ISSN 0918-4597

NRIM

Research Activities

1993

National Research Institute for Metals

Japan

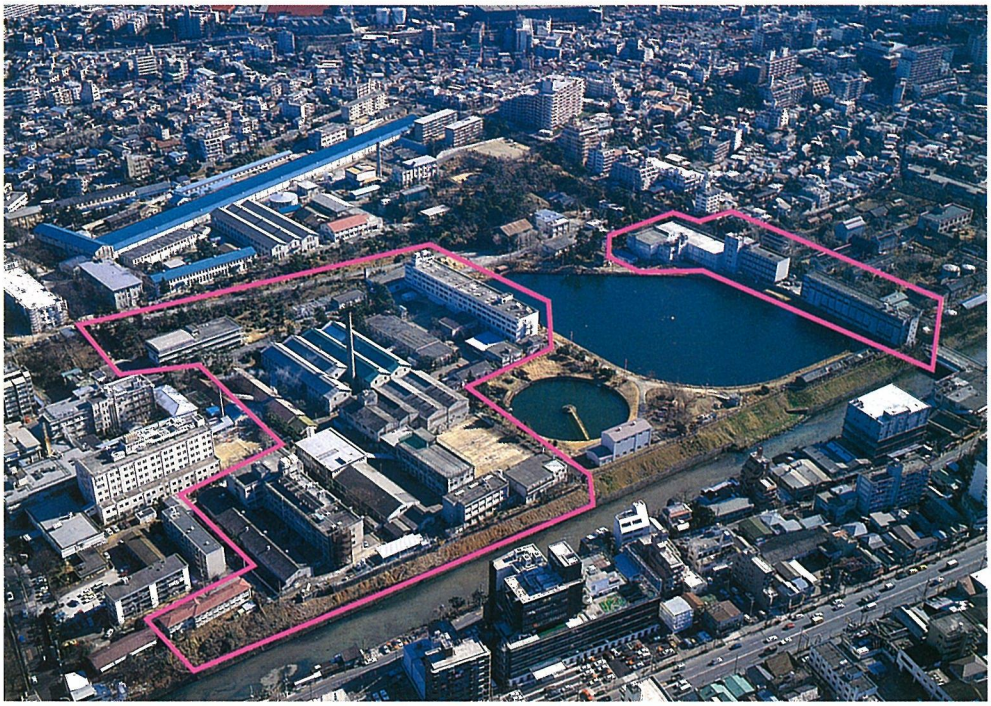

Meguro Main Site

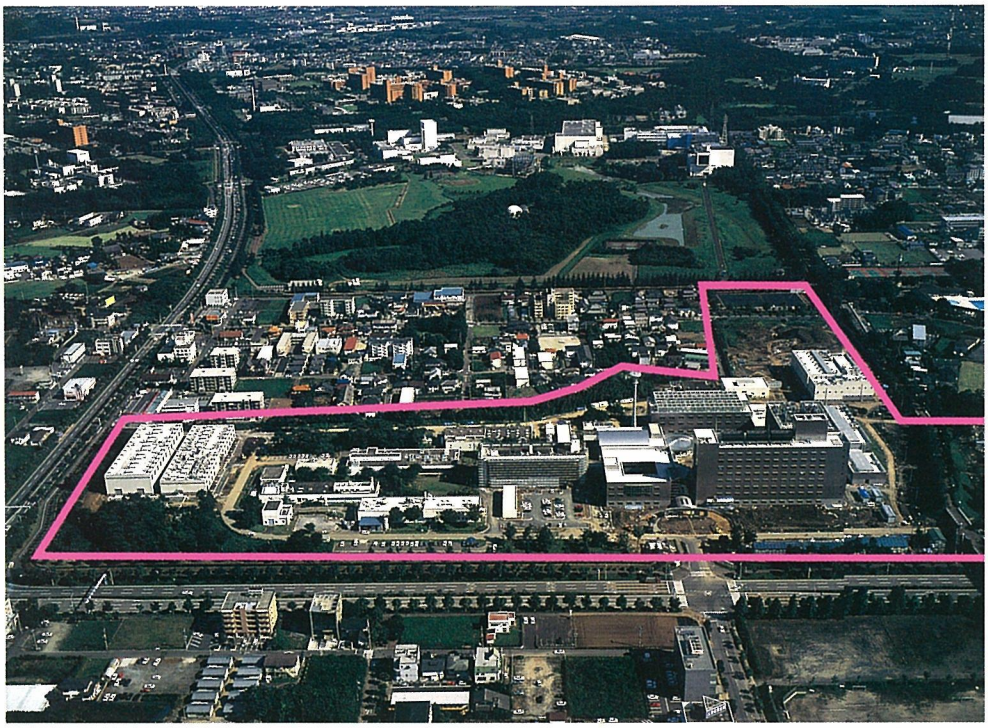

Tsukuba Laboratories

Preface

National Research Institute for Metals was established in 1956 as a research organization attached to the Science and Technology Agency of the Japanese Government. Since then, our Institute has played an important role in research and development of metals and alloys in Japan. Now NRIM has research staffs of over 300 people with a budget of about 8.6 billion yen (FY 1993) and is located at two sites; the main site in Tokyo and the branch in Tsukuba City.

The research activities of NRIM are concentrated on two fields. One is fundamental and applied research for advanced materials such as metallic and oxide superconductors, heat-resisting alloys, structural intermetallic compounds, etc. The other is research on reliability of materials to ensure safety of structural components and facilities. It includes the production of standard creep and fatigue data of Japanese commercial alloys, research on the failure mechanism, life prediction method and so on.

During the past 37 years, we have made several contributions to materials science and technology, especially in the fields of superconducting materials and superalloys. We have developed the bronze method to draw wires of metallic superconducting materials, and in 1988 our colleague found a new superconducting material of Bi-Sr-Ca-Cu oxide, which has T_c higher than 100 K. The computer aided alloy design method for superalloys was constructed, and several excellent heat-resisting alloys have been successfully developed. In the research on reliability of materials, we have been conducting the very long-term research programs on creep and fatigue properties, including creep rupture testing over 100,000 hr. We have published these data as the series of NRIM Creep and Fatigue Data Sheets, which we think are one of the most reliable sets of creep and fatigue data of commercial alloys. Through these programs, we have contributed to the progress in the life prediction technology and advanced materials assessment technology.

We are now unifying the whole Institute in Tsukuba City, and the new site will be completed in 1994. We will take this occasion to extend our materials research in the various fields, especially researches in high magnetic field, in ultra-high vacuum and in excited state assisted by high energy beams, and currently we are building their facility base. We expect this extension will bring about a new development of NRIM.

Kazuyoshi Nii

Dr. Kazuyoshi NII
Director-General

NRIM Research Activities 1993

Contents

Research Topics

❒ Electronic Structure of $YBa_2Cu_4O_8$

T. Oguchi and T. Sasaki, Materials Physics Division*

Keywords: $YBa_2Cu_4O_8$, Fermi surface, Hall coefficient, band theory, anisotropy

Several important experimental data of the copper-oxide superconductors have emerged as a result of highly controlled samples available. Transport properties are characterized by a large anisotropy due to the layered structure. Among the normal-state transport properties, Hall coefficient measurements provide useful information on the off-diagonal elements of the conductivity tensor, which can be directly compared with the Fermi surfaces derived by local-density band calculations.

Yttrium-barium-copper oxides, $YBa_2Cu_3O_y$ with y ~ 7 (Y123) and its low-temperature phase $YBa_2Cu_4O_8$ (Y124), which have a similar orthorhombic structure, reveal interesting similarity and dissimilarity in the properties, offering an important material field to study the electronic properties and mechanisms among the high-T_c superconductors.

In this study, we investigate the electronic structure of Y124 with particularly focusing on the Hall coefficient. The calculated Hall coefficient is in good agreement with experiment in its sign and magnitude and indicates a remarkably large anisotropy.

The electronic band structure of Y124 was calculated within the density functional formalism in the local density approximation. A perspective view of the calculated Fermi surfaces is drawn in figure 1. Two closed square-shaped and two open flat Fermi surfaces are associated mainly with two-dimensional CuO_2 plane and one-dimensional CuO chain bands, respectively, being crossing and anti-crossing each other. Similar but less significant two- and one-dimensional characters of the Fermi surfaces can be seen in Y123. Less dispersive feature along the k_z direction in Y124 than in Y123 is due to the facts that the energy position of the plane and chain π states in Y124 is lower than that in Y123 and the states near the Fermi energy are dominated by the σ states. This leads to a larger anisotropy in the transport properties of Y124 than that of Y123, as mentioned later.

In the Boltzmann theory, the electrical current in the presence of an electric field **E** and a magnetic field **B** is given as

$$j_\alpha = \sigma_{\alpha\beta}E_\beta + \sigma_{\alpha\beta\gamma}E_\beta B_\gamma + ..., \tag{1}$$

and the conductivity σ can be evaluated by

$$\sigma_{\alpha\beta} = e^2 \sum_{\mathbf{k}} \tau(\mathbf{k}) v_\alpha(\mathbf{k}) v_\beta(\mathbf{k}) \delta(\varepsilon(\mathbf{k}) - \varepsilon_F), \tag{2}$$

$$\sigma_{\alpha\beta\gamma} = -e^3 \sum_{\mathbf{k}} \tau^2(\mathbf{k}) v_\alpha(\mathbf{k}) \left\{ \left[v(\mathbf{k}) \times \nabla / \hbar \right]_\gamma v_\beta(\mathbf{k}) \right\} \delta(\varepsilon(\mathbf{k}) - \varepsilon_F), \tag{3}$$

with the relaxation time τ, the group velocity of electrons $v(\mathbf{k}) = \nabla\varepsilon(\mathbf{k})/\hbar$ and the Fermi energy ε_F. In equations (2) and (3), band indices are included implicitly in the **k** coordinates. The Hall coefficient of an orthorhombic crystal has three independent components,

$$R^H_{xyz} = \frac{E_y}{j_x B_z} = \frac{\sigma_{xyz}}{\sigma_{xx}\sigma_{yy}}, \tag{4}$$

with R^H_{yzx} and R^H_{zxy} given by cyclic permutation. If one assumes constant τ approximation in equations (2) and (3), τ cancels out of equation (4) and R^H can be evaluated without knowledge of τ. The group velocities have been evaluated with use of the Fermi surfaces calculated. In table 1, the calculated Fermi velocities, $\langle\langle v_\alpha^2 \rangle\rangle^{1/2}$, and the Hall coefficient for Y124 are listed along with those for $La_{2-x}Sr_xCuO_4$ (LSCO) and Y123 reported previously.

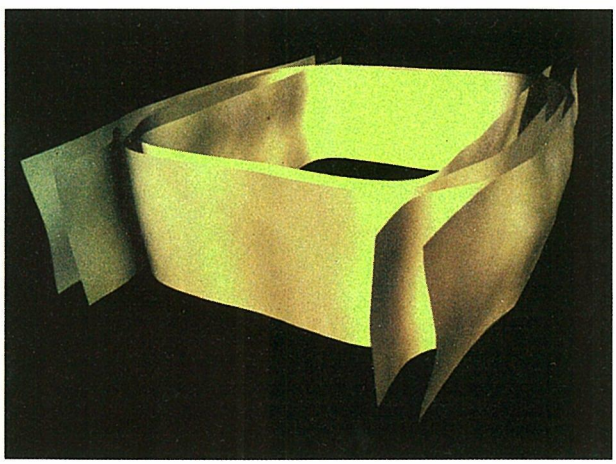

Fig. 1 A perspective view of the calculated Fermi surface of $YBa_2Cu_4O_8$. Two rounded-square cylinders and two almost-flat sheets are associated with CuO_2 plane and CuO chain bands, respectively, being crossing and anti-crossing each other.

*Hiroshima University

Table 1 Calculated density of states at the Fermi energy, $N(\varepsilon_F)$ (states/Ry cell), Fermi velocities, $\langle\langle v_\alpha^2 \rangle\rangle^{1/2}$ (10^7 cm/s), and Hall coefficient, $R^H_{\alpha\beta\gamma}$ (10^{-9} m^3/C), for $YBa_2Cu_4O_8$ and the related high-T_c superconducting oxides.

	$YBa_2Cu_4O_8$	$YBa_2Cu_3O_7$	$La_{1.85}Sr_{0.15}CuO_4$
$N(\varepsilon_F)$	42.5	76.0	28.4
$\langle\langle v_x^2 \rangle\rangle^{1/2}$	2.9	1.8	2.2
$\langle\langle v_y^2 \rangle\rangle^{1/2}$	4.7	2.8	2.2
$\langle\langle v_z^2 \rangle\rangle^{1/2}$	0.5	0.7	0.41
R^H_{xyz}	+0.18	+0.18	+0.18
R^H_{yzx}	−0.58	−0.38	−0.94
R^H_{zxy}	−0.03	−1.07	−0.94

(The notations, x, y and z, correspond to the directions, a, b and c, of the present material, respectively.) The present result of the Fermi velocities implies a larger anisotropy in Y124 than in Y123 and thus we may predict a larger anisotropy of σ in Y124 than in Y123. This is consistent with less three-dimensional character of the Fermi surfaces due to the existence of double CuO chains.

As for the Hall coefficient, trend in the sign of the components, which represents carrier character for a single isotropic parabolic band, coincides perfectly with those in Y123 and LSCO: When **B** is applied parallel to the c axis the carrier is *hole-like* while when B is in the *ab* plane it turns out to be *electron-like*. A coincidence of R^H_{xyz} even in magnitude may be accidental but quite interesting. The sign and magnitude of the observed Hall coefficient at room temperature (~ $+0.13 \times 10^{-9}$ m^3/C) correspond well to our calculated value of R^H_{xyz}.

References

1. *Electric Band Structure of $YBa_2Cu_4O_8$*, T. Oguchi, T. Sasaki and K. Terakura, Physica C 172 (1990): 277.
2. *Local-Density Band Structure of Y-Ba-Cu Oxides*, T. Oguchi, T. Sasaki and K. Terakura, Physica C 185–89 (1991): 1733.
3. *Calculation of the Hall Coefficient in $YBa_2Cu_4O_8$*, T. Oguchi, T. Sasaki and K. Terakura, in *Electronic Properties and Mechanisms of High-T_c Superconductors*, ed. by T. Oguchi, K. Kadowaki and T. Sasaki, Elsevier Sci. Pub. (1992): 407.
4. *Fermi Surface and Transport Properties of $YBa_2Cu_4O_8$*, T. Oguchi and T. Sasaki, J. Phys. Chem. Solids 53 (1992): 1525.

❒ X-ray Photoelectron Diffraction Studies of $Bi_2Sr_2CaCu_2O_{8+x}$

M. Shimoda, Materials Physics Division

Keywords: X-ray photoelectron diffraction, $Bi_2Sr_2CaCu_2O_{8+x}$, modulation

Introduction

X-ray photoelectron diffraction (XPD) is a newly developed and powerful tool for studying surface atomic geometries[1]. Unlike low energy electron diffraction (LEED) or reflection high energy electron diffraction (RHEED), which is also a surface analysis technique based on electron diffraction, XPD is quite unique in using photoelectrons as a probe. Because of the atom-specific nature and of the short inelastic attenuation length of photoelectrons, XPD brings the information about the local geometry around a specific element. Experimentally, the intensity distribution of photoelectron emission is measured with a high angle resolution by scanning both azimuthal angle (ϕ) and polar angle (θ)[2].

A remarkable feature of XPD is in exhibiting enhanced intensities of forward scattering, the forward focusing effect, which is prominent for the electrons with kinetic energies higher than a few hundreds of eV. We can expect from this effect intensity peaks to appear in the directions which linearly connect emitters with surrounding scatterers. Finding the forward scattering directions in observed XPD patterns is therefore a simple and useful way to understand the atom arrangements around the surface. It is also helpful to compare the XPD patterns with the simulated ones based on the single-scattering cluster (SSC) model, which is widely used and believed to give good results in the most cases.

In the present work, we applied XPD for the first time for studying the surface structure of $Bi_2Sr_2CaCu_2O_{8+x}$[3, 4], which is a layered material and has a pseudotetragonal average structure as shown in figure 1. It is also well known that this compound has an incommensurate modulation of the position and occupation of atoms along the b-axis with a periodicity of ~4.8b[5]. We prepared a clean surface of a $Bi_2Sr_2CaCu_2O_{8+x}$ single crystal by cleaving it *in situ* with Scotch tape and observed the XPD patterns of Bi 4f, Sr 3d, Ca 2p, Cu 2p and O 1s core level emission exited by Si Kα radiation (1740 eV) over much of 2π solid angle by rotating the sample. Note that we use here an abbreviation, $A^m \rightarrow B^n$, to express the event that photoelectrons emitted from A atom are scattered by B atom, where m and n denote the atoms on different layers as illustrated in figure 1.

XPD Patterns and Simulations

Figure 2 shows the Bi 4f XPD pattern as a gnomonic projection, a planar projection on a plane parallel to the surface, in order to present the lattice-like arrangements of scatterers. Most of the bright spots are the enhanced forward scattering peaks of $Bi^1 \rightarrow Bi^2$ scattering. This is easily confirmed by the simulation of the forward scattering directions; the result is shown in this figure, being superimposed on the experimental data, where patterns are shown in gnomonic projection, namely. It is clear that the simulated spots of $Bi^1 \rightarrow Bi^2$ forward scattering fall on the observed spots. The small deviations between the experimental data and the simulation are mainly due to the lattice modulation and the overlap of other scattering like $Bi^1 \rightarrow Sr^2$. The large contribution from $Bi^1 \rightarrow Bi^2$ scattering results from the large scattering cross section of Bi.

Figure 2 yields an important information about the termination of the crystal. If the Bi^0–O layer existed above the Bi^1–O layer, $Bi^1 \rightarrow Bi^0$ scattering would have given rise to stronger spots than $Bi^2 \rightarrow Bi^1$ scattering. However, the fact that any signal

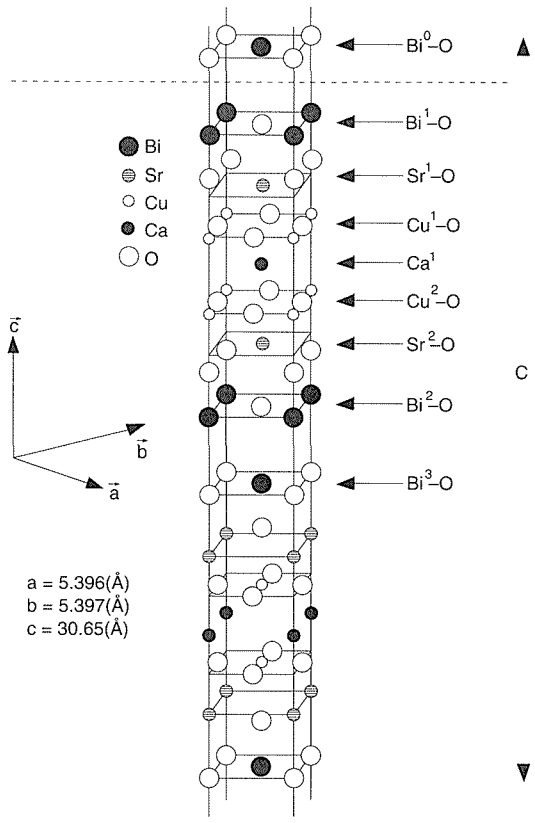

Fig. 1 The fundamental crystal structure of $Bi_2Sr_2CaCu_2O_{8+x}$.

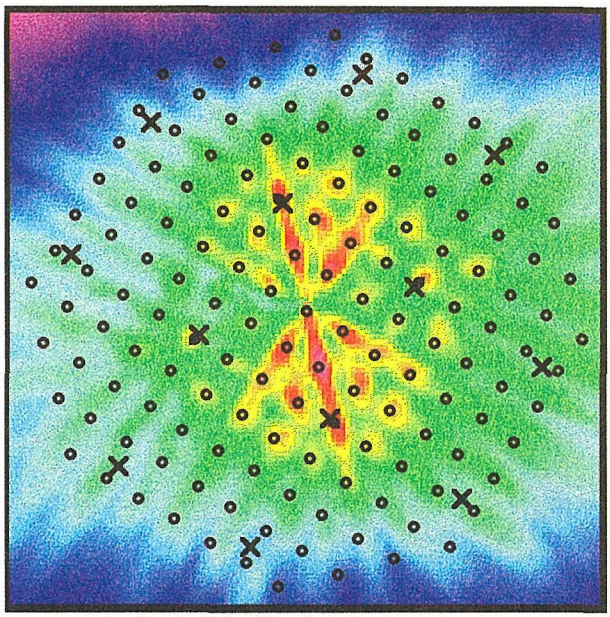

Fig. 2 Gnomonic projection of the Bi 4f XPD pattern. Simulated forward scattering directions of $Bi^1 \rightarrow Bi^2$ and $Bi^0 \rightarrow Bi^1$ are shown by ○ and ×, respectively.

from $Bi^1 \rightarrow Bi^0$ scattering, which would appear at × in the figure, was not detected means that the $Bi_2Sr_2CaCu_2O_{8+x}$ single crystal was terminated by the Bi^1–O layer.

We found that other observed XPD patterns were also regarded as the overlap of the forward scattering peaks which came from several types of emitter-scatterer combinations. Although these patterns are different from each other reflecting the local geometry around each emitter, there are some common features. First, the forward scattering peaks are fourfold symmetric in terms of the peak position. This is clearly due to the fact that we observed the emission from the (001) surface of the almost tetragonal crystal. Second, the intensity patterns are modulated in twofold symmetry, i.e., the emission parallel to the *bc* plane is stronger than that parallel to the *ac* plane. This fact is qualitatively in good agreement with the modulated structure. In addition, the forward scattering spots are rather broad and diffused. We found that the nature of the diffuseness is well explained by the forward scattering analysis with a cluster which is positionally modulated as in the bulk[5].

The same cluster was also used for the SSC calculation for more quantitative comparison. As shown in figure 3, the calculation is rather successful, except that the twofold symmetry is not well reproduced in some cases (e.g., at $\theta = 32°$ in Cu 2p XPD). We are unable to explain that at this stage.

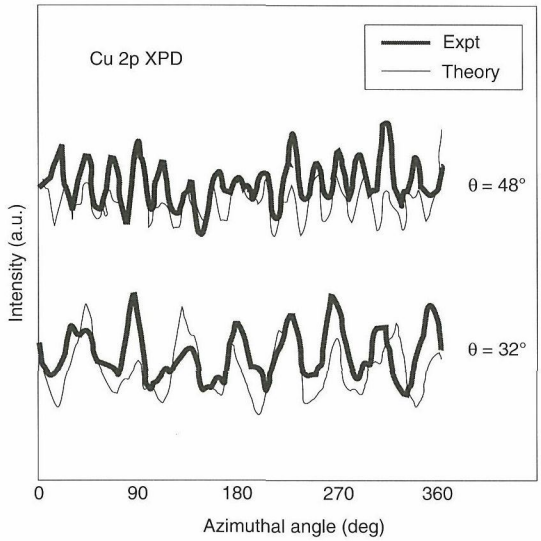

Fig. 3 A comparison of the experimental XPD patterns to the SSC calculations with a positionally modulated cluster for the case of Cu 2p emission. The parameters of modulation were taken from ref. 5.

However, taking it into account that the diffuse spots are well simulated by the modulated cluster, the clean surface of $Bi_2Sr_2CaCu_2O_{8+x}$ is to be expected to have basically the same modulated structure as the bulk.

We performed this work in cooperation with the group of Université de Fribourg, Switzerland.

References

1. *The Study of Surface Structures by Photoelectron Diffraction and Auger Electron Diffraction*, C.S. Fadley, in: *Synchrotron Radiation Research: Advances in Surface and Interface Science*, ed. R.Z. Bachrach Plenum, New York (1989): 421–518.
2. *Experimental Full-Solid-Angle Substrate Photoelectron-Diffraction Data at 1-keV Energies: Implications for Photoelectron Holography*, J. Osterwalder, T. Greber, A. Stuck and L. Schlapbach, Phys. Rev. B 44 (1991): 13764–67.
3. *X-ray Photoelectron Diffraction Studies of $Bi_2Sr_2CaCu_2O_{8+x}$*, M. Shimoda, T. Greber, J. Osterwalder and L. Schlapbach, Physica C 196 (1992): 236–40.
4. *Two Dimensional Photoelectron Diffraction Images of a Single Crystal $Bi_2Sr_2CaCu_2O_{8+x}$*, M. Shimoda, Butsuri, to be published (in Japanese).
5. *Rietveld Analysis of the Modulated Structure in the Superconducting Oxide $Bi_2(Sr, Ca)_3Cu_2O_{8+x}$*, A. Yamamoto, M. Onoda, E. Takayama-Muromachi, F. Izumi, T. Ishigaki and H. Asano, Phys. Rev. B 42 (1990): 4228–38.

❒ Modeling of Nano-structure in Ni-base Single Crystal Superalloys Theoretical Estimation and Experimental Verification

H. Harada, Materials Design Division

Keywords: Ni-base superalloy, computer modeling, cluster variation method, site occupation, atom-probe field ion microscopy

There is a constant drive to increase the temperature capability of Ni-base superalloys, as a means of improving thermal efficiencies in aero-engines. With this objectives in mind, a series of Ni-base superalloys were developed using our alloy design computer program established on our database by using regression analysis[1]. These alloys outperformed the industry standard alloys such as CMSX-4 and PWA1484.

In order to improve the alloy design computer program and to design alloys with further superior properties, more theoretical approach with Cluster Variation Method (CVM)[2] has been applied to the modeling of the nano-structure in superalloys. The estimation has been verified experimentally by Atom-probe Field Ion Microscopy (APFIM)[3].

Theoretical Estimation by CVM

The equilibrium between γ and γ' phases, including site occupations of alloying elements in the crystals, lattice parameters and so on, was calculated by using CVM. The principle of this method is as follows. The configurational entropy is calculated by using a tetrahedron nearest neighbor atom cluster shown in figure 1. The entropy per each lattice point of the γ' phase is written as:

$$S_{\gamma'} = -k\left[\sum_{ijkl} 2L(Z_{ijkl}^{ABBB}) - 3\sum_{ij}\left\{L(y_{ij}^{AB}) + L(y_{ij}^{BB})\right\} + \frac{5}{4}\sum_{i}\left\{L(x_i^{A}) + 3L(x_i^{B})\right\}\right] \quad (1)$$

where, z_{ijkl}^{ABBB} is the probability of finding atoms i, j, k and l in a tetrahedron nearest neighbor atom cluster. The summation is taken with all component atom species. The Al and Ni sublattices are denoted by superscripts A and B, respectively. y_{ij}^{AB} and y_{ij}^{BB} are the probabilities of finding atoms i and j in a nearest neighbor atom pair between the two sublattices and in the Ni sublattice. x_i^A and x_i^B are the probabilities of finding atom i at a lattice point belonging to the Al and Ni sublattices, respectively. k is the Boltzmann constant, and $L(\zeta) = \zeta \ln\zeta - \zeta$.

The enthalpy is calculated by using the Lennard-Jones pair potential, e(r); only the nearest neighbor pair interaction is taken into account, namely:

$$H_{\gamma'} = \frac{z}{2}\sum_{ij} e_{ij}(r)(y_{ij}^{AB} + y_{ij}^{BB}) \quad (2)$$

where z = 12 is the nearest neighbor coordination number in the fcc lattice. The atom configuration which minimizes the grand potential:

$$\Omega_{\gamma'} = H_{\gamma'} - TS_{\gamma'} + PV_{\gamma'} + \frac{1}{4}\sum_{i}\mu_i(x_i^{A} + 3x_i^{B}) \quad (3)$$

is sought under the restrictive condition:

$$\sum_{ijkl} z_{ijkl}^{ABBB} = 1 \quad (4)$$

Here, T, P, $V_{\gamma'}$ and μ_i are temperature, pressure, atomic volume and chemical potential of the i-th component, respectively. All corresponding equations for the γ phase are obtained by removing the subscripts A and B from the above equations. The equilibrium state between γ and γ' phases can be obtained by equalizing the grand potentials thus calculated for the phases, under the same values of P, T and μ.

Experimental Verification by APFIM

The nano-structure was analyzed by using APFIM. Very sharp needle-like samples were prepared by electropolishing of thin rods cut out of a single crystal superalloy specimen (TMS-63) crept at 1040 °C and at 137 MPa, the measured rupture life being 2657 h. The sample tip temperature was kept below 40 K during the analysis.

Figure 2 shows the FIM image. Each spot corresponds to each atom. The atomic layers on low index planes are clearly visible as coaxial rings. The dark line across the center of this figure was

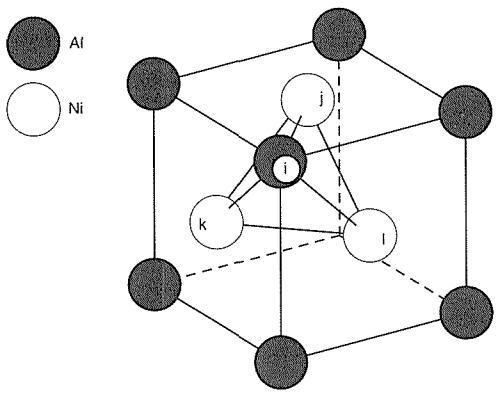

Fig. 1 Tetrahedron cluster for fcc structure used in the calculation.

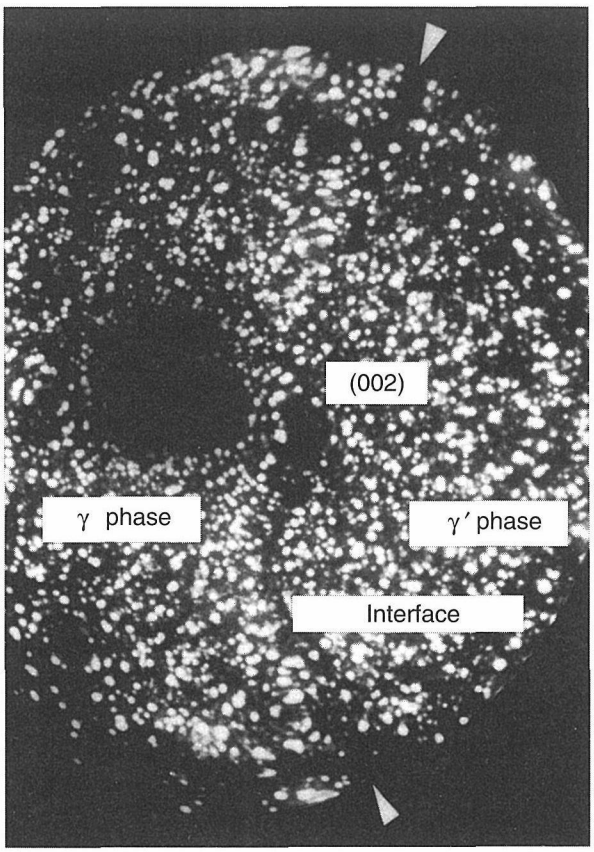

Fig. 2 FIM image of the γ/γ' interface

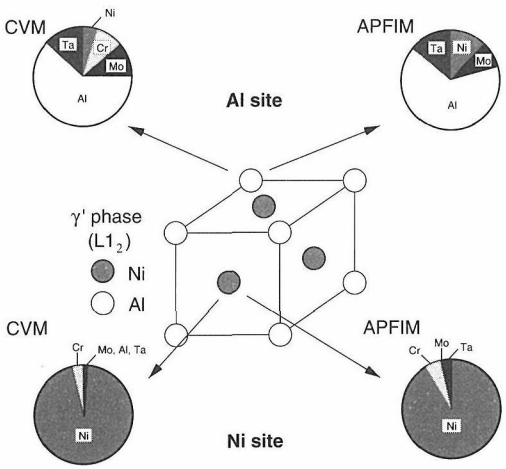

Fig. 3 Site occupancy in the γ' phase in a Ni-base single crystal superalloy

confirmed, using chemical analysis, to be the γ'/γ interface. The observed continuity of {200} planes across the phase interface is consistent with the coherency between the γ and γ'.

The site occupations of the solute elements are determined from the chemical analysis of the Ni + Al mixed layers and Ni-rich layers obtained by progressively stripping {200} planes of the γ' phase. The result is compared with the CVM calculation in figure 3. This figure demonstrates a very good agreement between the theoretical estimation and the experimental determination, except for the difference in Cr content at the Al site suggesting a need of a slight modification of interatomic potential parameters in the Lennard-Jones pair potential used in the CVM calculation.

CVM and APFIM thus match each other very well for establishing the computer model of nanostructures in alloys. The same approach is now being applied to other alloys including high temperature intermetallics like NiAl.

Acknowledgement

This work has been carried out in a collaboration. Professor M. Enomoto (CVM), Dr. A. Ishida, Dr. H. Murakami and Dr. H.K.D.H. Bhadeshia (APFIM) are to be mentioned for their major contribution. The APFIM work was performed in University of Cambridge, Department of Materials Science and Metallurgy, as part of the research activities of a collaborative research project, "Atomic Arrangement Design and Control Project," among University of Cambridge, Research Development Corporation of Japan (JRDC) and NRIM.

References

1. *Design of High Specific-Strength Nickel-base Single Crystal Superalloys*, H. Harada, T. Yokokawa, K. Ohno, T. Yamagata and M. Yamazaki, Proc. Conf. High Temperature Materials for Power Engineering 1990, Liege, Belgium, 24–27 Sept. 1990, 1319.
2. *Calculation of γ'/γ Equilibrium Phase Composition in Nickel-base Superalloys by Cluster Variation Method*, M. Enomoto, H. Harada and M. Yamazaki, CALPHAD 15 2 (1991): 143–58.
3. *Atom-probe Microanalysis of a Nickel-base Single Crystal Superalloy*, H. Harada, A. Ishida, H. Murakami, H.K.D.H. Bhadeshia and M. Yamazaki, Applied Surface Science, 67 (1993), 299–304.

❐ Cold Crucible Type Levitation Melting of Reactive Metals

A. Fukuzawa, Chemical Processing Division

Keywords: cold crucible, levitation melting, reactive metals

Introduction

Up to now, the contamination of molten metal by tramp elements from the crucible which is made of refractory materials and the reaction between metal and crucible have made it difficult to purify the reactive metals. Besides, there has been no crucible materials for homogeneous melting of refractory metals, for the melting point of some of refractory metals are higher than the crucible materials. For this reason, refractory metals and reactive metals such as niobium, titanium, zirconium and those alloys have been melted with the water cooled copper crucible by vacuum arc furnace, electron beam furnace, or plasma arc furnace. But these melting methods have following disadvantages; as the fusion of the melting stock is not performed completely by these methods, the homogeneous composition of molten metal cannot be obtained. In the case of addition of low melting point metals for alloying such as aluminum, vaporization of these elements makes it difficult to control the precise composition of alloys. Therefore, the development of melting method to be capable to deal with these metals and alloys has been expected to solve these problems.

Cold Crucible Type Levitation Melting

Levitation melting method using high frequency electric power is known as non-contacting melting method. But the weight of levitated metal by this method has been only a few grams up to now. Cold crucible type levitation method, of which crucible is assembled with electrically insulated segments, is thought to have a large capacity of levitation. Therefore, NRIM has been studying the development of the cold crucible type levitation melting induction furnace which enable to levitate and to melt a large amount of metals. In these several years, various kinds of trials on the cold crucible type non-contacting induction furnace have been made and many fundamental results concerning with the cold crucible have been obtained. Shape of cold crucible (number of segments, slit width, height of crucible, inner shape, etc.), coil shape (number of turns, cross section, diameter, position against crucible, etc.), levitating material (property of material, shape, etc.) and electric source (frequency, electric power, etc.) have been investigated and tested to make clear the relation between levitation force and these parameters of cold crucible devices with the combination of electromagnetic analysis by computer simulation. As a result, we have succeeded in the development of levitation melting device which can lift liquid metal around 2 kg.

Principle of Levitation Melting Device

Figure 1 shows the principle of cold crucible type levitation melting device. High frequency current being supplied to the coil which is wound around the cold crucible, high frequency magnetic field is induced, and the eddy current is induced by the magnetic flux both in the segments and the metal placed in the crucible. As the direction of the eddy current in the vicinity at the inner surface of the crucible is opposite to that at the surface of the metal to be melted, the metal is levitated by the repulsive force induced between eddy currents. Then, levitating metal is also heated and melted by eddy current induced in electromagnetic field.

There is a following equation among the levitation force acting between crucible and metal, frequency of electric current and physical property of levitating materials.

$$F = W\sqrt{\frac{2\mu}{\omega\rho}} \qquad (1)$$

where, F ; levitation force,
W ; electric power,
μ ; magnetic permeability,
ω ; angular frequency,
ρ ; electric resistance.

This equation means that the levitation force is proportional to the square root of reciprocal of electric source frequency and electric resistance of levitating material at a constant electric power.

Controlling Techniques for Optimum Levitation

As the physical properties such as density, melting point, electric resistance etc. vary according to the kind of metals and alloys, there are some cases where heating of materials in the crucible is not sufficient although applying enough electric current to the coil for levitating the materials. On the contrary, there are some cases where the materials of low density spring out from the crucible for too much levitation force even though electric current is sent for just only melting the materials. As electric resistance of metals increases with tem-

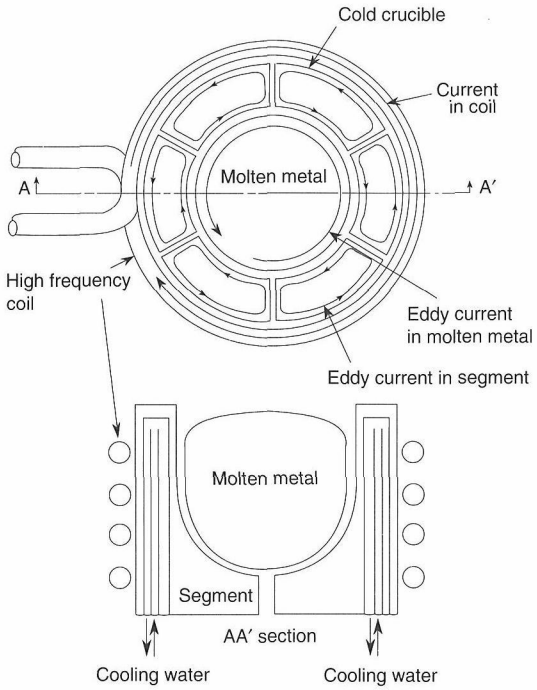

Fig. 1 The principle of cold crucible type levitation melting device

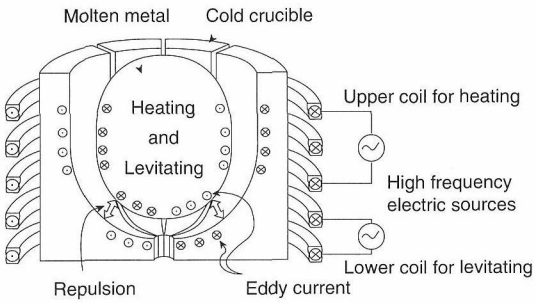

Fig. 2 The new conception of the cold crucible levitation melting developed by NRIM

perature rise (in the case of iron, 10 μΩ·cm at room temperature, 140 μΩ·cm at the vicinity of melting point), levitation force and heating speed decrease with temperature rise according to the equation (1). Thus, it is very difficult to control the stability of levitating and heating the materials in the case of using single electric power source.

To improve these disadvantages, we have been developing a new levitation control techniques; supplying different two frequencies. A new conception of levitation controlling is shown in figure 2. Two sets of coils are arranged around the cold crucible, and two high-frequency currents are supplied from two electric power source which have different frequency each other. The higher frequent currency is supplied to the upper coil, and the rather lower frequency current is supplied to the lower coil. The role of the lower coil is mainly levitation of material, for the levitation force is proportional to the square root of reciprocal of electric source frequency as shown by the equation (1). The role of the upper coil is mainly heating of material, for the eddy current in the material to be melted is more converged to the surface of the material and heating efficiency is improved with the increase of electric source frequency.

Thus, to use two electric power source and to design the shape of the cold crucible being adapted for levitating and heating make it possible to control the optimum levitation melting by regulating electric current and frequency arbitrarily even though the amount of material for melting or kinds of metals and alloys are varied.

A newly developed levitation melting device is composed of 24 segmented cold crucible which has 800 ml of inner volume and two sets of coils for heating and levitating. High frequency electric sources of 50 kHz, 450 kW and 3 ~ 10 kHz, 100 kW are connected to the upper and the lower coil, respectively. By using this configuration, 2.3 kg of titanium and same weight of Ti-Al (intermetallic compound) were able to be levitated and melted completely within 2 to 3 minutes after the start of supplying electric power (see figure 3).

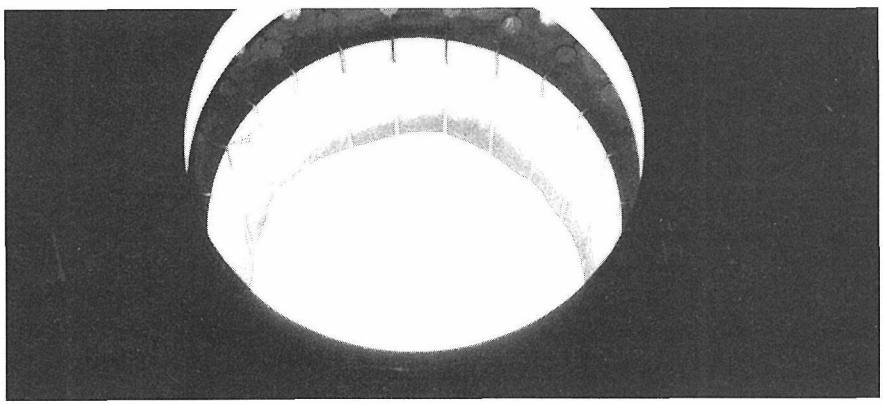

Fig. 3 2.3 kg of titanium under levitation melting

❒ Development of Ultra High Vacuum Equipment for Diffusion Welding with Controlled Surface Composition and Misorientation Angle

O. Ohashi and S. Meguro, Advanced Materials Processing Division

Keywords: ultra high vacuum, joining, surface composition, sulfur-rich layer, misorientation angle, semi-conductor device

Introduction

A National Project has been established in Japan which is interested in research for "Materials Interconnection" for advanced applications where a combination of material properties is necessary to produce high technology devices. However, the application of conventional welding techniques to join materials affects the original parent metal properties. Therefore, work at NRIM is being under taken to develop a low temperature and low pressure joining process for complex materials to prevent detrimental changes in material properties. Research on the effect of composition and structure at the bonding surfaces has led to a low energy joining technique. For this research, an ultra high vacuum equipment has been developed for diffusion welding, which incorporates a surface control and analysis unit.

Detail of Ultra High Vacuum Joining Equipment

Figure 1 shows a schematic diagram of the joining equipment. The equipment consists of chambers for specimen loading, pre-cleaning, joining, surface analysis and specimen traverse. The chambers used for joining, surface analysis and specimen traverse are maintained at an atmospheric pressure of 10^{-8} Pa by means of an ion pump and a molecular turbo pump. Specimens are placed into the loading chamber and moved to the surface analysis chamber and the joining chamber via interconnecting traverse chambers. Both surface composition analysis using auger electron spectroscopy and surface structural analysis using reflection high energy electron diffraction (RHEED) is carried out in the surface analysis chamber. An argon-ion bombardment source for controlling the surface composition is also located within this chamber. The joining chamber has devices for applying load (up to 2000 N) using a hydraulic pressure system, radio frequency (R.F.) heating (with a capacity to heat metals and ceramics to temperatures of 1000 °C) and specimen rotation enabling samples to be joined using different crystal orientations.

The following relationships have been investigated by using this equipment:

1. Surface composition, structure and joining phenomena of various metals.
2. Misorientation angle and joining phenomena of molybdenum and silicon.
3. Surface composition, structure and semi-conductor device function of silicon.
4. Misorientation angle and semi-conductor device function of silicon.

Experimental Results and Discussion

The relationship between changes in surface composition when heating in a vacuum and subsequent bonding phenomena was studied using this joining equipment. A variety of materials were used such as titanium, copper and SUS304 stainless steel. These materials could be joined to produce good bonds once oxides and contaminants based on oxygen and carbon were removed from the surface. Heat treatment in vacuum, was found to cause surface oxide dissociation due to the dissolution of oxygen into the base metal and oxide reduction by carbon. However, auger analysis of the surface revealed the formation of a sulfur-rich monolayer. It is thought that sulfur (in the bulk material) segregates to the surface and forms this sulfur-rich layer. The layer has the effect of preventing the adsorption of impurity elements such as oxygen and carbon which interfere with the joining process, but also lowers the bonding temperature. This is because the bonding temperature is determined by the temperature at which surface oxides dissociate and since the sulfur-rich layer dissociates at a lower temperature than surface oxides based on oxygen, lower bonding temperatures can be employed.

Therefore, a new, lower temperature diffusion bonding process has been developed. Unlike the

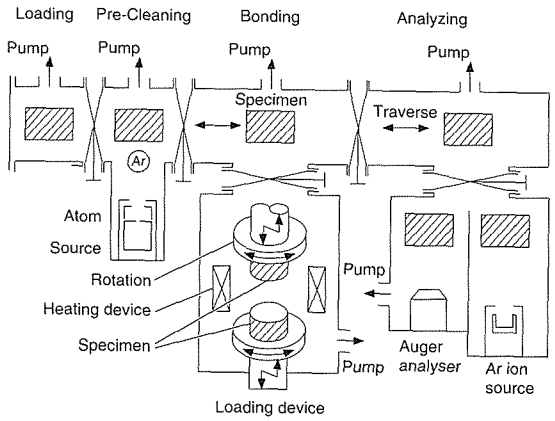

Fig. 1 Schematic diagram of joining equipment

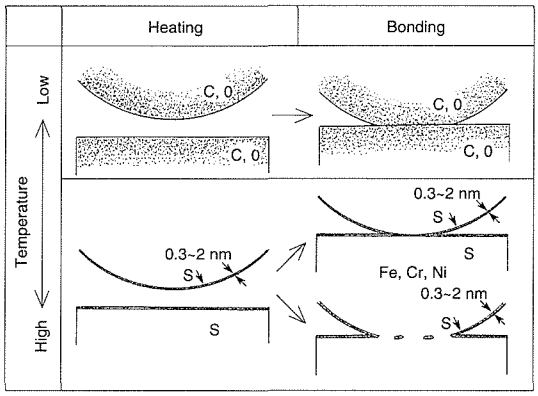

Fig. 2 Behavior of surface layer on bonding (Upper: Conventional Process, Lower: New Process)

Table 1 Bonding temperature of various materials in each process

	Copper	Titanium	SUS304
Conventional Process	800 °C	750 °C	800 °C
New Process	300 °C	650 °C	650 °C

conventional bonding process where the joint region is heated after the bonding surfaces are brought into contact, in this method specimens are heat treated in vacuum prior to bonding. Figure 2 shows a schematic comparing the bonding mechanisms at the joint interface during the conventional and new bonding processes. In table 1 the difference in bonding temperatures for various metals can be seen when conventional and new joining processes are compared.

Conclusions

1. Conventional diffusion bonding techniques consider highly clean surfaces as a method for reducing bonding temperatures. This work shows that the presence of a sulfur-rich monolayer at the joining surfaces considerably lowers the bonding temperature.
2. The presence of a sulfur-rich layer keeps the bonding surfaces free from further contamination and adsorption of impurity elements such as oxygen and carbon which interfere with the joining process.
3. A new, lower temperature bonding procedure can be suggested involving heat treatment of specimens in vacuum prior to joining.

❒ Structural Analysis of Argon-Helium Mixed Gas Tungsten Arcs

K. Hiraoka, Advanced Materials Processing Division

Keywords: gas tungsten arc, mixed gas, spectroscopy, electron density, plasma composition, electron temperature

It is well known that the arc characteristics are remarkably influenced by the introduction of a secondary gas in a gas tungsten arc (GTA) welding. These phenomena are still poorly understood. Moreover, although pure argon arcs have been investigated in detail, basic researches on mixed gas welding arcs are very scarce.

In this research, the structure of mixed gas arc plasmas is discussed from results obtained by three different spectroscopic methods.

Electron Density Profile

The method proposed by Ohji and Eagar[1], in which the electron density is estimated from the infrared radiation of the arc plasma, has been applied to the measurement of the electron density profile. For the electron density profile, a lens system mounted on a stage is used to obtain the radiance of a ϕ 0.2 mm spot of the arc plasma. The radiation is led to an IR-temperature meter with a PbS sensor through a quartz fiber and then the spectral radiance profile is obtained using the Abel conversion technique.

The resulting electron density profiles of 100 A argon-helium arcs at 1 mm below the cathode tip, are shown in figure 1. It is found that the measured electron densities decrease with increasing the helium content and that there are also remarkable drops in electron density at the arc center.

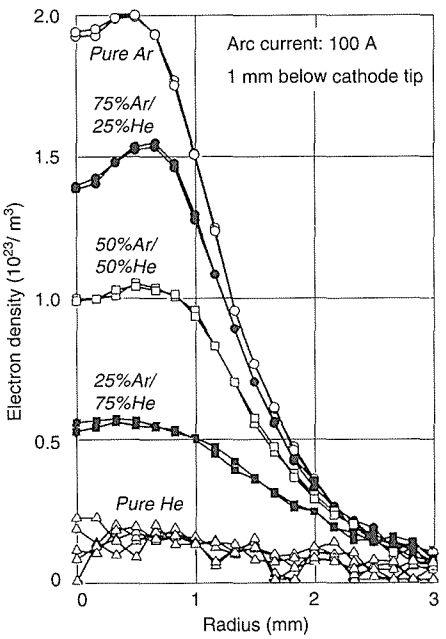

Fig. 1 Measured electron density as a function of the radial position in the arc for various argon-helium mixture ratios.

If the arc plasmas under consideration are in local thermodynamic equilibrium (LTE) and the plasma composition is homogeneous, these results suggest from the Saha relation diagram in an argon-helium mixed gas system that the electron temperature at the arc center decreases remarkably with increasing the helium content.

Plasma Composition at the Anode Surface

A new method was developed to estimate the plasma composition at a water-cooled copper anode by a mass spectrometer. In these experiments, a small amount of plasma gas is directly sampled through a hole (ID: 0.5 mm) in the anode plate and is analyzed. The helium concentration of the sampling gas is determined from the ratio of the helium spectrum peak value (H_{He}) to that of argon (H_{Ar}) in argon helium arcs.

In figure 2, the measured helium concentration at the stagnation point (arc center at anode) is shown as a function of arc length in 25%Ar-75%He arcs, and it is higher in the center of the arc plasma at the anode surface than that of shielding gas. The helium concentration clearly increases with the decrease in arc length.

It can be concluded that the gas composition is not homogeneous but depends on the position in the arc plasma. This effect should lead to lower electron densities in the center of the arc (shown in figure 1).

Plasma Spectroscopic Analysis

A new method using a monochromator is pro-

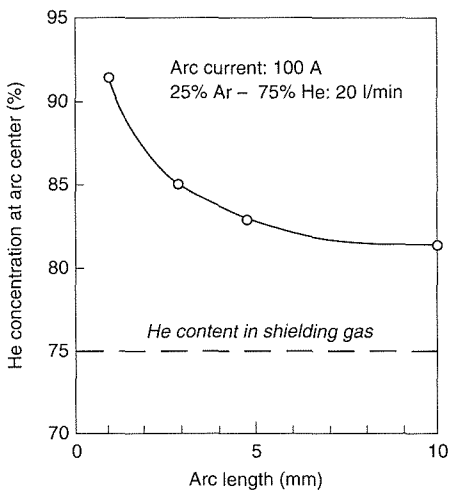

Fig. 2 Effect of arc length on helium concentration at the arc center.

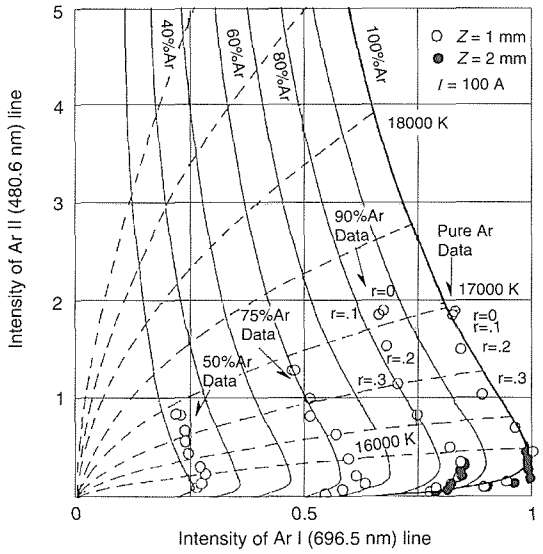

Fig. 3 Relationship between Ar I and Ar II intensities in argon-helium arcs.

posed to estimate simultaneously the position-dependent composition and temperature of the arc plasma. The setup of the light spectroscopic measurement is similar to that of the electron density measurements, and the end of the quartz fiber is led to a monochromator. The argon excited line spectrum intensity Ar I (696.5 nm) and ionized line intensity Ar II (480.6 nm) profiles are calculated from their measured radiation profiles using the Abel conversion technique. The local plasma composition and the electron temperature in argon-helium arcs can be estimated from the relative intensity ratio (Ar II/Ar I), assuming that the Ar-He arc plasma is in LTE. Although the electron density of arc plasmas and the plasma composition at the anode can be analyzed without the assumption of the existence of the LTE, this spectroscopic analysis depends on the existence of LTE.

Figure 3 shows the relationship between Ar I and Ar II intensities (circular marks) as a function of the radial position, as measured at 1 mm below the cathode tip of pure argon, 90%Ar-10%He, 75%Ar-25%He and 50%Ar-50%He arcs. Here, solid lines and broken lines show intensity relations and isotherms, respectively, calculated from the relative intensity equation combined with the Saha relation in the argon-helium mixed gas system. From this figure, the local plasma composition and the electron temperature are determined as a function of the radial position, and afterwards the electron density is calculated from the Saha relation.

Correlation of the Results Obtained by the Three Spectroscopic Methods

The helium concentration, the electron temperature and the electron density at the arc center (r = 0), 1 mm below the cathode tip (z = 1 mm), estimated from figure 3, are shown as a function of the helium content in the shielding gas using circular marks in figures 4(a), (b) and (c), respectively. In figure 4(a), the results estimated by the mass spectroscopic analysis in arcs with a 1 mm arc length are depicted using a solid line. A solid line in figure 4(c) shows results obtained in figure 1.

The results of all measurements show a good agreement. Therefore, this correlation of the results leads to a conclusion that the performed spectroscopic analysis of the structure of the Ar-He arc, under the assumption of LTE, is valid and effective, and that the composition in the mixed gas arc plasma is not homogeneous, but that the helium gas concentrates near the center of argon-helium arcs.

Reference

1. *Infrared Radiation from an Arc Plasma and its Application to Plasma Diagnostics*, T. Ohji and T.W. Eagar, Plasma Chem. Plasma Process 12 (1992): 403–19.

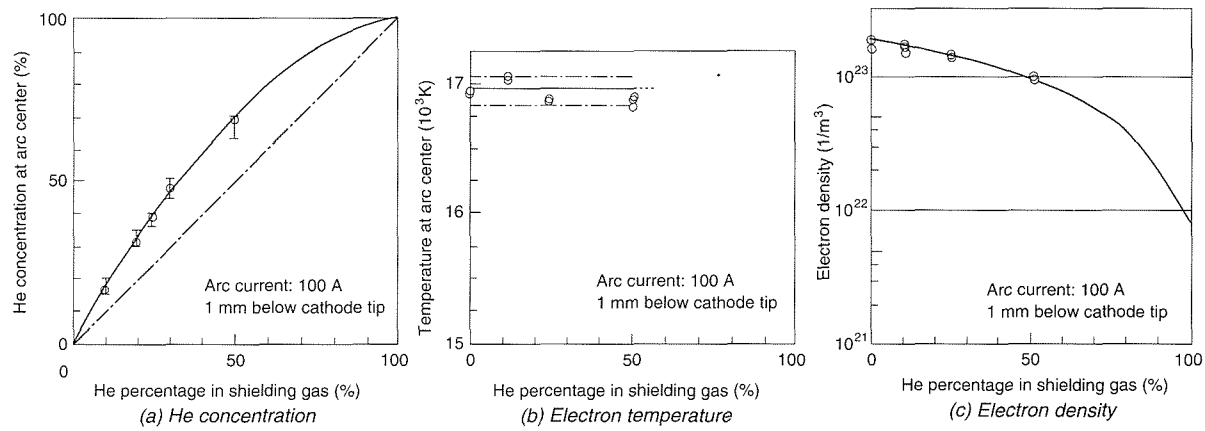

Fig. 4 Estimated plasma parameters at the center of the arc as a function of shielding gas composition.

❒ Scanning Tunneling Microscopy in Electrochemical Study of Materials Reliability—Electrodeposition Phenomena Related to Tunnel Current

H. Masuda, Failure Physics Division

Keywords: STM, electrodeposition, copper, tunnel current, $CuSO_4$

Introduction

It is important to understand the basic mechanism of the damage of materials by electrochemical reaction for improving the reliability of materials. Scanning tunneling microscopy is one of the best method to study this basic mechanism, because *in-situ* observation of electrochemical reaction can be done with the atomic resolution. We have studied the corrosion behavior of steels in 1% NaCl and 0.1% HNO_3 aqueous solution by the scanning tunneling microscope (STM)[1, 2] and the quantitative evaluation of corrosion was done by the subtraction between STM images. We also studied the initial stage of electrodeposition for copper on gold electrode in 0.1 M $CuSO_4$ + 0.6% H_2SO_4 aqueous solution by the STM. We have found that the enhanced electrodeposition occurred under STM tip when the tunnel current was increased. In this paper, the effect of potential and tunnel current on this phenomenon was discussed.

Experimental Procedure

The test specimen used was a pure gold plate of 5 mm × 3 mm × 1 mm in size mounted in heat hardened resin and polished with diamond paste up to 0.3 μm. The test cell was made from Teflon with diameter of 40 mm and height of 15 mm. The bipotentiostat proposed by Itaya[3] and the tunnel tip coated with epoxy resin except on the top were used to minimize the faradic current in the tip. STM was controlled by a 16 bit D/A converter and data of 256 × 256 points were obtained by a 12 bit A/D converter. The data were displayed on two monitors in real time with both bird's eye view image and 8 bit gray scale image. The tunnel head with the scanning range of 9 × 9 × 3 μm for x, y and z direction at maximum was used to get wide range information. The current-voltage curves were obtained in the STM cell with the scanning speed of 40 mV/min. The effect of tunnel current on the electrodeposition rate was studied at a constant tip potential (Et = 55 mV) with the STM tip being fixed at the center of the scanning area. The electrode potential was first set at 25 mV and then changed quickly to the test potential. The measurement of electrodeposition rate was started 2 seconds after the potential was changed. The effect of electrode potential on the electrodeposition rate was also studied at potentials of –10, –20 and –30 mV with the constant tunnel current of 18 nA. The electrodeposition rate of copper under the STM tip was measured directly from the Z-axis displacement of piezo actuator. All tests were controlled by a computer and the program was originally made with machine language and basic language.

Experimental Results

Figure 1 shows the current-voltage curves for gold and copper electrodes. The electrodeposition of copper on gold electrode started around –30 mV and the current-voltage curve of gold became similar to that of copper as the covering ratio of copper on gold electrode increased. Figure 2 shows the effect of tunnel current on the electrodeposition rate of copper at 0 V. The electrodeposition was started under the STM tip at 0 mV when the tunnel current is larger than 4 nA. The electrodeposition rate increased with the tunnel current and was reached 130 nm/sec at the tunnel current of 18 nA, which is more than 7500 times bigger than the equivalent current density of gold in this solution. The electrodeposition rate is usually strongly dependent on potential near corrosion potential. The observed electrodeposition, however, was independent on electrode potential in the test potential range. Figure 3(a) shows the STM image of gold electrode before the test in 0.1 M $CuSO_4$ + 0.6% H_2SO_4 aqueous solution at 25 mV. A pit produced by the tunnel tip is observed on the left center of the image. Figure 3(b) shows the STM image after the test in the same environment. It is clear that the electrodeposition occurred only under the STM tip. Considering that the electrodeposition rate is extremely fast and only dependent on the tunnel current, it is concluded that some part of the tunnel current is consumed to the electrochemical reaction.

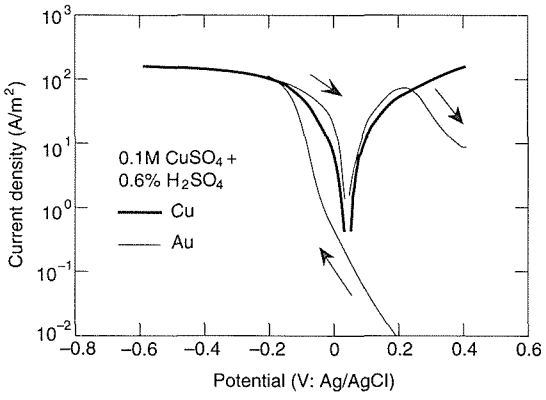

Fig. 1 Current-voltage curve of Au and Cu in 0.1 M $CuSO_4$ + 0.6% H_2SO_4 solution

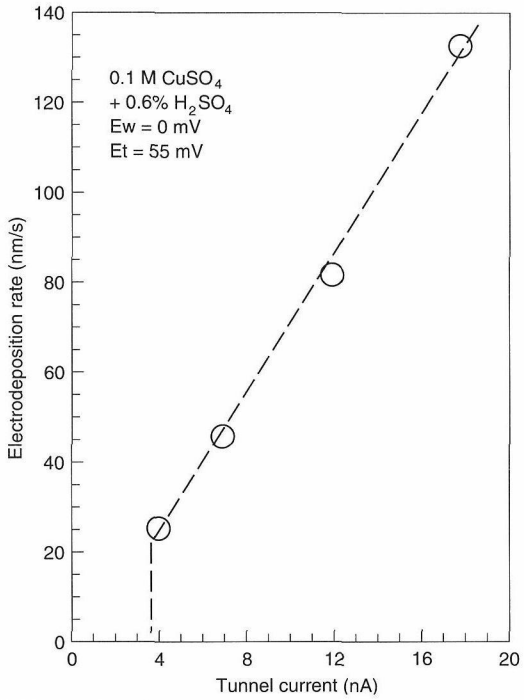

Fig. 2 Effect of tunnel current on electrodeposition rate of copper on gold electrode.

Future Work

We have found very interesting phenomenon related to tunnel current. This phenomenon can be applied for nano-processing. Further study is necessary to understand this mechanism.

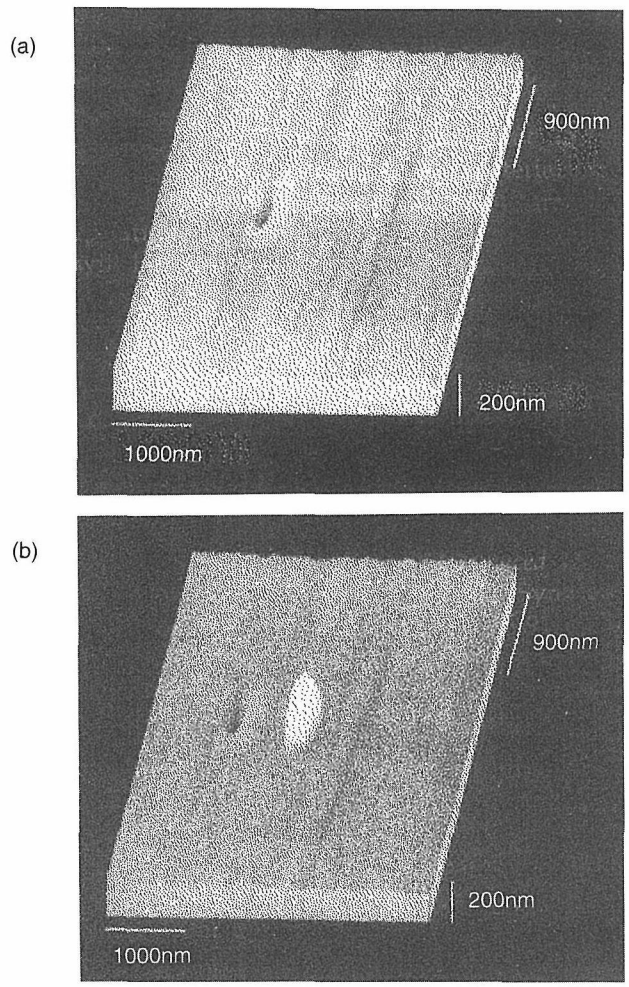

Fig. 3 STM image of gold electrode. (a) before test, (b) after test.

References

1. *Study on Micro-Corrosion Mechanism for Low Alloy Steel by Scanning Tunneling Microscope*, H. Masuda, N. Nagashima and S. Matsuoka, Zairyo-to-Kankyo 40 (1991): 754–59.
2. *In-Situ Observation on Metal Surfaces in Aqueous Solutions with an Electrochemical STM*, H. Masuda, N. Nagashima and S. Matsuoka, Trans. Japan Soc. Mech. Eng. 57A (1991): 328–35.
3. *Scanning Tunneling Microscope for Electrochemistry—A New Concept for the In-Situ Scanning Tunneling Microscope in Electrolyte Solutions*, K. Itaya and E. Tomita, Surface Science 1.2 (1988): L507–12.

❒ Atmospheric Corrosion Tests in South East Asia under Japan–ASEAN Cooperation in Science and Technology

T. Kodama, Environmental Performance Division

Keywords: atmospheric corrosion, international cooperation, surface coatings

In May 1983 the ex-Japanese Prime Minister Mr. Y. Nakasone proposed a cooperation program on science and technology during his visit to the countries of Association of Southeast Asian Nations (ASEAN). The objective of this program is to strengthen the basis of the science and technology in ASEAN countries and to share scientific achievement through cooperative research works. As for materials science, it is proposed that six projects be implemented at six individual ASEAN countries receiving financial support through Japan International Cooperation Agency (JICA). Among six projects of the program, four projects are related more or less to corrosion of metals indicating that concern of these countries in materials science is focused more on the materials evaluation and preservation than the production technology or new materials development. Seemingly, high temperature, high humidity and strong ultraviolet light in the tropics may affect metallic corrosion and polymer deterioration. However, corrosion data in this region are lacking in the corrosion atlas despite the needs for this kind of data in industries and governments of world's most rapidly progressing region. It is also feasible to evaluate the performance and corrosivity of materials in connection with global environmental pollution.

Although the main target of the program existed in cooperation on science and technology, it also had an aspect of official development assistance (ODA). One of the most important activities in this line was the donation of experimental equipment and facilities through JICA to the participating research institutes in ASEAN countries. JICA also assisted in human exchange program by dispatching technical experts to counterpart countries and accepting engineers and researchers to Japan as technical trainees.

Several national research institutes in Japan were assigned as counterpart agencies in individual projects for scientific and technical support. National Research Institute for Metals (NRIM) has been assigned as a supporting agency to the Philippine and Thai projects on atmospheric corrosion which are carried out at Industrial Technological Development Institute (ITDI) of Department of Science and Technology (DOST) of the Philippines, and Thailand Institute for Scientific and Technological Research (TISTR) of Ministry of Science, Technology and Environment (MOSTE) of Thailand, respectively. These two projects had common objectives and methodology in experiments although there existed slight difference in the selection of materials tested; more emphasis was placed on metallic coating in the Philippine team and on organic coatings in Thai team.

In parallel with the outdoor and related activities, laboratory corrosion tests using acceleration corrosion testers and electrochemical instruments have been carried out by local staffs at ITDI and TISTR. NRIM has offered training program in the field of electrochemistry, acceleration corrosion testing, instrumental and chemical analyses, and data analysis for the ASEAN counterparts.

Atmospheric Corrosion Studies in the Philippines and Thailand

The purpose of atmospheric corrosion tests is to express corrosivity of metals in tropical atmosphere as a function of time, meteorological factors and air pollutants. The methodology and materials selection for the corrosion of metals are the similar to those adopted by International Standard Organization (ISO). Materials selected for atmospheric exposure are shown in table 1. Exposure samples used are mostly common for both in Philippine and Thai projects.

Atmospheric exposure testing sites are selected from places which are characterized by 1) rural 2) urban 3) industrial and 4) marine environments. Most of sites selected are located within metropolitan Manila and Bangkok area except for one site in Northern Thailand (Chiang Mai). Exposed samples are retrieved at intervals of half, one, two, four and five years and are subjected to evaluation for corrosion loss or deterioration of coating . The effect of seasonal trend in corrosion was tested. Corrosion products analyses were carried out at the counterpart institutes using various instruments donated by JICA, or at NRIM as a part of training. At above exposure sites, also exposed were pollu-

Table 1 Materials for atmospheric exposure

Bare Metals	Carbon Steel, Cu, Zn, Al, Type 304 and 430 Stainless Steels
Metallic Coatings on Steel	Zn (Hot-dip and electric), Al, 5% Al-Zn and 55% Al-Zn
Organic Coatings on Steel	Epoxy, Polyurethane, Synthetic Rubber, Zn-rich Paint

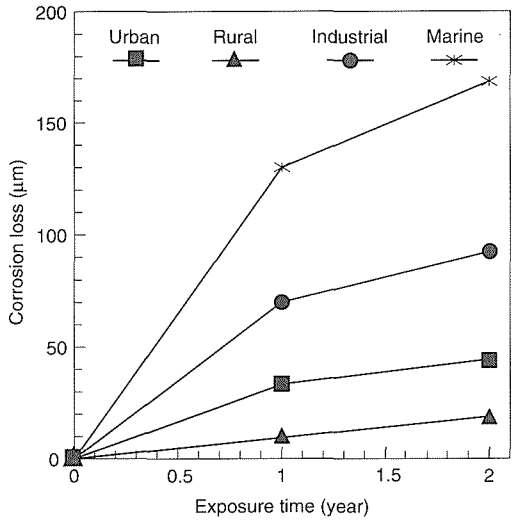

Fig. 1 Atmospheric corrosion loss of carbon steel at four exposure sites in Thailand expressed as a function of time.

tant collectors for sulfur dioxide, NOx or air-born salinity, which were subjected to chemical analyses at constant intervals.

Exposure tests started from 1988 as a five-year program. Although the tests are still running in both countries, some preliminary results are presented here. Figure 1 shows corrosion loss of carbon steel at four exposure sites in Thailand. Corrosion kinetics follow approximately in the form $M = kt^N$, where t is time and k and N are constants. The value of N ranged from 0.5 to 0.8, where N can be regarded as a parameter of the protectiveness of corrosion product (the smaller the more protective).

Figure 2 shows the corrosion rate of carbon steel expressed μm/year as a function of distance of exposure racks from shoreline. The data were obtained at Hua Hin, marine environment in Thailand. Corrosion decreases drastically with distance from shoreline and at a point 150 m apart, corrosion rate is of the same level as that of world average value. The similar trend of corrosion behavior was observed for zinc but was not distinct for copper.

Figure 3 shows the correlation between corrosion rate of carbon steel and zinc. Thailand corrosion data (indicated by square symbol) are overlapped over world wide corrosion data by ISO (49 exposure sites). It is concluded from this figure that the corrosion rate of steel is roughly 20 times as high as that of zinc. Except for one extreme data at marine environment in Thailand, corrosion rate in the tropics is not very high. The extreme data, indicated by an arrow in figure 3, was due to the proximity of exposure site to shoreline rather than tropical climate.

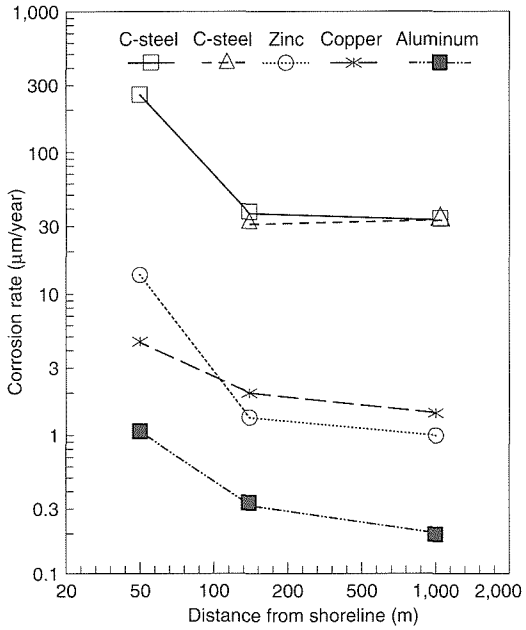

Fig. 2 Atmospheric corrosion rate of carbon steel as a function of distance from sea shoreline at Hua Hin, Thailand.

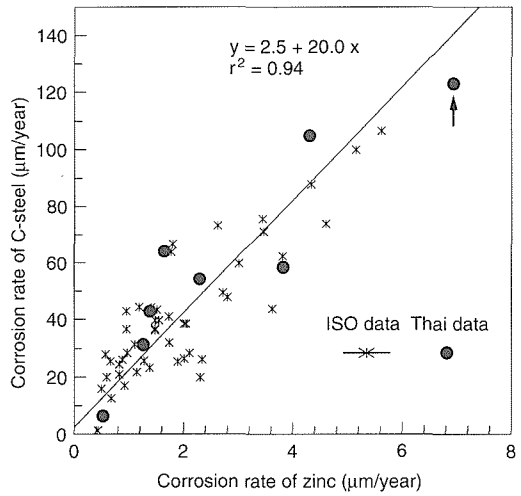

Fig. 3 Correlation between corrosion rate of carbon steel and zinc. Closed circles indicate Thai exposure data and asterisks show world wide data obtained by ISO.

Conclusion

A brief introduction of Japan–ASEAN Cooperative Program on Materials Science and Technology has been given with special emphasis on the Philippine and Thai projects on atmospheric corrosion. The Program was unique in the sense that it provides both cooperative research activities and economic and technical assistance. It is expected that the program will contribute to the foundation of corrosion research nucleus in respective countries and the fruits obtained by the project may provide new data corrosion in the tropics.

❒ Inherent Creep Strength Concept

K. Kimura, H. Kushima, K. Yagi and C. Tanaka, Environmental Performance Division*

Keywords: long-term creep strength, carbon steel, ferritic heat resistant steel, solid solution strengthening, inherent creep strength

Long-term creep strength is a fundamental and important property of metallic materials used for high temperature applications. Accurate assessment of long-term creep strength is required to design and maintain a reliability of high temperature apparatus such as power-generating plant. Inherent creep strength[1-3] is a new concept on creep property and useful idea to understand the mechanisms of long-term creep strength.

Inherent Creep Strength

Creep strength can be improved by addition of alloying elements and by controlling a morphology of microstructure through various effects such as precipitation strengthening, solid solution strengthening and work hardening. Since microstructure is unstable at the elevated temperature, however, creep strength decreases with increase in exposed time to high temperature. After long-term exposure at the elevated temperature, creep strength decreases to strength level of matrix, because microstructure is fully tempered or annealed and the strengthening effects correlated with morphology of microstructure such as precipitation strengthening has been lost. Consequently, creep strength of matrix itself is an important property which governs the long-term creep strength and we have named that as "Inherent Creep Strength."

Schematic illustrations concerning on the effects of decrease in creep strength and existence of inherent creep strength on long-term creep rupture property are shown in figure 1. Decrease in creep strength due to microstructural change makes stress vs. time to rupture curve steeply. In the long-term region, however, a slope of the curve decreases because of the advent of inherent creep strength. It is possible to assess long-term creep strength accurately from a viewpoint of inherent creep strength.

Effect of Solid Solution Strengthening on Inherent Creep Strength

A large scatter of the creep rupture strength is observed for the multi-heats of carbon steels (JIS STB 410: CAA–CAN) as shown in figure 2, and is caused by heat-to-heat variations of the inherent creep strength. Differences in the inherent creep strength are resulted from differences in Mo content from 0.005 to 0.019 mass% which is an effective element for solid solution strengthening. Drastic improvement of inherent creep strength by the addition of slight amounts of Mo to carbon steel is speculated and illustrated in figure 2. Carbon is also considered to be an effective element for improving inherent creep strength. Consequently, solid solution strengthening is a significant factor which governs inherent creep strength, since it strengthens matrix itself independent of the morphology of microstructure.

Inherent Creep Strength of Ferritic Heat Resistant Steels

10^5h creep rupture strength of the 10 different types of ferritic heat resistant steels are plotted against temperature and shown in figure 3. Inherent creep strength of the carbon steels with and without a slight amounts of Mo are also illustrated in the same figure. Although the logarithms of inherent creep strength of carbon steels decrease linearly with increase in temperature, solid solution strengthening due to a slight amounts of Mo

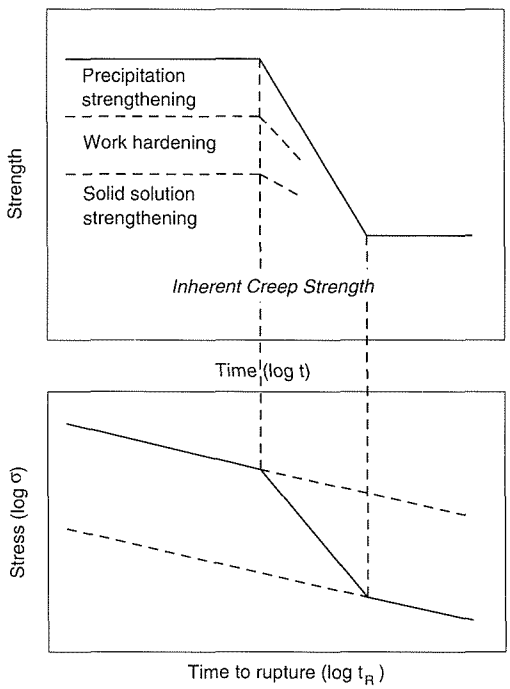

Fig. 1 Schematic illustrations concerning on the effects of changes in creep strength on long-term creep rupture property.

*Materials Design Division

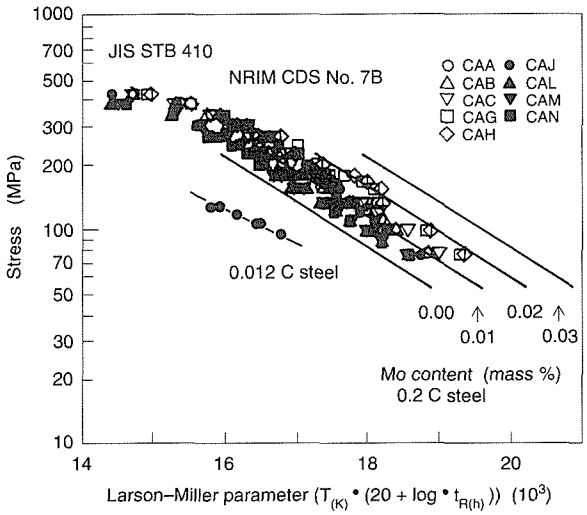

Fig. 2 Creep rupture properties of carbon steels with the evaluated inherent creep strength for carbon steels containing several amounts of Mo.

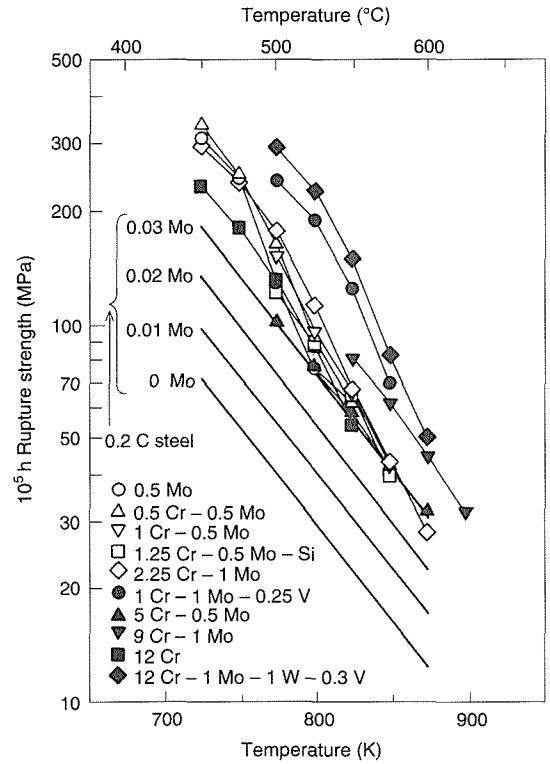

Fig. 3 10^5h creep rupture strength properties for 10 types of ferritic heat resistant steels including the evaluated inherent creep strength for carbon steels.

is effective independent of temperature. At the lower temperature, rupture strength of heat resistant steels are higher than that of 0.2C-0.03Mo steel and varies considerably from steel to steel. With increase in temperature, however, a scattering of the rupture strength decreases and rupture strength of most of the heat resistant steels except for 1Cr-1Mo-0.25V, 9Cr-1Mo and 12Cr-1Mo-1W-0.3V steels, converge to the same level as that of 0.2C-0.03Mo steel. Inherent creep strength of those heat resistant steels are evaluated to be almost the same as that of 0.2C-0.03Mo steel regardless of the short-term creep strength.

The concept of inherent creep strength is expected to make clear the mechanisms of long-term creep strength.

References

1. *Fundamental Properties of Long-term Creep Strength for Ferritic Heat Resistant Steels*, K. Kimura, H. Kushima, K. Yagi and C. Tanaka, Tetsu-to-Hagané (J. Iron Steel Inst. Japan) 77 (1991): 667–74 (in Japanese).
2. *Inherent Creep Strength for Ferritic Heat Resistant Steels*, K. Kimura, H. Kushima, K. Yagi and C. Tanaka, Proc. 5th Int. Conf. Creep and Fracture of Eng. Mater. and Structures (1993): 555–64.
3. *Fundamental Aspects of Inherent Creep Strength for Ferritic Steels*, K. Kimura, H. Kushima, K. Yagi and C. Tanaka, Proc. 7th JIM Int. Symp. (JIMIS) on Aspects of High Temperature Deformation and Fracture in Crystalline Materials (1993): 309–16.

❒ Shape Memory Thin Film of Ti-Ni Formed by Sputtering

A. Ishida and A. Takei, 3rd Research Team

Keywords: micromachine, shape memory, Ti-Ni, sputtering

Shape Memory Thin Films as Microactuators

Micromachines such as micromanipulators and fluid microvalves are expected to be used in the near future in various fields such as biotechnology, medicine and the semiconductor industry. In order to produce such a micromachine, the development of an effective microactuator is essential. The driving force of a microactuator can be obtained using various physical phenomena such as piezoelectric effect, electrostatic force and so on. Among them, the shape memory effect of Ti-Ni alloys seems to have attractive characteristics for a microactuator. They demonstrate large transformation strain and stress by heating and cooling and can also produce complicated motion by themselves. Therefore thin films of Ti-Ni are a promising candidate for a microactuator. In this study we demonstrate the promising properties of Ti-Ni thin films as microactuators by quantitative measurement of their shape memory effect.

Preparation of Ti-Ni Thin Films

Thin films of Ti-Ni were prepared by sputtering. The thin films were deposited on glasses in a 5 in r.f. magnetron sputtering apparatus using a Ti-50.0at.%Ni target. The substrate temperature, r.f. power and Ar gas pressure were kept at 523 K, 400 W and 0.67 Pa respectively[1]. The film thickness was in the range of 8 to 15 μm.

The thin films were removed from the glasses after the sputtering and then heat treated for 30 min at 973 K to produce crystallization of the Ti-Ni, homogenization of composition and relaxation of the stress induced during film deposition. Subsequently, some of the annealed specimens were aged for 1 h at 773 K to produce distribution of fine Ti_3Ni_4 particles.

Martensitic Transformation of Ti-Ni Thin Films

The martensitic transformation of the thin films was confirmed by differential scanning calorimetry (DSC) and x-ray diffraction. Figures 1(a) and 1(b) show the DSC results of thin films of Ti-50.4at.%Ni and Ti-51.4at.%Ni respectively. The thin film of Ti-50.4at.%Ni was prepared by placing Ti plates on the Ti-50.0at.%Ni target. The film of Ti-51.4at.%Ni was aged for 1 h at 773 K after annealing at 973 K to produce a dispersion of fine Ti_3Ni_4 particles in a matrix of Ti-Ni. In figure 1(a), two peaks can be observed. X-ray diffraction showed that the high temperature phase was B2 structure and the low temperature phase a monoclinic structure. Therefore the peak (M*) on cooling is related to transformation from the parent phase to the martensite. The other peak (A*) on heating is related to the reverse martensitic transformation. In figure 1(b), in addition to the above peaks, two other small peaks can be detected at higher temperatures than the martensite-related peaks. They seem to be related to R phase (R*) and reverse R phase (R'*) transformations.

Shape Memory Effect of Ti-Ni Thin Films

The shape memory effect was measured quanti-

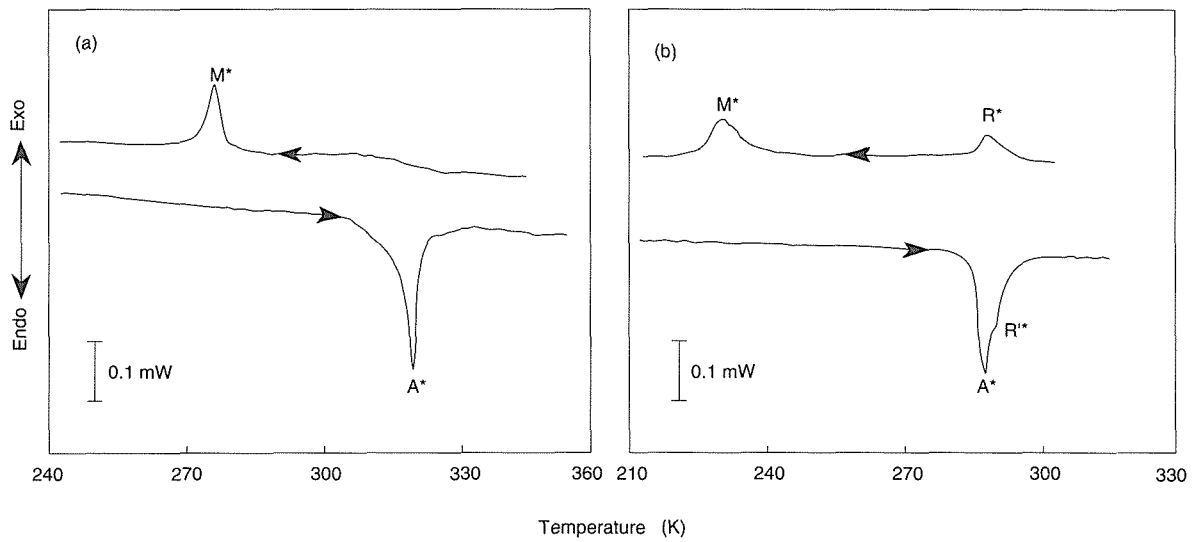

Fig. 1 DSC curves for thin films of (a) Ti-50.4at.%Ni after annealing at 973 K for 30 min and (b) Ti-51.4at.%Ni after a solution treatment at 973 K for 30 min followed by aging at 773 K for 1 h.

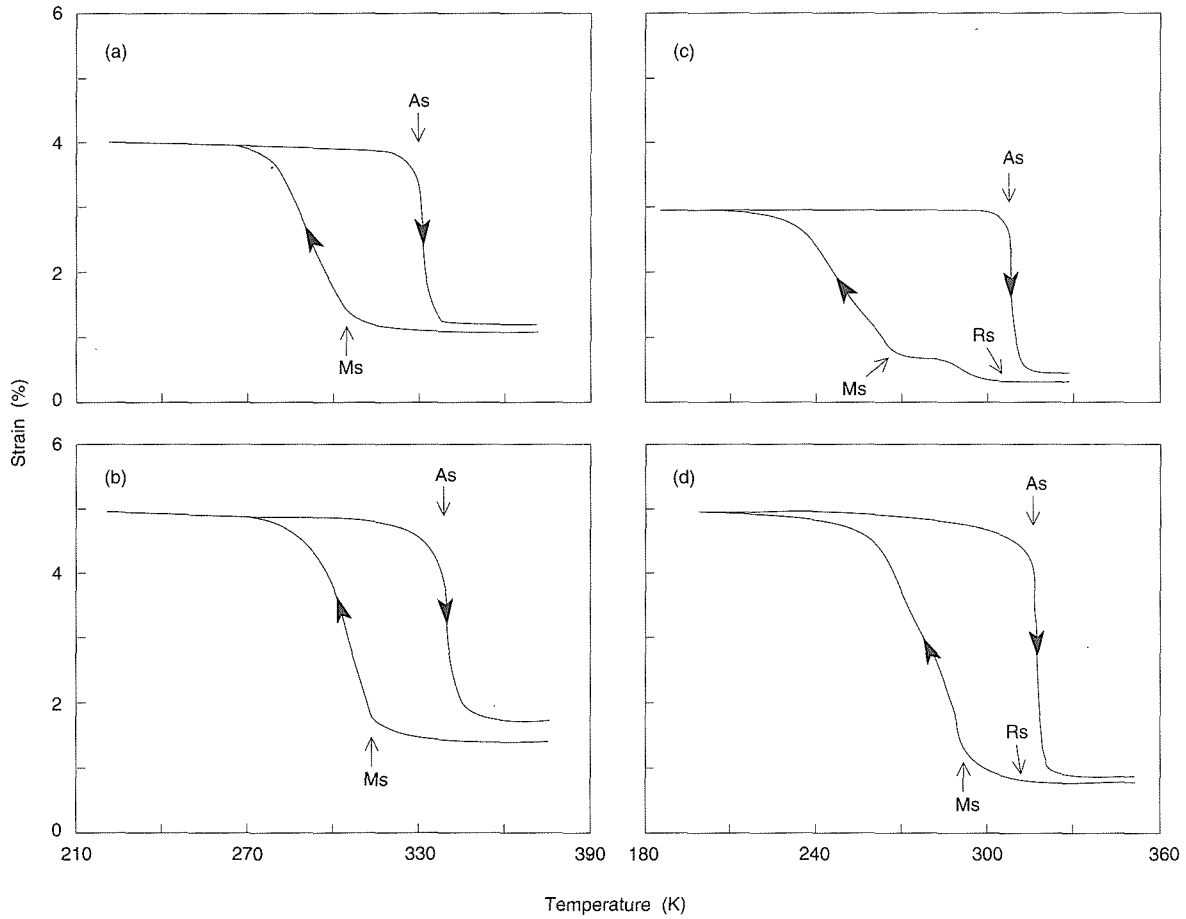

Fig. 2 Strain vs. temperature curves at constant loads of (a) 182 MPa and (b) 303 MPa for the Ti-50.4at.%Ni thin film and at constant loads of (c) 174 MPa and (d) 313 MPa for the Ti-51.4at.%Ni thin film.

tatively by changing the sample temperature under a various constant load of up to 300 MPa. This test involved loading at 373 K, cooling to 173 K at a rate of –10 K min^{-1} and heating to 373 K at a rate of 10 K min^{-1}. The sample size was 1 mm × 5 mm × (8–15 μm).

Figures 2(a)–(b) show the results for the thin film of Ti-50.4at.%Ni at constant loads of (a) 182 MPa and (b) 303 MPa respectively. The strains associated with both the martensitic and the reverse martensitic transformations were observed. The transformation strain increased with increasing load and reached 3.5% under a constant stress of 303 MPa (b). The plastic strain was 0.3% for this case.

Figures 2(c)–(d) show the results of the thermal cycle tests for the thin film of Ti-51.4at.%Ni at constant loads of (c) 174 MPa and (d) 313 MPa respectively. The strain related to the the R phase transformation was detected in addition to that related to martensitic transformation. These strains were recovered by the reverse transformations. The plastic strain was 0.1% for a constant stress of 313 MPa (f) and thus reduced compared with that of the 50.4at.%Ni thin film. This improvement can be attributed to precipitation strengthening with fine Ti_3Ni_4 particles formed by aging at 773 K.

The shape memory behavior mentioned above was almost comparable with that of bulk TiNi and it was found that the perfect shape memory effect can be obtained even in Ti-Ni thin films formed by sputtering. Further work on development of these shape memory thin films already started in 1993 and will last for a period of 5 years as will be mentioned in the different section, "Research in Progress 1990–91," of this journal.

Acknowledgement

This research was performed in collaboration with Dr. Miyazaki in Tsukuba University.

Reference

1. *Shape Memory Thin Film of Ti-Ni Formed by Sputtering*, A. Ishida, A. Takei and S. Miyazaki, Thin Solid Films 228 (1993): 210.

❐ Computerized Materials Data Evaluation Results of a VAMAS Round-Robin

Y. Monma, 5th Research Group

Keywords: creep, fatigue, database, data evaluation

When we build a factual materials database, one of the major considerations is how to implement the data evaluation methods and models for the retrieved data. Because we are more interested in properly evaluated results typically in tables and graphs than the numerical values of the raw data points. The comparison of the application of empirical and/or theoretical methods/models to the relevant data set is a procedure often taken during the data evaluation using a materials data system.

The objectives of the VAMAS (Versailles Project on Advanced Materials and Standards) TWA (Technical Working Area) 10 Materials databanks are correlated with the activities of international collaboration on the computerization of materials property information. As a project of the VAMAS TWA 10 in 1988–90, which was chaired by H. Kröckel of the CEC Joint Research Centre at Petten (The Netherlands) and J. Rumble of the NIST (USA), an interlaboratory comparison of data evaluation methods for creep and fatigue data of typical engineering steels and alloys was conducted with the cooperation of fifteen experts from five countries. The purpose of the round-robin work was to examine various problems of the procedures of the data analysis in computational modeling of materials strength[1].

Materials Property Data Distributed

From the early stage of computerization of materials property data, creep and fatigue data have been stored in many data processing systems worldwide. It is well recognized that there are at least several models commonly used for evaluation of creep and fatigue data. In July 1988 we distributed small amount of materials strength data from the NRIM Creep and Fatigue Data Sheets to about twenty experts who expressed their interest to join the round-robin. The raw, numerical data was listed in ASCII text format on a MS-DOS floppy disk. The materials included are carbon steel, low alloy steel, austenitic stainless steel and heat-resisting alloy. The material properties covered are stress-rupture, creep strain-time, high-cycle fatigue S-N, and fatigue crack growth.

Participants and Reporting

Each participant of the round-robin was asked to send back the results of data evaluation in numerical form such as the regression coefficients. Fifteen scientists/engineers from five countries submitted the results. We collected the results of eight reports for stress-rupture, five for creep strain-time, another five for high-cycle fatigue S-N, and four for fatigue crack growth. Several participants reported that they had difficulties when they transferred the data from the distributed disk to their systems. The technology of data interchange among different systems should be available to the materials community working with computerized data systems. So far no agreement on the logical format suitable to materials data interchange has been reached internationally. This adds further barrier to data import/export between computerized materials data systems.

The international activities to establish a neutral, machine-independent, standardized format for materials data interchange should be increased. The coordination of regional groups working on the issues in America, Europe and Asia is needed, preferably with joint experiments on materials data exchange through the international data communication network. Discussions on metadata, data models, and data format to be used for materials data interchange would be needed prior to such experiments.

Data Evaluation Methods/Models Used

There is a variety of analytical models for materials strength data that can be used in computerized data systems. In almost every case, the numerical values of materials data are treated statistically, or curve fitting to the model equation by use of the least squares regression procedure. Some of sophisticated models require non-linear optimization procedure such as weighted iterative computation. The selection of adequate model for the regression is a major concern in the implementation of data evaluation methods for materials strength data. One of the big issues is the choice of dependent-independent variables (X-Y or Y-X) for stress and life data. From purely statistical point of view it is obvious to assume the life as the dependent variable, but in practice we sometimes assume vice versa.

The knowledge and experience of valid data evaluation could be shared worldwide, if we build an inventory of data evaluation methods and models commonly used in computerized materials datas systems.

Comparison of Results

We developed a PC software package to plot the

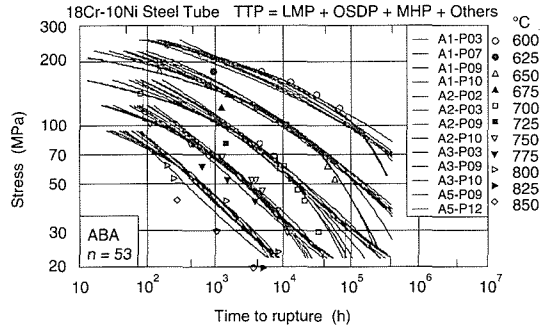

Fig. 1 Comparison of curve fitting to stress-rupture data for a heat of 304 stainless steel. A1, A2,...denote the model equation. P03, P03,...are the code for the participants.

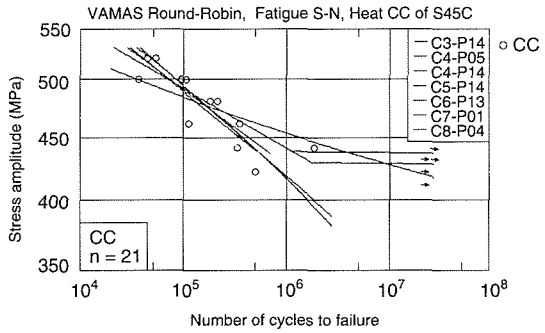

Fig. 2 Comparison of models for high-cycle fatigue S-N curves for a heat of carbon steel. C3, C4,...denote the model equation.

data and computed curves in order to reconstruct the submitted results into unified graphical formats. Figures 1 and 2 compare the results of curve fitting for stress-rupture and high-cycle fatigue, respectively. Here in figure 1, Model A1 is Larson-Miller, Model A2 is Orr-Sherby-Dorn, Model 3 is Manson-Haferd, and Model A5 is MCM (minimum commitment method). In figure 2, Model C3 is semi-log, Model C4 is log-log, Model C5 is asymptotic, Model C6 is the maximum likelihood, Model 7 is the staircase, and Model C8 is the combination of PCA (principal component analysis) and the probit method. (Note that the original graphs on CRT are in color to distinguish each model, but it is inevitable to reproduce here in monochrome. Refer to the demonstration disk attached to the VAMAS Report[2].) Generally the difference among the results by various methods is small for the "well-behaved" data set, while we find distinct curves for the "ill-natured" one. Fairly common and agreed models/methods of data evaluation are available for specific areas of materials properties such as the stress-rupture. But we found that occasionally there were considerable difference among the computed equations using nominally the same model.

A major origin of the difference in the results of computed S-N curves for a set of data, such as shown in figure 2, is how to treat the run-out (discontinued) data points. The treatments employed are classified into three groups: a) exclusion of the run-outs, b) inclusion of the run-outs as failed, and c) inclusion of the run-outs with a statistical procedure such as the probit method. Apparently the choice a) or b) is questionable, but it is a common practice. On the basis of major findings from the round-robin we proposed several recommendations, and some of them discussed above are pursued in the follow-up projects of VAMAS TWA 10.

References

1. *Significance of Data Evaluation Models in Materials Databases*, S. Nishijima, Y. Monma and K. Kanazawa, VAMAS Technical Report 6 (1990).
2. *Computational Models for Creep and Fatigue Data Analysis*, Y. Monma, K. Kanazawa and S. Nishijima, VAMAS Technical Report 7 (1990).

❒ Titanium-Based Metal Matrix Composites Reinforced with Ceramic Particulates

M. Hagiwara, Mechanical Properties Division

Keywords: titanium, mechanical properties, blended elemental powder metallurgy, particulate composite

Introduction

Titanium alloys are attractive materials for aircraft and automobile applications due to their high strength/weight ratio. However, the service temperature is limited to 600 °C due to a degradation of tensile strength, creep resistance and environmental resistance. Moreover, titanium alloys exhibit lower stiffness and poorer abrasion-related properties than nickel-based alloys.

The incorporation of relatively large-sized ceramic particulates into titanium matrices is expected to overcome these drawbacks. However, mechanical property data available for this type of composites are still lacking. Particularly, comparison with the matrix alloys have received relatively little attention.

In the present study, an attempt was made to produce titanium-based composites reinforced with TiB or TiC particulates using blended elemental (BE) powder metallurgy (P/M) route. The tensile, creep and smooth axial high cycle fatigue tests were done on the composites and the matrix alloys with emphasis on relating microstructure to these mechanical properties.

Microstructure and Mechanical Properties

Three kinds of composites, i.e., Ti-5Al-2.5Fe/15wt%TiB, Ti-5Al-13Cr/10TiC and Ti-6Al-2Sn-4Zr-2Mo/10TiB, were produced using proprietary blended elementals processing techniques, whereby FeB, Cr_3C_2 and TiB_2 were used as starting ceramic powder material to form TiB or TiC *in situ* in the matrix during the sintering step. The composites produced by this "internal reaction" technique are said to have three main advantages, i.e., more random dispersion of particulates, excellent bonding at the particulate/matrix interface and the lack of macroscopic flaws within the particulates, over those produced by the conventional "simple blending" technique[1].

The microstructures of matrix alloy and the composites are shown in figure 1. It is seen that the globular-shaped TiC particulates are dispersed reasonable randomly in the matrix. Microstructure differs significantly between the matrix alloy and composites, with the diameter of prior β grain (figure 1a) being markedly smaller in the composites. It seems that these dimensions are limited by the particulate spacing. No obvious interaction zone is visible in these three composites at the resolution available in optical and scanning microscopy.

The Ti-5Al-2.5Fe/15TiB composites achieved remarkably higher elastic modulus at room temperature, 151 GPa, 32 percent higher than that of an unreinforced Ti-6Al-4V, 114 GPa.

The ultimate tensile strength for Ti-5Al-2.5Fe/15TiB composites were superior to that of the matrix alloy in the whole temperature range examined, as shown in figure 2. Irrespective of the test temperatures, the tensile fracture initiated from the cracking within the particulate reinforcements. This may be indicative of excellent bonding at the interface. Ductility of composites was significantly lower than that of the matrix alloy. At room temperature, both Ti-5Al-2.5Fe/15TiB and Ti-5Al-

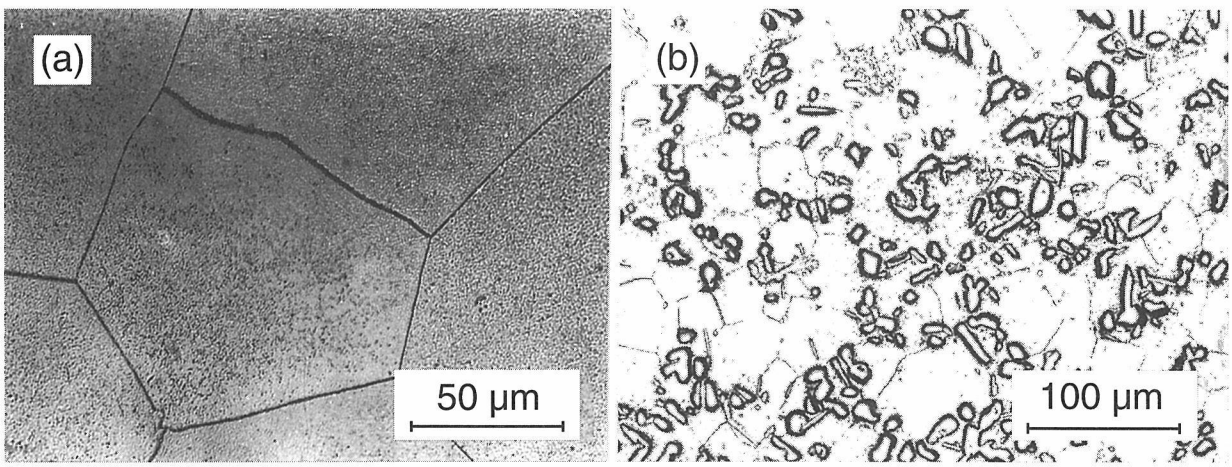

Fig. 1 Microstructures of (a) BE P/M Ti-5Al-13Cr matrix alloy and (b) TiC-reinforced composites.

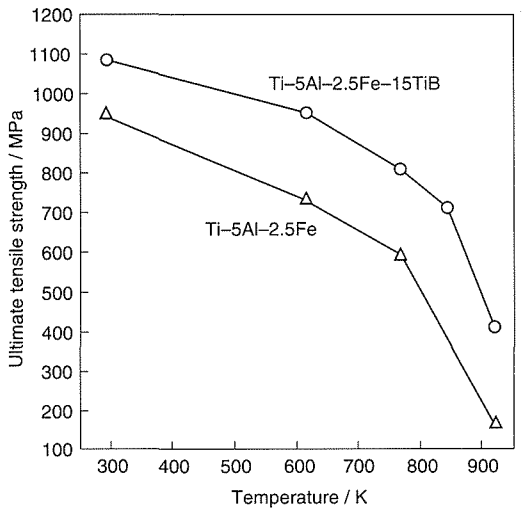

Fig. 2 Temperature dependence of UTS of BE P/M Ti-5Al-2.5Fe matrix alloy and TiB-reinforced composites.

13Cr/10TiC composites failed in a brittle manner before the ultimate tensile strength was achieved.

TiC-reinforced Ti-5Al-Cr based composites were creep tested at 923 K (650 °C), as shown in figure 3. It is seen that the dispersion of ceramic particulates provides superior creep properties when compared to those of the unreinforced matrix alloy.

High cycle fatigue data for Ti-6Al-2Sn-4Zr-2Mo/10TiB composites together with fatigue data for matrix alloy are shown in figure 4. It is seen that the composites result in a considerably higher fatigue strength especially in the high cycle range with very little scatter in test data, compared to those for the unreinforced matrix alloy. The lower fatigue strength observed in the low cycle range may be attributed to the poor ductility of these composites. The SEM examination of the fracture surfaces revealed that fatigue crack initiation is associated with the colony microstructure of matrix alloy.

These observations again demonstrate that the sufficient load transfer from the matrix alloy to the particulate reinforcements was achieved in the present composites.

Conclusion

The uniform dispersion of relatively large-sized ceramic particulates which have superior high temperature properties relative to the matrix alloy was found to be an effective method for improving properties such as elastic modulus, tensile and creep strength and high cycle fatigue properties of conventional titanium alloys. The property enhancement may be caused by the sufficient load transfer from the matrix alloy to the particulate reinforcements.

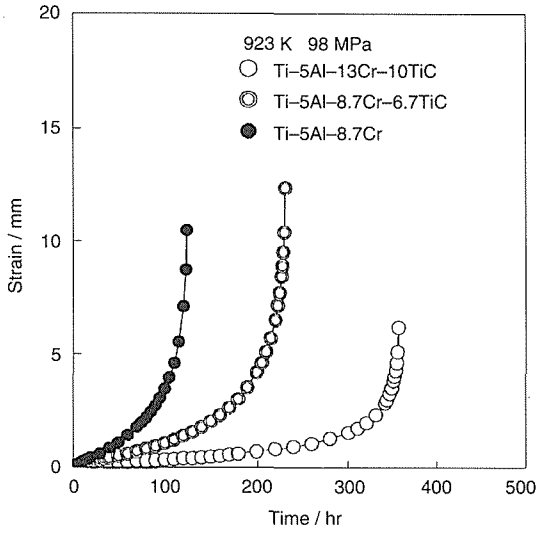

Fig. 3 Creep curves of BE P/M Ti-5Al-9Cr matrix alloy and TiC-reinforced composites.

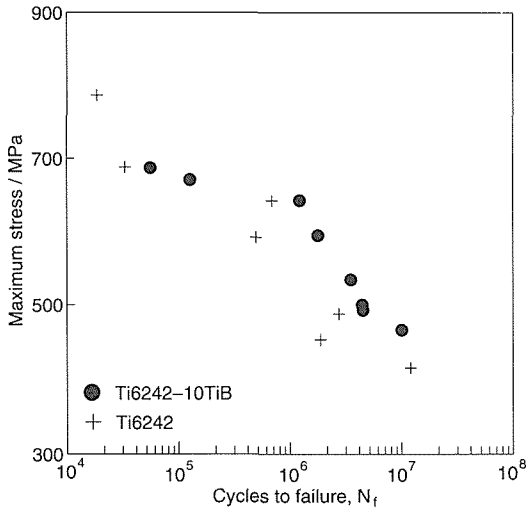

Fig. 4 Smooth axial fatigue data for BE P/M Ti-6Al-2Sn-4Zr-2Mo matrix alloy and TiB-reinforced composites.

More uniform dispersion and further refinement of the particulates through fabrication modifications such as the use of much smaller starting powder materials may lead to additional improvement in the mechanical properties of these P/M-processed composites.

Reference

1. *Mechanical Properties of Particulate Reinforced Titanium-Based Metal Matrix Composites Produced by the Blended Elemental P/M Route,* M. Hagiwara, S. Emura, Y. Kawabe, N. Arimoto and H.G. Suzuki, ISIJ Int. 32 (1992): 902–16.

❒ Fabrication of 300 Å Thick BiSrCaCuO Thin Films with T_c of 108 K

K. Saito, Surface and Interface Division

Keywords: BiSrCaCuo, thin films, Ar ions, low-energy cascade

From both scientific and technological points of view, it is significant to study how the superconducting transition temperature, T_c, or the critical current density, J_c, changes with the thickness of the film substance, and to investigate whether a minimum thickness for superconducting states exists or not. In the case of new high-T_c superconductors there has been a physical fact that T_c decreases with decreasing film thickness. It has been experimentally difficult to obtain high-T_c thin films of thicknesses below several tens of nanometers.

In this report we describe the synthesis of high-T_c (108 K) BiSrCaCuO thin films of 300 Å thickness by a combined use of sputter deposition and ion implantation techniques[1–5]. The film thickness of 300 Å corresponds to about a ten-unit-cell length of the Bi system.

Figure 1 shows a typical example of the resistivity-temperature curves obtained for 300-Å-thick films. After an Ar ion dose of 1×10^{12} ions/cm^2 at 10 K, the T_c of the films in the 90 K range decreased by about 5 ~ 9 K and increased to 108 K by postannealing at 730 °C. The low-temperature irradiation was necessary to reduce to a minimum undesirable chemical reactions and compositional changes during the ion bombardment. In this way, the T_c value of our 300-Å-thick films reached the maximum value so far observed in this system. The X-ray diffraction pattern showed that the thin film consists of 90% high-T_c phase and 10% low-T_c phase material. The result of magnetization measurements in a magnetic field of 100 Oe by a SQUID magnetometer is shown in figure 2, exhibiting a clear transition around 108 K in the zero-field-cooled and the field-cooled curves. J_c values of 10^3 ~ 10^4 A/cm^2 were obtained by a transport method in zero field at 77 K. J_c is found to be approximately proportional to $(1\text{-}T/T_c)^{1.34}$ in the temperature range of 70 ~ 100 K. Our thin films may contain weak links between the thin crystals or in grain boundaries, such as superconductor/insulator or normal metal/superconductor (SIS or SNS) junctions.

As the Ar ion dose was increased to 1×10^{13} ions/cm^2, the resistivity of the thin films increased markedly and exhibited a transition from metallic to semiconducting behavior. At the highest dose of 1×10^{14} ions/cm^2, the films became almost insulating. It was found that these heavily damaged samples were not fully recovered, and the T_c became lower than 70 K even after postannealing.

Figure 3 represents a SEM image of the film surface, revealing a directional array of thin crystals with very fine steps, resembling fish scales. The size of individual thin crystal grains exceeds 10 μm. It is interesting to note in figure 3 that needle-shaped precipitates, probably due to impurity phases, form along two well-defined crystallographic directions. This indicates that both of the a- and b-axes of the thin crystals are uniquely oriented over a wide area of the thin crystal arrays.

Now, we consider the role of Ar ions in terms of nuclear atomic collision. Table 1 lists calculated values of several important collision parameters for primary knock-on atoms in this system[6]. In our case almost all the 100 keV Ar ions are considered to pass through the 300-Å-thick thin films. It is shown that 100 keV Ar ions produce primary knock-on atoms (PKAs) with an average transferred energy T of the order of 1 keV. For such low-energy collision regime, atomic collision events approach the hard-sphere collision approximation, and the energy transfer becomes maximum for the case of equal masses of colliding

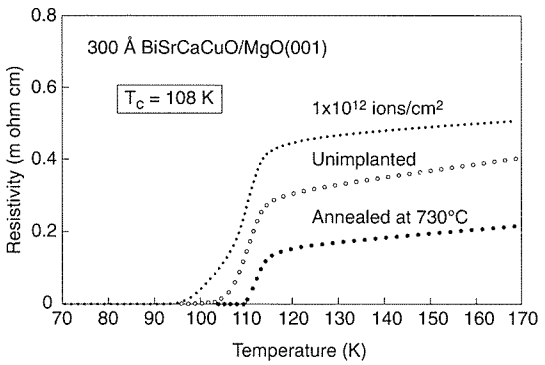

Fig. 1 Resistivity-temperature curves of 300-Å thick BiSrCaCuO system films, (a) before, (b) after irradiation with 100 keV Ar ions to 1×10^{12} ions/cm^2 at 10 K and (c) finally annealed at 730 °C for 0.5 h.

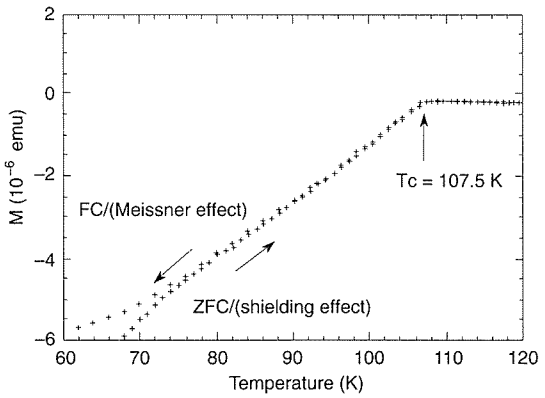

Fig. 2 Temperature dependence of magnetization for a 300-Å-thick sample.

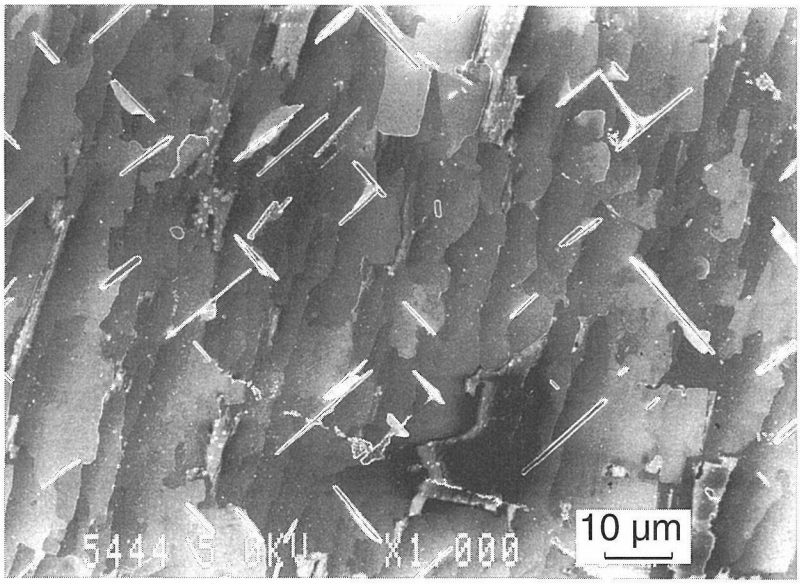

Fig. 3 SEM image of the film surface of a 300-Å-thick film.

Table 1 Calculated values of the nuclear stopping S_n, the displacement cross section σ_d, the average transferred energy T, the nuclear energy loss $(dE/dx)_n$, the electronic energy loss $(dE/dx)_e$, the mean ion range R_p and the straggling ΔR_p, respectively.

PKAs	S_n (eV*Å^2)	σ_d (Å^2)	T (eV)	$(dE/dx)_n$ (eV/Å)	$(dE/dx)_e$ (eV/Å)	R_p (Å)	ΔR_p (Å)
Bi	1515	1.002	1512	86.09	5.77	15.0	4.6
Sr	1407	0.850	1655	71.94	5.99	18.4	7.2
Ca	1178	0.748	1574	45.52	5.66	20.5	11.3
Cu	1323	0.805	1643	61.51	5.91	18.5	8.7
O	655	0.541	1210	16.72	3.92	26.2	20.8

atoms. Consequently, each PKA displaces self-atoms preferentially and forms individual cascades of specific volumes and specific defect densities. It should be noted that the mean ranges of all PKAs do not exceed the unit cell length, and thus almost all of the recoils remain within the unit cell. In this way, each PKA produces atomic displacement, mixing and shuffling on a microscopic scale within the volume of each cascade. By postannealing, the partly displaced or dislocated layered structure can be reformed into a more perfect one through short-range mass transport or diffusion of displaced atoms within the unit cells.

Finally, it is important to note that the capability of lowering the annealing temperature to 730 °C in the case of the irradiated specimens is advantageous to induce high-T_c phase formation by inhibiting competitive growth of the low-T_c phase.

References

1. *Fabrication of 300 Å Thick BiSrCaCuO Thin Films with T_c of 108 K by Use of Ion Implantation*, K. Saito and M. Kaise, Jpn. J. Appl. Phys. 31 (1992): L1047–50.
2. *Fabrication of 30 nm Thick Superconducting BiSrCaCuO Thin Films by Single-Target Magnetron Sputtering Method*, M. Kaise and K. Saito, J. Jap. Inst. Met. 57 (1993): 103–07 (in Japanese).
3. *Displacement Damage Effects and Related Phase Changes of Ar-Ion-Irradiated BiSrCaCuO System Superconducting Thin Films*, K. Saito and M. Kaise, Jpn. J. Appl. Phys. 31 (1992): 3533–38.
4. *Thermal Spike and Displacement Damage Effects in BiSrCaCuO Thin Films by Ar Ion Beams*, K. Saito and M. Kaise, Jpn. J. Appl. Phys. 31 (1992): 3539–45.
5. *Structural Changes and Annealing Behavior of Ar-Ion-Irradiated Superconducting BiSrCaCuO Thin Films*, M. Kaise and K. Saito, Jpn. J. Appl. Phys. 32 (1993): 942–48.
6. *The Stopping and Range of Ions in Solids*, J.F. Ziegler, J.P. Biersack and U. Littmark, ed. J.F. Ziegler, (Pergamon, New York) 1 (1987).

❒ Development of Long-Pulsed High-Field Magnets

T. Asano, Y. Sakai, M. Oshikiri, K. Inoue and H. Maeda, High Field Magnetic Research Station

Keywords: long-pulsed magnet, high magnetic field, Cu-Ag alloy wire

Introduction

Coils for a long-pulsed magnetic field have been developed at NRIM, in order to accomplish a final target to generate fields up to 80 T, in the Multi-Core Research Project on Superconductivity. A newly-developed Cu-Ag alloy wire with a 2 × 3 mm rectangular cross section, which has both high conductivity and high strength, was used to wind small multilayered coils. So far, maximum fields of 50.9 T and 62.7 T have been achieved in the magnet coils with a 20 mm inner winding diameter and a 15 mm one, respectively. However, the generation of 62.7 T resulted in destruction of the 15 mm inner diameter coil. On the other hand, we made several pulsed magnet coils of Cu-Ag wire, which were further reinforced by glass fiber winding between the coil layers. One of them generated a maximum field of 68.0 T in a 12 mm inner winding diameter.

Wire and Coil

The upper most generating magnetic field of the pulsed magnet is limited mainly by the following two parameters of coil material. The mechanical strength defines the upper limit of the stress generated by the Lorentz force and the conductivity determines the power which needs to generate the pulsed-field. So far, in Massachusetts Institute of Technology, a field of 68.4 T was obtained in a 12 mm inner winding diameter coil using Cu-Nb alloy wire with high strength and high conductivity. On the other hand, in Katholieke Universiteit Leuven, 67 T was achieved in 12 mm inner winding diameter coil with glass-fiber reinforcement between winding layers of Cu wire coil. Cu-Ag alloy wires with high conductivity and high strength, which were developed recently in NRIM[1], have advantages such as; 1) having homogeneous and reproducible properties, 2) showing high strength with relatively low reduction. Therefore in the Cu-Ag alloy wire the fabrication of a large cross sectional wire is much easier than in the Cu-Nb one. Small test coils were wound using the Cu-16at%Ag alloy wire with 2 × 3 mm rectangular cross section. The resistivities of the wire are 2.15×10^{-8} Ω.m at 300 K and 0.65×10^{-8} Ωm at 77 K. The ultimate tensile strength, the 0.2% yield strength and the elongation of the wire are achieved up to 1008 MPa, 930 MPa and 13% at 300 K, and those at 77 K are 1206 MPa, 1050 MPa and 10%, respectively. However, the strength of the Cu-Ag alloy wire wound actually into the coil was slightly reduced by annealing in order to reduce the spring-back force during the coil winding. On the wire surface, varnish was coated to adhere and seal the insulations. The wire size including the insulations was 2.35 × 3.35 mm in cross section.

The coil specifications are listed in table 1. In the coils there is no reinforcement of the winding between each layer. After winding coils vacuum impregnation of epoxy was done and cured below 393 K. Those coils were machined on its epoxy surface and then set into a support case made of stainless steel. Pulsed field generation tests were repeated with a full interval time to cool the coil down to 77 K.

Test Results

The #1 coil could generate the maximum field of 50.9 T without damage when a full power (125 kJ) of a capacitor bank charged up to the maximum voltage of 5 kV was discharged. The estimated maximum rising temperature of the conductor induced by this most powerful shot is about 300 K. This coil is still intact and being used for some experiments. In the #2 coil a smaller inner winding diameter of 15 mm was adopted for testing the bending tolerance of the conductor and for generating higher field. The maximum magnetic field of 62.7 T was generated as shown in figure 1. The estimated maximum temperature rising just after the maximum shot is more than 400 K. Without having damage due to the insulation failure this coil had experienced 7 times to generate magnetic fields exceeding 62 T and 27 times the fields above 50 T. During the operation the coil was expanded

Table 1 Coils specifications

Coil code	Winding inner diameter	α OD/ID	Coil length	Number of turns/layer	Number of layers	Bmax (T)	Tmax (msec)	Inter layer material
#1	20 mm	3.56	75	22	10	>50.7*	3.9	Epoxy
#2	15 mm	4.11	58	17.5	10	62.7	2.7	Stycast 2850FT
Mel47	12 mm	4.8	55	16	8	68.0	2.0	Epoxy

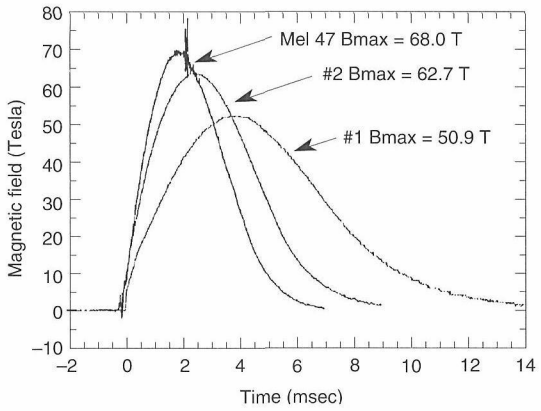

Fig. 1 Pulsed magnetic field generated by coils made of Cu-Ag alloy wire.

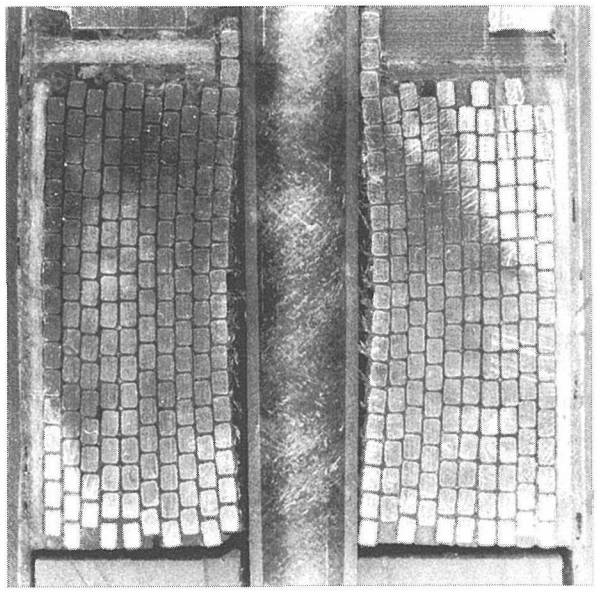

Fig. 2 The deformation of the winding coil layer observed on the sectioned #2 coil which were cut after the insulation failure.

as shown in figure 2. The inductance L of the coil began to increase gradually in the maximum field exceeding 50 T and the inductance change $\Delta L/\Delta B$ max became very large above 62 T. The insulation failure occurred between the first and the second innermost layers of the coil.

The feasibility of Cu-Ag alloy conductor for multilayered high-field long-pulsed magnet was proved in the coils without inter-layer reinforcements.

Future Plans

A long-pulsed magnet with the duration time over 20 ms may be necessary for measuring the high-field properties of metallic substances. To realize this demand, we have completed a new 1.6 MJ capacitor bank system as a current source of the long-pulsed magnet. The total capacitance of this bank is 128 mF. We are designing a large multilayered coil made of thick wire suitable for the large capacitor bank to realize a high-field long-pulsed magnet. We are now preparing a new coil winding machine as a next step to wind a thicker Cu-Ag wire into a large coil. On the other hand, the collaboration work with Katholieke Universiteit Leuven on winding this Cu-Ag alloy conductor with glass fiber reinforcement between the winding layers is also progressing. The glass fiber was wound as the reinforcement on every winding layer by controlling the tensile stress and the total winding number. We have fabricated several small pulsed coils with interlayer reinforcement, of which the test operations are being carried out now. One of them could generate a maximum field of 68 T in a 12 mm inner winding diameter[2].

References

1. *Development of High-Strength, High-Conductivity Cu-Ag Alloys for High-Field Pulsed Magnet Use*, Y. Sakai, K. Inoue, T. Asano, H. Wada and H. Maeda, Appl. Phys, Lett. 59 (1991): 2965–67.
2. *Cu-Ag Wire Pulsed Magnets With and Without Internal Reinforcements*, T. Asano, Y. Sakai, K. Inoue, H. Maeda, L.Van Bockstal, G. Heremans, L. Li and F. Herlach, to be published.

❒ Study on Vortex Dynamics in High Quality Single Crystalline High T_c Superconductors

K. Kadowaki, T. Mochiku, H. Takeya and K. Togano, 1st Research Group

Keywords: vortex dynamics, vortex pinning, single crystals

This research subject covers a broad area of fundamental material sciences of high T_c superconductors such as determination of phase relation of superconducting and non-superconducting compounds, single crystal growth, studies of electromagnetic properties including dc- and ac-resistivity, magnetic susceptibility, magnetization, high frequency conductivity and magnetic torque, and of thermal properties such as specific heat, thermal expansion, etc. Three permanent staff members and two research scientists in the second sub-group of the first research group as shown in figure 1 are currently engaged in this subject. Experimental facilities involved in this research are various kinds of furnaces for the heat treatment and synthesis of materials, especially the infrared mirror furnace with two halogen lamps as a heat source being used for single crystal growth of high T_c superconductors, high precision resistivity measurement facilities with horizontal fields up to 6 T being capable of measuring two axes high resolution angular dependence, an ac- and dc- magnetometer in fields up to 7 T, a high precision torque magnetometers, a SQUID magnetometer, and various kinds of analytic facilities.

Among a great deal of work carried out in the program, particular interest has been raised in the nature of the superconducting state in magnetic fields. Undoubtedly, one of fascinating and remarkable properties of superconductors is a superflow of gigantic electrical currents without resistance. In conventional superconductors the fundamental understanding of this phenomenon has been thought to be established thoroughly by the BCS (Bardeen, Cooper and Schrieffer) theory together with the idea of flux pinning mechanism of the vortex line that was just introduced by Abrikosov as a new-born concept more than 35 years ago. Since then, all properties related to the vortex state have been believed to be well understood by the static and/or dynamic nature of the vortex lines in a superconductor.

Recently, the resistivity in a superconductor in magnetic field has become a highly intriguing subject in physics, as to whether the dissipation associated with the supercurrent flow is originated by the conventional mechanism or not. The most crucial experimental test is to prove the mechanism causing the resistivity, which is the Lorentz force to drive motion of vortex in a conventional superconductor. Since the Lorentz force is related to the current and the field direction such that $\boldsymbol{F} = \boldsymbol{I} \times \boldsymbol{B}$, where $\boldsymbol{I}$ is the transport current flow and $\boldsymbol{B}$ is the magnetic induction, this can easily be tested by measuring the angular dependence of resistivity with respect to the current and field directions.

In order to prove this idea, first of all, it was essential to obtain extremely high quality single crystals. We have chosen the $YBa_2Cu_3O_{7-\delta}$ system as a first candidate for this purpose, since it ap-

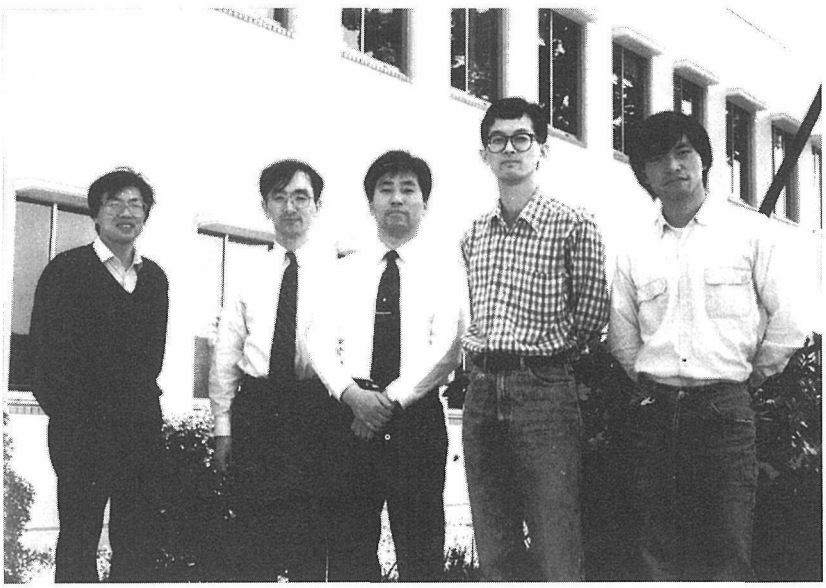

Fig. 1 A photograph of the member in the second sub-group of the first group, Dr. K. Kadowaki (center), Dr. H. Takeya, Dr. T. Mochiku, Mr. Y. Saito and Dr. S.L. Yuan (from right to left).

peared that the best quality of sample at that time may only be grown in this system among various kinds of high T_c superconductors. Shortly after that a high quality single crystalline $YBa_2Cu_3O_{7-\delta}$ has successfully been grown by a CuO-BaO rich flux method, though it was a tiny cubic sample with black shinny luster. The electrical resistivity and its angular dependence measurements have been performed immediately in horizontal fields up to 6 T. The results clearly showed negative evidence for the conventional picture that the Lorentz force is not the cause of resistivity[1]. Later on a more clear evidence has been proven by similar measurements on large single crystalline $Bi_2Sr_2CaCu_2O_{8+\delta}$ grown in the infrared mirror furnace[2]. Therefore, it is concluded that the Lorentz force do not play important role for the dissipation but there must be a new mechanism for the dissipation mechanism of supercurrent flow: superconducting fluctuations.

The concept of superconducting fluctuations in a superconductor is in fact not new but has been argued in relation to the restricted systems such as zero-, one- and two-dimensional systems. In these systems, the superconducting order is prevented from growing macroscopic size due to dimensional restriction, resulting in the fluctuating state of the order parameter. This argument is nothing but a pure statement from statistical mechanics in phase transitions. Since it is known that all high T_c superconductors has been recognized to be highly two dimensional due to the structural constraint that the superconductivity is realized only at the conducting CuO_2 plane and the other blocks in the structure are mostly non-metallic in-between CuO_2 planes. This leads to a natural consequence that all high T_c superconductors may show effects of two dimensionality on the superconducting properties, depending upon the electronic coupling strength of the CuO_2 layers.

The contribution of superconducting fluctuations in various physical quantities can be easily estimated by using Ginzburg criterion: $T/T_c - 1 \leq (1/32\pi^2)\{k_B/\Delta C\xi_{ab}^2(0)\xi_c(0)\}^2$. In conventional superconductors with three dimensions the range of superconducting fluctuations is in the order of 10^{-11} K with the coherence length of 10^3–10^4 Å, whereas it is about 1 K with the coherence lengths of $\xi_{ab} \approx$ 20 Å and $\xi_c \approx 0.3$ Å for the typical case of high T_c superconductors. Furthermore, this superconducting fluctuation region becomes even much wider in magnetic fields because of the reduction of the effective dimension in the system, resulting in the superconducting fluctuation region being 20–30 K in a magnetic field of a few Tesla.

At the present stage of our understanding on high T_c superconductivity, there is no discontinuity between high T_c superconductors and conventional ones. Although the appearance of phenomena in magnetic fields looks quite different, we interpret the difference as a different range of material parameters. For example, the prominent difference can be found in the phase diagram in magnetic fields as shown in figure 2. In highly anisotropic superconductors with short coherence length, the upper critical field $H_{c2}(T)$, which was the well defined phase boundary separating the normal state and the superconducting phase in conventional superconductors becomes fuzzy due to the strong superconducting fluctuations and is replaced by the irreversibility line, which makes inroads deeply into the vortex state in the phase diagram. Above the irreversibility line the superconducting fluctuations are playing major role in all physical quantities, while below the line the superconducting state is more or less similar to the conventional vortex state. It requires further intensive studies in the future to achieve more unified understanding of the properties related to the vortex state, especially to search for the mechanism to control the nature of the irreversibility line and the pinning forces in order to improve critical current characteristics in high T_c superconductors at higher temperatures.

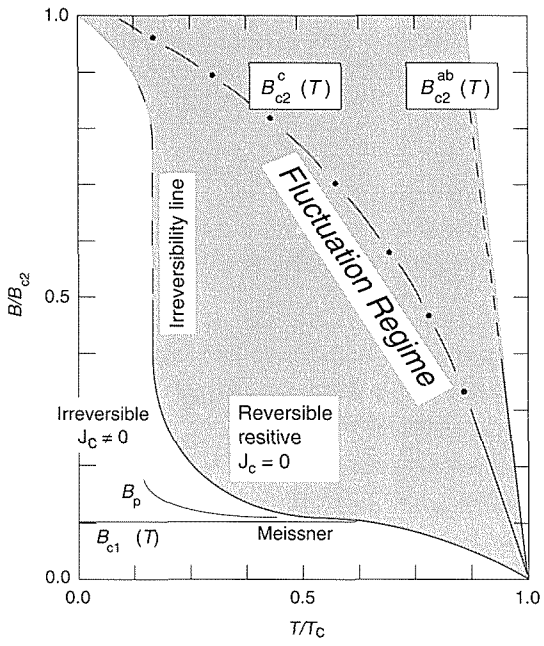

Fig. 2 The phase diagram of highly anisotropic superconductors with short coherence lengths.

References

1. *Broadening Phenomena of The Resistive Transition in Single Crystalline $YBa_2Cu_3O_{7+\delta}$ in Magnetic Fields*, K. Kadowaki, J.N. Li and J.J.M. Franse, Physica C170 (1990): 298–306.
2. *Vortex Dynamics and Unusual Vortex State of High T_c Superconductors*, K. Kadowaki, in *Electronic Properties and Mechanisms of High T_c Superconductors*, eds. by T. Oguchi, K. Kadowaki and T. Sasaki Elsevier Science Publishers B. V., North Holland (1992): 209–20.

❐ Computational Evaluation of Radiation Induced Stress Relaxation

J. Nagakawa, 2nd Research Group

Keywords: stress relaxation, irradiation creep, radiation damage, point defect, computer simulation

Radiation Induced Deformation—Macroscopic Deformation Induced by Atom-Size Point Defects

Radiation Induced Deformation results from a dynamic migration of radiation induced point defects biased by the externally applied stress. During the irradiation with energetic particles, point defects are continuously produced, migrate to meet and be annihilated with other kind of defects, form point defect agglomerates (dislocation loops), and are absorbed by network dislocations and loops. When the stress is applied, the strain field of point defects, particularly the strong one of interstitials, interacts with the stress field and their migrations are biased. In consequence, plastic strain is produced through the enhanced absorption and subsequent climb motion by dislocations or loops aligned to the stress and also through the active formation of loops on the aligned plane. Accumulation of such atomic scale phenomenon induces significant macroscopic deformation even in a condition that there is no deformation without irradiation.

Computer Simulation of Radiation Induced Deformation

Recently, a numerical calculation method has been developed at NRIM to simulate the radiation induced deformation. Since the radiation induced deformation is caused by the stress-biased migration of point defects, it can be evaluated most precisely by following the destiny of each defect. It is, however, wasting too much computational time that a rate theory approach has been adopted. Simultaneous differential equations are numerically solved for the following defect concentrations;

1. single interstitials,
2. single vacancies,
3. loop nuclei aligned to stress,
4. those non-aligned to stress,
5. interstitial loops growing on aligned planes,
6. those on non-aligned planes,
7. accumulated net interstitials in growing aligned loops,
8. those in growing non-aligned loops,
9. net interstitials absorbed by aligned network dislocations,
10. those by non-aligned network dislocations.

From the calculated defect concentrations, the irradiation induced deformation was evaluated at each iteration step using the following models;

1. PA (SIPA [Stress Induced Preferential Absorption] creep by network dislocations climb),
2. PAG (dislocation glide induced by SIPA climb),
3. SAIL (SIPA creep by growing interstitial loops),
4. SIPN (creep by stress-induced preferential loop nucleation).

It should be emphasized here that these mechanisms are operating simultaneously, competing with each other for the point defects.

This simulation technique was successfully used to evaluate the light-ion irradiation creep behavior of austenitic stainless steels[1].

Calculation of Radiation Induced Stress Relaxation

Stress relaxation is caused by a transformation of elastic strain to plastic strain. When there is no irradiation, this occurs only through thermally activated deformation in which deformation rate is proportional to the 4th–6th power of applied stress. However, with irradiation and consequent atomic displacements, the radiation induced deformation, in which the deformation rate is only linearly proportional to the stress, is responsible for the strain transformations. Figure 1 illustrates the significance of radiation induced stress relaxation, showing the relaxation curves of 321 stainless steel at 500 °C with and without irradiation calculated from the thermal and light-ion irradiation creep data. As can be seen, stress relaxation due to thermal deformation is dependent on the initial stress, but nonetheless it tends to be saturated irrespective of the stress level. On the other hand, radiation induced stress relaxation is independent of the initial stress level and steadily approaches the stress-free condition.

Aforementioned computer simulation technique has been applied to the evaluation of the radiation induced stress relaxation behavior for the cases with no irradiation creep data available. Structural materials for the light-water nuclear reactor cores receive rather low fluence of neutrons. It is, therefore, generally considered that irradiation creep is not a life-determining factor in these structural materials. However, the computational evaluation revealed that the stress relaxation is considerable as shown in figure 2 with experimental results[2]. Extended calculation indicates that the stress will be only about 10 MPa, i.e. 5% of the initial stress, after 10 years of irradiation.

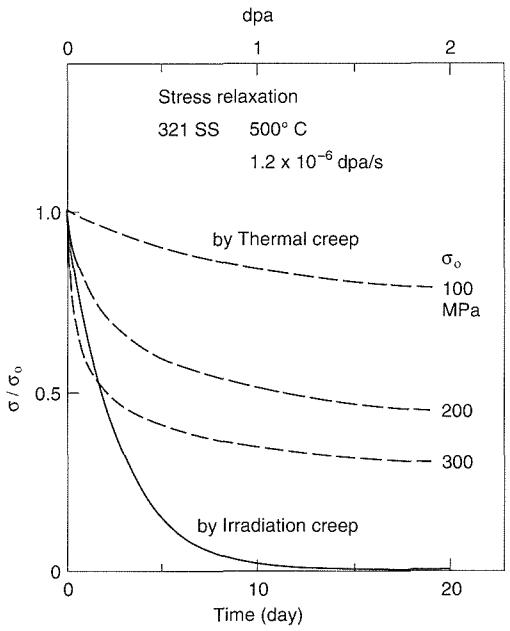

Fig. 1 Stress relaxation with and without irradiation

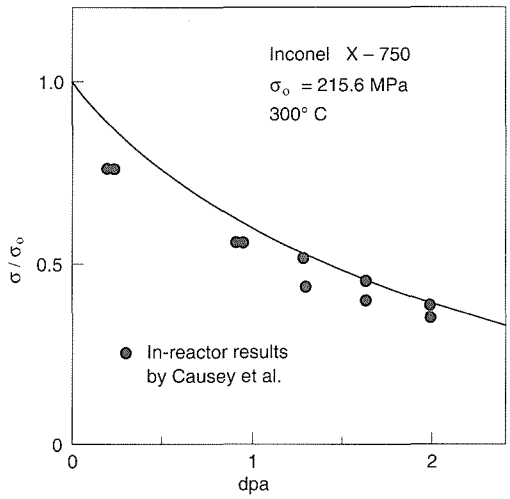

Fig. 2 Radiation induced stress relaxation in LWR core

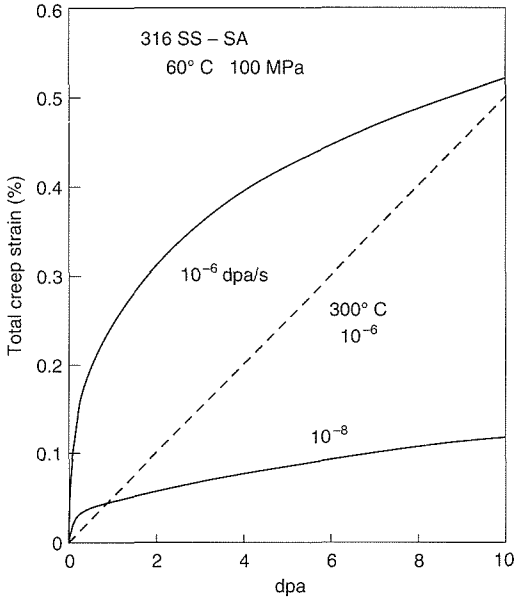

Fig. 3 Low temperature irradiation creep at 60 °C

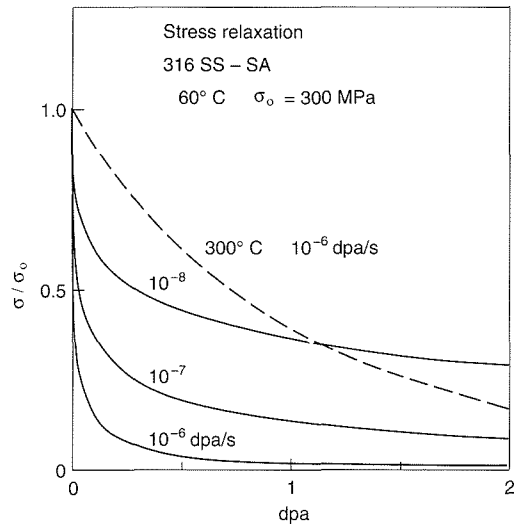

Fig. 4 Radiation induced stress relaxation at 60 °C

Recently, very significant creep strain, higher than those at 330 °C and 400 °C, has been reported for austenitic stainless steels irradiated to 60 °C. This result is of critical importance to the design of experimental fusion reactors like ITER (International Thermonuclear Experimental Reactor) of which structural materials will be irradiated below 100 °C at many portions of the core assembly. The aforementioned simulation has been applied to this "low temperature irradiation creep" as shown in figure 3, and it revealed that it is caused by the transient of point defect concentrations[2]. The total strain produced by the low temperature irradiation creep throughout the life time of ITER will be less than 1%, which can be regarded as within the design limit of fusion reactors. However, if this low temperature deformation is considered from the viewpoint of stress relaxation, detrimental effect is anticipated as shown in figure 4. At low temperatures, stress relaxes very significantly at a very early stage. This low temperature radiation induced stress relaxation has urged the ITER design of core portions to be changed from a bolted structure to a welded one.

References

1. *Computer Simulation of Early-Stage Irradiation Creep*, J. Nagakawa, N. Yamamoto and H. Shiraishi, J. Nucl. Mater. 179–81 (1991): 986.
2. *Calculational Evaluation of Radiation Induced Deformation*, J. Nagakawa, Proc. 4th ANER (1992): 387.

Research in Progress 1992–1993

❒ List of Research Subjects

Numbers with circle indicate subjects newly started from April 1993.

Numbers with square indicate subjects ended by March 1993.

Characterization/Properties

Electronic and nuclear properties

(1) Pressure Effects on Physical Properties of Magnetic Materials

(2) Theory of Structure and Properties of Surfaces and Interfaces

(3) First-Order Phase Transitions in Magnetic and Superconducting Materials at Low Temperatures

(4) Study of Electron Correlations and Quantum Transport Phenomena in 80 T Class Long Pulsed Magnetic Fields

5 Electronic Structure and Superconducting Mechanism in High-Temperature Superconductors

6 Database Development in Assistance of New Superconducting Materials Research

[7] Studies on Electronic and Magnetic Properties at High Pressure

[8] Theory of Structure and Electronic States in Systems with Randomness

[9] Relaxation Phenomena in Magnetic and Superconducting Materials

[10] Direct Observation of Vortex State in a Superconductor by Means of Magnetic Force Microscope

Atomistic arrangement

(11) Quantification Study on High Resolution Transmission Electron Microscopy

12 Structures of Transition Metal Oxides from the Bonding View Point

13 Molecular-Dynamics Study of the Nucleation Process at Solid-Liquid Interfaces

[14] High Resolution Transmission Electron Microscopic Study for Interfaces of Materials

Phase transformation and microstructures

15 Super-Microscopic Study on the Mechanism of Martensitic Transformation in Shape Memory Alloys

Surface and interface properties

(16) Structure and Electronic Properties of Silicides

17 Study on Changing the Properties of Metallic-Oxide Films for Increasing the Hydrogen Permeability

18 Effect of Oxidation on Mechanical Degradation of Metallic Materials

19 Study on Monolayer-controlled Materials by Using a Surface Tomographic Technique

20 Fabrication of Quantum Well Box Systems by Droplet Epitaxy for Advanced Optoelectronic Devices

[21] Crystal Growth on the Surface of Inter Metallic Compounds

Mechanical properties

(22) Toughness Improvement of Brittle Ceramics and Steels by Precipitation and Phase Transformation Control

(23) Study on Deformation and Fracture of Structural Materials at Cryogenic Temperatures

(24) Study on Deformation and Fracture under Irradiation

25 NRIM Fatigue Data Sheet Project-IV

26 Controlling and Recovering Methods for High Temperature Damage

27 NRIM Creep Data Sheets (IV)

28 Effect of Surface Film on Deformation of Bulk Matrix Material

29 Evaluation of Crack Initiation and Growth of Superalloys under Creep and Creep-Fatigue Conditions

30 Fatigue Behavior of Brittle Materials at Elevated Temperatures

31 Fatigue Crack Initiation Process in Corrosive Environment

32 High Temperature Deformation and Fracture in Polycrystalline Oxide Ceramics

33 Mechanism of Fretting Fatigue Failure in Metallic Materials

[34] Tensile Fracture Mechanism of Continuous Ceramic Fibers

Measurement and evaluation

(35) *In-situ* Measurement of Local Strain in High Temperature Range of Material and Detection of Defects by the Laser Speckle Method

(36) Correlation between Plasma Parameters and Evaporation in Free Arcs

(37) On-line Determination of Order Parameters in Alloys from Electron Diffraction by CCD Camera System and Its Application to Examination of Ordering Process

(38) Electrochemistry and Modeling of Corrosion of Metals under Thin Water Layer

(39) Studies on Advanced Characterization Methods of Metals and Alloys Using Synchrotron Radiation

40 *In-Situ* Analysis/Evaluation of Radiation Damage in Materials

41 Characterization and Control of Elementary Functions of Materials in the Localized Fine Area

42 Study on Detection and Evaluation of Radiation Damages in Extreme Particle Fields

43 Development of Advanced Technologies for X-ray Microtomography

44 Advanced Techniques Physical Analyses for Metals

45 Evaluation of Metallurgical Structure with a Fuzzy Logic

46 Sensitive Instrumental-Analysis of Metallic Materials by Direct Methods and Separation Methods

47 Study on Mechanism of Ion Production in Low Temperature Plasma

48 Database Systems for R&D of Superconducting Materials

49 Modeling and Evaluation of Advanced Materials—A Coordinated Interlaboratory Research Effort

50 Sensing and Analysis of Material Damage Formation Processes

51 Atomic Scale Evaluation of Material Damage in Aqueous Solution

52 Research on Quantitative and Intelligent Nondestructive Evaluation Techniques for Materials and Structures of High Reliability

53 Quantitative Evaluation of Fracture in Materials for Casks

54 Real Time Evaluation of Fatigue Damage during Crack Propagation under Random Loadings

55 Chemical Analysis of Organotin in Marine Environmental Samples

56 Development of Extremely High Field Magnets

[57] Vaporization and Ionization by Arc Plasma

[58] Measurements of Transient Phenomena Due to Beam-Solid Interaction

[59] On-line and Precise Measurement of the Intensity Distribution in Electron Diffraction Pattern by Using Cooled CCD Camera

[60] Characterization of Metals and Alloys Using Synchrotron Radiation

[61] Rutherford Backscattering and Particle Induced X-ray Spectroscopy Studies of Thin Film Oxide Superconductors

[62] Evaluation and Application of Cu-Ag Alloy as Conductor Material in High Field

[63] Coil-Winding Procedure for High-Strength/High-Conductivity Wire

[64] Study on Measurement and Evaluation Methods for Superconducting Properties

Simulation and theory

(65) Evaluation and Life Prediction of Material Strengths by "DIMS" System

66 Development of Material-design-technique for Mechano-chemical Attack on Lightweight Heat-resistant Materials

67 Self-organizing Information-base System Used for Creative Research and Development

68 Study on the Trend of Application of New Super Conductors

69 Computer Aided Design Tools for the Development of Materials

70 Basic Research to Establish Design Techniques for Advanced Materials

[71] Development of Knowledge Based System for Materials Life Prediction

[72] Predictions of Materials Strength and Endurance under Irradiation Using Ion Beam

[73] A New Computational Approach to the Micromechanics of Heterogeneity in Advanced Structural Materials

Materials

Non-ferrous materials

74 Disintegration Phenomena in Intermetallic Compounds

75 Microstructural Refinement and Mechanical Properties of Titanium Alloys

Intermetallic compounds

(76) Basic Researches on Intermetallic Compounds for Structural Applications

(77) Study on Sintering of TiAl Intermetallic Compound

78 Fundamental Study of Microstructures and Properties to Develop High Performance Materials for Severe Environment (II-High Temperature Intermetallic Compounds)

79 Improvement of Mechanical Properties of Intermetallic Compounds by Crystal Growth Control

80 Fatigue Fracture Mechanisms for TiAl Intermetallic Compounds at High Temperatures

81 High Ionic Conductivity of Solid Electrolyte

82 High Performance Materials for Severe Environments-I (Microstructure and Properties of Intermetallic Compounds with High Specific Strength)

[83] Preparation of Spontaneous Exothermic Metals and Its Application

[84] Production and Character Evaluation of Functional Intermetallic Compounds

Composites

(85) Thermal Stability of Intermetallic Compound Matrix Composites Reinforced with Fibers

[86] Thermal Effects in Hetero-Phase Materials

Materials for mechanical application

87 Intelligent Structural Materials

88 Development of Metal Matrix Composites for High Temperature Use Through Combinations of Advanced Powder Metallurgy Processes

Materials for electronics application

(89) Thermal and Electrical Properties of II–IV and V–VI Thermoelectric Semiconductors

(90) Structure Control and Electromagnetic Properties of High Temperature Superconductors

91 Purification of Active Metals for the Preparation of Superconductive Materials

92 Development of $Bi_2Sr_2CaCu_2O_x$ Tapes and Coils

93 Development of High-T_c Superconducting Thick Films and Tapes by Various Spraying Methods and by Internal Oxidation

94 Development of High-Field Multifilamentary Superconductors Made by Intermetallic Compounds

95 Development and Characterization of Superconducting Materials for Fusion Reactor Magnet Use

96 Fabrication of Oxide Superconductors Using YAG Laser Irradiation

[97] Development and Evaluation of Advanced Superconducting and Cryogenic Materials

Magnetic materials

(98) Magnetocaloric Effect on Size-controlled Magnetic Materials for the Production of Ultra-low Temperatures

99 Fundamental Research into Intelligent Materials with Cooperative Molecules or Atoms

100 Fabrication and Physical Properties on Metallic Substances with Mesoscopic Sizes

[101] Fabrication and Magnetic Properties of Metallic Clusters with Sub-Nanometer Size

Materials for energy application

(102) Study on Highly Resistant Mechanism to Radiation Damage

103 Environmental Degradation of Structural Materials for Light Water Reactors

104 Assessment of Strength and Structural Materials Database for Weldment in FBR (Fast Breeder Reactor) Components

105 Fundamental Research on Application of New Functional Materials to Passive Components

106 Material Chemistry in the Extreme Conditions under Irradiation

107 Research on Distributed Database for Advanced Nuclear Metals

108 R & D of Advanced Heat-Resistant Structural Materials for Very High Temperature Gas-Cooled Reactors

[109] Study on a Porous Gas-Diffusion Electrode

[110] Development of the Fusion Reactor First Wall Materials Resisting to Plasma and Radiation Damage

Materials for environmental performance

111 Improvement of Wear Properties of Metallic Medical Materials

112 Synthesis of New Functional Materials by the Application of Host-Guest Reactions

[113] Corrosion Resistance of Synthetic Barriers in Geological Disposal of Spent Nuclear Fuels

[114] Corrosion Resistance of Coated Materials in Natural Environment

[115] Achievement, Measurement and Application of Extremely High Vacuum

Bio-Materials

(116) Basic Study on Reaction between Materials and Bacteria

(117) Fundamental Study on Biocompatibility of Materials

[118] Evaluation of Biocompatibility of a Ti-6Al-4V Alloy in a Pseudo Body Fluid under Fretting Fatigue Load through a Cell Culture Method

Processing

Separation and synthesis

119 Fundamental Study on Preparation and Characterization of the Metal Complexes Possessing a Peculiar Molecular Structure

120 Alloying Method Using Decomposition of Metal Halides

[121] Literature Survey on Elimination of Specific Toxic Metallic Ions

[122] Survey Research on Utilization of Biological Function to Separation and Extraction Process

Gaseous process

(123) Development of Shape Memory Thin Films Formed by PVD Method

124 Precise Composition Control of Ordered Alloys by Chemical Transportation Techniques

125 Synthesis and Characterization of Oxide Superconductors

126 Study on Fabrication Process of High-T_c Oxide Superconductors

127 Processing and Development of Isotopically Controlled Materials (ICM)

Liquid state process

(128) Metastable Phase Solidification from Undercooled Liquid by Introducing External Nucleation Seed

129 Purification of Metals by Non-Contacting Melting Method

130 Extraction from Metal to Gas Phase

131 Basic Techr.ology Development of Materials Processing in a Short-Duration Microgravity Environment

132 Solidification Processing for Fine-grain Structure Materials

133 Measurements, Analyses and Evaluations of Specimens Made by FMPT

Solid state process

(134) Metallurgical Analysis of Micro-Machining Region

135 Cooperative Phenomena of the Transformation Variants

[136] Materials Properties Induced by Transformation Superplasticity

[137] Metallurgical Analysis of Cutting Region

[138] Comprehensive Research and Development of Special Structural Ceramics Using Colloid Processing

Powder processing

(139) Study on Solid State Chemical Reaction, its Propagation and Materials Synthesis

(140) Fundamental Study on Creation of Micro Stereome Fabrics by Powder Technology

(141) Characterization of Composite Ultrafine Particles

(142) Synthesis and Characterization of Advanced Materials Utilizing Colloidal Dispersed Systems

143 Coating of Fine Powders by CVD Technique in Fluidized Bed

144 Development of Particles Assembly Technology for Integration of Functions

145 Properties of Raw Powder of Superconductor for High Pressure Forming

146 Study on Rapidly Solidified Powders for Superconductive Materials

147 Preparation and Characterization of Ultrafine Powders Used for Making Oxide Superconductors

[148] Combustion Synthesis for Production of Ceramic and Intermetallic Materials

[149] Production and Characterization of Advanced Powders

Joining

(150) Fundamental Study on Brazing under a Micro Gravity

151 Corrosion of Dissimilar Metals Joints in Reactor Fuel Reprocessing Plants

[152] Joining of Intermetallic Compounds Utilizing Resistance Heating by Direct Current

[153] Low Energy Joining with Controlled Surface Composition and Misorientation Angle

[154] Effects of Temperature Distribution on Capillary Gap Penetration

Composite process

(155) Study on the Melting Effects of Spray Particles on Properties of Deposited Coatings

156 Forced Infiltration Process for Making Composite Structures

157 Coating Formation by Molten and Electrified Powders

Process with aid of beam technology

158 Diagnostics of Laser Photoionization Induced Plasma

159 Study on Evaporation Process by High Energy Density Beams

160 Study on Synthesis of Special Compounds by a Combined Use of Ion Implantation and Deposition

[161] Study on Molten Metal Behavior in Surface Modification Process with High Temperature Heat Sources

Processing in special environment

(162) Development of New Material Phases in the Extremely High Vacuum

163 Development of Quantum Microstructure in Ultra Clean Vacuum

❒ Research Programme

Characterization/Properties

Electronic and nuclear properties

① Pressure Effects on Physical Properties of Magnetic Materials

April 1993 to March 1996
T. Matsumoto, Materials Physics Division
Keywords: magnetic properties, the Kondo effect, α- and γ-Ce

Targets of this research program are to clarify the electronic and magnetic properties of magnetic materials by using high pressure techniques. We are interested particularly in the attracting phenomena caused by the interactions between electrons in the electronic states modified in solid. Typical examples of related problems are the Kondo effect, electron with enormous mass, and valence fluctuation etc. in rare earth compounds.

The magnetic properties of α- and γ-Ce have been investigated by means of the measurements of magnetic susceptibility at high pressure. The magnetic susceptibility of γ-Ce obeys the Curie-Weiss law and the Weiss temperature is considerably increased with increasing pressure. On the other hand, the susceptibility of α-Ce becomes nearly temperature independent at higher pressure. These behavior can be semiquantitatively explained by the single impurity Kondo picture giving the characteristic temperatures as a function of volume which is contracted by the applied pressure.

Related Papers

Presure Effects on the Yb Valence State in $YbIn_{1-x}Ag_xCu_4$ *(x = 0–0.2)*, T. Matsumoto, T. Shimizu, Y. Yamada and K. Yoshimura, J. Magn. Magn. Mater. 104–07 (1992): 647.

Effect of Pressure on Magnetic Susceptibility in α- and γ-Ce, T. Naka, T. Matsumoto and N. Mōri, submitted to the proceedings of LT20, Eugene, Oregon, 1993.

② Theory of Structure and Properties of Surfaces and Interfaces

April 1993 to March 1996
T. Oguchi, Materials Physics Division
Keywords: electronic structure, structural stability, surface, interface

We study theoretically the structural and electronic properties of several surface and interface systems. The analysis is based on the density-functional (DF) electronic theory within local-density approximation (LDA).

Particular attention will be paied on alkali-metal adsorbed transition-metal surfaces, artificial interfaces such as multilayer films and chemisorption on semiconductor surfaces. Newly developed atomic-force method will be applied to determine the adiabatic potential of the systems and the structural stability will be discussed in relation to experimental observations.

Further developments on methodological and numerical techniques will be also tried to make it possible to perform large-scale numerical calculations.

Related Papers

Density-Functional Molecular-Dynamics Method, T. Oguchi and T. Sasaki, Prog. Theor. Phys. Suppl. 103 (1991): 93–117.

Linear-Augmented-Plane-Wave Based Car-Parrinello Method and Its Application to Cu Surfaces, T. Oguchi and T. Sasaki, in *Computer Aided Innovation of New Materials II*, ed. by M. Doyama, J. Kihara, M. Tanaka and R. Yamamoto (Elsevier, 1993): 107–10.

Augmented-Plane-Wave Force Calculations for Transition-Metal Systems, T. Oguchi, in *Interatomic Potentials and Structural Stability*, ed. by K. Terakura and H. Akai (Springer-Verlag, 1993): to appear.

③ First-Order Phase Transitions in Magnetic and Superconducting Materials at Low Temperatures

April 1993 to March 1996
M. Uehara, Surface and Interface Division
Keywords: first-order phase transition, metastable state, quantum tunneling, magnetic relaxation

In disordered magnetic systems like Sm(CoCu)5, magnetic domain walls move between pinning centers provided by the disorder. At high temperature this is known to occur via thermal activation; at low temperature we have shown previously that there is a crossover to quantum tunneling. Such behavior of the magnetic relaxation is related to the general nature; first-order phase transition in which a macroscopic system in a metastable state undergoes transitions to a lower state. The decay of a metastable state is also observed in type-II superconductors. We study the magnetic relaxation

in high-T_c superconductors. We have shown that the dynamics of vortices in Bi and Y-samples of high-T_c superconductors can be described on a very coherent way by using the mean relaxation time τ defined at a constant level of mixed state. The mean energy barrier E which is associated with this relaxation time is found to be proportional to the reciprocal magnetic field in both samples, $E \propto (1/H - 1/H_0)$. The temperature dependence of this energy barrier is also found the same for both samples above a crossover temperature Tcr = 6 K and 8 K, $E \propto [1 - (T/T_c)^2]$. Below their crossover temperatures both samples show a change in the mechanism of relaxation: the relaxation is no longer thermally activated but independent on temperature. This is attributed to the quantum tunneling of vortices. The studies on magnetic relaxation in conventional ("low-T_c") superconductors and ferromagnetic systems are currently in progress.

Related Papers

Noncoherent Quantum Effects in the Magnetization Reversal of a Chemically Disordered Magnet, M. Uehara and B. Barbara, J. Physique 47 (1986): 235–38.

Field and Temperature Dependence of the Mean Penetration Rate of Fluxons in the Mixed State of High T_c Superconductors, M. Uehara and B. Barbara, J. Phys. I France 3 (1993): 863–70.

Microscopic Quantum Tunneling in Ferromagnetic Particles, B. Barbara, L. Sampaio, A. Marchand, M. Uehara, C. Paulsen, J.L. Tholence and D. Fruchart, JJAP Series 9 (1993).

④ Study of Electron Correlations and Quantum Transport Phenomena in 80 T Class Long Pulsed Magnetic Fields

April 1993 to March 1998

K. Kadowaki, 1st Research Group

Keywords: pulsed high magnetic field, quantum transport phenomena

This research plan is newly set starting this year in order to intensify research activities in the 80 T class long pulsed high magnetic field facilities, which are under construction in part of the High Magnetic Research Station (Tsukuba Magnet Laboratories). It has been recognized that the long pulsed high magnetic field technique is a most attractive and a unique methods to generate extreme high magnetic fields, which can be covered field ranges in the vicinity of 100 T region, far beyond the upper limit of field ranges (approximately 32 T) by means of steady current magnet technologies. The experimental setup is a unique system in the sense that, first of all, it is non-destructive so that it is possible to make reliable physical measurements. Secondly, although the generated field is pulsed, it has sufficiently long duration time (10–100 msec.) for most of physical measurements. This is essential for studies of conducting materials such as metals, alloys, intermetallics, organometallic compounds, etc. This brings us most competitive and challenging opportunities among the high magnetic field laboratories in the world.

Recently, we have shown that the copper-silver alloys have superior properties to ever known conductor materials with sufficiently low resistivity at the operating temperature. This material problem (mechanical strength and conductivity) has long been the major problem to be overcome in order to generate higher fields. The preliminary result of testing of magnet made of such wires showed greatly improved performance. The generated magnetic field so far exceeded 68 T with the pulse duration time of about 5 msec. This value is the world highest record using a single solenoid. Further optimization among many physical parameters is currently undergoing in order to reach higher magnetic fields.

For physical measurements, the high sensitivity magnetization measurement system and transport measurement system are under construction for the study of currently interesting systems such as highly correlated electron system, high temperature superconductivity, rare earth intermetallics, hard magnetic materials, organometallic compounds, two dimensional electron systems, mesoscopic systems, etc.

5 Electronic Structure and Superconducting Mechanism in High-Temperature Superconductors

April 1988 to March 1994

T. Oguchi, Materials Physics Division

Keywords: high-temperature superconductor, theory, electronic structure

The high-temperature superconductor (HTSC) is a potential material for a variety of applications. Despite a great deal of effort of basic research on electronic structure and properties of HTSC, the superconducting mechanism has not been clarified yet. In this work, we have studied electronic structure of HTSC based on band-structure calculations with the local-density approximation (LDA).

The electronic structure of La_2CuO_4 has been investigated for two different crystal structures, K_2NiF_4 and Nd_2CuO_4. The calculated band structure shows importance of the position of oxygen atoms outside CuO_2 planes in realizing two-dimensional character of the electronic structure near the Fermi energy (E_F). The high density of states just below E_F obtained for the Nd_2CuO_4 structure implies relative instability when doping holes, being consistent with the observed fact that no hole-doping is possible in Nd_2CuO_4.

LDA band calculations have been performed for $YBa_2Cu_3O_y$ (y = 6 or 7) (abbreviated as Y123). Several characteristic aspects have been derived by comparing with other HTSC's. Importance of the energy separation between Cu-*d* and O-*p* states was pointed out in connection to photo-emission experiments. Significance of the *p-p* hopping between the nearest oxygen atoms was also discussed.

The electronic structure of $YBa_2Cu_4O_8$ (Y124) has been calculated. Overall characteristics of the electronic structure are quite similar to those of Y123. A large energy-level lowering of oxygen *p*-states at chain sites was found. This result may explain the relative stability of the oxygen ions in Y124. Some differences in the Fermi surfaces between Y123 and Y124 were also suggested in conjunction with anisotropic transport properties.

Quite recently, Hall coefficient of Y124 has been calculated by analyzing the Fermi surface based on the Boltzman transport theory. The obtained Hall coefficient is in good agreement with experiment in its sign (carrier character) and magnitude (carrier concentration). We have derived an important relation between the Hall coefficient and anisotropy of the in-plane resistivity, which may give us a clue for the mechanism of anomalous temperature behavior of the Hall coefficient.

Related Papers

Implications of Band-Structure Calculations for High-T_c Related Oxides, K.T. Park, K. Terakura, T. Oguchi, A. Yanase and M. Ikeda, J. Phys. Soc. Jpn. 57 (1988): 3445–56.

Electronic Band Structure of $YBa_2Cu_4O_8$, T. Oguchi, T. Sasaki and K. Terakura, Physica C 172 (1900): 277–81.

Local-Density Band Structure of Y-Ba-Cu Oxides, T. Oguchi, T. Sasaki and K. Terakura, Physica C 185–89 (1991): 1733–34.

Calculation of the Hall Coefficient in $YBa_2Cu_4O_8$, T. Oguchi, T. Sasaki and K. Terakura, in *Electronic Properties and Mechanisms of High-T_c Superconductors*, ed. by T. Oguchi, K. Kadowaki and T. Sasaki (Elsevier, 1992): 407–09.

Fermi Surface and Transport Properties of $YBa_2Cu_4O_8$, T. Oguchi and T. Sasaki, J. Phys. Chem. Solids 53 (1992): 1525–32.

6 Database Development in Assistance of New Superconducting Materials Research

April 1988 to March 1994

Y. Asada, Material Design Division

Keywords: oxide superconductors, database, graphic data

Since the discovery of high-T_c oxide superconductors an enormous amount of research papers have been reported. Numerical database on these superconducting materials, therefore, is necessary for the researchers in this field. We developed in this study a numerical database "SUPERCON": The data on superconducting properties (T_c, higher and lower critical magnetic fields, coherence length, penetration depth, energy gap, etc) and related properties (Hall coefficient RH, thermopower s, thermal conductivity κ, specific heat C, etc) are collected from the published papers. More than 4000 records of data are stored up to now in our database "SUPERCON". Graphic data of temperature dependence of RH, s, κ, C are also stored in the form of digital data.

We retrieved the temperature dependence of Hall coefficient RH for $YBa_2Cu_3O_z$ from "SUPERCON" and compared among them. Although they have similar temperature dependence the values at 300 K scatter beyond error in measurement. It suggests that the numerical values depend on some unknown parameters which have not been explicitly described in the literature.

Related Papers

Data Tables of High-T_c Oxide Superconductors, Y. Asada, Bulletin of the Japan Institute of Metals 30 (1991): 832–38 (in Japanese).

Numerical Database of High-T_c Oxide Superconductors, Y. Asada, to be published in Cryogenic Engineering (in Japanese).

7 Studies on Electronic and Magnetic Properties at High Pressure

April 1990 to March 1993

T. Matsumoto, Materials Physics Division

Keywords: specific heat, magnetic susceptibility, magnetic phase transition, CeP, RFe_2O_4 (R = Y, Er)

We are interested in the pressure effects on physical properties. One of the important purposes of this research program is to clarify the change in the physical properties through the reduction of the interatomic distance caused by external pressure. We have developed the original apparatuses in order to measure the magnetization and specific heat under pressure with a high accuracy, and applied them to the investigation on the physical properties of oxide superconductors and rare earth compounds.

The effect of pressure on the magnetic phase transition of CeP has been investigated by the measurement of the specific heat up to 0.5 GPa. CeP is one of the cerium monopnictides with the NaCl-type structure, and exhibits the magnetic transition at about 10 K. This work shows that the peak at 10 K splits into two peaks with increasing pressure. One of the peaks remains at 10 K, but the other goes up monotonically with increasing pressure at a rate of 20 K/GPa. This large pressure

dependence suggests that the exchange interactions controlling the magnetic property are sensitive to the applied pressure.

Pressure dependence of magnetic susceptibilities of RFe_2O_4 (R = Y, Er) has been also measured up to 0.6 GPa above about 100 K. Two magnetic phase transitions, T_L and T_H, are observed in the temperature range of 200–250 K at ambient pressure for both compounds. Except for the increase in T_H of $ErFe_2O_4$, the transition temperatures are depressed with increasing pressure. The reduction of the transition temperatures is explained as the volume effect on the first order phase transition from their volume changes. Because no structural change occurs at T_H in $ErFe_2O_4$, the pressure dependence of T_H is interpreted in terms of the 10/3 law for the volume dependence of superexchange interaction.

Related Papers

High Pressure Specific Heat Investigation of the Magnetic Transition in CeP, A. Matsushita, Y. Okayama, S. Takayanagi, N. Mōri, T. Matsumoto, Y.S. Kwon, Y. Haga and T. Suzuki, Solid State Commun. 84 (1992): 761.

Magnetic Properties of the Two Dimensional Antiferromagnets RFe_2O_4 (R = Y, Er) at High Pressure, T. Matsumoto, N. Mōri, J. Iida, M. Tanaka, K. Siratori, J. Phys. Soc. Japan 61 (1992): 2916.

Crystal Structures of the Two Dimensional Antiferromagnets RFe_2O_4 (R = Y, Er) and Their Magnetic Properties Under Pressure, T. Matsumoto, N. Mōri, J. Iida, M. Tanaka, K. Siratori, F. Izumi and H. Asano, Physica B 180 & 181 (1992): 603.

8 Theory of Structure and Electronic States in Systems with Randomness

April 1990 to March 1993

T. Oguchi, Materials Physics Division

Keywords: electronic structure, defects in solid, structural stability

We investigated theoretically the structure and electronic states of bulk materials which contain imperfections such as point defects, stacking faults or phase boundaries. The analysis is based on the density-functional (DF) electronic theory combined with the molecular-dynamics (MD) method (abbreviated as DF-MD method). The DF-MD method provides an useful tool to determine the optimum atomic arrangement as well as the electronic states affected by the imperfections.

First of all, physical backgrounds and concepts of the DF-MD method have been studied intensively. Numerical techniques and algorithms involved in the method have been examined in details by performing small-scale calculations for silicon molecules. It was demonstrated that the method enable us to carry out an *ab initio* MD simulation for real materials and has several great advantages over the conventional methods for electronic-structure calculations. Some new concepts which are necessary to extend to metallic systems were also discussed.

Formation energies for stacking faults of Al have been evaluated with the DF-MD method. We considered twin and intrinsic stacking faults in the present work. To model these faults, supercell geometry which contains repeated fault planes was used. The formation energies calculated by taking full atomic relaxations into account are in fairly good agreement with the experimental values. It was found that only small atomic relaxations occur, which is consistent with close-packed structure of the faults.

It is well known that highly-conductive ZnSe promises realization of new devices such as blue LED's. However, no stable *p*-type ZnSe sample has been fabricated so far. Here, the origin of the instability of *p*-type ZnSe has been studied with the DF-MD method. Based on the total energies calculated for Li-doped ZnSe and host ZnSe, we have proposed a new compensation mechanism for a Li acceptor in ZnSe and have shown that Li is not suitable as the *p*-type dopant of ZnSe.

An extension of the DF-MD method has been recently carried out in order to make an application to a system with spatially localized electrons feasible. For the purpose, linear-augmented-plane-wave (LAPW) functions were adopted as the basis set. Several atomic-force calculations for bulk Si, Cu surface, Cu oxide and ferromagnetic Fe systems have shown an efficiency and high accuracy of the LAPW base method.

Related Papers

Li Impurity in ZnSe: Electronic Structure and the Stability of the Acceptor, T. Sasaki, T. Oguchi and H. Katayama-Yoshida, Phys. Rev. B 43 (1991): 9362–64.

Density-Functional Molecular-Dynamics Method, T. Oguchi and T. Sasaki, Prog. Theor. Phys. Suppl. 103 (1991): 93–117.

Density-Functional Molecular Dynamics Calculations for Defects in Si and Al, T. Oguchi and T. Sasaki, in *Molecular Dynamics Simulations*, ed. by F. Yonezawa (Spriger-Verlag, 1992); 157–66.

Linear-Augmented-Plane-Wave Based Car-Parrinello Method and Its Application to Cu Surfaces, T. Oguchi and T. Sasaki, in *Computer Aided Innovation of New Materials II*, ed. by M. Doyama, J. Kihara, M. Tanaka and R. Yamamoto (Elsevier, 1993): 107–10.

Augmented-Plane-Wave Force Calculations for Transition-Metal Systems, T. Oguchi, in *Interatomic Potentials and Structural Stability*, ed. by K. Terakura and H. Akai (Springer-Verlag, 1993): to appear.

[9] Relaxation Phenomena in Magnetic and Superconducting Materials

April 1990 to March 1993
M. Uehara, Surface and Interface Division
Keywords: magnetic relaxation, metastable state, domain wall motion, magnetic after effect

Recently much attention has been given to the dynamical nature in magnetic and superconducting systems such as spin glasses, amorphous magnets and high-T_c superconductor. We study the magnetic relaxation phenomena in which a macroscopic system in a metastable state undergoes transitions to a lower state via thermal excitation or quantum fluctuations through the barrier. It was shown that the thermal activation mechanism responsible for the diffusion of ferromagnetic domain walls in a $SmCo_{3.5}Cu_{1.5}$ single crystal shows a strong anomaly below a temperature of 50 K. This effect, initially attributed to quantum fluctuations, has been studied in more detail. In particular it was shown that the evolution of the magnetic after effect at low temperature fits a simple model where an effective temperature $T^* \sim 10$ K accounts for energy fluctuations of domain walls at zero Kelvin. This temperature coincides with the characteristic frequency, $\omega_0 \sim 10^{12}$ sec^{-1} of domain wall vibrations in metastable equilibrium. At lower temperature, collective jumps of magnetization in a metastable state were observed in a reversed magnetic field. Such behavior strongly suggests the existence of simultaneous wall motion on the scale of the sample, due to thermal "avalanche effect," associated with dissipation, and initiated by wall tunneling events on a microscopic scale. The magnetic relaxation in superconducting $Bi(Pb)_2Sr_2Ca_2Cu_3O_y$, $YBa_2Cu_3O_7$ and in high-quality single crystalline $Bi_2Sr_2CaCu_2O_8$ have been also studied.

Related Papers

Noncoherent Quantum Effects in the Magnetization Reversal of a Chemically Disordered Magnet, M. Uehara and B. Barbara, J. Physique 47 (1986): 235–38.

Staircase Behavior in the Magnetization Reversal of a Chemically Disordered Magnet at Low Temperature, M. Uehara, B. Barbara, B. Dieny and P.C.E. Stamp, Phys. Lett. A 114 (1986): 23–26.

Anomalous Demagnetization Process at Low Temperature in Nd-Fe-B Magnets, Y. Otani, J.M.D. Coey, B. Barbara, H. Miyajima, S. Chikazumi and M. Uehara, J. Appl. Phys. 67 (1990): 4619–21.

[10] Direct Observation of Vortex State in a Superconductor by Means of Magnetic Force Microscope

April 1992 to March 1993
K. Kadowaki, 1st Research Group
Keywords: superconducting vortex state, magnetic force microscope

Studies of vortex state in high T_c superconductors are very important in order to understand the nature of superconductivity in magnetic fields, since the critical current densities show an unusual behavior and eventually diminish at high temperatures, where most of application is waiting for.

The purpose of this research subject is to initiate a new technique to study microscopically the vortex state by means of the newly developing sensitive local probe such as STM (Scanning Tunneling Microscope), AFM (Atomic Force Microscope) and MFM (Magnetic Force Microscope), etc. These techniques have such advantages compared with the conventional Bitter method or the optical imaging technique using YIG that, firstly, the spatial resolution is more than 10^3 times greater so that each vortex, even the internal structure of vortex can be investigated in great detail. Secondly, the sensitivity of these techniques is in general much higher than that of the conventional ones. As far as the magnetic structure of the vortex as well as the phenomenological study of the pinning properties is concerned, MFM is most favorable. This technique is, however, still premature and is currently developing at the present stage of research. We introduced a new compact sized STM system with atomic spatial resolution as well as the magnetic field sensitive detection system with a magnetic force chip, which is expandable to low temperatures in ultra-high vacuum in the future. It is hoped that this new technique will provide rich information of the vortex state and will be a most powerful tool to study microscopic nature of vortex state.

Atomistic arrangement

(11) Quantification Study on High Resolution Transmission Electron Microscopy

April 1993 to March 1996
S. Ikeda, Surface and Interface Division
Keywords: HRTEM, structure image, $Na_{0.9}Mo_6O_{17}$, Y_2O_3, slow scan CCD camera

Quantification of high resolution electron microscopic images and electron diffraction intensities is expected to produce much more information than that obtained by the conventional method using the photographic film. For example, light atoms usually do not be recorded on photo films when they are included in a crystal together with heavy atoms. In the case of $Na_{0.9}Mo_6O_{17}$ crystal, only molybdenum atoms can be seen on a print of high resolution electron micrograph. In the present study, a slow scan CCD camera-image processing, which has a dynamic range of 10^4, is attached

to a high resolution electron microscope, JEM-4000EX, with a point to point resolution of 0.17 nm. Intensity contribution of Na and oxygen atoms is expected to be recorded on a processed image taken by the CCD camera.

In a preliminary experiment, intensity distribution of the electron diffraction pattern has examined to detect a and b directions in the (001) plane of Y_2O_3. In this case, kinematical structure factors of h00 are same as 0h0, which means determination of a and b directions is difficult since this electron diffraction pattern has almost four fold symmetry. In the present experiment, it was found a slight beam convergence induces intensity difference between h00 and 0h0, that make possible to identify a and b directions. The intensity difference between h00 and 0h0 is caused by dynamical scattering of electron beam. A slight off axis incident beam enhances multiple reflection and, consequently, make it possible to do clear identification for a and b directions.

12 Structures of Transition Metal Oxides from the Bonding View Point

April 1992 to March 1994

M. Okochi, Materials Physics Division

Keywords: transition metal oxides, binding nature, $Na_xMo_6O_{17}$, $Ba_2Sr_2CaCu_2O_{8+x}$, ZrO_2-12mol% CeO_2

Transition metals oxides are characterized by the structures of crystalline coordination compounds with interatomic bonds by sharing of electrons between metallic atoms and the neighboring oxygen. The bonding view point is a potential conception to make the microscopic binding nature clear in three dimensional array of atoms and gives the conceptional understanding about the binding nature in the compounds like metal oxides.

We have got a new knowledge about the bonding nature as follows:

Firstly, we have observed structure changes for single crystal $Na_xMo_6O_{17}$ under the irradiation of electrons in a 400 kV-type high resolution transmission electron microscope. The alkali metal occupies the isolated interlayered position between the free ends of frame structure. The alkali metal breaks away from the crystal under the irradiation and causes local recombination of oxygen to deformed frame structure. i.e., the structure changes of the crystal. This fact shows that the alkali metal is bounded in a weak bonding to the frame structure.

Secondly, the structure of $Ba_2Sr_2CaCu_2O_{8+x}$ (001) surface has been investigated by an XPS diffraction technique. Observed XPD patterns were analysed on the basis of the so-called forward focusing effect and we obtain information about the modulated structure, i.e., the modulation at the surface is similar to that in the bulk and a single crystal has the weakest bonding between the double Bi-O layers, and consequently, it cleaves there.

Thirdly, low-temperature phase transition in ZrO_2-12mol% CeO_2 has been studied by Fourier transform infrared spectroscopy (FTIR), paying attention to bond strengths in the bond. It was found that this material undergoes the tetragonal to monoclinic phase transition at ~120 K, revealing the Bu and Au modes at 574 cm^{-1} and 740 cm^{-1}, accompanied with the monoclinic phase. Temperature dependence of infrared reflectance spectra of Bi_2MoO_6, $Bi_2Mo_2O_9$ and $Bi_2Mo_3O_{12}$ had been measured and discussed in term of the bond length/bond strength relationship.

13 Molecular-Dynamics Study of the Nucleation Process at Solid-Liquid Interfaces

April 1991 to March 1994

K. Kusunoki, Materials Physics Division

Keywords: molecular-dynamics simulation, nucleation, solid-liquid interface

We have studied the solidification mechanisms at solid-liquid interfaces using a molecular-dynamics simulation under the constant-pressure and the periodical boundary conditions (PBC). We applied the Lennard-Jones (L-J) type interatomic potentials for the construction of a model system of stacking A- and B-monoatomic crystals with fcc structure. The total number of A and B atoms are 1050 and 1470, respectively. The system is heated up to the melting temperature of the A-crystal, and then cooled down. In the course of this process, we observed that the melt A-material began to crystallize onto the flat surface of the B-crystal. However, the solidification front, where we observed creations and dissipations of clusters with an ordered structure, was not always parallel to the A/B interface. In every case of the simulation run, the solidification of the A-material resulted in generating a new crystal with an hcp structure, being different from its initial form. This might come from the use of the L-J type interatomic potentials and the PBC in the present system. It is to be noted that a large number of vacancies of about 1% are formed occasionally in the A-material after the completion of its crystallization.

14 High Resolution Transmission Electron Microscopic Study for Interfaces of Materials

April 1990 to March 1993

S. Ikeda, Surface and Interface Division

Keywords: HRTEM, Y_2O_3, $Bi_2Sr_2CaCuO_x$, ion track, irradiation induced structural images

We have studied structure images of Y_2O_3 and $Bi_2Sr_2CaCu_2O_x$ by means of a 400 kV-type High Resolution Transmission Electron Microscope (HRTEM).

The HRTEM image of $Ia\bar{3}$ structure was first observed for a crystal of Y_2O_3; where, inherent existence of oxygen-vacancies shift positions of Y-atoms by 0.035 nm from the cationic position of the CaF_2-type structure. Using an electron microscope with a point-to-point resolution of 0.17 nm, structure images different from the CaF_2 type structure were obtained. A staggered configuration of the spotting image corresponding to the shifted Y-atoms was observed for the (110) plane. Positions of oxygen vacancy chains in the (111) image could be detected by an image since the spacing of the atomic columns of Y-atoms is modified by the presence of the oxygen vacancy chain.

It is well known that ion irradiation enhances the irreversibility fields of $Bi_2Sr_2CaCu_2O_x$ superconducting material and increases the values of intragrain J_c. We have observed the irradiation induced structural damages in this oxide-tape of 15 μm thick by using the HRTEM. Highly damaged areas consist of long continuous cylindrical columns which vary from 2 to 8 nm in diameter. The core of the column is surrounded by an anisotropic strain field. The T_c reduces by irradiation of $10^{12}/cm^2$.

Annealing at 573 K after the irradiation, induces partial recovery of the values of T_c and J_c. The amorphous portion in the columnar defect reduces by the annealing, contributing to the reduction of the efficiency of flux pinning.

Related Papers

Structure Images of Y_2O_3 Corresponding to the Shift of Y-atoms, S. Ikeda and K. Ogawa, J. Electron Microsc. 41 (1992): 330.

High Resolution Electron Microscopy Observation of Defects in 180 Mev Cu^{11+} Ion-Irradiated $Bi_2Sr_2CaCu_2O_8$ Crystals, B. Chenevier, S. Ikeda, H. Kumakura, K. Togano, S. Okayasu and Y. Kazumata, Jpn. J. Appl. Phys. 31 (1992): L777.

Low-Temperature Annealing Effect on Superconducting and Structural Properties of Ion-Irradiated $Bi_2Sr_2CaCuO_x$ Crystals, B. Chenevier, H. Kumakura, S. Ikeda, K. Togano, S. Okayasu and Y. Kazumata, Jpn. J. Appl. Phys. 31 (1992): L1671.

HREM Observation of the Effects of 180 MeV Cu^{11+} Ion-Irradiation on the Crystal Structure of $Bi_2Sr_2CaCuO_x$, B. Chenevier, S. Ikeda, H. Kumakura, K. Togano, S. Okayasu and Y. Kazumata, Materials Research Forum 129 (1993): 17.

Phase transformation and microstructures

15 Super-Microscopic Study on the Mechanism of Martensitic Transformation in Shape Memory Alloys

April 1992 to March 1995

S. Kajiwara, Physical Properties Division

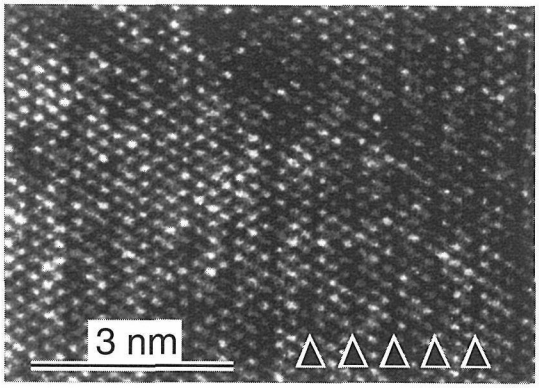

Fig. 1 Structure image of R phase in TiNi

Keywords: transformation, structure image, R Phase, shape memory

The purpose of this study is to clarify the mechanism of martensitic transformation in shape memory alloys by obtaining the structure image from high resolution electron microscope. The materials used in this study are a Ti-50.6Ni (at%) alloy and an Fe-13.4Mn-11.5Si-9.0Cr-4.7Ni (at%) alloy. The former alloy has been a very famous shape memory alloy for these thirty years and the latter is a cheap and rust proof Fe-based shape memory alloy which has been developed recently. In the former alloy, much attention has recently been paid to the transformation to R phase. The hysteresis of the transformation from the parent phase (b.c.c.) to R phase and its reverse transformation is very small, and it is considered that this transformation characteristic can be applied to some special use. However, the crystal structure of R phase is not clear yet. One of the characteristics of the diffraction pattern of the crystal structure is the extra spots which appear at the points corresponding to the one third of 011 reciprocal lattice vector. In this study, the structure image corresponding to these extra spots were taken by high resolution electron microscope. Figure 1 shows one of the results. In this picture, the arrays of <111> atoms are resolved, and vertical dark striations (indicated by arrows) can be seen with a period of three times that of {110} plane, which is considered to be due to the long periodicity of R phase.

Two kinds of specimens which have different degrees of shape recovery were used with regard to an Fe-13.4Mn-11.5Si-9.0Cr-4.7Ni alloy. One is a thermomechanically heated-treated specimen, which was cold-rolled by 10% and heated for 10 min at 970 K and another is a solution-treated specimen. The degree of shape recovery is 80 and 50%, respectively. The structure images were observed by high resolution electron microscope and it was found that the microstructure of the former specimen consists of the mixture of the parent phase (f.c.c.) and martensite (h.c.p.) on the nanometer scale, but the microstructure of the latter one

is not a mixture of them. The existence of the parent phase in martensite phase on an ultra fine scale is considered to contribute to the improvement of the degree of shape recovery.

Surface and interface properties

⑯ Structure and Electronic Properties of Silicides

April 1993 to March 1996
T. Hirano, Chemical Processing Division
Keywords: silicides, single crystal, interface, high-pressure

The purpose of the study is to investigate the structure and the electronic properties of metal disilicides. We will study that under two circumstances, i.e., at silicon/disilicide interface and under high-pressure.

In the former, the interface is formed by the growth of Si on single-crystalline substrates of transition-metal disilicides (M_TSi_2). M_TSi_2 is selected for the following reasons; (1) there are few experiments about semiconductor/metal interface formed on metal surface, and (2) Schottoky barrier height (SBH) of Si/disilicide interface is sensitive not only to the kind of metal but also to the structure of the interface. The structure of the interface is observed using transmission electron microscope, TEM. The electronic property will be studied using SBH measurements.

The experiments under the latter condition are carried out using a multi-anvil apparatus. We use alkaline-earth metal disilicides (M_ASi_2, M_A = Ca, Sr, Ba) as samples because of their characteristic Si atom configurations and large compressibilities of M_A atoms. When the sample is compressed, it undergoes phase transition. The structure and electronic properties of the high pressure phase will be discussed using x-ray diffraction and electrical resistivity measurements under pressure. Furthermore, we are going to discuss about the similarity among the transformation sequence under pressure in three M_ASi_2.

17 Study on Changing the Properties of Metallic-Oxide Films for Increasing the Hydrogen Permeability

April 1991 to March 1994
M. Amano, Physical Properties Division
Keywords: oxide film, hydrogen penetration, reaction method, hydrogen separation

It has been found that palladium-coated V-15at%Ni alloy membrane is a promising material for hydrogen separation. It shows good resistance to hydrogen embrittlement with hydrogen permeability larger than those of Pd-Ag alloy membranes. However, it reveals a conspicuous hydrogen-trapping phenomenon below 473 K. The phenomenon is mainly caused by the oxide film under the palladium overlayer. It is difficult to remove oxide film before palladium coating even in a high vacuum. The aim of this study is to increase the hydrogen permeability of oxide films on metals and alloys based on V_a elements by changing the composition and structure of the films through a reaction method. It has been found that the deposition of a few nanometer lanthanum or yttrium before palladium coating markedly suppresses the hydrogen-trapping phenomenon below 473 K for the V-15at%Ni alloy membrane. The depth profile of Auger electron spectroscopy analysis for the oxide film revealed that the vanadium oxide was reduced and the oxide consisting mainly of lanthanum or yttrium was formed underneath the palladium overlayer. The reaction method is applied to vanadium and niobium membranes.

18 Effect of Oxidation on Mechanical Degradation of Metallic Materials

April 1991 to March 1994
Y. Ikeda, Failure Physics Division
Keywords: spalling, diffusion, S segregation, Cr_2O_3 coating, REM, Y_2O_3

The results of our previous works showed that the spalling of Al_2O_3 coating film on alloys was promoted by S segregation at the coating film/alloy interface, but that the segregation and spalling were suppressed through either of rare earth metals (REM) addition or Y_2O_3 dispersion in alloys. The Y_2O_3 dispersion retarded furthermore the diffusion of alloying elements into the coating film, while REM addition did not have retardation effect. With the purpose of obtaining further information for the spalling and diffusion we used Cr_2O_3 coating film.

The surface segregation of S at 1100 K was examined on several alloys in Auger electron spectroscopy system. The same kinds of alloys were coated with Cr_2O_3 and cyclically heated up to 1100 K for spalling test or kept constant at 1200 K for diffusion test. Both REM addition and Y_2O_3 dispersion suppressed the S surface segregation and the spalling of Cr_2O_3. But the suppression of spalling was not so drastic as the case of Al_2O_3 film. The diffusion of alloying elements such as Cr and Mn occurred more rapidly into Cr_2O_3 film than Al_2O_3 film. Result of simulation experiment showed that Y_2O_3 dispersion would retard the diffusion of alloying elements into Cr_2O_3 film although somewhat less effectively than Al_2O_3 film.

Related Paper

Y_2O_3 Dispersion Effect on Al_2O_3 Protective Coating Examined on the Basis of Five Models, Y. Ikeda, K. Nii and M. Yata, ISIJ Int. 33 (1993): 293–306.

19 Study on Monolayer-controlled Materials by Using a Surface Tomographic Technique

April 1992 to March 1995
Y. Yoshihara, 4th Research Group
Keywords: monolayer-controlled deposition, surface tomography, epitaxy, angle-resolved spectrometer, real-time measurement

Top-most surface regions can be considered to be a new phase which has different chemical properties and atomic geometries from those of the bulk. This unusualness of surface region is stem from the redistribution of surface atoms in order to minimize the surface free energy, which causes various interesting phenomena such as surface segregation, surface precipitation, surface reconstruction etc. On the other hand, recent development of micro-electronics technology has enabled a monolayer-scale deposition of molecules or atoms, which has a possibility of development of artificially designed materials. Therefore, one of the main purposes of this project is to establish an elemental technique for synthesizing such kinds of artificially surface-controlled materials by using a thermodynamically equilibrium state or a molecular beam epitaxy method. Another theme of this project is to develop a new analytical method for surface tomography, that is to say, SET (Surface Electron-spectroscopic Tomography) in order to clarify both of atomic concentrations and atomic arrangements of the above monolayer-controlled materials in a layer-by-layer manner. This project can be divided into three categories as follows.

1. Synthesis of monolayer-controlled materials.
   As a model sample for monolayer-controlled material, epitaxially grown monolayer and multilayer graphite have been deposited on the surface of Ni(111) by using the surface precipitation of dissolved carbon atoms. Structure and kinetics have been studied preliminary by AES, ARXPS and LEED.
2. Acquisition of high-resolution spectra of emitted electrons.
   In order to obtain fundamental data for electron scattering by atoms in the surface regions, a new highly energy-resolved and angle-resolved electron spectrometer has been designed and constructed, in which a concentric hemispherical analyzer with a small acceptance angle can move along the hemisphere above the specimens to be measured.
3. Development of a real-time technique for surface tomography.
   Since monolayer-controlled deposition is a kind of dynamical surface process, it is required that a surface tomography can be performed in a real-time manner. In order to do that a new direct visualization mirror type analyzer has been roughly designed.

20 Fabrication of Quantum Well Box Systems by Droplet Epitaxy for Advanced Optoelectronic Devices

April 1991 to March 1996
N. Koguchi, Surface and Interface Division
Keywords: quantum well boxes, molecular beam epitaxy, GaAs, GaAlAs, sulfur-termination

Predictions of enhanced electron mobility device and advanced semiconductor laser with high monochromized and low threshold current density have been made for the applications of quantum well box systems. It is necessary to grow many nm-size epitaxial microcrystals to fabricate the quantum well box system. Molecular beam epitaxy (MBE) is successfully used in the growth of finely layered structures and quantum well wires. However, comparable success has not been achieved in the production of structures for quantum well boxes.

We have proposed a new MBE growth method called droplet epitaxy for the fabrication of some III-V compound semiconductor epitaxial microcrystals. This method is based on V-column element incorporation into the III-column element droplets deposited on the inert substrate for the monolayer adsorption of the III- and V-column elements. We have found that the III-V compound semiconductor surfaces terminated with a VI-column element such as S, Se or Te are suitable for the growth of epitaxial microcrystals by droplet epitaxy. Numerous GaAs epitaxial microcrystals with rectangular bases and (111) facets were fabricated on an S- or Se-terminated GaAlAs surface. The average base size of the GaAs microcrystals was about 10 nm × 10 nm. The growth mechanism is a vapor-liquid-solid mechanism. We can use this method to fabricate GaAs quantum well boxes.

Related Papers

New MBE Growth Method for InSb Quantum Well Boxes, N. Koguchi, S. Takahashi and T. Chikyow, J. Crystal Growth 111 (1991): 688–92.

Microcrystal Growth on an Se-terminated GaAlAs Surface for the Quantum Well Box Structure by Sequential Supplies of Ga and As Molecular Beams, T. Chikyow and N. Koguchi, Appl. Phys. Lett. 61 (1992): 2431–33.

Growth of GaAs Epitaxial Microcrystals on an S-terminated GaAs Substrate by Successive Irradiation of Ga and As Molecular Beams, N. Koguchi and K. Ishige, Jpn. J. Appl. Phys. 31 (1993): 2052–58.

Growth of GaAs Epitaxial Microcrystals by Droplet Epitaxy (Review), N. Koguchi, Bulletin of Jpn. Inst. Metals 32 (1993): 485 (in Japanese).

21 Crystal Growth on the Surface of Inter Metallic Compounds

April 1990 to March 1993
T. Hirano, Chemical Processing Division

Keywords: surface, interface, $CaSi_2$, $CoSi_2$

The purpose of this study is to investigate the surface properties of intermetallic compounds and characteristics of the metal/semiconductor interface formed on intermetallic compound surfaces. Especially, we focus on two subjects, (1) the surface of calcium disilicide ($CaSi_2$) and (2) Si/Cobalt disilicide ($CoSi_2$) interface.

Surface of $CaSi_2$

The crystal of $CaSi_2$ shows layer-by-layer packing structure in which hexagonal Si bilayers alternate with hexagonal Ca monolayers along the [111] direction. The single crystal of $CaSi_2$ exhibits a very smooth cleaved (111) surface just like mica. The cleaved $CaSi_2$ (111) plane exhibited atomically smooth terraces with steps, and secondary electron microscope (SEM) images showed a dark and bright contrast on the terrace. The Auger intensities showed a clear contrast corresponding to the SEM image contrast: The intensity of Si *LVV* was high in the dark region and low in the bright region, while the intensity of Ca *LMM* was reversed. The surface termination of the cleaved $CaSi_2$ (111) was quantitatively determined from AES point analysis such that the dark region was terminated in the Si bilayer and the bright region in the Ca monolayer. The results showed that cleavage occurs between the Ca monolayer and Si bilayer.

Si/$CoSi_2$ interface

Si was grown on $CoSi_2$ (111) substrate at 400 °C using a magnetron sputtering method after cleaning the substrate with RCA solution. Schottoky barrier height (SBH) was measured with a current-voltage method. The value of SBH is 0.65 eV and this is in agreement with the previously reported value. For a further study, it is necessary to control the structure at the interface. To its end, a molecular-beam-epitaxy Si growth is under experiment.

Related Papers

Single Crystal Growth and Electrical Properties of $CaSi_2$, T. Hirano, J. Less-Common Metals 167 (1990): 329–37.

Surface Analysis of Cleaved Single-Crystalline $CaSi_2$ by Auger Electron Spectroscopy, T. Hirano and J. Fujiwara, Phys. Rev. B 43 (1991): 7442–47.

Mechanical properties

㉒ Toughness Improvement of Brittle Ceramics and Steels by Precipitation and Phase Transformation Control

April 1993 to March 1996

F. Abe, Mechanical Properties Division

Keywords: toughness, zirconia ceramics, martensitic steels, precipitation, phase transformation

The purpose of the present research is to investigate the microstructural evolution in brittle materials, such as zirconia ceramics and neutron-irradiated martensitic steels, and to improve their toughness by microstructural control.

Stress-induced transformation from tetragonal to monoclinic phase near a proceeding crack tip is responsible for the high fracture toughness of partially stabilized zirconia ceramics. The stability of tetragonal phase is hence a primary need for transformation-induced toughening and can be controlled by several microstructural and chemical factors, such as grain size, tetragonal particle size and alloy composition. In this research, the precipitation behavior of tetragonal particles from the supersaturated solid solution of cubic matrix and the subsequent tetragonal to monoclinic phase transformation behavior are systematically investigated for zirconia ceramics containing 4-8mol% CaO, 4-10mol%MgO or 15mol%Y_2O_3 by means of TEM and dilatometry. The change in fracture toughness K_{IC} induced by phase transformation is evaluated by means of indentation method.

Irradiation effects on ductile-to-brittle transition temperature (DBTT) and fracture properties are of great concern for fusion applications of ferritic/martensitic steels. In this research, the relationship between irradiation hardening/embrittlement and microstructural factors, such as carbides, dislocations and lath-martensite subgrains, is investigated for martensitic 9Cr steels developed at NRIM by means of tensile and Charpy impact tests and TEM, after irradiation in Japan Materials Testing Reactor (JMTR). The final goal is to suppress the irradiation embrittlement by controlling the precipitation of carbides and the distribution of dislocations produced by martensitic transformation.

㉓ Study on Deformation and Fracture of Structural Materials at Cryogenic Temperatures

April 1993 to March 1996

K. Nagai, Mechanical Properties Division

Keywords: cryogenic temperature, plastic instability, fatigue strength, fracture toughness

Deformation mechanism in a small strain range determines the mechanical properties of metals and alloys at cryogenic temperatures. A uniform plastic strain is very small at liquid helium temperature due to plastic instability in a small strain-range. In this study, therefore, a method to measure a micro-strain precisely in liquid helium has to be developed, and then a monotonous plastic flow under load-controlled deformation, an alternating plastic flow under constant strain-range deformation, and a low temperature creep flow are investigated mainly for austenitic stainless steels.

Fracture criterion such as fracture toughness or fatigue strength is practically a function of metallurgical factors. However, the intrinsic contribution of microstructure on the fracture criterion has not yet been clarified quantitatively. Cryogenic test has merits to extract the intrinsic effect of microstructure: 1) Fracture behavior is often influenced by chemical reactions like oxidation, atomic diffusion etc. However, the chemical effects are minimized in a cryogenic temperature regime. 2) Material strength has a strong effect on the criterion and also varies with microstructure. In the cryogenic regime, the material strength changes with test temperature without varying microstructure. In this study, long-term fatigue strength under load-controlled fatigue test is primarily determined for typical cryogenic structural alloys like nickel steels, titanium alloys and aluminum alloys. The microstructural effect on fatigue properties and fracture toughness is elucidated for two-phase alloys such as ferritic steels and titanium alloys.

㉔ Study on Deformation and Fracture under Irradiation

April 1993 to March 1998

J. Nagakawa, 2nd Research Group

Keywords: irradiation, radiation damage, deformation, fracture

Among the various changes in materials properties induced by neutron irradiation, a change in mechanical properties is one of the most important property alterations in the structural materials for nuclear reactors. The change causes a significant influence on endurance of the structural components.

The effects of irradiation on the mechanical properties can be classified into two groups. One is the post-irradiation effect, e.g., the irradiation embrittlement, caused by radiation-induced defects those can survive long after the irradiation. The other effect is an *in-situ* type, e.g., irradiation creep, which is induced by the free point defects dynamically produced and migrating during irradiation. NRIM has been successfully carrying out the irradiation creep evaluation using the NRIM small cyclotron accelerator and the *in-situ* testing equipment. Also, a computer simulation study has been performed to analyze and predict the deformation behavior of materials under irradiation from aspects more than a simple irradiation creep, for example, radiation induced stress relaxation and transient behavior at low temperatures.

A new research project has been initiated since this fiscal year to experimentally evaluate, analyze and theoretically predict the interaction between deformation and fracture properties of materials under irradiation. The loading conditions of the core components in nuclear reactors are mostly combination of constant and cyclic stress or constraint. Therefore, the radiation induced deformation such as irradiation creep or radiation induced stress relaxation must be strongly influencing the fracture behavior like fatigue in the materials under irradiation. An equipment which can carry out a creep-fatigue type testing under light ion irradiation will be constructed this fiscal year and connected to the NRIM cyclotron after the completion of a new irradiation chamber next year. Effects of nuclear transmutation products like helium or hydrogen on the deformation-fracture interaction will also be examined using the NRIM cyclotron and new equipments.

Related Paper

Calculational Evaluation of Radiation Induced Deformation, J. Nagakawa, Proc. of the 4th Int'l Symp. on Advanced Nuclear Research (1992): 387–91.

Collaboration Research

Effect of Transmutation Products on the Mechanical Properties of Nuclear Materials (with JAERI, Oct. 1992 to Mar. 1995).

25 NRIM Fatigue Data Sheet Project-IV

April 1990 to March 1994

S. Nishijima, Failure Physics Division

Keywords: fatigue of metals, standard reference data, steels and alloys, aluminum alloys

This project is aiming at the establishment of standard reference data on the basic fatigue properties of Japanese engineering materials most commonly used for machines and structures under fluctuating loads.

The work has been conducted since 1975 under successive five-year-term programs. In the present term IV, emphasis is put on the ambient temperature properties of high strength steels and aluminum alloys, intermediate temperature properties of steels for pressure vessels, and high-temperature time-dependent properties of heat-resistant alloys. A brief summary of NRIM fatigue Data Sheets is given in table 1.

In parallel with the testing program, series of basic researches are being conducted to understand materials behavior and mechanisms of degradation under fatigue environment. Some of the latest concerns are: equivalence of steels and aluminum alloys in terms of strain based fatigue strengths, quantitative evaluation of the effect of non-metallic inclusions in hard materials, cyclic softening mechanism of weld metals, interaction of strain aging at intermediate temperatures, elaboration of a new time-temperature parameter method predicting creep-fatigue interaction processes, and so on.

Table 1 Summary of NRIM Fatigue Data Sheets, as of March 1993

Subtheme	Items Investigated	Issued
Machine Structural Materials	High-/Low-Cycle Properties on: carbon/low-alloy steels, stainless steels, carburizing steels, spring steels, tool steels, aluminum alloys	32
Welded Joints of Structural Materials	High-/Low-Cycle and Crack Growth Properties looking at the Effect of: specimen size, welding procedure, stress ratio, weld/HAZ materials, and for aluminum alloys, as well	20
Elevated Temperature Materials	Time Dependences in High-/Low-Cycle Properties for: carbon/low-alloy steels, stainless steels, and heat-resisting alloys	20

The output data thus validated by the basic researches have been published and exchanged worldwide with scientific and technical organizations. An on-line data service is available from the Japan Information Center for Science and Technology since 1990. It is anticipated that the NRIM Fatigue Data Sheet Project contributes largely to the safe and effective use of engineering materials.

Related Papers

Fundamental Fatigue Properties of JIS Steels for Machine Structural Use, S. Nishijima, NRIM Special Report, SR-93-02 (1993): 34pp.

Effect of Yield Strength on Basic Fatigue Strength of Welded Joints, A. Ohta, Y. Maeda, and N. Suzuki, Fatigue and Fracture of Engineering Materials and Structures 16 (1993): 473–79.

Parameter Analysis for Time-Temperature Dependence in Low-Cycle Fatigue, K. Yamaguchi, K. Kobayashi, K. Ijima and S. Nishijima, (accepted for publication in Trans. ASME).

26 Controlling and Recovering Methods for High Temperature Damage

April 1991 to March 1994

N. Shinya, Failure Physics Division

Keywords: grain boundary cavities, sintering, self-recovering, life extension

Low ductility fracture of metals after long term high temperature creep results from the progressive accumulation of grain boundary cavities throughout the creep process. So that, the acquirement of technologies for controlling and recovering the cavities are important for the development of reliable heat resisting alloys and as well as for the maintenance of high temperature components. In this work, a sintering mechanism and a self-recovering mechanism of cavities are studied, and a creep life extending system, based on control of the cavities, is being developed.

Sintering of grain boundary cavities

Samples of a low alloy steel were crept to induce grain boundary cavities, and then annealed or compressively crept to make the cavities shrink. The progressive sintering of the cavities due to the treatments was monitored using the highly sensitive density measurement technique. The results show that sintering rates under compressive creep are rapid and depend proportionally on compressive creep rates, whereas annealing causes only slight sintering. Two models of diffusional and constrained cavity growth are applied for the calculation of sintering rates. It is shown that the sintering rates calculated using the constrained cavity growth model are coincident with the experimental data.

Extension of creep life

The investigation for the rejuvenation of material to prolong its creep life is concentrated on the elimination of grain boundary cavities induced by creep. To eliminate the cavities, stress-free annealing, hot isostatic pressing and compressive creep were conducted by interrupting creep test. The results of repetitive creep/sintering cycle test are as follows:

1. Stress free annealing had no significant effect on the rupture life. The limiting life extension is due to insufficient sintering of the cavities and over aged microstructure.
2. Hot isostatic pressing and compressive creep remove completely the cavities, and extend the rupture life considerably.

27 NRIM Creep Data Sheets (IV)

April 1991 to March 1996

C. Tanaka, Environmental Performance Division

Keywords: NRIM Creep Data Sheets, heat-resistant metallic materials, long-term creep and rupture tests

The objectives of this program are the collection of 10^5 h creep and rupture strength data in long-term creep and rupture tests on heat-resistant metallic materials, the publication of these data as the series of NRIM Creep Data Sheets, the investigation on long-term creep deformation behavior and creep rupture properties of these material, and the development of evaluation method for long-term creep and rupture strength at high temperature.

This program has been continued since 1966 in order to obtain long-term creep testing data of many kinds of domestic steels and alloys. NRIM Creep Data Sheets of four kinds of materials as listed in Table 2 were published in fiscal year 1992. As short-term creep rupture data on mod. 9Cr-1Mo and 9Cr-2Mo steels were obtained, long-term creep and creep rupture tests up to about 10^5 h were started. The manuscript of Technical Document concerning creep and rupture testing techniques, which have been accumulated during the period of this program, is being produced.

Table 2 NRIM Creep Data Sheets which were published in fiscal year 1992

Year of Issued	No.	Material
September, 1992	37A	25Cr-12Ni-0.4C Steel Castings, JIS SCH 13
September, 1992	39A	Ni Based 15.5Cr-2.5Ti-0.7Al-1Nb-7Fe Superalloy Bars for High-Temperature Service, JIS NCF 750-B
March, 1993	22B	Fe based 15Cr-26Ni-1.3Mn-2.1Ti-0.3V Superalloy Forgings for Gas Turbine Discs
March, 1993	34B	Ni based 19Cr-18Co-4Mo-3Ti-3Al-B Superalloy Castings and Forgings for Gas Turbine Blades

Long-term creep and rupture strength of steels and alloys at high temperature was investigated using the creep data and the ruptured specimens which have been obtained in NRIM Creep Data Sheets project. The main subjects investigated are as follows; (1) long-term creep strength of ferritic steels was evaluated on an inherent creep strength concept. The inherent creep strength of these steels seems to be dependent on carbon and very small amount of molybdenum; (2) the creep deformation behavior of 1Cr-0.5Mo and 1.25Cr-0.5Mo-Si steels was evaluated using a modified θ projection concept. Creep deformation behavior and rupture strength for these materials were expressed well using two parameters by which the softening behavior was described; (3) heat-to-heat variation of creep-rupture strength for SUS 347 steel was studied in view of microstructural change and damage formation; (4) Iso-stress tests were conducted on NRIM Creep Data Sheet steels and alloys in order to verify the applicability of the present method to prediction of remaining life.

These activities are expected to contribute to ensuring safety and reliability of structural components of high temperature plants and developing new materials.

Related Papers

Governing Factors of the Inherent Creep Strength of Ferritic Steels, K. Kimura, H. Kushima, K. Yagi and C. Tanaka, Report of 123rd Com. on Heat-Resisting Metals and Alloys, JSPS 33 (1992): 131–41 (in Japanese).

Evaluation of Creep Deformation and Rupture Life of 1.3Mn-0.5Mo-0.5Ni Steel by Modified θ Projection Concept, H. Kushima, T. Watanabe, K. Yagi and K. Maruyama, Tetsu-to-Hagane 78 (1992): 918–25 (in Japanese).

Effect of Microstructures on Creep Rupture Properties for SUS 347H, H. Tanaka, M. Murata, K. Yagi and C. Tanaka, Report of 123rd Com. on Heat-Resisting Metals and Alloys, JSPS 33 (1992): 313–21 (in Japanese).

28 Effect of Surface Film on Deformation of Bulk Matrix Material

April 1991 to March 1994

K. Kanazawa, Environmental Performance Division

Keywords: fatigue crack initiation, dynamic ultra micro hardness tester

A surface crack is not easy to initiate under high-temperature, high-cycle fatigue in air environment, as films at the specimen surface prevent dislocations from slipping off from the surface. This project aims at studying the effect of surface films on deformation of bulk matrix material to evaluate the resistance of surface films to fatigue crack initiation from the surface.

As an example of surface films, oxide film formed on a matrix surface of low alloy steel has been examined. Hardness of oxide film and its thickness are measured by using a dynamic ultra micro hardness tester. The hardness is higher than that of the matrix.

29 Evaluation of Crack Initiation and Growth of Superalloys under Creep and Creep-Fatigue Conditions

April 1991 to March 1994

K. Yagi, Environmental Performance Division

Keywords: creep crack growth, creep-fatigue crack initiation and growth, superalloy

The understanding of crack initiation and growth behavior under creep and creep-fatigue loading conditions is important for life prediction of high temperature structural components. In this study, the crack initiation and growth behavior of superalloys under creep and creep-fatigue conditions is being investigated in terms of microscopical creep fracture mechanisms.

Creep crack growth behavior

The creep crack growth tests of Inconel 713C were conducted at 1173 K and 1273 K. Creep crack growth rate *da/dt* could be characterized by C^* parameter even in this brittle material except for the initial transition stage of crack growth. The effect of size and configuration of γ' phase on *da/dt* is being investigated.

The long-term creep crack growth tests were conducted on SUS 316 steel and NCF 800H alloy. The effect of intergranular creep damaged zone ahead of the crack tip on *da/dt* was studied.

Creep-fatigue crack initiation of Fe-base superalloy

The systematic interrupted creep-fatigue tests were conducted on NCF 800H alloy. The number of intergranular cavities and the A parameter were measured on these interrupted specimens. The contours of constant A parameter from which the remaining creep-fatigue life could be predicted were made.

The creep-fatigue crack growth tests are being conducted on SUS 316 steel and NCF 800H alloy under some conditions at which the different three types of crack growth, i.e. wedge-type, transgranular, and cavity-type intergranular fracture are observed.

Related Papers

Long-term Creep Crack Growth Behavior of 316 Stainless Steel, M. Tabuchi, K. Kubo and K. Yagi, J. Soc. Mat. Sci. Japan 41 (1992): 1255–60.

Relationship Between Creep Damage Mode and Creep-Fatigue Interaction for SUS 321 Steel, K. Kubo, O. Kanemaru and K. Yagi, J. Soc. Mat. Sci. Japan 42 (1993): 1–7.

30 Fatigue Behavior of Brittle Materials at Elevated Temperatures

April 1992 to March 1995

Y. Kawabe, Mechanical Properties Division

Keywords: cyclic fatigue, elevated temperatures, ceramics

The development of ceramics is being watched with knee interest, because they are very promising as structural components for engineering applications where metallic materials are not available. Since many of them are subjected to static or cyclic loading at elevated temperatures for prolonged periods, it is important to understand fatigue behavior at elevated temperatures. Nevertheless, there are very few studies on the cyclic fatigue behavior of ceramics at elevated temperatures.

In a prior study, we have evaluated fatigue properties for various kinds of nontransforming ceramics at room temperature and suggested a crack resisting-reactivating model as fatigue mechanisms. However, it is doubted if this mechanism is available at elevated temperatures. Recent studies have shown that cyclic loading has a beneficial effect at high temperature, compared to static loading. Such results are inexplicable by any fatigue mechanisms proposed for room temperature so far. Systematical investigation for various kinds of ceramics is, thus, required to understand the difference at room and high temperatures.

As the first stage of this work, cyclic fatigue crack growth behavior in normally sintered silicon nitride was investigated over a range from room temperature to 800 °C. It was found that the crack growth rate are markedly affected by temperature, especially in lower stress intensity factors. It is supposed that such influence of temperature is responsible for environmental effect and/or viscous flow behavior of glassy phase which is changed with increase of temperature.

Related Paper

Cyclic Fatigue of Ceramic Materials: Influence of Crack Path and Fatigue Mechanisms, S. Horibe and R. Hirahara, Acta Metall. Mater 39 (1991): 1309–17.

31 Fatigue Crack Initiation Process in Corrosive Environment

April 1991 to March 1994

R. Hamano, Mechanical Properties Division

Keywords: corrosion fatigue , pre-crack deformation, early fatigue crack growth, high strength, slip localization

Fatigue lives of structural materials extremely decrease in corrosive environments, in comparison with laboratory air. However, we have no definite mechanisms on how the corrosive environments play an important role on the crack initiation or crack propagation process of fatigue. Therefore, it is needed to investigate the environmentally-assisted fatigue damages in the processes such as (a) pre-crack cyclic deformation, (b) microcrack initiation with its early propagation, and (c) long crack growth.

In the present study, the emphasis is put on the processes of pre-crack cyclic deformation and early crack propagation of high strength materials.

We examined the fatigue crack initiation processes in atmospheres of purified argon and saturated water vapor at 293 K, using notched specimens of high strength aluminum alloys. Load ratio of 0.1 and sinusoidal wave of a frequency of 1.0 Hz were employed. In the purified argon gas, fatigue cracks oriented with an angle of 45 degrees to the notch root surface and propagated along slip line directions, i.e., maximum shear stress directions. In the saturated water vapor, however, the directions of fatigue crack easily deviated from maximum shear stress mode to maximum tensile stress mode. This early transition of fatigue cracks from shear stress mode to normal stress mode be attributable to the environmental embrittleness susceptibility of materials in saturated water vapor. The above results suggest strongly that environmental effects on pre-crack cyclic deformation and crack nucleation processes are of importance.

32 High Temperature Deformation and Fracture in Polycrystalline Oxide Ceramics

August 1992 to March 1995

K. Hiraga, Mechanical Properties Division

Keywords: oxide ceramics, intergranular glassy phase, tensile deformation, cavitation

This study aims at clarifying the role of intergranular glassy phase and cavitation in the high temperature deformation and fracture of fine-grained oxide ceramics. For this purpose we have been trying to intentionally introduce some kinds of glassy phases into high purity zirconia- and alumina-base oxides. We are examining the deformation behavior of these oxides as a function of

temperature, strain rate, grain size and the thickness of the glassy phases under uniaxial tension in vacuum. The analysis of cavity growth in the deformed oxides with and without the glassy phases is also in progress by applying theoretical models to cavity size distribution functions measured with a high resolution SEM.

33 Mechanism of Fretting Fatigue Failure in Metallic Materials

April 1991 to March 1994
M. Sumita, Mechanical Properties Division
Keywords: fatigue, fretting, failure mechanism, contact pressure, relative slip amplitude

Fretting damage is known to have a detrimental effect on fatigue behavior of structural materials. Many factors control the fretting fatigue. This research was planned aiming a fundamental understanding of the mechanism of fretting fatigue failure from a microstructural viewpoint.

One of the important factors which influences fretting fatigue strength is the behavior of stick region on the contact area. We found that the fretting fatigue life exhibited a minimum at low contact pressure and a maximum at intermediate contact pressure. The mechanism was explained by the stress concentration at the fretted area accompanied by the change of slip mode. Cracks are initiated at the boundary between the stick region and slip region on the contact area.

We also found that the fretting fatigue life exhibited a minimum at low relative slip amplitude. The phenomenon could be explained by the same mechanism on the minimum in the fretting fatigue life appeared in the contact pressure dependence. The behavior of the stick region seems to be controllable.

In order to examine the role of second phase in the above mechanism, metal matrix composites and surface modified metallic materials were prepared.

Related Paper

Effect of Contact Pressure on Fretting Fatigue of High Strength Steel and Titanium Alloy, K. Nakazawa, M. Sumita and N. Maruyama, ASTM STP (1992): 115–25.

[34] Tensile Fracture Mechanism of Continuous Ceramic Fibers

April 1990 to March 1993
C. Masuda, Failure Physics Division
Keywords: ceramic fiber, tensile strength, probability, fracture mechanism

Several kinds of continuous ceramic fibers are used for reinforced materials in composites such as plastic matrix-, metal matrix- or ceramic matrix-composites. Tensile strength of those composites is strongly depends on the strength of the reinforcement fibers. In order to obtain the basic data of the strength of mono-filament, tensile tests have been performed in this study for the ceramic fibers of boron fiber, silicon carbide fiber and carbon fiber in relation to their probability of strength and fracture mechanism.

In these fibers, cracks were observed to start from many kinds of defects: pores which situated at surface, inside of fibers, at the interface between inner core fiber and mantle or between silicon carbide and carbon coat. Cracks propagate by forming mirror zone, mist zone and hackle zone until final failure occurs. It is considered that the mirror zone be formed by slow crack growth, because mirror zone is very flat. On the while, the hackle zone be formed by fast crack growth, because the aspect of fracture surface is very irregular. There are many small debris on the corrosion surface of the mist zone. It is suggested that main cracks stop and form many subcracks at their tips to dissipate strain energy. In the case of silicon carbide fiber, however, whose surface being coated by carbon the crack initiation was not clear.

The depth of mirror zone is discussed in relation to the maximum stress intensity factor for the fibers. This intensity factor is constant for surface fracture, and for the interior mirror zone of inner fracture, though the magnitude of the factor for the latter is one half as large as that for the former. The slope of the probability of fracture strength was small for large initial defects on Weibull probability graph.

The data obtained in this study are surely very useful to analyze the fracture strength and discuss the fracture process in metal matrix or ceramic matrix composites reinforced with boron fibers, silicon carbide fibers and/or carbon fibers.

Related Paper

Tensile Fracture Mechanism for Boron Fiber, Y. Tanaka and C. Masuda, The Soc. Mat. Sci. Japan 40 (1991): 869–74.

Measurement and evaluation

(35) *In-situ* Measurement of Local Strain in High Temperature Range of Material and Detection of Defects by the Laser Speckle Method

April 1993 to March 1996
Y. Muramatsu, Advanced Materials Processing Division
Keywords: laser speckle method, dynamic strain, *in-situ* strain measurement, high temperature

A laser speckle method for strain measurement is a unique method which is able to measure responsively the surface strain of any materials

without contact. This method has been developed for the static strain measurement, for example in the tensile tests. We have been made sure that the laser speckle method is also available for the *in-situ* dynamic strain measurement in high temperature range during the welding process. We confirmed that the laser speckle method is able to follow the dynamic strain and it shows correct tendencies qualitatively.

An improvement of a quantitative measuring accuracy, however, is our main objective of next three years. For this purpose, the calibration of this method in high temperature range and checking some effects by the fundamental movement of the specimen, a rigid body motion, local distortion or local expansion against the detectors should be done.

Moreover, it is expected that the relation between high temperature defects which occurred in a stainless or aluminum plate and the local strain can be examined from a new standpoint, using this method.

Related Paper

Application of the Laser Speckle Method to Strain Measurement in the Welding Process, Y. Muramatsu and S. Kuroda, Jpn. Quarterly J. of Japan Welding Society 10 (1992): 125–31.

(36) Correlation between Plasma Parameters and Evaporation in Free Arcs

April 1993 to March 1996

K. Hiraoka, Advanced Materials Processing Division

Keywords: plasma structure, current density, spectroscopy, probe measurement

The goal of this new research program is to find out basic parameters by which the evaporation behavior can be controlled at a melting anode material in free arcs containing an active gas. For this purpose, both plasma structures (such as local plasma composition, temperature and electron density in front of anode) and anode modes classified with current density must be discussed under various arc conditions at the same time.

As a first step of this research, a light spectroscopic method developed to analyze local composition and temperature of a mixed gas arc plasma at more than 15,000 K (as shown in 93's topics in NRIM Research Activities) will be modified in order to apply to the plasma below 15,000 K near the anode. Then, the obtained electron density will be compared with that estimated by a stark-broadening method. These comparison will verify the existence of a local thermodynamic equilibrium in the lower temperature plasma region.

Secondly, a method developed to estimate the current density distribution at a melting anode (as shown in 91's topics) will be constructed in a chamber for arcs containing the active gas, and then the degree of current concentration at the anode will be investigated as the arc conditions and the plasma gas components change.

From the procedures mentioned above, it is expected that the correlation between plasma structures near the anode and the evaporation depended current distributions at the anode is made clear.

(37) On-line Determination of Order Parameters in Alloys from Electron Diffraction by CCD Camera System and Its Application to Examination of Ordering Process

April 1993 to March 1995

T. Kimoto, Materials Characterization Division

Keywords: order parameter, on-line determination, cooled CCD camera, ordering process

Long-range order (LRO) parameter can be determined from the ratio of intensities of superlattice and fundamental spots, and short-range order (SRO) parameter can be determined from the intensity distribution of diffuse scatterings. If we use conventional film to record electron diffraction pattern, however, it is impossible or very difficult to determine order parameters by measuring the electron diffraction spots intensities because the detectable range of intensities (dynamic range) on film is very small (usually 10–100). Therefore, quantitative examinations of order parameters have been performed so far by using x-ray and/or neutron diffraction. If we use x-ray or neutron diffraction technique, however, it takes a lot of time (1–3 weeks) to determine order parameters and it is impossible to determine order parameters in a very small region (less than 0.01 mm).

One of the objectives of the present research is to develop the on-line system to determine precisely LRO and SRO parameters from electron diffraction by using the cooled CCD camera detection system attached to a transmission electron microscope (TEM). The system has been developed from April 1992 to March 1993. The dynamic range of the cooled CCD camera is between 40,000 and 64,000. The following steps are necessary in order to develop so-called "on-line order parameter determination system:"

1. To make a theory which determines order parameters from electron diffraction pattern from the fundamental diffraction theory, considering inelastic scattering effects,
2. To make a computer program based on the theory in (1) in order to realize the on-line determination of order parameters,
3. To improve the system by comparing the order parameters obtained by the system with those obtained by the x-ray diffraction technique.

The other objective in the present research is to examine ordering process by using the developed "on-line order parameter determination system." The following researches are planned:

1. To examine how order parameter varies with location by determining order parameter in several small regions,
2. To examine the effects of super-saturated vacancies, which are introduced by annealing at high temperature and rapid quenching, on ordering process,
3. To examine the effects of specimen thickness on ordering speed, which is important in the thin specimen for electron diffraction.

(38) Electrochemistry and Modeling of Corrosion of Metals under Thin Water Layer

April 1993 to March 1996

T. Kodama, Environmental Performance Division

Keywords: thin water layer, kelvin probe, potential distribution

Wet corrosion reaction occurs through thin layer of water on metal surfaces. The examples of this case are atmospheric corrosion, indoor corrosion, dew point corrosion etc.. These electrochemical reactions occur on the boundary between thin layer of water and metal surface. The reaction rate in this case is generally larger than that of bulk solution environment, because of higher activity of mass transfer or accelerated diffusion. Little information is available on the mass-transfer and distribution of local electrochemical potential or current because of experimental difficulties in the measurements of these values. Our purpose of this study is clarifying wet corrosion mechanism through thin water layer by using a non-contact type vibrating electrode technique.

To study metallic corrosion under thin water layer, we attempt to prepare prototype models of a non-contact electrode (Kelvin probe) and an electrochemical cell. In this cell, the thickness of water layer on metal surface can be controlled from a few hundreds to 10 μm. A probe with 1 to 0.5 mm diameter will be prepared for the purpose of measuring the distribution of local electrode potential. Finally, our purpose is the development of a probe with a smaller diameter for microscopic measurement of potential distribution on metal surface. Electrochemical measurement by using a micro-reference electrode (conventional contact-type electrode) will also be carried out for the purpose of comparing potentials, measured by the non-contact probe and conventional one. From the measurement by these probes, we will extend the project for the determination of mass-transfer through thin layer water and distribution of potential or current on metal surface.

(39) Studies on Advanced Characterization Methods of Metals and Alloys Using Synchrotron Radiation

April 1993 to March 1998

K. Ohno, 1st Research Team

Keywords: synchrotron radiation, near-surface analysis, grazing incidence reflectometry, labo-XAFS

New generation storage ring provides an extremely high intensity in high energy region, typically, 40–100 keV, where any other appropriate x-ray source has not been developed so far. The major advantages of the storage ring, namely the parallel-beam, higher intensity and easy wavelength selectivity, are highly attractive for the development of the new characterization methods of metals and alloys. This program includes the following categories:

Near-surface analysis and multi-layer thin film analysis

The parallel-beam x-ray source is promising for the characterization of the surfaces and buried interfaces of multi-layer thin films by grazing incidence x-ray reflectometry. The source allows us to employ a specular reflection technique to characterize the surface uniformity, oxidation layer thickness, density and interface-roughness of the multi-layer films. The program includes the development of a high angular resolution reflectometer and a least-square refinement of techniques for high precision reflectivity analysis.

Development of analytical techniques with high energy SR source

X-ray fluorescence/absorption spectroscopic analyses of heavy elements using K-lines absorption edges are promising from a point of high sensitivity. Elastic and inelastic scattering in high energy region are also attractive for characterization of materials. Besides the experiments using SR, this program treats some instrumentation in a laboratory scale. Development of a labo-XAFS facility is one of the most important topics. In the previous study, a new x-ray generator, which provides extremely high tube current at low tube voltage, has been developed, and used for the conventional transmission XAFS experiments. Furthermore, it has a capability to enable the fluorescent XAFS measurements that are important to characterize trace chemical species. Instrumentation of the fluorescent mode is planned in this program.

40 *In-Situ* Analysis/Evaluation of Radiation Damage in Materials

April 1988 to March 1994

K. Furuya, Materials Characterization Division

Keywords: radiation damage, *in-situ* analysis,

dual-beam ion irradiation, SUBNANOTRON, 1 MV TEM, Si, 70 keV Ar^+, 20 keV H^+

Radiation damage of metallic materials is characterized by the atomic displacements associated with the destruction of crystalline structure by the irradiation of energetic particles such as neutrons and ions. Many types of defects and defect clusters are supposed to be produced by this atomic process and the resultant microstructure generally become complicated with the formations of dislocation loops, voids, precipitates and so on. For the basic understanding of radiation damage, it has been strongly desired to clarify the process of atomic displacement. *In-situ* observation in the transmission electron microscope (TEM) is one of the fascinating method to investigate the structural evolution induced by particles bombardments and implantations.

The purpose of this research is to develop a new facility for *in-situ* analysis of the microstructural aspects of materials under dual-beam ion irradiations. The facility so-called "SUBNANOTRON" consists of 1 MeV TEM with two ion accelerators. The voltage of 1 MeV for electron was chosen for the resolution lower than 0.15 nm, for enough thickness of the specimen and enough volume at the specimen position where stressing, heating and cooling will be conducted. The analytical tools such as MAD, EDS and EELS are essential to characterize the complicated structural changes of irradiated materials. The construction of the SUBNANOTRON is in progress and will be completed at the end of 1993.

A special effort for supporting the SUBNANOTRON has been performed by using a standard 200 kV TEM incorporating with two types of small ion accelerators which can produce 100 keV heavy ions and 30 keV inert gas ions such as H and He. Several specimens of Si have been irradiated in this system and dynamic process of crystal/amorphous transition was observed in the images taken by a fiber optically coupled TV camera, and recorded with a VTR through a real time image processor. Si(100) and (111) thin films were easily amorphized by the irradiation of 70 keV Ar^+ to a fluence of 1×10^{19} ions/m^2 and small particles of Si crystals detected in this process indicated the heterogeneous transition from crystal to amorphous. Even in the very low fluence less than 1×10^{17} ions/m^2, Ar^+ ions can generate the small area of amorphous and irregularity in the crystalline structure. From the results that 20 keV H^+ irradiation to a fluence of 1×10^{22} ions/m^2 did not show crystal/amorphous transition, it can be concluded that the defect structures by the irradiation play an important role on this transition.

Related Paper

Direct Observation of Radiation Damage and Lithography Process by Using Ion Irradiation in the Electron Microscope, K. Furuya and N. Ishikawa, Proc. BEAMS (1992): 437, Tokyo (in Japanese).

41 Characterization and Control of Elementary Functions of Materials in the Localized Fine Area

April 1989 to March 1994

K. Furuya, Materials Characterization Division

Keywords: focused ion beam (FIB), TERM, micro-lithography, gas

Bulk functions of materials are controlled by the physical and chemical properties in localized fine area ranging from 10^{-6} to 10^{-9} m. Especially, the electronic and magnetic properties of metals and semiconductors are considered to come from the heterogeneity in the materials such as surfaces, grain boundaries and domains. Focused ion beam (FIB) has increased usefulness for creating artificial heterogeneity by ion implantation, etching and lithography with submicron dimensions. However, the microstructural aspect and elementary functions of fabricated area by FIB could not be analyzed in the conventional experiments. The purpose of this research is to develop a new equipment for *in-situ* analysis of materials under the micro-lithography by FIB in the transmission electron microscope (TEM).

The equipment called "FIB/TEM" consists of a 200 kV standard TEM with 25 kV Ga^+-FIB. FIB system is mounted in the specimen column of TEM and the focusing with the working distance of 100 mm made it possible to micro-fabricate the semiconductor specimens at a beam spot of 150 nm and intensity of 75 pA during TEM observation. The deflection of FIB ions was negligible in the magnetic field of TEM. In addition to TEM observation, the cathodoluminescence spectroscopy (CL), energy dispersive x-ray spectroscopy (EDS) and electron energy loss spectroscopy (EELS) are attached to characterize the basic physical properties of the localized fine area.

The specimen used in this study is GaAs (100), which was ion milled to TEM thin films. FIB micro-lithography during TERM observation was carried out on the thin section of Gas at a magnification of 30 k in both of area and line scanning modes. About 50 nm of thickness was removed after the thinning of 30 sec and there is no evidence of the formation of secondary defects clusters. It was found by SAD patterns that the remained film became partial amorphous phase due to FIB ions damage. One interesting result was the formation of Ga particles at about 100 nm diameter on the micro-fabricated surface, which was considered due to both of Ga ion implantation by FIB and As evaporation from the Gas specimen. For the next step, double layer thin film of semiconductors will be examined for the purpose of clarifying the ion beam micro-fabrication process.

Related Paper

Direct Observation of Radiation Damage and Lithography Process by Using Ion Irradiation in the Electron Microscope, K. Ferry and N. Ishikawa, Proc. BEAMS (1992): 437, Tokyo (in Japanese).

42 Study on Detection and Evaluation of Radiation Damages in Extreme Particle Fields

April 1992 to March 1998

N. Kishimoto, Materials Characterization Division

Keywords: extreme particle field, *in-situ* measurement, photoconduction, DLTS

Combined particle fields of ion and photon exert strong interactions with materials and are potent to distinguish elementary processes and to explore novel properties. Especially if both high energy and high density of ion and photon are attained, unexplored non-equilibrium effects will be expected, by virtue of their contrastive effects of momentum, energy, excitation modes etc. The extreme particle field is also an important aspect for practical environments of high energy devices, such as fusion reactors, MHD generators etc. The main purpose of this research program is to detect and evaluate non-equilibrium and non-linear processes of materials in the extreme particle fields, associated with radiation damages.

Since 1992, techniques of combined irradiation and *in-situ* measurements have been developed using high-energy light ion from the NRIM cyclotron. *In-situ* optical measurements are promising to reveal electronic states of the radiation damages but the optical sensors are weak in the secondary radiation fields. Consequently, we have employed a photoconduction method for crystalline silicon, where the specimen in itself acts as the sensor. An optical monochrometer was installed into the cyclotron system and fully-remotely operated. The spectral changes in photoconductivity was traced along with the deuteron irradiation. The basic photoconductivity due to the band-to-band transition drastically decreased with increasing the deuteron fluence. It indicates that a carrier trapping process of damages is dominant. On the other hand, a broad tail spectrum emerged below the edge of the basic spectrum and relatively increased with increasing the deuteron fluence. This implies that damage states were detected by the photoconduction method and that they also supply the charge carriers as the deep centers.

To observe dose-dependent energy states of the deep centers, we have also installed a DLTS (Deep Level Transition Spectroscopy) apparatus into the same target chamber, equipped with a cryogenic system.

Related Paper

A Fast and Accurate Infrared Pyrometer Combining Two-Wavelength Comparison with Single Waveband Detection, N. Kishimoto and H. Amekura, Sensor Technology 12 (1992): 18 (in Japanese). To be published in Japanese Sensor Newsletter, Case Western Reserve University (1993).

43 Development of Advanced Technologies for X-ray Microtomography

April 1992 to March 1995

Y. Yamauchi, Materials Characterization Division

Keywords: CT, tomography, microtomography, x-ray, three-dimension

X-ray computerized tomography has been widely utilized in the applications for relatively large objects, such as in medical diagnostics of human bodies or in industrial inspection of manufactured components. In those applications the required spatial resolution is usually in the order of 1 or 0.1 mm at most and is limited by the number of pixels on the image. The effective number of pixels is circumscribed by the dynamic range of detected x-ray signal or the steepness of x-ray absorption. Further a mass of data storage and computational power have to be considered. However, if it is allowed to restrict the size of objects fairly small, the constraints would be alleviated. The limited number of pixels may not affect the pixel size nor the resolution of image. Based on this idea, we are developing the x-ray microtomography device. In the previous project, high resolution tomographies of a small object were accomplished with the parallel beam projection using a conventional point x-ray source. Then we extended the function of the device to three-dimensional. In this project we have been studying advanced technologies which improve the spatial resolution of tomographs and which provide another function to analyze chemical composition.

Asymmetric reflection seems to be a promising technique to magnify x-ray images. We have obtained magnified image of factor 10 by Si(511) reflection with a normal focus Cu tube source. A lead glass capillary plate which consists of channels of 10 μm in diameter and 2 mm in length was used to reduce the diverging angle of primary beam.

Introducing spectrum modulation of x-rays, an evaluation of chemical composition by the micro-CT was tried and its capability for qualitative analysis has been confirmed. Spectra of x-rays were modulated by thin film filters.

44 Advanced Techniques Physical Analyses for Metals

April 1991 to March 1994

Y. Tamura, Materials Characterization Division

Keywords: structure analysis, surface structure analysis, composition analysis

The purpose of this investigation is to develop higher performance techniques of physical analyses for advanced materials with the help of data processing by micro-computers. Physical analyses include x-ray diffraction, electron probe micro-analysis, transmission electron microscopy, scanning electron microscopy and optical microscopy.

The scope of the investigation is as follows:

1. Techniques of crystal structure analyses
   a. Crystal structure analyses by XRD
      i. Study on new x-ray analysis. A preliminary investigation is carried out to determine a long range order parameter in binary alloys by a newly developed x-ray diffractometry method, comparing with the parameters by former methods, such as x-ray diffractometry or ALCHEMI method.
      ii. Study on quantitative analysis. A computer software is intended to develop, by which the crystal structure of unknown substances can be identified on the basis of the x-ray diffraction data.
      iii. Study on surface structure analysis. An application technique of the x-ray total reflection method is studied in order to obtain the information of crystal surface structures.
   b. Crystal structure analyses by HREM
      Study on lattice image structure analysis. The structural analysis of lattice images are performed on metal/ceramic interfaces by means of a high resolution electron microscopy.
2. Techniques of materials composition analysis
   Software study on a computer processing of EPMA data are developed for the purpose of highly accurate on-line micro-analysis.
3. Application
   On request, physical analysis and consultative function are performed.

45 Evaluation of Metallurgical Structure with a Fuzzy Logic

April 1992 to March 1995

M. Fukamachi, Materials Characterization Division

Keywords: computer-image analysis, fuzzy logic, electron microscopy, distribution of chemical elements on metallurgical structures

In order to carry out an accurate and rapid computer-image analysis of metallurgical structures, the feasibility of an application of fuzzy logic to a computer-image simulation has been studied. Fine metallurgical structures can be revealed with the electron microscopy. Usually, the numerical computer-image simulation is necessary to analyze and to evaluate the fine metallurgical structures. It is difficult to give accurate numerical values to many parameters which characterize the geometry of electron microscopy and the operating conditions to obtain a satisfactory image simulation.

The method to simulate microscope images of the secondary and the reflected electrons has been studied with an application of fuzzy logic. Only two parameters are used in the image simulation. These are the parameters to represent the amount of generation of the signal electrons and the efficiency of detector to collect the electrons. With this method, the distribution of chemical elements on metallurgical structures can be obtained rapidly by separating the image contrast caused by the local distribution of chemical elements from that of the uneven geometry of specimen surface.

46 Sensitive Instrumental-Analysis of Metallic Materials by Direct Methods and Separation Methods

April 1991 to March 1994

R. Hasegawa, Materials Characterization Division

Keywords: inert gas fusion, GD-MS, GF-AAS, ICP-AES, separation

Aiming at the development of fundamental techniques for the sensitive instrumental analyses of metals, alloys and related materials, studies on the following three items including direct methods and separation methods have been carried out. Main targets for each item in this fiscal year are as follows.

Study on direct analysis of solid samples

1. Determination of trace oxygen in low melting point metals (Pb, Zn and their alloys) by inert gas fusion-infrared absorption method using a graphite capsule.
2. Evaluation of relative sensitivity factors of the alloying elements in steels by glow discharge mass spectrometry (GD-MS) using a flat cell.

Study on direct analysis of liquid samples

1. Efficient atomization of analytes in a modified graphite furnace atomic absorption spectrometry (GF-AAS) and precise determination for high melting points matrices (Ta, Mo and V) and for a solution of high concentration.
2. Application of a long plasma torch in the inductively coupled plasma atomic emission spectrometry (ICP-AES) with end-on observation and time-resolved measurement.

Study on separation analysis of liquid samples

1. Determination of trace elements in nickel by co-precipitative separation and ICP-AES.
2. Simultaneous analysis of multi-elements for the determination of trace impurity elements in pure metals by ICP-AES following a simple separation procedure.

3. Determination of trace silicon in high purity metals (Cr, Ni and Mn) and titanium alloys by molybdosilicic acid blue spectrophotometry following fluoride separation.
4. X-ray fluorescence analysis of aqueous sample solutions with their pretreatment.

The investigation also includes the improvement of analytical techniques available for the chemical analysis of the various samples which are provided from other divisions of the Institute.

47 Study on Mechanism of Ion Production in Low Temperature Plasma

April 1991 to March 1994

M. Saito, Materials Characterization Division

Keywords: glow discharge mass spectrometry, matrix effect, absolute determination

In a direct current glow discharge mass spectrometry, the ion intensity signals of elements have been found to be greatly increased when Ar/H_2 or Kr/H_2 gas mixture containing small amounts of H_2 was used as discharge gas. This method was also applied to the determination of relative standard factor (RSF) (Fe = 1) by using the reference materials of steels, copper, aluminum, heat-resisting alloy and indium. The results obtained by the proposed method were founded to be free from matrix effects, compared with those from the conventional method using Ar gas as a discharge gas.

In addition, by the combination of Ar/H_2 gas mixture and liquid nitrogen cell cooling system, a linear relationship was found between the RSF value and ionization potential of elements. This method shows the possibility of the accurate determination of almost elements in solid samples without standard reference materials (absolute determination).

48 Database Systems for R&D of Superconducting Materials

April 1989 to March 1994

S. Nishijima, Failure Physics Division

Keywords: superconductors, high-T_c oxides, factual database, knowledge base

This project aims at the development of factual database systems on the high-T_c superconducting materials by coordinating many laboratories from industries, universities and national institutions. It is however not simple to build a database for those superconductors where the mechanism and theory are not well established so far. Efforts were made for the first years to improve sample reproducibility and establish common practices for the properties evaluation through replicated measurements of common samples by the participants.

A prototype database is built at NRIM and core data from the coordinated experiments have been

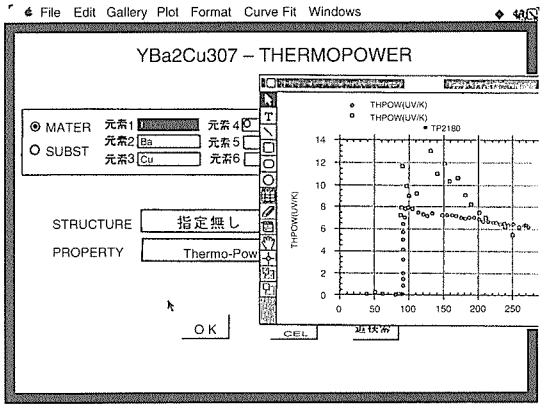

Fig. 2 An image of search-and-show in 'Correlation Finder' system

installed. It includes a variety of physical, chemical and electronic informations on typical high-T_c superconductors of different configurations. Current additions are, for example, the basic properties on monocrystals of $La_{2-x}Sr_xCuO_4$, $YBa_2Cu_3O_7$ and $Bi_2Sr_2CaCu_2O_3$, Ag-sheathed wires of $Bi_2Sr_2Ca_2Cu_3O_z$, and films of $Bi_2Sr_2CaCu_2O_z$, and so forth.

Data collection is facilitated by a common package for input and handling of experimental raw data. A comprehensive database, including detailed experimental data and extracted data from literature, as well, is being built on a workstation, which will be linked to a knowledge base under development for R&D of new materials. A more compact and handy database on PCs is under preparation in collaboration with the National Institute of Standards and Technology of USA.

49 Modeling and Evaluation of Advanced Materials—A Coordinated Interlaboratory Research Effort

April 1992 to March 1994

S. Nishijima, Failure Physics Division

Keywords: advanced materials, property evaluation, modeling, VAMAS project

Advanced materials are considered as one of the key subjects for further development of science and technology in the coming new decades. This research is aiming at the development of materials models to describe the behavior and properties of selected advanced materials through analysis and comprehension of physico-chemical mechanisms in their elementary processes. It covers the establishment of rationalized methods for evaluating their properties, especially in concert with the international activities of Versailles Project on Advanced Materials and Standards (VAMAS).

The work is conducted as a nation-wide coordinated research project and financed by the special coordination funds of Science and Technology Agency. NRIM forms an important task force with its 38 research staffs, and at the same time, bears a role to harmonize combined efforts of more than

50 participating research groups, each belonging to industrial, university or national laboratories.

Materials modeling is currently investigated about the strength properties including fatigue and fracture on: (1) inter-metallic compounds (IMC) of TiAl system, (2) metal matrix composites (MMC), as SiC fiber reinforced Ti alloys, and (3) ceramic matrix composite (CMC), as SiC fiber reinforced SiC. Daido Steel Co., Mitsubishi Heavy Industries and Toshiba Corporation are involved in the project and supplying test materials of IMC, MMC and CMC, respectively. An X-ray micro-beam tomographic technique is under development to assist with the analysis of those advanced composite materials.

VAMAS Project as a whole is actually at the stage of reviewing its activities in individual task working areas (TWA). NRIM is taking initiative to open a new TWA on (1) MMC; it continues to take essential part in TWAs: (2) creep crack growth, (3) surface chemical analysis, (4) superconducting materials, (5) cryogenic structural materials, and (6) materials property data systems.

50 Sensing and Analysis of Material Damage Formation Processes

April 1991 to March 1994

N. Shinya, Failure Physics Division

Keywords: damage monitoring system, piezoelectric polymer, electron Moiré method

In this work, a damage monitoring system and advanced analytic techniques for damage formation processes are being developed. The main research program and results are as follows.

1. Local strain sensing methods have been developed for damage detection in structural materials. As a strain sensor, piezoelectric polymers were coated on the surfaces of aluminum sheets. Local strains in the tensile tested aluminum sheets were measured by an operational amplifier circuit with a scanning probe, and then observed using the voltage contrast technique in a scanning electron microscope. The preliminary results indicate that these methods using piezoelectric polymers are sensitive and useful for detection and measurement of local static strains in structural materials.
2. A new Moiré method for the measurement of high temperature deformation, which uses electron beam lithography and scanning exposure of the electron beam, has been developed. This new Moiré method makes it possible to observe the scanning electron microscope image and the Moiré fringe at the same time, to obtain a clear Moiré fringe without an image processing system, and also to determine the highly localized deformation at elevated temperature. Using this method, the microcreep deformation such as grain boundary sliding, coarse slip and localized strain in pure copper specimens has been measured.

51 Atomic Scale Evaluation of Material Damage in Aqueous Solution

April 1992 to March 1994

H. Masuda, Failure Physics Division

Keywords: *in-situ* observation, STM, tunnel current, electrodeposition, nano-processing

In-situ observation was done by the scanning tunneling microscope (STM) to study the electrodeposition behavior of copper on gold electrode in 0.05 M $CuSO_4$ + 0.3% H_2SO_4 and 0.1 M $CuSO_4$ + 0.6% H_2SO_4 aqueous solutions. A rapid electrodeposition occurred under the STM tip when the tunnel current was increased while the STM tip being fixed at the center of the scanning area. An original program was developed to apply these phenomena for nano-processing. Figure 3 shows the characters of NRIM drown by using the program.

52 Research on Quantitative and Intelligent Nondestructive Evaluation Techniques for Materials and Structures of High Reliability

April 1991 to March 1994

C. Masuda, Failure Physics Division

Keywords: nondestructive evaluation, frequency response, acoustic microscopy, laser-ultrasonics, composite materials

In this research, it is intended to develop nondestructive evaluation techniques and systems based on various ultrasonic measurement techniques to maintain the reliability of newly de-

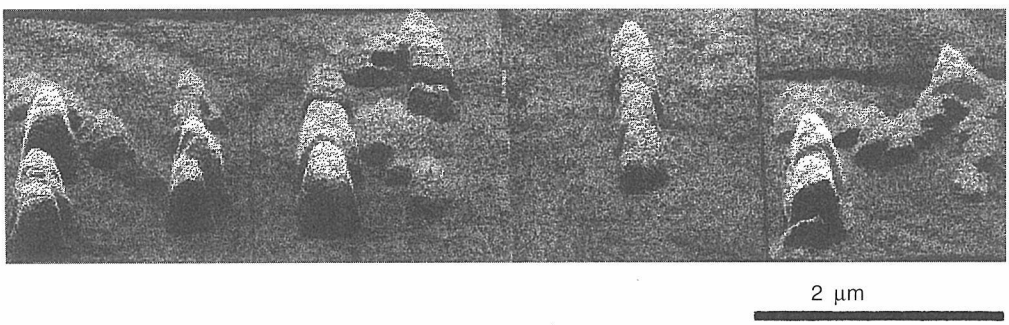

Fig. 3 NRIM drown by electrodeposition of copper

veloped structural materials. This research is sponsored by STA and supported by members of various institutions, universities and companies. The following four sub-themes are carried out in our laboratory.

Ultrasonic measurement of highly attenuating materials

The technique to evaluate microstructure and flows in materials characterized by ultrasonic high attenuation is investigated by means of measurement of ultrasonic frequency response. Detecting the frequency spectral change of ultrasonic waves, attenuation and velocity characteristics of materials were instantly obtained. Grain sizes of stainless steels were estimated and compared to results obtained by the traditional ultrasonic method using multiple reflecting wave forms which are difficult to be obtained in attenuative materials.

Measurement using acoustic microscopy

Microscopic ultrasonic measurement of Rayleigh wave velocity by a usage of V-Z curve property obtained from scanning acoustic microscope (SAM) is investigated for the evaluation of microscopic physical property of advanced materials. Improvement of SAM system has been carried out for the precise velocity measurement of the anisotropic materials and external stress loaded materials. As a trial, aluminum alloys with anisotropic microstructure induced by rolling and external applied load were evaluated using the system.

As results, obvious relation between the velocity and the stress were obtained, and difference of the relations between directions of the anisotropy was also observed. Furthermore, using SiC/Al composite, velocity variation related to the density of SiC fiber was detected by the system.

Laser-ultrasonics

Ultrasonic imaging system using laser-ultrasonic techniques is investigated for non-contact evaluation of materials in a small region. For development of the system, elemental mechanisms of laser beam scanning, signal processing for quantitative ultrasonic detection, and non-contact ultrasonic detection by Fabry-Perot interferometry have been constructed. Experimentally, non-contact ultrasonic detection by a Fabry-Perot interferometer was evaluated for improvement of the detection on rough surface specimens, and sharewave detection by a heterodyne interferometer was also examined.

Flaw evaluation in inhomogeneous and anisotropic materials

A purpose of this sub-theme is to clarify ultrasonic property of materials with complex structure and inhomogeneity, such as composites. Experiments were conducted on standard metal matrix composites including one or several layers of fibers. For analysis of ultrasonic phenomenon in complex materials, new computer simulation technique of elastic waves based on FDM was also developed. The simulation is characterized with applicability for specimens, inclusions, flaws with free shape and anisotropic elasticity in 3 dimensions. As results of calculations, ultrasonic characteristics of hexagonal elastic materials and layered materials with anisotropy were correctly simulated.

53 Quantitative Evaluation of Fracture in Materials for Casks

April 1992 to March 1994

T. Yasunaka, Environmental Performance Division

Keywords: fracture toughness, low temperature embrittlement, carbon steel, nodular cast iron

Shipping containers (casks) for radioactive materials must maintain structural integrity even when subjected to accident of impact loading at low ambient temperature. In ferritic steels, low temperature embrittlement occurs. For the evaluation of material for casks, brittle or unstable fracture is an important consideration and application of fracture mechanics is appropriate.

The objective of this study is to characterize the behavior of dynamic fracture toughness of a carbon steel and a ferritic nodular cast iron and to develop the precise evaluation method for these materials.

In the ductile fracture region of cast iron, plain strain fracture toughness divided by yield stress was found to be independent of loading rate and temperature. This parameter can be regarded as a material constant of cast iron. Using this parameter, the evaluation of fracture toughness for the cast iron can be simplified. Evaluation of the cast iron by small bend specimens is also attempted because the microstructure in the direction of wall thickness is inhomogeneous and uses of small specimens are desirable.

Furthermore, in view of large amount of scatter in the ductile-brittle transition range the evaluation of fracture toughness of the carbon steel is studied.

Related Paper

Dynamic Fracture Toughness and Evaluation of Fracture in a Ferritic Nodular Cast Iron for Casks, T. Yasunaka and K. Nakano, Proceedings 10th Int. Sympo. on Packaging and Transportation of Radioactive Materials (1992): L1304–10.

54 Real Time Evaluation of Fatigue Damage during Crack Propagation under Random Loadings

April 1991 to March 1994

A. Ohta, Environmental Performance Division

Keywords: fatigue crack, random loading, crack closure, residual stress

The fatigue crack propagation properties in a tensile residual stress field which is the usual condition for the fatigue crack propagation in real welded structures were investigated. In this condition, the fatigue cracks always open. That is, the applied stress intensity factor ranges coincide with the effective ranges of stress intensity factor. Therefore, we defined these properties to be the basic fatigue crack propagation properties.

In order to simulate the above condition to get the basic fatigue crack propagation properties, specimens were heat treated by heating only a central part at 780 °C and cooling the surrounding part by water jacket. By this heat treatment, the tensile residual stresses were induced in the middle part of specimen. The tensile residual stresses avoided the fatigue crack closure.

A two-step programmed test which is the simplest type of random loading was performed on these specimens. It was revealed that the transitional phenomena appeared in a residual stress free specimen disappeared in the heat-treated specimen. The avoidance of the fatigue crack closure improved that the fatigue crack propagation rate just after the sudden change of loading could be predicted from data obtained by the constant amplitude test.

Related Papers

Fatigue Crack Propagation in a Tensile Residual Stress Field Under a Two-Step Programmed Test, A. Ohta, A.J. McEvily and N. Suzuki, Int. J. Fatigue 15 (1993): 9–12.

Minor Role of Fractographic Features in Basic Fatigue Crack Propagation Properties, N. Suzuki, T. Mawari and A. Ohta, Int. J. Fracture 54 (1992): 131–38.

Effect of Young's Modulus on Basic Crack Propagation Properties near Fatigue Threshold, A. Ohta, N. Suzuki and T. Mawari, Int. J. Fatigue 14 (1992): 224–26.

55 Chemical Analysis of Organotin in Marine Environmental Samples

April 1991 to March 1996

H. Okochi, Director of Special Research

Keywords: organotin, inductively coupled plasma mass spectrometry, solid-phase extraction, micellar liquid chromatography, sea water

Inductively coupled plasma mass spectrometry has been used as a detector for several organotin compounds which were separated with the use of micellar liquid chromatography. Triphenyltin chloride, diphenyltin chloride, monophenyltin chloride, tributyltin chloride, and dibutyltin chloride were separated with a 40 mM tris (hydroxymethyl) amino-methane micellar mobile phase containing 75 mM NH_4NO_3, 3% acetic acid and 20% ethanol. The analytical column was YMC-Pack FL-C4 (30 × 4.6 mm) and the injector with 100 ml sample loop was used. The detection limits (3 σ of blank values) and sensitivities of five species of organotin compounds are shown in table 3. The reproducibilities of peak areas are shown in table 4. The RSDs of peak areas were obtained for 5 replicate injections of 50 ng Sn of organotin compounds.

The solid phase extraction of organotin compounds in sea water has been developed using a polymer of stylene derivative/metacrylic ester as a solid phase adsorbent. The recoveries of organotin compounds were measured by atomic absorption spectrometry. To prepare water samples, methanol was added to be 50% v/v to an artificial sea water containing organotin standard solutions and then pH was adjusted to 0.5 with nitric acid. The water samples were forced through the cartridge at a flow rate at 4.5–5 ml min^{-1}. Elution was by gravity flow of 10 ml methanol. The recoveries of TPT and TBT were more than 90%, while those of DPT and DBT were about 30 and 60%, respectively.

Table 3 Detection limits and sensitivities of four species of organotin compounds

Tin species	Detection limit (pg)	Sensitivity (cps/ng)
MPT	97.1	2.24×10^3
DPT	52.4	8.24×10^3
DBT	35.4	1.19×10^4
TPT	24.5	1.76×10^4
TBT	27.2	1.52×10^4

Table 4 Reproducibilities of peak areas

Tin species	RSD (%)
MPT	5.39
DPT	1.73
DBT	1.80
TPT	0.72
TBT	0.83

56 Development of Extremely High Field Magnets

April 1988 to March 1995

H. Maeda, 1st Research Group

Keywords: 80 T class long-pulsed magnet, 40 T class hybrid magnet, 20 T class large-bore superconducting magnet, high resolution magnet

For evaluating the high-field properties of high-T_c oxide superconductors, we are developing several high-field facilities, such as 80 T class long-pulsed magnet, 40 T class hybrid magnet, 20 T class large-bore superconducting magnet, and high resolution magnet.

Although Cu-(5-30)at%Ag alloy has been found to be the best new conductor for pulsed magnet

due to its promising combination of high conductivity and high tensile strength, it is very difficult to wind the thick Cu-Ag alloy wire into a coil because of its strong spring-back force. By using a thin rectangular Cu-Ag alloy wire of 2 mm × 3 mm, we have succeeded in fabricating a small pulsed magnet, which can generate 62.7 T in a winding diameter of 15 mm. By collaborating with Katholieke Universiteit Leuven we have made several pulsed magnets which were reinforced by the glass fiber winding between the layers of Cu-Ag wire. Their operation tests are progressing now. One of them could generate 68 T in an inner winding diameter of 12 mm.

The 40 T class hybrid magnet system is designed to be composed of a 15 T superconducting magnet with a clear bore of 400 mm, and a polyhelix-type water-cooled resistive magnet generating an incremental field of 25 T in a clear bore of 30 mm. The all parts of the water-cooled magnet system have been nearly constructed. All the pancake windings of superconducting cable have been finished. The test operation of the superconducting magnet will be performed at the end of 1993. By the end of 1994 all the system will have been constructed and tested.

Test operation of the 20 T class large bore superconducting magnet system has been continued this year. The third inner coil made of a new (Nb, Ti, Ta)$_3$Sn conductor were tested and found to be able to generate up to 21.1 T in a 50 mm free bore under the back-up field of 18 T generated by the middle coil and the outer coil. This is the new world record as not only the magnetic-field strength but also the clear bore size, because the last world record performed by a superconducting magnet was 20.7 T in a 32 mm free bore.

By using the high resolution magnet system we have performed to measure the physical properties such as NMR of oxide superconductor, its ultrasonic absorption, its flux creep, dHvA of organic superconductor, its SdHvA, dHvA of heavy fermion, large magnetic resistivity of metallic superlattice, and NMR of organic compounds and glass. Particularly, we have succeeded in an observation of the conduction electrons, whose effective masses are 120 times larger than that of free electron. This success proves the very high resolution faculty of this system.

Related Papers

Development of 40 Tesla Class Hybrid Magnet System, K. Inoue, T. Takeuchi, T. Kiyoshi, K. Itoh, H. Wada, H. Maeda, T. Fujioka, S. Murase, Y. Wachi, S. Hanai and T. Sasaki, IEEE Trans. Magn. 28 (1992): 493–96.

Development of 20 Tesla Class Superconducting Magnet with Large Bore, T. Kiyoshi, K. Inoue, K. Itoh, T. Takeuchi, H. Wada, H. Maeda, K. Kuroishi, F. Suzuki, T. Takizawa and N. Tada, IEEE Trans. Magn. 28 (1992): 497–500.

High-Field Facilities Under Development and Construction in NRIM, Japan, K. Inoue, T. Asano, T. Kiyoshi, Y. Sakai, T. Takeuchi, K. Itoh and H. Maeda, Physica B 177 (1992): 7–15.

Development of High Resolution Magnet System and Applications—A Step Toward NRIM High Field Magnet Laboratories, H. Aoki, S. Uji, T. Shimizu, Cryogenic Engineering 27 (1992): 21–29 (in Japanese).

57 Vaporization and Ionization by Arc Plasma

April 1991 to March 1993

A. Okada, Advanced Materials Processing Division

Keywords: vaporization, GTA, anode, molten pool, current distribution

The anode configuration and its behavior on the molten pool surface in a gas shielded tungsten arc (GTA) weld due to the vaporization on the surface is being made clear from the measurement of the current distribution on the surface up to the present.

The vaporization is influenced by the arc length and the axial plasma velocity which are related to an extent of the higher temperature plasma region on the molten metal surface. It is made clear that the anode region size is reduced with a decrease in the arc length and with a less acute cone angle at the electrode tip.

Moreover, a method is developed to reduce anode region size. Ar gas jet is applied to the circumference of the molten pool and a centripetal Ar gas flow from the circumference is formed. The anode region is constricted by covering a region in shore of the molten pool with the centripetal Ar gas flow.

This control can be verified by the measurement of the current distribution on the molten pool surface. In the stationary GTA with arc length of 4 mm, current of 150 A and shield gas flow rate of 15 l/min, when the total Ar gas flow rate of 10 l/min was applied through 4 tube control nozzles, the radius of anode region was reduced to 2.5 mm from 4.5 mm.

Related Papers

Anodic Spot Current on Molten Pool in Stationary GTA Welding, A. Okada and H. Nakamura, Quarterly J. Japan Weld. Soc. 11 (1993): 88–94 (in Japanese).

Formation of Multiple Anode Spots in Stationary GTA Welding, A. Okada and H. Nakamura, Quarterly J. Japan Weld. Soc. 11 (1993): 253–59 (in Japanese).

Anode Behavior in GTA Welding and Its Effect on Melting Thin Plate, A. Okada and H. Nakamura, submitted to Quarterly J. Japan Weld. Soc. (in Japanese).

Basic Parameters in Heat Transport in Ar-He Mixed Gas Arcs, J. Zijp and K. Hiraoka, submitted to Trans. of Japan Weld. Soc.

[58] Measurements of Transient Phenomena Due to Beam-Solid Interaction

April 1990 to March 1993

N. Kishimoto, Materials Characterization Division

Keywords: pulsed-beam perturbation, strain measurement under 10 MeV D irradiation, resonant creep

Microstructural evolution in irradiated materials results from dynamical balances between generation and relaxation of point defects. A transient response of a material to a pulsed-beam perturbation conveys kinetic information of the damage processes.

Strain measurement under 10 MeV D irradiation has been conducted for Fe-Ni-Cr alloy and type 316 stainless steel, under uniaxial loading. High strain resolution (10^{-5}) under beam heating has been accomplished by a fast/accurate temperature control system i.e. He-jet cooling, fast resistance monitoring and DC heating, and newly developed infrared-pyrometry etc. The continuous irradiation for about 10 hrs was switched to a square-wave (pulse width τ_p = 10 msec – 1000 s), at a damage rate of 2×10^{-7} dpa/s.

The pulse-width dependences of strain change have revealed overall response behaviors of the austenitic alloys and we have found out a resonant creep for the first time. The resonant peaks in strain emerged at τ_p = 50 – 100 s for the both austenitic alloys. Such large positive creep had never been observed under the continuous irradiation. Especially for the 316 steel, the solution-annealed specimen showed the resonant creep but little strain change for the cold-worked one.

This finding is important not only technologically but also from a fundamental aspect. In the next fusion devices such as ITER, pulsed irradiation may cause a significant deformation in austenitic steels even at such low dose and slow pulsing rates.

The resonant behavior was elucidated in terms of a point-defect kinetic model. The pulsing time at resonance corresponds to a characteristic time of transient enrichment of interstitial atoms and the pulsation drastically increases the net defect flux into the loops. This resonant creep may be an experimental evidence to support a creep mechanism of stress-induced interstitial nucleation, rather than conventional models of dislocation motion.

Related Paper

A Fast and Accurate Infrared Pyrometer Combining Two-Wavelength Comparison with Single Waveband Detection, N. Kishimoto and H. Amekura, Sensor Technology 12 (1992): 18 (in Japanese). To be published in Japanese Sensor Newsletter, Case Western Reserve University (1993).

[59] On-line and Precise Measurement of the Intensity Distribution in Electron Diffraction Pattern by Using Cooled CCD Camera

April 1992 to March 1993

T. Kimoto, Materials Characterization Division

Keywords: cooled slow-scan CCD camera, electron diffraction intensity, YAG scintillator, optical fiber plate

If we use a conventional film to record an electron diffraction pattern, it is impossible to measure precisely the intensity distribution in the pattern because the detectable range of intensity (dynamic range) on film is very small (usually 10–100). The on-line measurement of electron diffraction intensity is also impossible if we use a film or an imaging plate whose dynamic range is 1,000–10,000. The objective of the present research is to develop the system for the on-line and precise measurement of electron diffraction intensity distribution by detecting diffracted electrons with a CCD camera in a transmission electron microscope (TEM).

In the developed system, the diffracted electrons are converted to be photons by YAG scintillator ($Y_3A_5O_{12}$: Ce^{3+}). The photons from YAG scintillator are then led to the cooled CCD camera by the optical fiber plate. The intensity distribution of photons is detected and converted to the electric signal by the CCD camera. The electric signal is transferred from the CCD camera to a personal computer through A/D converter. After analyzing with a computer, the on-line and precise electron diffraction intensity profile is successfully printed or shown on CRT.

The thickness of YAG scintillator was reduced to be less than 0.05 mm in order to minimize spreading of photons which causes location error in the detection of electrons. The length of the optical fiber plate was successfully chosen to be 10 cm to reduce effectively the influence of x-rays from TEM and YAG scintillator on CCD camera, as well as to prevent the frost on YAG scintillator which is cooled by thermal conduction through the fiber plate attached to the cooled CCD camera. The diameter of each fiber was about 0.01 mm. The dark current of less than 0.8 e-/pixel/sec in CCD camera was realized in order to get high accuracy of measurement by cooling electrically the CCD camera to be –45 C as well as by adopting multi-phase pin (MPP) mode. The CCD camera had very high dynamic range from 40,000 to 64,000, and the pixel number was 512 × 512. The accumulation of electron intensity was successfully carried out by

using slow-scan type CCD camera with a shutter.

60 Characterization of Metals and Alloys Using Synchrotron Radiation

April 1990 to March 1993

T. Saito, Materials Characterization Division

Keywords: synchrotron radiation, near-surface, labo-XAFS, x-ray CT, diffractometry

Use of synchrotron radiation (SR) as a powerful research tool in materials characterization has grown tremendously in recent years. In the present program, from a view point of a materials characterization, new analytical techniques and apparatuses as well as their practical applications have been extensively studied.

Near-surface study using grazing incidence x-ray experiments

In analyses of thin films using grazing incidence x-ray techniques, it is important to simulate behavior of electric vector in the material, reflectivity and intensity of fluorescent x-rays. The computer program MUREX (Multiple reflections of x-rays) has been developed for this purpose, and is now widely distributed. This program contains the codes for determining layer thicknesses and surface/interface roughness from an experimental data by our new technique.

Development of labo-XAFS facilities

A new electron gun was designed as an x-ray source for labo-XAFS. We have succeeded to get high tube current of 900 mA at low tube voltage of 20 kV, with forming a narrow focal spot of ca. 0.1 mm in width. This x-ray source enables to obtain a good quality spectrum in a short time without relying on synchrotron x-rays.

Evaluation of structure and defects by x-ray CT

SiC/A6061 composites were observed during the tensile test with *in-situ* x-ray CT using SR. A 3-dimensional image reconstructed from several CT images have revealed that the distribution of fibers and many pull-outs at the end of fibers were clearly observed.

Crystallographic analysis of superalloys using SR parallel-beam diffractometry

A diffractometer with a hot stage was developed to measure the lattice parameters of γ and γ' phase in Ni-base single crystal superalloys under high temperatures. The superalloys have γ' precipitates which are of an ordered L12 structure in γ-matrices of a disordered FCC structure.

The apparent thermal expansion coefficients of lattice parameter of the γ' precipitates were smaller than those of the γ-matrices from 800 ° to 1200 °C.

Related Papers

High-Intensity X-ray Line Focal Spot for Laboratory Extended X-ray Absorption Fine-Structure Experiments, K. Sakurai, Rev. Sci. Instrum. 64 (1993): 267–68.

Observation on Fibers in Long Fiber Reinforced Metal Matrix Composites by X-ray Computed Tomography Using Synchrotron Radiation, C. Masuda, Y. Tanaka, K. Usami, T. Hirano, Y. Imai, I. Shiota, E. Furubayashi and H. Iwasaki, Nondestr. Evaluat. 8/9 (1992): 779–86.

Determination of the Coherency Strain of Gamma and Gamma Prime Phases in Ni-base Superalloys at High Temperatures, K. Ohno, T. Yokogawa, T. Yamagata, H. Harada and K. Ohsumi, Adv. X-ray Anal. 36 (1993): (in press).

61 Rutherford Backscattering and Particle Induced X-ray Spectroscopy Studies of Thin Film Oxide Superconductors

April 1992 to March 1993

K. Nakamura, 1st Research Group

Keywords: RBS, PIXE, oxide superconductors, thin films

The purpose of this study is to establish reliable analytical method in thin films by applying Rutherford Backscattering (RBS) combined with Particle Induced X-ray Emission (PIXE). Although RBS is the most reliable method for thin film analysis, its poor mass resolution for heavier elements makes it difficult to analyze the systems containing heavier elements with closer mass number. Particle Induced X-ray Emission (PIXE) combined with RBS is expected to solve these problems.

The advantage of RBS-PIXE analysis is that the data can be acquired simultaneously under the same beam conditions, and that the characteristic x-ray yield can be calibrated by the backscattering yield of the projectile ions. Thus, we have established a series of calibration curves for the analysis of thin oxide films containing various cationic elements and have succeeded to determine composition of superconducting films containing elements with closer mass number.

Detecting a trace amount of impurities accidentally or intentionally incorporated in the film is one of the most important aspects of PIXE analysis in the present investigation. Recently we have applied PIXE analysis to the BSCCO films and have found that Curie-Weiss behavior of the BSCCO films caused not only from Fe and Ni impurities incorporated from the stainless steel holder during sputter-deposition but also from a trace amount of Fe dissolved in single crystal MgO substrate. As described above, RBS-PIXE analysis provides us with a strong analytical meaning to a complete quantitative analysis of oxide superconductor films.

62 Evaluation and Application of Cu-Ag Alloy as Conductor Material in High Field

April 1992 to March 1993
H. Maeda, 1st Research Group
Keywords: Cu-Ag alloys, high tensile strength, high conductivity, resistive magnet material

The development of conductor material with high mechanical strength is indispensable for fabricating resistive high-field magnets, such as a pulsed magnet and a water cooled magnet. Recently, we have found that the heavily cold-worked Cu-Ag alloys showed some excellent properties as the conductor material. When the Cu-Ag alloys including 10 ~ 16 at% Ag were cold-worked into wires or plates with several intermediate annealings at 450 °C, they exhibited not only high tensile strength above 1 GPa but also high conductivity above 80% IACA at room temperature.

In this year we made many Cu-16 at% Ag alloy plates at 0.5–0.7 mm in thickness, 159 mm in width, and 635 mm in length, and then sent them to the Francis Bitter National Magnet Laboratory (FBNML), where the plates are being worked into Bitter-type plates with many cooling channels and being constructed into a Bitter-type water-cooled magnet. At the end of 1993 the water-cooled magnet will be tested in a hybrid magnet of FBNML, which have the world's highest-field record of 34 T, to evaluate the Cu-Ag alloy plate as the conductor material for high-field water-cooled magnet. The obtained data will become very valuable when we will construct a new water-cooled magnet system in the near future.

Related Papers

Development of High-Strength, High Conductive Copper-Silver Alloys, Y. Sakai, K. Inoue, T. Asano and H. Maeda, J. Japan Inst. Metals 55 (1991): 1382–91 (in Japanese).

Development of High-Strength, High-Conductivity Cu-Ag Alloys for High-Field Pulsed Magnet Use, Y. Sakai, K. Inoue, T. Asano, H. Wada and H. Maeda, Appl. Phys. Lett. 59 (1991): 2965–67.

63 Coil-Winding Procedure for High-Strength/High-Conductivity Wire

April 1992 to March 1993
H. Maeda, 1st Research Group
Keywords: Cu-Ag alloy wires, high tensile strength, high conductivity, pulsed magnet material, winding procedure

A high-strength conductor material is indispensable for fabricating a high-field magnet. However, it is very difficult to wind a high-strength wire into a solenoid due to its large spring-back force. Recently we have successfully developed new Cu-Ag alloy wires which exhibit not only high tensile strength above 1 GPa but also high conductivity above 80% IACS. On the other hand, Katholieke Universiteit Leuven has successfully developed a new winding procedure of a pulsed magnet with internal reinforcement. Therefore we began to study the new pulsed magnet made on the promising combination of the new conductor material and the new winding procedure.

At first we fabricated several Cu-16at%Ag alloy thin wires with 2 mm × 3 mm in cross sections which can be wound into small solenoids due to its relatively small spring-back force. We sent them to Katholieke Universiteit Leuven, where the wires were wound into several small coils by using the new winding machine developed by Katholieke Universiteit Leuven. A glass fiber was wound as the internal reinforcement on every winding layer by controlling its tensile stress and its total winding number. After winding the coils were impregnated with Epoxy resin for reinforcement. The operation tests of these coils are progressing now at both sides. One of them could generate a maximum field of 68 T in an inner winding diameter of 12 mm. The value is comparable to the world highest-field record generated by a long pulsed magnet.

Related Papers

Development of High-Strength, High-Conductive Copper-Silver Alloys, Y. Sakai, K. Inoue, T. Asano and H. Maeda, J. Japan Inst. Metals 55 (1991): 1382–91 (in Japanese).

Development of High-Strength, High-Conductivity Cu-Ag Alloys for High-Field Pulsed Magnet Use, Y. Sakai, K. Inoue, T. Asano, H. Wada and H. Maeda, Appl. Phys. Lett. 59 (1991): 2965–67.

64 Study on Measurement and Evaluation Methods for Superconducting Properties

April 1990 to March 1993
H. Wada, 1st Research Group
Keywords: standardization, critical current, standard reference device

This is a collaboration program of NRIM with NIST (National Institute of Standards and Technology, Boulder, Colorado), based on the Japan–US Agreement on Cooperation in Research and Development in Science and Technology, and covers the following topics;

1. stress effects on critical currents in advanced superconducting materials,
2. ac losses in advanced superconducting materials, and
3. critical currents in oxide superconductors.

In fiscal year 1992 collaborative work was focused on the development of standard oxide superconductor devices for interlaboratory critical-

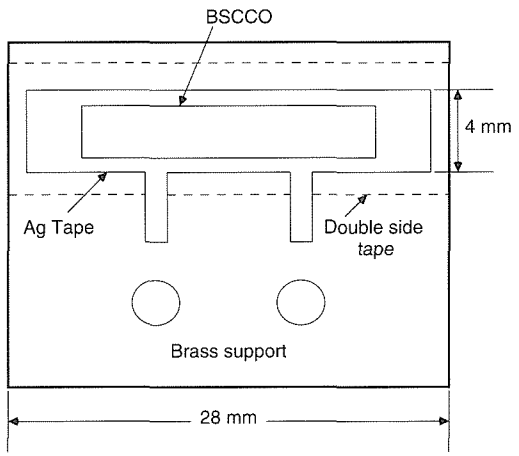

Fig. 4 An example of standard reference device for critical current measurement

current (I_c) measurement comparison. First, standard reference devices (SRD) were designed through discussions between two laboratories. Second, Bi-based 2212 phase samples for SRD were fabricated at NRIM using the so-called doctor-blade method. Fig. 4 shows an example of thus developed SRD. I_c measurements were then carried out, whereby effects of measurement variables were examined. The followings were found;

1. soldering heat and Joule heating at current terminals during measurement can reduce I_c,
2. sample cooling rate below 100 K/min does not appreciably affect I_c, while it has substantially reduces I_c over 100 K/min due to thermal differential stresses occurring between the brass-support and the oxide, and
3. I_c of the samples studied does not remarkably change with time.

Based on the present results, comprehensive research work including an international inter-laboratory measurement comparison program will be planned to establish guidelines for the critical current measurement in oxide superconductors.

Related Paper

n-Value and Second Derivative of the Superconductor Voltage-Current Characteristic, L.F. Goodrich, A.N. Srivastava, M. Yuyama and H. Wada, IEEE Transactions on Magnetics (1993) in print.

Simulation and theory

(65) Evaluation and Life Prediction of Material Strengths by "DIMS" System

April 1993 to March 1994
N. Nagata, 5th Research Group
Keywords: material strength, database, life prediction

This research is the follow-up of the previous work on the development of knowledge based system for material life prediction. The previous work has been done for constructing an integrated system for life prediction of advanced materials by combining the factual database on material strengths under creep, fatigue and corrosive environments. An integrated database management system, DIMS (Dialogical Integrated system for Material Strength database) which works in a UNIX operating environment with X-Windows has been developed.

In this research high temperature water environment is chosen as an environment to be investigated from the viewpoint of the technological requirement. Material strengths related to corrosion fatigue in high temperature water environments simulating light water reactor environments are databased and analyzed in the DIMS system in terms of influential factor of water chemistry such as dissolved oxygen concentration, conductivity, pH. Data related to stress corrosion cracking are analyzed in relation to test method, influential factor and elemental process of damage.

In addition elaboration of the material life prediction technique using the DIMS system, systematization of knowledges which has so far been obtained and construction of knowledge bases on material strength are scheduled. Construction of a prototype prediction system for material strength based on the knowledge base system will be tried.

66 Development of Material-design-technique for Mechano-chemical Attack on Light-weight Heat-resistant Materials

April 1989 to March 1994
I. Tomizuka, Physical Properties Division
Keywords: material design, mechano-chemical attack, light-weight heat-resistant material, intermetallic compound, C/C-composite material, oxide-despersion strengthened superalloy

Mechano-chemical attack on intermetallic materials

Effect of various factors of heat-treatment on hardness was elucidated for a cast Ni_3Al intermetallic. Effect of holding time at a cathodic potential on cathodic and anodic current densities were investigated in the specified acid for a series of TiAl-based materials. Scale formation in the course of heating to 1000 °C at a constant rate of heating was observed in a thermomicroscope for 4 types of TiAl-based materials.

Mechano-chemical attack on carbon-fibre-reinforced carbonaceous composite materials

Degradation of various types of C/C-composite materials in oxidizing atmosphere was observed *in-situ* in a thermomicroscopy.

Mechano-chemical attack on light-weight super-heat-resistant oxide-dispersion-strengthened alloys

Effect of various species of dispersed oxides in an Fe-Cr alloy on a tensile deformation behavior

was observed and discussed at 4 temperatures from 300 K through 1073 K.

Oxidation behavior of a yttria dispersed nickel-base alloy was observed and a manuscript on the results was submitted to "Zairyo-to-Kankyo."

Related Papers

Hot Corrosion in a Burner Rig Tester of the Ni-base Alloy on a Single Tie-line, Y. Koizumi, I. Tomizuka, S. Nakazawa and H. Numata, Zairyo-to-Kankyo 42 (1993): 86–92.

High Temperature Oxidation of C/C-composites and Their Components from Viewpoint of Material Design, A. Miyazaki, I. Tomizuka, S. Nakazawa and Y. Koizumi, Zairyo-to-Kankyo 41 (1992): 597–604.

High Temperature Oxidation a Series of Nickel-base Superalloys on a Single Tie-Line and its Extension, S. Nakazawa, I. Tomizuka, Y. Koizumi and A. Miyazaki, Zairyo-to-Kankyo 41 (1992): 379–84.

Prediction of Burn-off of a C/C-composite in Air and in O_2/N_2 Gas Mixtures, A. Miyazaki, I. Tomizuka, S. Nakazawa and Y. Koizumi, Zairyo-to-Kankyo 41 (1993): 83–88.

67 Self-organizing Information-base System Used for Creative Research and Development

April 1991 to March 1994

K. Hoshimoto, Materials Design Division

Keywords: self-organizing, information-base, materials design, dictionary, knowledge converter

In the domain of metals and alloys one can never find any two species that have precisely identical internal structure even if the chemical composition and outer shape are the same; which means that one can not specify the object exactly in the database of materials properties. Therefore the specification of material has inevitably an ambiguity. Specialists create new materials by combining basic theories, factual data and qualitative knowledge with their full skill and experiences, while the information on materials today is increasing day by day beyond the quantity which one person can deal with. The objective of the present study is to develop a self-organizing information-base system for materials design. To realize the system, the investigation of fundamental procedures has been made to select and organize various types of information automatically with the aid of computer for producing new materials.

The knowledge on materials being fuzzy ones, the answer that the system can offer contains fuzziness inevitably to some extent. For these reasons, a knowledge retrieval system has been constructed in the previous study by which the knowledge included in the research articles are collected and stored in the computer, and in the response to the queries expressed by natural language (Japanese in this case) of user, the system retrieves and shows the related knowledge to the user. Information on the data source and experimental procedures were also stored together with the experimental results and conclusions.

The system to be developed in the study will treat the fundamental knowledge on materials and the actual data of materials properties along with the above mentioned information.

In 1991 fiscal year, two tools for gathering information into the computer have been developed. The first searches for new words from the text fed into the computer by using OCR and put them in the dictionary automatically. It also assists to construct a thesaurus in consultation with the user. The second is a knowledge converter by which a text cut out from a document is transformed to a knowledge treatable by the computer.

In 1992, a conversational system to retrieve information from the knowledgebase by using natural English languages has been designed and a prototype system has been realized.

Related Paper

Development of a Knowledgebase System for Computer-Assisted Alloy Design, K. Hoshimoto, submitted to IUMRS-ICAM-93, August 31–September 4, 1993, Tokyo.

68 Study on the Trend of Application of New Super Conductors

April 1988 to March 1994

K. Hoshimoto, Materials Design Division

Keywords: energy technology, future technology

The development of High T_c Superconductors will give revolutional influences not only to the field of science but to the economy or social affairs. The investigators of the new superconductors should recognize this fact. From this point of view, studies have been started on the trend of application of new super conductors, which include the investigation of the possibilities of application of new superconductors to the industries of energy and also to the future technology.

69 Computer Aided Design Tools for the Development of Materials

April 1991 to March 1994

K. Hoshimoto, Materials Design Division

Keywords: computer aided development of materials, sensory test, micrographic data, materials database, knowledge on materials, materials design

The objective of the study is to extend fundamental tools used for the computer aided development of materials. The following three subjects have been studied.

Development of statistical tools for materials design

To develop an expert system of materials design and selection by using computer, it is necessary to obtain the quantitative correlation between microstructure and mechanical properties. Sensory tests followed by the analysis using a multi-dimensional scaling method have been adopted for the investigation of the relationship between the micrographic data of structure and of various properties in a Ti-6Al-4V alloy. It has been concluded that specialists in the field of materials science evaluate mainly from three characteristics of the geometry, the anisotropy and the size in a variety of microstructures. Moreover, good correlations were observed between the extracted characteristics of microstructures and mechanical properties.

Optimization of the implementation of materials data

As a part of the scheme for optimization of the structure of the materials database, the most efficient way to computerize binary phase diagrams obtained from literature has been studied. An intelligent man-machine interface for the retrieval of data has been developed which accept the user who lacks the knowledge on the special language of database management.

Organization of knowledge on materials and its application to materials design

Information expressed by different format or recorded by different media have been analyzed and an optimal way has been explored for organizing the knowledge of the materials so as to be the most suitable for the application to materials design.

Related Paper

Characterization of Image Data by Sensory Test, K. Kaneko, Y. Kurihara, K. Hoshimoto, M. Yamazaki and M. Fujita, *Computer Aided Innovation of New Materials II* (edited by M. Doyama et. al.), Proc. of CAMSE '92, Yokohama, Sept. 22–25, 1992: 1501–04.

70 Basic Research to Establish Design Techniques for Advanced Materials

April 1989 to March 1994

T. Tsujimoto, Materials Design Division

Keywords: lattice misfit, thermodynamic calculation, C/C-composite

Establishment of structure design and property design sub-systems are carried out for each material, such as Ni-base superalloy, Titanium alloy, and C/C-composite materials. In Ni-base superalloy, single crystal superalloys containing Re were examined by alloy design program in terms of the microstructural parameters and high temperature properties to clarify the strengthening mechanism, and the strongest alloys were searched for by the alloy design program. It was found that the control of lattice misfit was the most important for the design of ultra-high strength SC-superalloys. In Titanium alloy, thermodynamics aided design method for $\alpha + \alpha_2$ high temperature Titanium alloys was constructed by means of the two sub-lattice model in Ti-Al-Sn-Zr-Nb-Si systems. And it was confirmed that addition of Nb and Si improved creep strength. In C/C-composite materials, rate of oxidation was observed on carbon fibers, resion carbons and composite materials. Oxidation rate of CCCM was not given by a rule of mixture of components, while the activation energy of the rates was given by one. For expert system, intelligent alloy design system was developed using alloy design program for Ni-base superalloys. In this system, additional data are used to improve accuracy and reliability of the program.

Related Papers

Computer Analysis on Micrrostructure and Property Nickel-base Single Crystal Superalloys, H. Harada, T. Yamagata, T. Yokokawa, K. Ohno and M. Yamazaki, Proc. 5th Int. Conf. on Creep and Fracture of Engineering Materials and Structures, Swansea, U.K. March (1993): 245–54.

Thermodynamics Aided Design of $\alpha + \alpha_2$ High Temperature Titanium Alloys (Ti-Al-Sn-Zr-Nb-Si), H. Onodera, K. Ohno, T. Yamagata and M. Yamazaki, Proc. 7th World Conf. on Titanium, San Diego, June (1992), (to be published).

Collaboration Research

Atom Arrangement Design and Control. (Univ. of Cambridge, U.K.)

Computer Modelling of Alloys. (Rolls-Royce plc, U.K.)

71 Development of Knowledge Based System for Materials Life Prediction

April 1988 to March 1993

N. Nagata, 5th Research Group

Keywords: life prediction, database, knowledge base

We have planned to build an integrated system for the advanced materials life prediction, by combining the factual database on materials strength data and the knowledge base on our scientific and empirical understanding of materials deformation and fracture process. This research program has been carried out in the three fields of creep, fatigue and corrosion and the different factual materials properties databases for each field have been built by using the engineering workstations (EWS), which are connected with each other through a network communication system.

The advanced-integrated database management system, named as DIMS (Dialogical Integrated system for Material Strength database) was newly developed. The system, which works in a UNIX operating environment with the X-Windows system, can analyze the desired data set extracted from the database and find the combinations among characterized items of materials, not to mention the managing capability of the database. In the field of fatigue, for instance, many possible combinations among the characterized items of materials fatigue properties have been obtained by using the DIMS and through these combinations the significant paths from the characterized materials properties to the fatigue lives have been found, which has resulted in the empirical mathematical models for the life prediction. By using these empirical models, we have developed the new algorithm for predicting the fatigue strengths and lives of notch members. In the field of creep, rupture database has been combined in the DIMS and is ready to be analyzed. An optimized time-temperature-parameter method was applied to the well-balanced creep rupture data sets of ferritic steels and austenitic steels and an elaborate algorithm for time-temperature dependence was obtained. Consolidation of environmental strength data to the DIMS has remained incomplete due to the complication of meta-data and strength data.

[72] Predictions of Materials Strength and Endurance under Irradiation Using Ion Beam

April 1988 to March 1993

J. Nagakawa, 2nd Research Group

Keywords: irradiation creep, stress relaxation, radiation damage, computer simulation

Among the various changes in materials properties induced by neutron irradiation, a change in mechanical properties is one of the most important property alterations in the structural materials for nuclear reactors. The change causes a significant influence on endurance of the structural components. It is, however, almost impossible to obtain a complete set of irradiation data necessary for the engineering design of nuclear reactors of the next generation such as fusion reactors, because of technical difficulties and a high cost of irradiation tests.

Materials behavior under irradiation is especially difficult to be evaluated. It cannot be estimated from the pre- and/or post-irradiation properties. It is, therefore, highly desirable to develop a prediction method of the materials properties under irradiation. A theoretical calculational method has been developed to evaluate radiation induced deformation, based on a computer simulation of point defect kinetics under stress. This method was applied to the radiation induced stress relaxation in 316 stainless steel at low temperatures, which could be expected in the ITER (International Thermonuclear Experimental Reactor). Following are the results;

1. Although significant stress relaxation is also induced at higher temperatures, e.g., 300 °C, extremely swift stress relaxation takes place at low temperature, e.g., 60 °C which is the inlet temperature of the coolant water in ITER. This results from a transient, high concentration of point defects in the matrix, which lasts until vacancies reach the defect sinks and it takes more than a year at 60 °C.
2. Even with a very low atomic displacement rate at the back side of the blanket, i.e., two orders of magnitude lower that at the first wall, radiation induced stress relaxation at 60 °C is still significant enough to reduce the stress to half in a few years.

Related Papers

Computer Simulation of Early-Stage Irradiation Creep, J. Nagakawa, N. Yamamoto and H. Shiraishi, J. Nucl. Mater. 179–81 (1991): 986–89.

Calculational Evaluation of Radiation Induced Deformation, J. Nagakawa, Proc. of the 4th Int'l Symp. on Advanced Nuclear Research (1992): 387–91.

[73] A New Computational Approach to the Micromechanics of Heterogeneity in Advanced Structural Materials

April 1992 to March 1993

Y. Nakasone, 2nd Research Group

Keywords: computational mechanics, micromechanics, singular integral equation, heterogeneity

The present study proposes a new computational approach to the micromechanics analysis of heterogeneity often found in advanced structural materials. The proposed approach attempts the computerization of the Type-I equivalent inclusion method, one of the most powerful theories in solid mechanics for analyzing materials with such heterogeneities as inclusions, precipitates, strengthening particles, etc. This method, however, requires advanced mathematics, and thus is difficult to treat or even theoretically unsolvable in a closed form. In order to avoid these difficulties, the present approach employs the finite element discretization scheme and evaluate the mechanical properties of advanced structural materials by using digital computers.

The governing singular integral equation has been discretized to obtain a computer code for two-dimensional elastostatic problems by the aid of the symbolic formula manipulation. The integrand has the $1/r$ and $1/r^2$ singularity for the two- and three-dimensional case, respectively. The discretization is carried out by using triangular

and tetrahedral finite elements having the special polar coordinates for the respective case which can theoretically eliminate the above singularities in Cauchy's sense.

The formulation has been completed, and found very similar to that encountered in the direct boundary element method in which interior points need to be investigated. The three-dimensional formulation can be obtained in the same manner. The FORTRAN computer code has been developed on a high-performance engineering workstation having a main memory capacity of 32 Mbytes and a computational speed of up to 20 MFLOPS.

Related Papers

A Theory of Fatigue Crack Initiation in Solids, T. Mura and Y. Nakasone, Trans. ASME 57-1 (1990): 1–6.

Free Energy Formulation of Fatigue Crack Initiation along Persistent Slip Bands: Calculation of S-N Curves and Crack Depths, G. Venkataraman, Y-W. Chung, Y. Nakasone and T. Mura, Acta Metall. Mater. 38-1 (1990): 31–40.

Numerical Equivalent Inclusion Method, Y. Nakasone, A. Safadi and T. Mura, Proc. the 1990 Annual Meeting of JSME/MMD 900-86 (1990): 374–76 (in Japanese).

Materials

Non-ferrous materials

74 Disintegration Phenomena in Intermetallic Compounds

April 1992 to March 1995

K. Kawahara, Physical Properties Division

Keywords: manganese intermetallic compound, disintegration, pulverization

Though MnAl compounds are stable in the air, addition of carbon results in natural disintegration to fine powder in a few days.

It has been found that a 47.5Mn-47.5Al-5C (atomic%) alloy shows the following phenomena: (1) the plate-like carbides dispersed in the matrix react with the moisture in the air, (2) the expansion in volume results from the reaction, thus the cracking occurs along the center of carbides, (3) through the path produced by cracking the moisture gas reaches new carbides in the interior and generates reaction products that consist of methane and hydrogen gases, (4) the cracks propagate into the matrix and unite mutually, (5) small particles are formed in several places, subsequently the specimen is disintegrated to fine powder.

The survey work is carried out for finding new intermetallic compounds which show disintegration in the air.

75 Microstructural Refinement and Mechanical Properties of Titanium Alloys

April 1991 to March 1994

T. Kainuma, Mechanical Properties Division

Keywords: Ti-3-8-6-4-4, mechanical properties, microstructural refinement, hydrogen absorbing

Recently, metastable beta-type titanium alloys have drawn attention because of their excellent formability. However, a rapid grain growth is known to occur when they are annealed at temperatures, above the beta transition temperature Tβ. Then, a metastable beta-type alloy with a composition of Ti-3Al-8V-6Cr-4Mo-4Zr(Ti-3-8-6-4-4), which is resistant to grain growth even at temperatures above Tβ, was developed for applications requiring cold formability and high strength.

The aim of this work is to reveal the mechanism of microstructural refinement of grain size, substructure and alpha phase precipitation due to thermomechanical treatment and the hydrogen absorbing treatment in Ti-3-8-6-4-4 alloy. The mechanical properties of the alloy with the refined microstructures will also be evaluated.

Microstructural refinement and mechanical properties

The grain refinement for Ti-3-8-6-4-4 alloy is mainly achieved by heavy cold-rolling, followed by short time recrystallization method. The addition of silicon to the alloy substantially help refine the grain size. The substructural refinement in the alloy is achieved by the combination of various annealing conditions and various reduction ratios of cold-rolling. The relationship between the grain refinement and the alpha precipitate morphology is currently being determined.

Microstructural refinement by hydrogen addition

Previously we have shown that hydrogen absorption and formation of dislocation structures induced by the absorption, occurs during the specimen preparation of the beta-type titanium alloy, such as the cold rolling, the emery polishing, the diamond cutting and the water quenching.

In this work, we have tried to understand the absorption mechanism of hydrogen by changing composition of atmosphere. In addition, the dislocation structure has been examined for the Ti-3-8-6-4-4 alloy charged with hydrogen. It was shown that the high dislocation density is caused by pinning effect due to hydrogen atoms which retards the recovery of dislocations introduced by the thermomechanical treatments. The possibility

of the further refinement of microstructure using hydrogen effect is also being studied.

Intermetallic compounds

(76) Basic Researches on Intermetallic Compounds for Structural Applications

April 1993 to March 1996

M. Nakamura, 3rd Research Group

Keywords: intermetallic compound, TiAl, transition in elongation, high temperature creep, grain morphology control

TiAl base intermetallic compounds have received considerable attention as candidates for high temperature structural applications. Although they have advantages of high melting point, high strength at high temperatures, high elastic moduli and reasonable oxidation resistance, improvement of both room temperature ductility and strength at higher temperatures above 1000 °C is required.

In this work, a transition phenomenon in tensile ductility of TiAl base alloys will be investigated. V– containing TiAl is reported to exhibit transition in elongation at about 200 °C and to have relatively good ductility above 200 °C, although it exhibits poor ductility at room temperature. It is useful for improvement of room temperature ductility to study the deformation behavior near a transition temperature in elongation. The creep strength at high temperatures is also required to study for high temperature structural applications, but there are not many researches on tensile creep behavior of TiAl base alloys. The creep behavior in tension will thus be studied at high temperatures above 800 °C.

The microstructure control of TiAl base alloys will be studied for improvement of mechanical properties at high temperatures. The alloys with an equiaxed, fine grained structure is known to have relatively good ductility at room temperature and to exhibit superplasticity at about 1000 °C. Meanwhile, the alloys with large grains or grains elongated parallel to a loading direction are required for high strength at high temperatures. Although the fine grained structure is prepared by thermo-mechanical processing, it is very difficult to control the grain growth and to prepare the microstructure with preferred orientation of grains. The control of grain morphology of TiAl base alloys will thus be studied using thermo-mechanical processing.

The resistance to thermal shock of transition metal carbides and borides with a much higher melting point will also be studied for much higher temperature structural applications.

(77) Study on Sintering of TiAl Intermetallic Compound

April 1993 to March 1995

Y. Muramatsu, Chemical Processing Division

Keywords: TiAl intermetallic compound, powder metallurgy, densification, microstructure, oxygen content

TiAl intermetallic compound is promising as a lightweight high-temperature material. It has a specific gravity of 3.9, excellent oxidation resistance, high strength at high temperatures and so forth. However, this material has not yet been industrially used because of its brittleness and poor workability. The powder metallurgical technique is considered as one of the attractive manufacturing techniques. This study is intended to develop sintering methods which allow a mass production of TiAl near-net shaped bulk components with high densities and high dimensional precision.

Up to now, we investigated the sintering behavior of various starting powders. For the starting powder which showed excellent sinterability, we examined the influence of compositional differences from the stoichiometric composition on densification characteristics. We also examined microstructure and oxygen content of sintered TiAl. These examinations made clear that the densification characteristics were greatly influenced by the compositional differences and Ti-rich TiAl showed excellent sinterability in comparison with Al-rich TiAl. The microstructure of Ti-rich TiAl consisted of two phases of TiAl and Ti_3Al, while that of Al-rich TiAl was composed of single phase of TiAl. The oxygen content was less than 0.4 mass%.

78 Fundamental Study of Microstructures and Properties to Develop High Performance Materials for Severe Environment (II-High Temperature Intermetallic Compounds)

April 1990 to March 1997

T. Yamagata, Materials Design Division

Keywords: Nb_3Al + Nb two phase structure, oxidation behavior

The project is a part of a national research project to develop various heat resisting materials which withstand severe environment. Target of the project is to develop high temperature intermetallic compound such as Niobium aluminide which possess mechanical properties of ductility at room temperature and 75 MPa tensile strength at 2073 K. Effect of alloy composition on structure and oxidation property was investigated. Intermetallic compound Nb_3Al (A15 phase) is a typical brittle material. In order to get ductile materials, two phase structure, composed of Nb_3Al and Nb phase (A2) ductile in equilibrium state at 2073 K, was searched in Nb-Al binary and Nb-Al-X ternary alloys. In binary alloys, A15, A15 + A2 and A2 structures were obtained in 20 ~ 23at%Al, 18at%Al and 16at%Al compositions respectively.

In ternary alloy, Mo, W, Ta, Hf, Ti, Zr and Cr were substituted for 4at%Nb and Si, Ni, Co to 4at%Al. Two phase structure was observed on Nb-18Al-4Ta and Nb-18Al-4W alloys heat treated for 1.44×10^4 S at 2073 K. Hardness test showed that two phase structure had ability to resist crack propagation. Addition of W and Ta enhanced the ability. For oxidation property, weight change of Nb-Al binary alloys with various Al compositions was observed at various temperatures in oxygen, in a commercial nitrogen, or in N_2-20%O_2 gas mixture. The alloys were far more sensitive to chemical attack by these gases as compared with TiAl or Ni_3Al.

79 Improvement of Mechanical Properties of Intermetallic Compounds by Crystal Growth Control

April 1992 to March 1997

T. Hirano, Chemical Processing Division

Keywords: unidirectional solidification, floating zone method, Ni_3Al, room-temperature ductility

The objective of this study is to improve the mechanical properties of intermetallic compounds by crystal growth control. Recently, we have found that unidirectional solidification using a floating zone method remarkably enhances the room-temperature ductility of Ni_3Al without addition of alloying elements such as boron. We call this method FZ-UDS. Stoichiometric Ni_3Al grown by FZ-UDS exhibits more than 60% tensile elongation at room temperature. Even Al-rich Ni_3Al can be ductilized by FZ-UDS. FZ-UDS is a new promising method to improve brittle intermetallic compounds.

In this study three subjects are stressed. First, crystal growth technique is developed in detail. Columnar grained Ni_3Al which is closely related to the large ductility is grown by FZ-UDS. Favorable growth conditions for this structure are clarified. Secondly, the solidified structure, especially grain boundary structure, is characterized. It became clear that this structure contains a large amount of low energy boundaries. Thirdly, the mechanical properties and deformation behaviors are studied.

80 Fatigue Fracture Mechanisms for TiAl Intermetallic Compounds at High Temperatures

April 1991 to March 1994

K. Yamaguchi, Failure Physics Division

Keywords: TiAl, intermetallic compounds, fatigue strength, fatigue fracture surface

Titanium aluminide alloys based on gamma TiAl are of great interest for practical applications as aerospace material and motor components due to their low density, high strength and good oxidation resistance at high temperatures. To make full use of their attractive and excellent properties, it is important to study the dynamical behavior such as fatigue strength as well as the static one.

Two sample materials for fatigue experiments were prepared from 7 kg ingots by skull melting and casting. The nominal compositions are A:Ti-33.9mass%Al and B:Ti-36.3mass%Al, respectively. The material A has a tensile fracture elongation of 2.2% which is the maximum among as-cast materials ranging from 28 to 38 mass% in Al. The microstructure of as-cast sample A consisted of large grains containing full lamellar morphology of γ(TiAl) and α_2(Ti_3Al) phases. The material B showed mixed microstructure with γ phase and lamellar structure. The volume fraction of γ phase was approximately 20%.

Both materials showed good fatigue resistance at room temperature and at 800 °C. Especially, A was superior to B at both temperatures.

The fatigue fracture surfaces consisted mainly of transgranular mode reflecting lamellar structures for sample A. As for the sample B, transgranular mode reflecting γ phase was also observed. On the specimen surface, persistent slip bands were observed in γ grains.

Related Paper

Fatigue Properties and its Mechanisms of Ti-Al-V Intermetallic Compounds, K. Yamaguchi, M. Shimodaira and S. Nishijima, J. Iron and Steel Inst. 78 (1992): 134–40 (in Japanese).

81 High Ionic Conductivity of Solid Electrolyte

April 1992 to March 1995

H. Nakamura, Environmental Performance Division

Keywords: ionic conductor, solid electrolyte, charge carrier, electrical conductivity

Recently, research works on solid high ionic conductor have been mainly focused on oxygen ion conductor such as ZrO_2, proton conductor such as $SrCeO_3$ and sodium ion conductor such as β-Al_2O_3.

One of the reasons why no other solid electrolytes have been developed as high ionic conductor is that cracks caused by grain growth or voids along grain boundaries tend to initiate in the sintered materials prepared for the solid electrolyte.

The purpose of this study is to synthesize a new solid electrolyte consisting of oxides and sulfates (M_2O – B_2O_3 – M_2SO_4, M = Li, Na, K) of which grain boundaries or voids were decreased by a rapid quenching method, and to investigate the suitable composition of the compound in solid-liquid coexisting composition range by various thermal analytical methods.

Furthermore, the electrical properties of the electrolyte can be evaluated by the measurement of

electrical conductivity, the investigation of polarizing behavior, the determination of charge carrier, the comparison of electron motive force for concentration cell with that for theoretical one, etc.

Related Paper

Electrical Conductivity of Solid Beryllium Sulfide, H. Nakamura, Y. Ogawa, A. Kasahara and S. Iwasaki, J. Japan Inst. Metals 56 (1992): 1408–13.

82 High Performance Materials for Severe Environments-I (Microstructure and Properties of Intermetallic Compounds with High Specific Strength)

April 1990 to March 1996

M. Nakamura, 3rd Research Group

Keywords: intermetallic compound, TiAl, microstructure, thermo-mechanical processing, mechanical property, high temperature oxidation

Light-weight, heat-resisting intermetallic compound TiAl is a candidate for a structural use in severe environments for a space plane etc., and the knowledge of various properties of TiAl base alloys is required for a practical use in such an environment. In this research program, the mechanical properties are systematically studied for TiAl base alloys whose composition and microstructure are well controlled, and then the fundamental methods to control microstructure which gives the optimum properties for a practical use to materials are discussed. Thus, TiAl base alloys with various microstructures and compositions have been prepared by heat-treatment and thermo-mechanical processing using isothermal forging above 1000 °C, and the effect of microstructure on mechanical properties like strength, ductility, etc. has been studied. The environmental effects on mechanical properties like room temperature tensile properties, etc. and high temperature oxidation behavior have also been studied.

Related Papers

Morphology of α_2 Phase in γ-TiAl-Base Alloy Ingots, T. Aritomi, K. Ogawa, K. Honma, K. Sato and T. Tsujimoto, Materials Science and Engineering A149 (1991): 41–51.

Microstructural Evolution and Tensile Properties of Ti-rich TiAl Alloys, T. Takeyama, Materials Science and Engineering A152 (1992): 269–76.

83 Preparation of Spontaneous Exothermic Metals and Its Application

April 1990 to March 1993

T. Fujii, Chemical Processing Division

Keywords: skelton structure, exothermic metals, compound

We have previously shown that a spontaneous generation of heat can easily take place in air atmosphere from the bulk material of Ni-Al and Co-Al alloys after leaching. These materials are called "Spontaneous Exothermic Metals." This year Al-Ni-Co ternary alloys containing 50 wt%Al and 10 ~ 40 wt%Co were prepared by a self-propagating high-temperature synthesis (SHS) method under a vacuum of 1×10^{-3} Pa for the purpose of refinement of microstructure. These alloys are leached to dissolve the Al element in an alkaline aqueous solution at about 373 K. The measurement of the exothermic characteristics was conducted with a newly designed thermobalance.

The results obtained at present stage are summarized as follows.

1. The alloys produced by SHS were composed of several kinds of intermetallic compounds with Ni_2Al_3, $NiAl_3$, Co_2Al_5 and Co_2Al_9 binary phases and $Ni_xCo_yAl_z$ ternary phase.
2. After leaching, the x-ray diffraction pattern showed all intermetallic compounds with a large line broadening, suggesting the skelton structure.
3. The leached compounds had stable spontaneous exothermic reaction in air atmosphere and maximum spontaneous exothermic temperatures were 895 K to 1150 K in proportion to the amounts of Co.
4. On the leached surface of Ni_2Al_3 and Co_2Al_9 phases the particles consisting of NiO and CoO less than 70 nm in diameter existed much more frequently after spontaneous exothermic reaction.

84 Production and Character Evaluation of Functional Intermetallic Compounds

April 1988 to March 1993

M. Nakamura, 3rd Research Group

Keywords: intermetallic compounds, coatings, thermoelectric compounds, combustion synthesis, TiAl

Many intermetallic compounds are candidates for new functional and structural materials with peculiar and excellent properties which conventional metals and alloys are not endowed with. The basic research works on intermetallic compounds like transition-metal aluminides, silicides and so on for functional and structural applications have been carried out. Fabrication and application of the intermetallic compounds like TiAl, NiTi, $FeSi_2$, Bi_2Te_3 etc. have also been studied.

Sub-themes:

1. Intermetallic Compound Coatings for High Temperature Corrosion Resistance.
2. Development of High Performance Thermoelectric Intermetallic Compounds.
3. Combustion Synthesis of Intermetallic Compounds.

4. Development of Light-Weight Heat-resisting Materials Based on TiAl Intermetallic Compounds.
5. Effect of Weightlessness on Microstructure and Strength of Ordered TiAl Alloys.

Related Papers

Aluminized Coatings on Titanium Alloys and TiAl Intermetallic Compounds, A. Takei and A. Ishida, High Temperature Corrosion of Advanced Materials and Protective Coatings (1992): 317.

Studies on the Holes of P-type $Bi_2Te_{2.85}Se_{0.15}$ Single Crystal, H.T. Kaibe, M. Sakata and I.A. Nishida, J. Phys. Chem. Solid 51 (1990): 1083–87.

Superplasticity in a Vanadium Alloyed Gamma Plus Beta Phased Ti-Al Intermetallic, D. Vanderschueren, M. Nobuki and M. Nakamura, Scripta Metallurgica et Materialia 28 (1993): 605–10.

Composites

(85) Thermal Stability of Intermetallic Compound Matrix Composites Reinforced with Fibers

April 1993 to March 1995
Y. Shinohara, Physical Properties Division
Keywords: TiAl matrix composite, B fiber, W fiber, protection layer, BN, TiB_2

Heat resistive materials which can be used above 1373 K are essential to the development of the space-plane, the fusion reactor and the high-efficient turbine engine. TiAl intermetallic compounds (IMCs) have higher strength and toughness than metals and ceramics at elevated temperatures. The TiAl matrix composite reinforced with fibers is hopeful for a structural material above 1373 K.

Reinforcements for TiAl matrix are SiC, B and W fibers. B and W fibers are tougher than SiC fibers, while are more reactive with TiAl. No reinforcement besides SiC fibers has been applied to the TiAl matrix composite. However, if the protection layers against the interfacial reaction are developed, it will be possible to utilize B and W fibers of higher toughness for reinforcements.

TiB_2 and BN have both little reactivity and good wettability with TiAl. Therefore, we will study on the B and W fibers with protection layers of TiB_2 or BN, and carry out the following subjects.

Formation of TiB_2 and BN layers and optimization of layer thickness

The B fibers are coated with Ti by using PVD method, and are heat treated to form TiB_2 layers. The W fibers are coated with BN by CVD. The fibers with thin protection layers may react with TiAl. On the contrary, the thick layers may cause the degradation of fiber strength. The optimum thickness of protection layers are investigated.

Effect of surface morphology on the strength of W fiber

When the protection layer has insufficient shear strength for stress transfer between the W fiber and the TiAl matrix, roughening of the fiber surface is effective in transferring stress. However, the roughening may decrease the fiber strength. Effect of the surface morphology on the fiber strength is investigated.

[86] Thermal Effects in Hetero-Phase Materials

April 1990 to March 1993
I. Shiota, Physical Properties Division
Keywords: FRM, thermal cycling, SiC fiber, Ti, Ti-6Al-4V

Major target of fiber reinforced metals (FRM) is high temperature applications. However, the strength of the FRM is deteriorated by reaction products at the interface between fiber and matrix. The effects of continuous heating of FRM had been studied in the previous research. On the other hand, the effects of thermal cycling on FRM were studied in this study.

SiC fiber was used as the reinforcement, and pure Ti and Ti-6Al-4V were used as the matrices. FRMs were fabricated at 1183 K under 39 MPa for 1.8 ks in a vacuum. The thermal cycling test was carried out at a heating rate of 8.3 K/s to 1123 K, and was held at the temperature for 360 s, consequently cooled down to 623 K. After the sample reached 623 K, the next thermal cycling was started. The time required for 1 cycle was 960 s. Total holding time at 1123 K for three samples were 32.4, 126 and 360 ks, respectively. The tensile strength of the FRMs was measured at room temperature.

The layer structure of reaction products was observed at the interface between the fiber and the matrix, which was similar to that of the sample of continuous heating. The degradation in tensile strength of the FRMs after continuous heating of 126 ks was approximately 5%. On the other hand, 20 to 30% of degradation was observed after the thermal cycling at total holding time of 126 ks. In the case of FRM with pure Ti matrix, the degradation rate was constant up to 360 ks. However, in the case of FRM with the alloy matrix, the degradation rate gradually decreased. Many fibers were pulled-out from the matrix in the FRM with pure Ti matrix after 126 ks. Severe grain growth and cleavage of pure Ti were observed after 360 ks. On the contrary, many dimples, which show the ductile fracture, were observed in the alloy matrix, and cleavage area was small. On the other hand, the tensile strength of the extracted fibers from the thermal cycled FRM with pure Ti was 40% lower than that of the fibers from continuously heated one. In the case of the alloy matrix, little difference was observed between them.

From these results, it is concluded that the degradation in tensile strength of FRMs after short time thermal cycling was attributed to the decrease in stress tansference from the matrix to the fiber. The radial stress was introduced by the shrinkage of matrix during cooling after fabrication at a high temperature, and the stress was relaxed by the thermal ratchet effect after the thermal cycling. In the case of longer thermal cycling, the degradation in strength of FRMs was due to coarsening of the matrix grain and degradation of the fiber. It has been found that the strength of FRMs can be improved by the intermixed structure of α and β phase, which prevents the grain growth.

Related Papers

The Relationship between Interfacial Reaction and Tensile Strength of SiC Filament Reinforced Ti Alloy Composites, Y. Imai, Y. Shinohara, S. Ikeno and I. Shiota, Proc. 5th Japan–US Conf. Comp. Mat. (1990): 347–54.

Deterioration Factor of SiC/Ti Alloy Composite after Heat Treatment, Y. Imai, Y. Shinohara, S. Ikeno and I. Shiota, ISIJ International 32 (1992): 917–22.

Materials for mechanical application

87 Intelligent Structural Materials

April 1991 to March 1996

S. Matsuoka, Environmental Performance Division

Keywords: intelligent material, material damage, self-sensing, self-restoring, nanotechnology

Recently, a new material concept, known as intelligent material or smart material, has been proposed and developed to establish the reliability of engineering structures such as air crafts, space structures and nuclear power plants. The intelligence of the material is defined as self-detectability for environmental changes and feasibility of sensing, processing and actuating.

In this study, fundamental research has been carried out in order to impart the intelligent functions to the metallic materials for structural use. Small cavities which do not deteriorate the mechanical properties exist in the materials. An attempt has been made to implant the sound-emitted material, phase transformed material or surface film controlled material into the cavities. The implantation could make the material possible to self-sense and self-restore the damage during operation. A nanotechnology based on the scanning tunneling microscope (STM) and atomic force microscope (AFM) has also been developed to evaluate the intelligent functions of the materials from atomic scale viewpoint.

Y_2O_3 oxide particles with about 30-nm-diameter dispersed in the Fe-20Cr alloy were found to control the elevated-temperature fatigue crack growth. The control function was related to the fact that Y_2O_3 particles suppressed spalling of oxide film at the crack tip through trapping sulfur element. Fractograpy in atomic scale was developed by STM and AFM. The hardness measurement method in nanoscopic scale was also developed, especially applying the nanofabrication by STM and AFM. These will be used to evaluate the intelligent structural materials.

88 Development of Metal Matrix Composites for High Temperature Use Through Combinations of Advanced Powder Metallurgy Processes

April 1991 to March 1994

M. Hagiwara, Mechanical Properties Division

Keywords: titanium, mechanical properties, powder metallurgy, titanium matrix composite

Titanium alloys are ideally suited for airframe and gas turbine engine components because of their unique mechanical properties. However, the service temperature is limited to 600 °C due to a rapid degradation of creep strength, metallurgical stability and environmental resistance. However, there still has much room to develop advanced titanium alloys having superior combinations of high-temperature strength, creep resistance, stiffness, corrosion resistance and thermal stability for future aircraft components available at temperatures up to 1000 °C.

The application of powder metallurgy processes can be considered as one possible route to expand the service temperature of titanium alloys due to extended alloy solubility, very fine and metastable microstructure and more homogeneous compositions. Powder metallurgy also provides a flexible process for manufacturing composites reinforced with relatively large size (1 ~ 40 μm) ceramic particles.

Our research group has been devoted to the production of titanium based metal matrix composites using advanced powder metallurgy processes such as plasma rotating electrode process (PREP), melt spinning method and proprietary blended elemental method, with emphasis on relationship between composition/microstructure and high-temperature mechanical properties.

Related Papers

Mechanical Properties of Particulate Reinforced Titanium-based Metal Matrix Composites Produced by the Blended Elemental P/M Route, M. Hagiwara, S. Emura, Y. Kawabe, N. Arimoto and H.G. Suzuki, ISIJ Int. 32 (1992): 906–16.

Microstructures and Tensile Properties of Titanium-Based Composites Produced by Powder Metallurgy, M. Hagiwara, S. Emura, J. Takahashi, Y. Kawabe and N. Arimoto, Proc. 7th World Conf. Titanium (1992): to be published.

Materials for electronics application

(89) Thermal and Electrical Properties of II–IV and V–VI Thermoelectric Semiconductors

April 1993 to March 1995

I. Nishida, Physical Properties Division

Keywords: thermal conductivity, thermoelectric property, energy conversion, $Bi_{2-x}Sb_xTe_{3-y}Se_y$, $Mg_2Si_{1-x}Ge_x$

Thermoelectric (TE) materials have been widely used for the direct energy conversion systems. These materials convert thermal energy to electric power with quick response and without noises and mechanical vibration. Recently, the thermoelectric generator is mainly used for the electric source in the space, marine and polar region, and the thermoelectric cooling system is mainly used for the precise controlling the temperature of semiconductor processing equipments, optical and electronic devices. Therefore, the TE materials with high conversion efficiency have been attracted much.

The TE materials with high efficiency are given by the three characteristics, i.e., high thermoelectric power and electric conductivity and low thermal conductivity (κ). For the TE materials with very low values of κ, such as $Bi_{2-x}Sb_xTe_{3-y}Se_y$ and $Mg_2Si_{1-x}Ge_x$ etc., it is very difficult to obtain the reliable value of κ.

The aim of this study is to establish more precise technique for the measurement of κ by means of the Harman's method and PAS (Photo Acoustic Spectroscopy).

(90) Structure Control and Electromagnetic Properties of High Temperature Superconductors

April 1993 to March 1998

K. Togano, 1st Research Group

Keywords: high temperature superconductors, critical current density, flux quantum, tape, film, vapor deposition

New superconductors such as high-T_c oxides are not only in scientific interest but also key materials for further progress of superconductivity applications in various advanced technological fields. From this point of view, the research program conducts following researches to establish the base of superconductivity applications.

Study on the relationship between microstructure and critical properties

The objective of this research is to study the effects of various microstructural features, such as grain alignment, phase distribution, defects produced by irradiation and structure change caused by intercalation, on critical current density J_c of high temperature superconductors (HTSC). Attempts of producing long tape and its coil test of HTSC are also carried out in order to study the possibility of power applications of HTSC.

Understanding of the electromagnetic behavior of HTSC

The objective is to understand the origin of peculiar behavior of flux quantum in HTSC. For this purpose, high quality single crystal of HTSC is prepared, from which precise information on electromagnetic properties can be drawn. New model of flux quantum state is proposed and discussed with the possibility of J_c improvement.

Structure control by film deposition techniques

Structure control in atomic layer level is carried out for HTSC by using MBE and alternative sputtering techniques. New techniques of film analysis such as RHEED-TRAXS and RBS-PIXE are also developed. Those techniques of deposition and analysis are essential to achieve well control of crystal structure, which is one of the keys to realize electronic applications of HTSC.

Microstructure control by vapor deposition technique

The objective is to apply vapor deposition techniques to the conductor fabrication of HTSC. Thin and thick films are synthesized by various deposition techniques of laser ablation, sputtering and thermal flash plasma, etc. The effects of grain alignment, inclusions and material of buffer layer on superconducting properties are studied to optimize the processing parameters.

91 Purification of Active Metals for the Preparation of Superconductive Materials

April 1987 to March 1994

T. Fujii, Chemical Processing Division

Keywords: sintering method, melt-growth method, $YBa_2Cu_3O_x$

In order to examine in more detail the superconducting characteristics of $YBa_2Cu_3O_x$ ceramics prepared by sintering and melt-growth methods, effect of purity of the starting materials on superconductivity such as the critical transition temperature, T_c, and the critical current density, J_c, was investigated.

It has found that the zero resistance and the critical current density depend strongly on the purity of starting materials and preparation methods. For the case of the melt-growth ceramic sample, a coarse-grained 123 phase structure was observed, while the higher zero resistance temperatures between 90 K and 92.9 K with transition widths narrower than 2.4 K, which remarkably depends on the concentration of impurities were achieved. In contrast, for the case of sintering ceramics sample, a uniformed and fine-grained 123

phase structure was observed, while the zero resistance temperatures between 87.9 K and 89.6 K and the values of transport J_c of 150 to over 500 A/cm^2 (at 77 K, 0 T) were obtained, which also depend upon the concentration of impurities.

These superconducting characteristics can be discussed in terms of the grain shape and size of $YBa_2Cu_3O_x$ phases as a result of purity of the starting materials and preparation procedures.

92 Development of $Bi_2Sr_2CaCu_2O_x$ Tapes and Coils

April 1989 to March 1994
H. Kumakura, 1st Research Group
Keywords: melt-texturing, pancake coil, generated magnetic field

$Bi_2Sr_2CaCu_2O_x$ (2212) pancake coils have been fabricated using 2212/Ag composite tapes prepared by continuous dip-coating method and melt-solidification process. Ag tapes were dipped into slurry composed of 2212 powder and organic materials and the tapes were coated with slurry on both sides. The length of the composite tapes was 6 m. These tapes were wound into coils with small gap between each turns and heat treated. At first, the coil was heated at 500 °C to remove organic materials, heated up to 885 °C, just above the melting point of 2212, slowly cooled down to 835 °C at a rate of 5 °C/min. and cooled to room temperature at a rate of 300 °C/min. Heat treatment was carried out under Bi atmosphere in order to suppress vaporization of Bi from the 2212 layer. 2212 layers on both sides of the Ag tape have grain oriented microstructure and show excellent critical current density. After the heat treatment, myler tape was inserted along the gap of the coil for insulation. The coils were then wound tightly and fixed by impregnating wax or epoxy resins. The size of the pancake coils were 41 mm in inner diameter, 14 mm in outer diameter and 12 mm in height. These pancake coils were stacked together to obtain double and triple stacked coils.

Coil performance tests were carried out in bias magnetic fields at various temperatures. Generated magnetic fields at 4.2 K by the double stacked coil were 1.64 T, 1.25 T and 0.54 T in bias magnetic fields of 0 T, 6 T and 23 T, respectively. The generated field decreased with increasing temperature. However, 0.7 T was generated even at 21.5 K. These results suggest that the 2212 coil can be used at a temperature range between 4.2 and 20 K.

This research was performed in collaboration with Asahi Glass Co. Ltd. and Hitachi Cable Co. Ltd.

Related Papers

Fabrication and Properties of $Bi_2Sr_2CaCu_2O_8$/Ag Composite Tapes and Coils, H. Kumakura, H. Kitaguchi, K. Togano, H. Maeda, J. Shimoyama, T. Morimoto, K. Nomura and M. Seido, Cryogenics 32 ICMC Supplement (1992): 489–95.

Improvement of Reproducibility of High Transport J_c for $Bi_2Sr_2CaCu_2O_y$/Ag Tapes by Controlling Bi Content, J. Shimoyama, N. Tomita, T. Morimoto, H. Kitaguchi, H. Kumakura, K. Togano, H. Maeda, K. Nomura and M. Seido, Jpn. J. Appl. Phys. 31 (1992): L1328–31.

93 Development of High-T_c Superconducting Thick Films and Tapes by Various Spraying Methods and by Internal Oxidation

April 1988 to March 1995
H. Maeda, 1st Research Group
Keywords: high-T_c superconductor, film, plasma spraying, flame spraying, internal oxidation, magnetic shielding

We have studied the superconducting properties, compositions and microstructures of Bi-based and Y-based high-T_c oxide thick films and tapes prepared by plasma spraying, flame spraying and internal oxidation. Especially, we have fabricated a prototype vessel for superconducting magnetic shielding, which is very useful for medical application such as neuromagnetics.

(Bi, Pb)$_2Sr_2Ca_2Cu_3O_{10}$ thick films with a thickness of about 770 μm were prepared by plasma spraying on the outer surface of a Ni-based alloy pipe (320 mm in diameter, 660 mm in length and 1.6 mm in thickness). A Ag buffer layer with a thickness of about 50 μm was plasma-sprayed to prevent the interdiffusion between the oxide layer and the substrate pipe. The films were post-annealed for 100 h at 1110 K and shows a T_c of 101 K and a J_c of 170 A/cm^2. The magnetic shielding effect, S, which is (applied magnetic field strength)/(measured magnetic field strength inside the pipe), were measured by a RF-SQUID magnetometer at an applied field of 4×10^{-4} T parallel to the pipe axis. The values of S show above 10^3 at the inner center position equal to the pipe diameter from the pipe end. We detect no difference in S in the frequency range of 0.1–10 Hz.

Flame spraying using a mixed gas of oxygen and acetylene was also applied to fabricate Bi-based high-T_c thick films. $Bi_2Sr_2Ca_1Cu_2O_8$ films with thickness of 300 μm to 1 mm were prepared on a Ag plate substrate heated at 673 K. The films have a T_c of about 90 K without post-annealing.

Three types of Ag alloys including compositions of YBa_2Cu_3, $Bi_2Sr_2Ca_1Cu_2$ and (Bi, Pb)$_2Sr_2Ca_2Cu_3$ were internally oxidized at temperatures of 973–1023 K and annealed at various temperatures. Continuous high-T_c oxide layers are formed in the Ag matrix. T_c's of the samples almost equal to those of bulk samples and I_c's are about 50 A.

94 Development of High-Field Multifilamentary Superconductors Made by Intermetallic Compounds

April 1992 to March 1995
K. Inoue, 1st Research Group
Keywords: multifilamentary superconductor, Nb_3Al, diffusion reaction

Nb_3Al is one of the promising superconductors having superior high-field properties to those of the commercially produced Nb_3Sn. Multifilamentary Nb_3Al conductor can be produced by an ultrafine composite process, in which a lot of Al alloy cores were inserted into a Nb matrix. Then, the resulting composite was cold-drawn into a wire and heat treated at 750–900 °C to form Nb_3Al filament by diffusion reaction. However, the J_c of the Nb_3Al MF conductors are relatively low in high fields because of their relatively low H_{c2}. To improve the H_{c2} of Nb_3Al conductors, we have tried to heat the composite wire at very high temperatures above 1500 °C for 0.1 ~ 1 sec by pulsed Joule heating. Although H_{c2} (4.2 K) was improved by the pulsed Joule heating, the low-field J_c was degraded showing peak effect in J_c-B property. The peak effect may be caused by the grain growth due to the long time heating. Therefore, we are now trying to cool down the composite wire rapidly just after the pulsed Joule heating.

We have found that Ag additions increase the formation rate of Nb_3Al in the diffusion reaction between Nb and Al. Therefore, we have studied the diffusion reaction between Nb and Al-added Ag-based alloy. At first a Nb rod was inserted into an Ag-Al pipe. The resulting composite was cold-drawn into a wire and then heat treated at 800–850 °C to form Nb_3Al layer. The best superconducting properties were obtained when Ag-5at%Al alloy was used as the matrix material. However overall J_c of the single-core composite is very small, because the thickness of formed Nb_3Al layer is very thin, being less than 0.3 μm. Multifilamentary Nb_3Al conductor has been fabricated to increase the volume fraction of Nb_3Al which is formed between Nb core and Ag-5at%Al alloy matrix. Overall J_c(4.2 K) of 10^7 A/m^2 at 3 T is obtained for the 59 × 59 core multifilamentary conductor. The value is not enough for the practical superconductor application. However, the process is very similar to the bronze process for fabricating commercial Nb_3Sn conductors. Therefore, the application of this process to the production of practical large-scaled superconductor seems to be relatively easy, which will be investigated in collaboration with Hitachi Cable Ltd.

Related Papers

Multifilamentary Nb_3Al Wires Reacted at High Temperature for Short Time, M. Kosuge, Y. Iijima, T. Takeuchi, K. Inoue, T. Kiyoshi and H. Irie, to be published in IEEE Trans. on Supercon.

Superconductivity of Nb_3Al Formed by Solid State Reaction of Nb with Ag-Based Alloy, T. Takeuchi, M. Kosuge, Y. Iijima and K. Inoue, to be published in IEEE Trans. on Supercon.

95 Development and Characterization of Superconducting Materials for Fusion Reactor Magnet Use

April 1989 to March 1994
H. Wada, High Magnetic Field Research Station
Keywords: BiSrCaCuO tape, critical current, strain

The purpose of this study is to develop high field superconducting materials for fusion reactor use. New, promising superconducting materials are characterized and evaluated under conditions that the materials may be experienced when wound to a superconducting magnet which should confine and control plasma in the reactor.

In fiscal year 1992 effects of neutron irradiation on the critical temperature of Nb-tube processed Nb_3Al wires and effects of tensile strain on the critical current of Ag-sheathed single- and multicore superconducting tapes of BiSrCaCuO were studied.

The critical temperature of Nb_3Al wires was decreased monotonously with neutron fluence. At a fluence of 3.9×10^{18} n/cm^2 (E > 0.1 MeV) the depression of the critical temperature relative to its unirradiated value was about 9%. Effects of neutron irradiation on the critical current of these wires are to be studied.

Ag-sheathed BiSrCaCuO tapes were fabricated by a powder metallurgy process. When uniaxial tensile strain was applied at low magnetic fields and 4.2 K, critical currents of these tapes were almost unchanged up to a certain strain and irreversibly decreased beyond this strain. This irreversible degradation in critical current occurs abruptly in monocore tapes, while it is a gradual decrease in multicore tapes.

Related Paper

Effects of Strain on Critical Currents in Ag-Sheathed BiSrCaCuO Tapes, T. Kuroda, M. Yuyama, K. Itoh and H. Wada, Advan. Cryog. Eng (Mater.) 38 (1992): 1045–51.

96 Fabrication of Oxide Superconductors Using YAG Laser Irradiation

April 1989 to March 1995
H. Wada, 1st Research Group
Keywords: YAG laser, Bi-based oxide superconductor, screen printing

The purpose of this study is to develop a simple and feasible fabrication method by com-

bining thin layer technology (screen printing) with highly controllable heat treatment technology (YAG laser).

Non-superconducting precursors of Bi-based 2223 oxide superconductor were layered on MgO and Ag substrates by a screen printing method. These precursor samples were then irradiated using a YAG laser apparatus equipped with a movable X-Y stage on which they were mounted.

YAG laser irradiation to the moving non-superconducting precursors alone did not convert them to high-superconducting temperature phase, 2223. This is because of the following;

1. the optimum reaction temperature range for the formation of the 2223 phase is very narrow around 845 °C,
2. the melting point of precursor is around 900 °C, and
3. on irradiation the sample temperature readily goes up beyond 900 °C and quickly goes down below 800 °C, resulting in the formation of 2212 and 2201 and not 2223.

Thus, irradiated samples were heat treated at 860 °C for 1 hour. Then, the samples showed superconducting transition between 110 K and 92 K, indicating the formation of 2223. However, critical current densities of these samples were still rather low.

It is planned to apply this fabrication method to YBaCuO superconductors, since it is known that critical current densities of YBaCuO are improved by the existence of non-superconducting phase precipitation from molten state.

[97] Development and Evaluation of Advanced Superconducting and Cryogenic Materials

April 1990 to March 1993

H. Maeda, 1st Research Group

Keywords: V_3Si multifilamentary superconductors, modified bronze process, carnot magnetic refrigerator, rare earth garnet single crystal, high cycle fatigue, cryogenic temperature

Three major materials have been studied to contribute to the development of advanced superconducting technologies.

1. Although the diffusion reaction between V and Cu-Si alloy (bronze process) is known to be available for production of V_3Si superconductor, non-superconductive phase V_5Si_3 is formed initially and then eventually converted to V_3Si. Then long heat treatments at high temperatures are necessary for appreciable V_3Si layer growth, thereby yielding grain growth of V_3Si and lowering the J_c of V_3Si compound.
   Recently we have successfully fabricated the V_3Si multifilamentary superconductors with high overall J_c's by a new modified bronze process. In this process the combination of reducing V filaments to 1 μm and adjusting overall V/Si ratio to 3 allows the completion of diffusion reaction in short time to decompose the initially formed V_5Si_3 and to produce mostly V_3Si without grain growth. The overall J_c (4.2 K) values obtained so far are 1.3×10^9 A/m^2 at 5 T and 1×10^8 at 12.5 T, which is 10 times larger than those of the conventional V_3Si wires. These values are comparable to those of Nb_3Sn multifilamentary wires produced by the bronze process for a.c. use.
2. For two austenitic steels, JN1 (0.022C-4.14Mn-14.74Ni-24.43Cr-0.330N) and YUS170 (0.015C-0.78Mn-13.52Ni-25.06Cr-0.368N), high cycle fatigue strength (S-N) data have been accumulated at 4 K, 77 K and 293 K. The steels have the basically similar chemical compositions but Mn content and almost the identical tensile properties. At the cryogenic temperatures, the fatigue strength of the two is almost the same until around one million cycles; however, the JN1 shows obviously lower fatigue strength than the YUS170 over one million cycles. The S-N curve at 4 K of each steel approaches to that at 77 K at higher cycles and at more than one million cycles finally both curves overlapped. Fatigue cracks are initiated at specimen surface at higher stress and at specimen interior.
3. Several key components of carnot magnetic refrigerator which provides below 1 K has been developed. Graphite was tested as the thermal switch for the expelling heat portion of the cycle. The thermal switch ratio is more than 10 and the heat transfer rate is ~1 W/K with the molecular heat conduction of ^{3}He. Large scale rare earth single crystals of $(Dy_{1-x}Y_x)_3Ga_5O_{12}$ with x = 0 – 0.6 have been grown and thermodynamic properties are measured. The magnetic transition temperatures were below ~500 mK and the thermal conductivity largely depends on the temperature and the magnetic field. The material is found to be useful for not only a magnetic refrigerant but also a thermal switch. ^{3}He heat pipe is also developed for absorbing heat switch and preliminary cycle operation of the whole system is now tested.

Related Papers

V_3Si Multifilamentary Superconductor Produced by a Modified Bronze Process, T. Takeuchi and K. Inoue, to be published in J. Appl. Phys.

Deformation Structures in High-Cycle Fatigue of 0.1N-32Mn-7Cr Steel at Cryogenic Temperatures, O. Umezawa and K. Ishikawa, Adv. Cryog. Eng. 38 (1992): 141–48.

Carnot Magnetic Refrigerator Operating between 1.4 and 10 K, T. Numazawa, H. Kimura, M. Sato and H. Maeda, Cryogenics 33 (1983): 547–54.

Magnetic materials

(98) Magnetocaloric Effect on Size-controlled Magnetic Materials for the Production of Ultra-low Temperatures

April 1993 to March 1995
M. Sato, Physical Properties Division
Keywords: magnetocaloric effect, magnetic refrigeration, ultra-low temperature

Production of low temperature environment is one of the key technologies for applications of superconducting magnets and devices. However, conventional gas-expansion cycles are not effective below 1.8 K. Magnetic refrigeration has been successful to provide Liquid He I and II with high efficiencies and is also one of the most promising candidates to obtain ultra-low temperatures below 1 K conveniently. This study is focused on the production of ultra-low temperatures by the magnetic refrigeration. In particular, we have chosen two approaches to get both the low magnetic transition temperatures and the large magnetocaloric effects by controlling the magnetic interaction size. One is to make use of magnetic interactions in nanometer-scale magnetic particles. Entropy changes by the applied magnetic field will be enhanced by the strong magnetic interactions in the nanocomposite. Another is to dilute a garnet magnetic refrigerant with non-magnetic substitutions of rare-earth ion by Y^{3+} such as $(DyY)_3Ga_5O_{12}$. This is effective to decrease the magnetic transition temperature. Material preparations and theoretical analysis are in progress.

99 Fundamental Research into Intelligent Materials with Cooperative Molecules or Atoms

April 1992 to March 1995
I. Nakatani, Physical Properties Division
Keywords: micromagnetics, ultrahigh-resolution electron-beam lithography, ferromagnetic fine particle lattice, magnetic dipolar wave

Micromagnetics is concerned with ferromagnetic fine structures whose dimensions lie in the same order of magnitude as the thickness of the magnetic domain walls. Ferromagnetic fine particles are widely applied to recording media, permanent magnets, magnetic fluids, etc. At present, the magnetic properties of strongly interacting particles have not been fully described. If the microscopic status of the individual particles can be specified in terms of magnetization, magnetic anisotropy and dynamic motion of magnetic spins, considerable progress of micromagnetics and their applications are foreseen. For clarifying these problems, it is required to study on the suitable system of fine particles with controlled sizes, shapes, morphology, relative orientation and spacing.

In this project, ultrahigh-resolution electron-beam lithograhpy is used to fabricate such fine particle systems or micro structured systems that the fine particles or fine stripes of Mo-Permalloy or Co-Cr alloy with the size of deep submicron meter are arrayed with regular arrangement on substrates of single crystal Si wafers or glass plates coated by diamond-like graphite. Such systems are called fine particle lattices. The fabrication was made by direct electron-beam writing on the PMMA resist overlaid on the substrate, development, etching process in oxygen plasma, vacuum deposition of Mo-Permalloy or Co-Cr alloy and lift-off process. The lattices consist of 10^5–10^6 identical particles arrayed with rectangular or triangular symmetries with identical spacing between adjacent particles. Highly accurate magnetization measurements, measurements on ferromagnetic resonances and observation on the local distribution of magnetic polarization were made to investigate micromagnetism on fine particle lattices. For the samples of the fine stripe arrays of Mo-Permalloy, multiple resonances were observed on their ferromagnetic resonance spectra. Each stripes is bounded to all other stripes in the array by the local field coming from dipole-dipole interaction between the stripes. Dynamic motion of the magnetic moment of the stripe system was analyzed using an equation of motion involving the dipole-dipole interactions. It was concluded that the magnetic dipolar standing wave with long wavelength are exited in the uniform r-f field in the array.

100 Fabrication and Physical Properties on Metallic Substances with Mesoscopic Sizes

April 1992 to March 1995
I. Nakatani, Physical Properties Division
Keywords: mesoscopic scale material, iron-nitride magnetic fluid, subnanometer micro-cluster, TiB_2whisker, metastable compound of iron-nitride

Mesoscopic scale materials are such materials that have sizes intermediate between atomic or molecular sizes and sizes of bulk materials. Mesoscopic materials consist of 10 ~ 10^5 atoms. Characteristics on the mesoscopic materials arise from the confinement of various types of electric state to the small volume in the materials. The interest of this project is focused on the fabrication and on the novel properties of the mesoscopic scale materials.

The research program is divided into the following 4 items.

1. Research on synthesize of iron-nitride magnetic fluids, having the highest magnetization more than 0.3 Tesla and the lowest viscosity of 2000 mPa·s, are on going by the method of vapor-

liquid reaction. Chemical binding between the absorbed molecule of amine and the iron-nitride fine particles are clarified by photoelectron spectroscopy. Superparamagnetic properties of the magnetic fluids are studied by magnetization measurements, ferromagnetic resonances and Mössbauer effect measurements. New type of magnetic composites that ultrafine particles of iron-nitride are dispersed and suspended in resins are studied. Some application of magnetic fluids to active dumpers for automobile, inductors for radio frequency circuits, magnetic toners for xerography and cosmetic colors are being made coordinating with some Japanese private companies.

2. Preparations of microclusters of ferromagnetic metals of Fe or Co, subnanometer in size, are tried by the ultrahigh-vacuum evaporation on the substrate cooled by liquid nitrogen. The size effects on cooperative phenomenon of ferromagnetism will be clarified by measurements of magnetization and Mössbauer spectroscopy on those fine particle systems.
3. Titanium diboride (TiB_2) has a high toughness and has a high electric conductivity. In this project, whiskers of TiB_2 were successfully grown by CVD reactions of the system $TiCl_4$-BBr_3-H_2 or the system $TiCl_4$-BBr_3-Ar using the catalyses of the Ti-Ni alloy powder or the Si powder. While in the CVD system of $TiCl_4$-BBr_3-$SiHCl_3$, TiB_2 whiskers were not obtained. Their crystallographic, electric and mechanical properties are being studied.
4. Microwave-plasma CVD reaction is applied to synthesize metastable new phases of iron-nitrides. Magnetic properties of the new phases are studied in terms of the ferromagnetic interaction between the iron atoms.

Related Papers

Iron-Nitride Magnetic Fluids Prepared by Vapor-Liquid Reaction and Their Magnetic Properties, I. Nakatani, M. Hijikata and K. Ozawa, J. Magn. Magn. Mater. 122 (1993): 10–14.

Mössbauer Studies of Iron Magnetic Fluids Prepared by Evaporation Methods, T. Furubayashi and I. Nakatani, J. Magn. Magn. Mater. 122 (1993): 74–77.

Effects of Heat Treatment on Properties of Co Magnetic Fluids, H. Yamamoto, T. Kanno and I. Nakatani, J. Magn. Magn. Mater. 122 (1993): 15–18.

Curie Paramagnetism of Chromium Ultrafine Particles, T. Furubayashi and I. Nakatani, J. Appl. Phys. 73 (1993): 12–13.

Iron-Nitride Fine Particles and Iron-Nitride Magnetic Fluids, I. Nakatani, (to be published in Seramics) (in Japanese).

[101] Fabrication and Magnetic Properties of Metallic Clusters with Sub-Nanometer Size

April 1992 to March 1993

T. Furubayashi, Physical Properties Division

Keywords: clusters, evaporation, magnetic properties

Much attention has been attracted to the problem of how magnetic properties of ferromagnetic materials are modified when the size is reduced to very small dimensions. For example, it has been shown that iron particles of about 2 nm in diameter are still ferromagnetic as the bulk iron. It may possibly occur that ferromagnetism disappears by reducing the size, say, below 1 nm. The purpose of this project is to fabricate magnetic clusters embedded in non-magnetic matrixes and investigate their magnetic properties. The method of fabrication is by evaporating a ferromagnetic and a non-magnetic materials at the same time in a vacuum around 10^{-8} Torr. We are trying to fabricate clusters with the size below 1 nm by varying preparation conditions, evaporation speed, substrate temperature, etc. Structural and magnetic studies are now in progress.

Materials for energy application

(102) Study on Highly Resistant Mechanism to Radiation Damage

April 1993 to March 1996

H. Shiraishi, 2nd Research Group

Keywords: resistance to radiation damage, neutron irradiation, irradiation embrittlement

This program consist of following subprograms;

1. Modeling and evaluation of fracture behavior under complex irradiation environment.
2. Analysis of micro-mechanistic property of advanced material.
3. Material chemistry in the extreme conditions under irradiation.
4. Processing and development of isotopically controlled materials.
5. Study on deformation and fracture under irradiation.
6. Research on distributed data base for advanced nuclear materials.

The first subprogram listed above is reported here. The reports on the other subprograms are given elsewhere.

Helium embrittlement is thought to determine the upper limit of application temperature of materials in a fusion reactor core design. It is well understood that this embrittlement is caused by existence of helium bubbles produced by (n, alpha) reaction on the grain boundary. For development of metals and alloys having excellent performance under neutron irradiation environment, quantitative relationship between mechanical property and bubble morphology on the grain boundary must be established.

Two dimensional elastic-plastic finite element method was applied for this object. Under the neutron irradiation, the yield point increases and the work hardening coefficient decrease rapidly, for example, in 316 stainless steel. The work hardening coefficient of this steel is about 0.3–0.5 for unirradiated condition. The effect of variation of the work hardening coefficient from 0.3 to 0.01 was investigated. Also, the effect of such parameters as bubble density and bubble size is evaluated.

For the estimation of helium embrittlement sensitivity, the strain concentration factor was defined as a ratio of maximum plastic equivalent true strain in bubble containing specimen to that with no helium bubble. With decrease of work hardening coefficient, strain concentration factor initially increases gradually, but this factor goes up sharply when the work hardening factor is around 0.1–0.03. Strain concentration shows a trend of saturation with further decrease of work hardening. This result means that there is a critical work hardening coefficient value above which helium embrittlement becomes serious. In contrast, the effect of bubble density was moderate.

The high temperature and slow strain rate is necessary to cause helium embrittlement because of helium bubble growth on the grain boundary. These two factors also reduce the work hardening coefficient and are considered to accelerate helium embrittlement through strain concentration mechanism.

103 Environmental Degradation of Structural Materials for Light Water Reactors

April 1991 to March 1996

N. Nagata, 5th Research Group

Keywords: acoustic emission, straining electrode, low cycle fatigue

The purpose of this research is to clarify the elemental process of environmentally assisted cracking (EAC) of structural materials for LWR in high temperature water and to systematize the related data for life prediction of components. In this year, following two research items R & D of evaluation techniques for initiation and growth of microscopic local damage and clarification of elemental process of local damage were conducted.

A new acoustic emission (AE) sensor applicable to high temperature water was developed in order to determine the modes of local damage by analyzing the original wave form from AE signals. This sensor can be directly installed to the specimen in the autoclave without any wave guide. Basic analyses such as original wave form, frequency response by using the new device were successfully completed.

The dissolution behavior of fresh metal surface that revealed in the solution of H_3BO_3 + $Na_2B_4O_7$ at 523 K was investigated using a straining electrode device. It was found that the repassivation of the fresh surface was completed within 12 ms, and no effect of applied potential on dissolution current and repassivation behavior were observed.

The effect of crevice corrosion environment on low cycle fatigue of a low alloy steel in high temperature water simulated LWR coolant conditions was investigated by means of applying a split collar made from the same material onto the test section of the fatigue specimen. It was seen that the fatigue life of the specimen with collar was a little longer than that of the specimen without collar when the total strain range decreased. This may be due to the environmental effect which is more striking for the extended immersion in the test solution, in which the dissolved oxygen concentration in the crevice decreases with increasing time.

Related Papers

Low Cycle Fatigue Behavior of Pressure Vessel Steels in High Temperature Pressurized Water, N. Nagata, S. Sato and Y. Katada, ISIJ International 31 (1991): 106–14.

Effect of Dissolved Oxygen Concentration on Fatigue Crack Growth Behavior of A533B Steel in High Temperature Water, Y. Katada, N. Nagata and S. Sato, ISIJ International 33 (1993): 877–83.

104 Assessment of Strength and Structural Materials Database for Weldment in FBR (Fast Breeder Reactor) Components

April 1991 to March 1996

Y. Monma, 5th Research Group

Keywords: creep, database, FEM, stainless steel, welded joint

The purpose of this study is to improve the prediction of the creep properties of thick welded joints from that of the base and weld metals of 316FR (0.01C-0.07N-18Cr-11Ni-2Mo) stainless steel for the FBR vessel. Three types of specimens were prepared by two methods of narrow-gap GTAW (gas tungsten arc welding) large specimens from the full-thickness (50 mm): joint, small specimens (ϕ10 mm) of the base and weld metals.

Full-thickness specimens as well as small ones from the base metals have been subjected to creep tests at 550 °C up to 30,000 h. Based on the moiré interferometry using a CCD (charge coupled device) camera, we have developed a new technique to measure the strain distribution of the creep interrupted joint specimens with full-thickness. We found the local variability of the strain distribution in the welded joint. The creep strength of the center of multi-layer weld metal is more pronounced than that at the surface parts.

This is because of the heat treatment effect during the multi-pass welding. Most of the creep strain is concentrated in the base metal part, while little strain is observed in the weld metal.

Materials constants for the creep constitutive equation determined from the results of small specimens are fed into the FEM (finite element method) simulation of creep behavior. It has been shown that the application of "damage parameter" proposed by Rabotonov provides significant improvement for the prediction of creep.

105 Fundamental Research on Application of New Functional Materials to Passive Components

April 1990 to March 1994
T. Ishihara, 5th Research Group
Keywords: shape memory characteristics, thermal cycle, SCC

In order to apply shape memory alloys to the equipment for the security of the nuclear power plant, it is necessary to evaluate the characteristics of the shape memory alloys in some environments. In this study, (1) effect of thermal cycle on the shape memory characteristics and (2) stress corrosion cracking (SCC) susceptibility in high temperature water were evaluated in an Fe-based shape memory alloy.

1. An Fe-13.3Mn-5.68Si-5.18Ni-9.15Cr (wt%) alloy has been used for various types of thermal cycle tests. The following shows one of the results of "constant load/thermal cycle test." Tensile specimens were solution treated at 1050 °C for 30 min. and water quenched. A stress of 315 MPa was applied to the specimen at room temperature and heated to 200 °C under the stress, and then cooled to room temperature. This thermal cycle was repeated ten times. In the first cycle, the elongation of the specimen increases with increasing temperature due to plastic deformation, and then further increases during cooling, which is due to the stress-induced transformation. After the third cycle, the hysteresis of the elongation-temperature curve changes very little, that is, the shape memory characteristics become more stable by the thermal cycle because of the "training effect." Since the amount of residual martensite is increased by the thermal cycle, the starting temperature for stress-induced transformation is also increased by the thermal cycle.
2. SCC susceptibility of Fe-Mn-Si-Ni-Cr alloy was evaluated in high temperature water. The specimen heat treated at 827 K for 3.6×10^3 s was tested in pure water at 561 K containing 0.2 ppm of dissolved oxygen by using slow strain rate test technique. The notched specimen was elongated at the cross head speed of 1 μm/60 s. The fractured surface was observed by scanning electron microscope. No trace of SCC was found on fractured surface. As a result, it was shown that the Fe-Mn-Si-Ni-Cr alloy was immune to SCC in high temperature water of low oxygen concentration.

106 Material Chemistry in the Extreme Conditions under Irradiation

April 1989 to March 1994
M. Kitajima, 2nd Research Group
Keywords: irradiation, dynamic process, surface reaction, surface lattice disordering

Irradiation causes both chemical and physical attacks upon material surface. The purpose of this research is to elucidate mechanisms of the irradiation activated surface reaction and to develop new analytical techniques for that with emphasis on the real-time observation of dynamic process. Kinetic or phenemenological modeling on the surface reaction and surface damage processes is also our target. From this viewpoint we have investigated time-dependent behaviors of the graphite surface, silicon and other materials during and after ion irradiation, by using a real-time Raman measurement technique which we had developed in this research project. We have obtained very new results on lattice disordering and its relaxation kinetics. *In situ* real-time ellipsometry is also performed to study growth kinetics of ultra thin films on the surface during oxygen (or hydrogen) plasma discharge, and plasma characteristics are examined using the Langmuir probe, emission spectroscopy and mass spectroscopy to compare with the surface reaction rate. The real-time ellipsometry has revealed that the oxidation rate strongly depend on plasma density and changes in dielectric property dominate the time-dependence of the optical phase shifts at an early stage of the plasma oxidation of silicon surface. In addition to these researches, we are performing studies on surface chemical reaction process using pulse laser techniques.

Related Papers

Raman Studies of Graphite Lattice-Disordering Kinetics under Low-Energy He Ion Irradiation, K.G. Nakamura and M. Kitajima, Phys. Rev. B45 (1992): 5672–74.

Initial Damage in Graphite under Ion Irradiation Studied by Real-Time Raman Measurements, M. Kitajima and K.G. Nakamura, J. Nucl. Mater. 191–94 (1992): 356–60.

Thermal Relaxation of Ion-Irradiation Damage in Graphite, E. Asari, M. Kitajima, K.G. Nakamura and T. Kawabe, Phys. Rev. B47, 11143–48.

Growth of Silicon Oxide on Silicon in the Thin Film Region in an Oxygen Plasma, M. Kitajima, H.

Kuroki, H. Shinno and K.G. Nakamura, Solid St. Commun. 83 (1992): 385–88.

Experimental Study of Plasma Effect on Oxidation of Solid Surface, M. Kitajima, H. Kuroki, H. Shinno and T. Kawabe, Proc. 1992 Int. Conf. Plasma Physics (European Physical Soc., 1992): 2155–58.

107 Research on Distributed Database for Advanced Nuclear Metals

April 1991 to March 1996

M. Fujita, 2nd Research Group

Keywords: Data-Free-Way, distributed database, advanced nuclear materials, to share data, type 316 stainless steel

New material-searching using database systems is required for nuclear technology. But it is very difficult at present to describe numerous nuclear materials properties because of their complexity in nature and pre-standardized status of information on new materials. The stored data consist of the properties under environments form normal to severe states, such as high temperature, stress loading and/or corrosive ones under heavy irradiation. Therefore, a wide spectrum of special knowledge of different fields is necessary.

A distributed database system, for designing and selecting has been built under the cooperation of National Research Institute for Metals (NRIM), Japan Atomic Energy Research Institute (JAERI) and Power Reactor and Nuclear Fuel Development Corporation (PNC). The system is called as "Data-Free-Way" and has been built since April of 1990. This project is to build the system within five years, focussing on advanced nuclear materials, such as new structural metals, intermetallic compounds, ceramics and composites. Input data will be captured from results of Fundamental Research on Nuclear Materials supported by Science and Technology Agency of Japan

In the pilot system, a new method to share data and meta data among the databases of the respective institutes is demonstrated. The merits to share data and the methods to obtain the knowledge in the distributed data system were discussed through irradiation data on tensile and creep properties of type 316 stainless steel. Comprehensive data sets were established on the basis of the system; thermal neutron data from JAERI, fast neutron data from PNC and ion irradiation data from NRIM. It is concluded that the major merits are that the knowledge of material technology is able to be expressed by numerical values, since a large number of data examined under various conditions are considered in analysis.

Related Papers

Development of a Distributed Database for Advanced Nuclear Materials, M. Fujita, Y. Kurihara, H. Nakajima, N. Yokoyama, F. Ueno, S. Kano and S. Iwata, Proc. 4th Int. Simp. on Advanced Nuclear Energy Research (1992): 402–09.

Function and Utilization of Data-Free-Way System, M. Fujita, Y. Kurihara, H. Nakajima, N. Yokoyama, F. Ueno, S. Kano and S. Iwata, CAMSE '92 (1992): 81–84.

108 R & D of Advanced Heat-Resistant Structural Materials for Very High Temperature Gas-Cooled Reactors

April 1990 to March 1995

T. Tanabe, 3rd Research Group

Keywords: high temperature gas-cooled reactor, material-design, testing-and-evaluation

In order to fulfill the national demand for advanced structural materials for high temperature gas-cooled reactors, we have carried out the R & D of new heat-resistant materials for very high temperature use up to 1,373 K by combining the material-design and the testing-and-evaluation technologies. The present status of the R & D is as follows.

Development of advanced heat-resistant materials

The investigations of cavitation behavior of typical ODS alloy, Inconel MA754, under creep or tensile condition at high temperatures revealed that the existence of two kinds of boundaries in the alloy (the recrystallized boundary and the quasi-boundary consisting mainly of two dimensional aggregate of dense oxide inclusions) affects its ductilities and/or its strengths. The crack-like cavities on the former boundaries grow remarkably faster than the round cavities on the latter boundaries, which explains the anisotropic creep and tensile ductilities of the alloy. As to the strength, it was found that on the quasi-boundaries of the specimens aged at 1373 K for 3.6 Ms, argon precipitates and grows during tensile testing at temperatures higher than 1273 K, leading to the reduction of the strengths in the alloy.

Development of advanced material testing-and-evaluation technologies

Creep rupture tests and creep crack growth tests of MA754 were carried out at 1273 K in air and in impure helium environment. The alloy exhibits the degradation of creep rupture lives in the longer time duration than 3.6 Ms. It was also found that the creep crack growth lives are longer in air than in impure helium and creep crack growth rate is remarkably faster when the elongated grain boundary is perpendicular to the stress axis than when the boundary is parallel to the axis.

Related Papers

Creep Damage of Hastelloy XR at Very High Temperatures in Simulated HTGR Helium Gas, Y. Nakasone

et. al. *Creep: Characterization, Damage and Life Assessment*, ASM International, ed. by D.A. Woodford, C.H.A. Townley and M. Ohnami (1992): 551–55.

Creep Crack Growth Behavior of Ni-26Cr-17W-0.5Mo Alloy in Air and Helium Gas Environment at 1273 K, M. Tabuchi et. al. *Creep: Characterization, Damage and Life Assessment*, ASM International, ed. by D.A. Woodford, C.H.A. Townley and M. Ohnami (1992): 297–304.

Creep Crack Growth Behavior in Ni-base Superalloys in 1273 K Helium Gas Environment, Y. Nakasone, et. al. J. Nucl. Sci. and Tech. 29 (1992): 422–26.

Application of Creep Damage Rules to a Nickel-base Heat-resistant Alloy Hastelloy XR, H. Tsuji (JAERI), T. Tanabe et. al., J. Nucl. Mater. 199 (1992): 43–49.

109 Study on a Porous Gas-Diffusion Electrode

April 1990 to March 1993

M. Kobayashi, Chemical Processing Division

Keywords: fuel cell, antimonic acid, lithium

Fuel cells have many attractive features for power utilities desiring urban power generation, and are promising in the following decades. Pilot plant of phosphoric acid fuel cell have already been operated in several places in the world. They are operated at ca. 200 °C, which poses severe problems for the constituent materials. Though the operating condition of an alkaline fuel cell is milder, the rate of oxygen reduction and hydrogen oxidation is slow. The aim of this study is to seek effective electrocatalysts and electrode materials to overcome the above disadvantage.

A simple test is to screen out good electrocatalysts from many candidate materials. The catalytic properties are roughly evaluated by measuring the cathodic polarization curve of suspension in an alkaline solution under O_2 bubbling at 50 °C. Following the rough screening, cathodic polarization is measured at 50 °C using disk samples. Noble metals on the activated carbon are used to prove the effectiveness of the above two step screening.

As an electrode material, antimonic acid is prepared from lithium antimonate. A particular sample of lithium antimonate is packed in a column and nitric acid solution flows down through the sample bed to exchange the lithium ion by hydrogen ion. The ion exchanged antimonic acid is a selective adsorbent of lithium ion, and is also expected as the electrode material of the fuel cell. The kinetic study is carried out, and it is found that the ion exchange rate strongly depends on the temperature. XRAD shows that the antimonic acid prepared at 60 °C has a different structure from that prepared at room temperature. The effect of the prepared temperature of antimonic acid on the efficiency of the oxygen reduction is future subjects.

110 Development of the Fusion Reactor First Wall Materials Resisting to Plasma and Radiation Damage

April 1987 to March 1993

H. Shiraishi, 2nd Research Group

Keywords: C-B-Ti composites, high heat flux materials, functionally gradient materials, helium embrittlement, 9 Cr heat resistant ferritic steel, ZrO_2, microstructure control by phase transformation

High heat flux materials

High thermal conductivity and high heat flux resistance are necessary for plasma facing materials of nuclear fusion reactor. Carbon materials such as graphite or carbon fiber composites are primary candidates at present for those purposes. Recently, carbon materials with boronized surface layer (B_4C) have been used as plasma facing materials, and significant improvement of plasma confinement performance has been obtained in various nuclear fusion facilities such as JT-60U.

However, thermal conductivity of B_4C is much lower than that of the carbon material so that the improvement of this property is required. As a solution for this problem, we have synthesized C-B-Ti materials. Samples of these materials were prepared by hot press and sintering from powders of carbon, boron and titanium. X-ray diffraction analysis revealed that the samples consisted of TiC, TiB_2 and graphite. Measured thermal conductivity of each sample was higher than that of B_4C and close to those of TiC or TiB_2.

Thermal shock resistance of the sample were evaluated by electron beam tests and it was found that samples containing small fraction of graphite had higher thermal shock resistance than those with no graphite. Some samples with composition gradients along the thickness (functionally gradient materials) showed the highest thermal shock resistance.

Radiation damage resistance of microstructure controlled materials

It was revealed that the 9 Cr ferritic steels have higher resistance to helium embrittlement than austenitic 316 stainless steel. The helium bubbles were trapped by finely dispersed carbides and lath boundary in 9 Cr steel. The finer helium bubble distribution in 9 Cr steel than in 316 steel is considered to be the reason of obtained excellent property of the ferritic steel.

Study on microstructure control for function generation of high melting point materials

Stress-induced transformation of tetragonal to monoclinic phase is responsible for the high fracture toughness of zirconia ceramics. In this research, the effect of high-temperature pre-heat

treatment on the transfromation behavior of tetragonal phase was investigated for a sintered ZrO_2 – 8 mol% CaO by means of dilatometry in the temperature range between room temperature and 1473 K. The tetragonal phase present in as-sintered specimen was stable up to 1473 K and virtually no transformation occurred. The pre-aging at 1673 K enhanced the phase transformation of tetragonal to monoclinic: the tetragonal phase transformed to monoclinic at about 1095 K during cooling and the monoclinic to tetragonal at about 1360 K during heating. The present results indicate that the high temperature heat treatment caused an instability of tetragonal phase, although the detailed mechanism is not clear at present.

Related Paper

Thermal Properties of Boron-Carbon-Titanium Compounds as Plasma Facing Materials, T. Tanabe, T. Baba, A. Ono, M. Fujitsuka, T. Shikama and H. Shinno, J. Nucl. Mater. 191–94 (1992): 382–85.

Materials for environmental performance

111 Improvement of Wear Properties of Metallic Medical Materials

April 1992 to March 1994

A. Hoshino, Physical Properties Division

Keywords: medical materials, titanium alloy, stainless steel, fretting corrosion test, tribological properties

Although titanium alloys are excellent corrosion resistant materials under static condition, their wear resistance is little known under the fretting condition. In order to understand the degradation mechanism and improve the tribological properties of titanium alloys for surgical implants, an in vitro fretting corrosion test of Ti-6Al-4V alloy was carried out in saline solution at 37 °C.

It was found that the corrosion potential of Ti alloy becomes electrochemically less noble than 316 L stainless steel during the fretting corrosion test. The weight loss and anodic current of Ti alloy was remarkable comparing with those of stainless steel at controlled potential of 0 mV (SCE). When Ti alloy was electrochemically coupled with stainless and tested at controlled potential of 0 mV, no wear reducing effect was observed during the continuous fretting corrosion test.

Related Paper

Consideration on Coupling Application of Biomedical Titanium Alloy with Stainless Steel, A. Hoshino, Zairyo-to-Kankyo 42 (1993): 291–96.

112 Synthesis of New Functional Materials by the Application of Host-Guest Reactions

April 1990 to March 1995

M. Amano, Physical Properties Division

Keywords: insertion/extraction reaction, ionic conductor, hydrous pentavalent oxide, proton conduction

The aim of this project is to synthesize new functional materials by applying insertion/extraction reactions. We are trying to synthesize new ionic-conductor materials by using ion exchange processes. Hydrous pentavalent oxides have been selected as the object materials, because they are known to possess interesting ion exchange properties and some hydrous oxide of Sb, Nb, and Ta, e.g., $HSbO_3 \cdot xH_2O$ and $HNbO_3 \cdot xH_2O$, are known as proton conductors. These compounds can be prepared by acid treatment of alkali metal compounds such as $LiSbO_3$, $KSbO_3$, $NaSbO_3$ and $LiNbO_3$. Different crystal structures of hydrous oxide can be obtained by changing the preparation process and starting materials. We have prepared monoclinic $HSbO_3 \cdot xH_2O$ from $LiSbO_3$ and cubic $HSbO_3 \cdot xH_2O$ from $KSbO_3$.

The proton conduction in the prepared samples has been studied by using an impedance analyser as a function of temperature, frequency and humidity. The mechanism of proton conduction in the prepared samples will be investigated by means of NMR, TGM and FTIR.

113 Corrosion Resistance of Synthetic Barriers in Geological Disposal of Spent Nuclear Fuels

April 1988 to March 1993

T. Kodama, Environmental Performance Division

Keywords: geological disposal, corrosion rate monitoring, electrochemical impedance, solubility diagram

In the nuclear fuel cycle system proposed by Atomic Energy Commission of Japan, high level nuclear waste separated from spent fuel after reprocessing is molded into metallic containers in the form of solidified glass which is to be disposed of in deep geological repositories. In this system, radioactive waste must be isolated safely until radioactivity has been reduced to a nonhazardous level and a durability of 1000 years is expected for metallic containers. In advance of the proposed construction of a nuclear disposal and repository in the forthcoming century, it is desirable that sufficient data be prepared for the guarantee of nuclear safety. For this purpose we have studied corrosion and life prediction of metals for the use of nuclear waste disposal containers.

Corrosion monitoring in simulated geological environment

Electrochemical impedance measurements have been carried out in simulated geological environment for corrosion rate monitoring. A simulated solution for electrochemical measurement was pre-

pared by adding sodium-bentonite clay to water at a concentration of 10 g kg^{-1} followed by the separation of the clay by filtration and centrifugal method. For electrochemical impedance measurement the small sinusoidal potential polarization was impressed on electrode using a potentiostat and the response in current was analyzed by a frequency response analyzer. In the impedance spectrum of carbon steel sample in the simulated geological solution as a parameter of frequency (Nyquist plot), two semicircles were observed indicating that the corrosion process proceeds via two rate processes. The first process with a smaller time constant was independent of electrode potential and its radius decreased with temperature. The second one was dependent on both electrode potential and temperature indicating that charge transfer occurs on this step.

Water chemistry in geological environments

For the description of chemical environments of geological disposal sites, we have developed a computer code for the automatic construction of Eh-pH diagrams useful in the interpretation of electrochemical reactions with charge transfer. The code was revised to include the construction of a solubility diagram that can be used for such reactions as dissolution of corrosion products or glasses, and adsorption of fission products to minerals and clays. Various diagrams have been prepared for the simulation of dissolution/deposition reactions in geological environment.

[114] Corrosion Resistance of Coated Materials in Natural Environment

April 1989 to March 1993

T. Kodama, Environmental Performance Division

Keywords: atmospheric corrosion, paint/metals, pollutant analysis, combined acceleration tests

As a part of Japan–ASEAN Cooperation on Science and Technology, which is in progress under auspices of the Japan International Cooperation Agency (JICA), NRIM has been in charge of supporting projects on atmospheric corrosion carried out at national research institutes in Thailand and the Philippines by participating in the planning of experiments and technical discussion and by dispatching experts to these countries. Because of the necessity of prolonged exposure time for corrosion test and the accomplishment of technology transfer, the projects are to be extended for two years beyond the originally scheduled period up to the autumn of 1992. In parallel with the overseas experiments on atmospheric corrosion, laboratory works on metal/polymer adhesion, mass transfer through paint films and surface treatment have been carried out at NRIM with participants from ASEAN countries.

Atmospheric corrosion in tropical areas

In Thailand and the Philippines, atmospheric exposure tests are in progress for bare metals and steels with organic and inorganic coatings at several exposure sites selected from different atmospheric conditions. In parallel with the exposure test, meteorological and pollution data are collected periodically by local staff. Exposed samples are regularly checked and a part of the samples are collected for inspection at a constant interval. The inspection include mass loss, instrumental analyses of corrosion products and degradation of polymer films. NRIM members periodically visited counterpart research institutes in Thailand and the Philippines for the evaluation of corrosion data.

Corrosion control at metal/coating interface

Photo-degradation of polymer films was investigated by combined infrared test using a Fourier transform infrared spectrometer (FTIR) and ultraviolet (UV) irradiation. Four types of polymer films with and without white pigments were prepared on glass plates using a bar coater to a thickness of 15 μm. After drying at 50 °C, sample films were exposed to UV light with a xenon lamp. The intensity of UV radiation was 17 W m^{-2}. Among four samples tested epoxy and alkyd film gave extra absorption bands peaks after UV irradiation at 1724 cm^{-1} and 1167 cm^{-1}, indicating oxidation occurred after breakdown of CH bonds.

Absorption increased with increasing exposure time and decreased by the addition of white pigment particularly by TiO_2, which is due to the absorptive effect of rutile to UV.

[115] Achievement, Measurement and Application of Extremely High Vacuum

April 1991 to March 1993

M. Tosa, Surface and Interface Division

Keywords: extremely high vacuum, boron nitride, sliding friction, hydrogen permeation

Extremely high vacuum system less than 10^{-10} Pa is the key technology to advance surface analyses and thin film preparations remarkably. Small outgassing is the necessary property of the material for the achievement and application of the extremely high vacuum system. Boron nitride with hexagonal structure is inert to the adsorption of gases, but it was difficult to prepare boron nitride layer on the surface of stainless steels directly at low temperature. We previously found that the precipitation temperature of boron nitride went down to 900 K on the surface of type 304 stainless steel doped with boron and nitrogen and also found that the precipitation temperature went down to 600 K on the surface of deposited film of mixed boron nitride and stainless steel. The purpose of this work, therefore, is to apply the surface precipitation of boron nitride to the lubricant layer

suppressing adhesion during sliding manipulation and to the barrier layer against the diffusion of doped atom in the extremely high vacuum.

We prepared the rf-magnetron sputtered film of mixed boron nitride and type 304 stainless steel on the type 304 steel substrate and annealed the specimen in the vacuum of 10^{-6} Pa at 700 K for 24 hours to cover the whole surface of the specimen with boron nitride uniformly. We developed a pin on a plate type tester for sliding friction in a vacuum and found that the frictional resistance of boron nitride precipitated film on the type 304 steel substrate was lower than that of stainless steel deposited substrate and mechanically polished substrate as atmospheric pressure went down to 10^{-5} Pa. This shows that precipitated boron nitride can be a good lubricant for smooth specimen manipulation system causing little outgassing in the extremely high vacuum. An apparatus for evaluating hydrogen penetration showed that hydrogen permeating rate of boron nitride covered type 316L stainless steel was less than one-tenth of no boron nitride covered type 316L steel. This shows that precipitated boron nitride can be a barrier layer against the hydrogen permeation. Thermal desorption spectroscopy and electron stimulated desorption method revealed that the barrier mechanism against hydrogen penetration mainly consisted of the disruption of recombination of hydrogen at the top surface of boron nitride layer due to the specific crystal structure of hexagonal boron nitride.

Bio-Materials

(116) Basic Study on Reaction between Materials and Bacteria

April 1993 to March 1995
H. Masuda, Failure Physics Division
Keywords: bacteria, QCM, STM

It is well known that some bacteria have special ability to oxidize metals. This ability of oxidizing metals is very useful for refining materials if the reaction rate is comparatively fast. We, therefore, employ the quartz crystal microbalance (QCM) system to find the better condition for bacteria reaction. In this system, material oxidizing by bacteria is coated on the quartz crystal of 10 MHz. The oxidation rate is directly measured from the frequency shift of the quartz crystal as shown in Figure 5. The accuracy of this system is less than 1 Hz corresponding 4.2 ng/cm^2 of weight change. The scanning tunneling microscope (STM) is also used to understand the mechanism of the reaction between materials and bacteria.

(117) Fundamental Study on Biocompatibility of Materials

April 1993 to March 1998
M. Sumita, Mechanical Properties Division

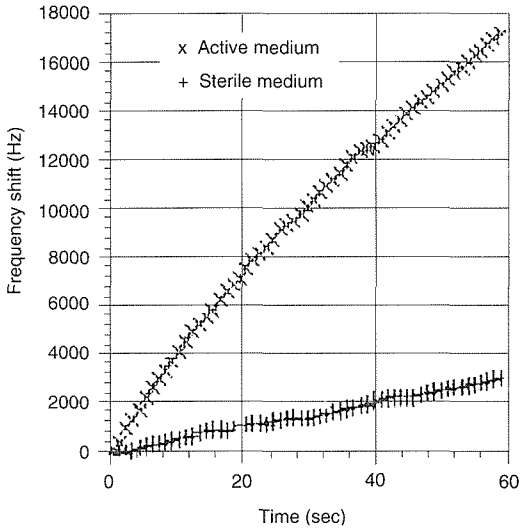

Fig. 5 Effect of bacteria on dissolution of Cu. Frequency shift corresponds the amount of dissolution of Cu.

Keywords: biomaterial, state analysis, pseudo-body fluid, toxicity against cell proliferation, cell adhesion, fretting fatigue

With the increase in number of the old aged, those who have to be implanted biomaterials in their body increase. It is important that the materials exist and function in their body without any trouble for many years until they die. Release of metallic ions and debris from materials implanted in body should be avoided, because they always or infrequently cause carcinogenicity, physical deformity enhancement and allergies. Unexpected failure of materials implanted also should be avoided, because the resultant reoperation forces the patient physical and mental pains. Therefore, non toxicity, adhesion to tissue, control in bioreaction caused by foreign bodies, sufficient resistance to corrosion and wear, and long fatigue life are considered as necessary characteristics for the biomaterials used in vivo conditions.

As metallic materials had the higher strength and the higher toughness than all of the other materials, 316L stainless steel, Co-Cr-Mo alloy, Ti-Al-V alloy etc. have experimentally been used as the biomaterials. However, no biomaterials, which have no problems in biocompatibility, exist.

The content of the present research subject is as follows:

1. Quantitative evaluation of toxicity of materials through cell culture method, and analysis of the relationship between the critical value of toxicity and state analysis of a very small amount of material in the pseudo-body fluid in which fretting fatigue was performed.
2. Measurement of the adhesion force of a cell to the surface of a material, and observation of cell degeneration caused by foreign body and mechanical stimulus.
3. Evaluation of fretting fatigue strength of materials in a pseudo body fluid.

118 Evaluation of Biocompatibility of a Ti-6Al-4V Alloy in a Pseudo Body Fluid under Fretting Fatigue Load through a Cell Culture Method

April 1992 to March 1993
M. Sumita, Mechanical Properties Division
Keywords: biomaterials, metallic ions, debris, toxicity, cells (MC3T3-E1), proliferation rate

Metallic components implanted in the human body sometimes fail due to fretting fatigue in the corrosive conditions produced by body fluids. Among biomaterials, use of titanium alloys is increasing because they have the higher strength to density ratio and the higher resistance to corrosion. However, titanium alloys may corrode in body fluids under fretting fatigue loading, because the process may be considered to be disruption of the existing passive film and exposure of fresh metal surfaces to body fluids at the fretted area and at the crack tip during the fretting fatigue cycle.

The fretting fatigue test was carried out in a pseudo body fluid at a stress frequency of 2 Hz using an annealed Ti-6Al-4V alloy. The fretting fatigue strengths at 5×10^6 cycles were 150 MPa in the air and 110 MPa in the pseudo body fluid in which the temperature was controlled at 310 K and the oxygen content was reduced to about one fifth compared with that saturated with air. Fe, Al, Ti, Ni, and V of the order of 5 to 10 ppb were detected in the pseudo body fluid after testing for 45 days by a graphite furnace atomic abstraction spectrophotometry.

In order to evaluate the toxicity of the above elements in the fluid, an in-vitro test was carried out through a cell culture method. The toxicity in the fluid containing the elements which was diluted with PBS(–) solution of 2 times of the volume was about three times higher than that in the control fluid.

Processing

Separation and synthesis

119 Fundamental Study on Preparation and Characterization of the Metal Complexes Possessing a Peculiar Molecular Structure

April 1991 to March 1994
H. Isago, Chemical Processing Division
Keywords: phthalocyanine, preparation, cerium, mixed valence, bismuth

Phthalocyanine and its related compounds containing metal elements have been known as one of the most important organic pigments so far and also have been intensively studied as a group of new materials in recent years. Indeed, it was found in this laboratory that bis(phthalocyaninato)lanthanoid(III) complexes exhibited remarkable electrochromic properties in organic solvents and in solid state as thin film. In these compounds, a hole is created in the complex molecule.

This research work consists of the following two subjects; 1) preparation and characterization of bis(phthalocyaninato)cerium complex and its derivatives which show exceptional properties among a series of bis(phthalocyaninato)lanthanoid(III) complexes and 2) an attempt to prepare the first bismuth complex ligating a phthalocyaninate ring or rings.

In the former subject, our interest is mainly placed on the behavior of the 4f electron on the cerium ion in the bis(phthalocyaninato)cerium complex. In this complex, the cerium is found to be in mixed valence state between trivalent and tetravalent states by electronic, infrared, ESR, and XPS spectra. It is probable that the 4f orbital of the cerium is largely hybridized with a phthalocyanine π orbital. In the latter subject, it is of interest whether the bismuth-phthalocyanine complex has a similar structure to those of the bis(phthalocyaninato)lanthanoid(III) complexes and whether the bismuth complex shows similar properties. It is because that a bismuth(III) ion has a close ionic radius to those of lanthanoid(III) ions with the same coordination number. Moreover, coordination chemistry of the phthalocyanine complex of the other group 15 elements in the periodic table as well as bismuth has been scarcely studied and hence a development of a new field of chemistry and material science is expected.

120 Alloying Method Using Decomposition of Metal Halides

April 1991 to March 1994
G. Omori, Advanced Materials Processing Division
Keywords: alloying, decomposition, metal halides, zirconium, magnesium

The purpose is to obtain basic information on an alloying method using decomposition phenomena of metal halides. An investigation is conducted with several zirconium containing materials for the alloying to magnesium.

Magnesium alloys containing zirconium have been expected in many sides of applications requiring high strength, because zirconium is an

important grain refiner in magnesium. There are, however, many problems in practical alloying procedure. Elemental zirconium is not an efficient agent to use because of its high melting point and high oxidation tendency.

Magnesium was melted in a crucible of mild steel under SF_6 atmosphere in an electric furnace. For the first step, adding zirconium to magnesium was done by using the powder or the briquet of $ZrCl_4$ fixed with a phosphorizer.

$ZrCl_4$ powder is light, fluffy and extremely hygroscopic, and sublimates easily at 604 K. Briquetted $ZrCl_4$ under dry argon gas atmosphere, however, is much easy to use and alloying efficiency is high. An attempt is made to introduce zirconium into magnesium at low temperature using various zirconium halides or complex halides. Characteristics of the alloys obtained are measured.

[121] Literature Survey on Elimination of Specific Toxic Metallic Ions

April 1992 to March 1993

I. Tomizuka, Physical Properties Division

Keywords: radioactive element, Chernobuyli disaster, adsorption

The literature survey is concerned with procedures which allow economical and swift elimination of the very diluted metallic ions from soils and waters that were scattered over a very wide range of environment from atomic power stations or likes by inevitable consequences, accidents or negligence.

The survey was performed in two fields.

The first was concerned with a very small amount of radioactive traces which leaked from relevant plants by one or other inevitable consequence. A typical example was iodine. According to literatures so far obtained, USA was a major source of the literatures. The element is eliminated by active carbons and other adsorbents.

The second was the radioactive species which had leaked from power stations or other disused plants by accidents or negligence. A typical example is those from Chernobuyli disaster, but other examples in Sea of Japan and Ural region are reported in recent time. Information in this field have been reported to be available owing to declassification of the files kept in KGB of former USSR, notably from government of Ukrainian Republic. Although some of the reports were brought to Japan at the opportunity of International Conference on Basic of Adsorption in Kyoto in the spring of 1993, several important papers have been advertised but not published presumably due to economical difficulty in Ukraina. According to reports so far obtained most of them deal with contamination. Papers on elimination procedures are limited.

A guest researcher is invited in 1993 from a related research institute in Kiev, Ukraina. As much more recent information is expected from him, the survey is to be switched to the research which is connected with his visit.

[122] Survey Research on Utilization of Biological Function to Separation and Extraction Process

April 1992 to March 1993

T. Ozaki, Chemical Processing Division

Keywords: biological function, extraction process, membrane, metallic elements

Possibility of application of biological function of selective transport and accumulation of metallic elements to artificial or industrial separation and extraction process is surveyed.

Survey on microbe possessing concentrative ability of metal and its compound

Taking into consideration to direct utilization of biological function in separation and extraction processing, literatures related to microbe possessing concentrative ability of metal and its compound were surveyed. In almost all the circumstances of the surface of earth, whether ordinary or extreme, existence of microbes possessing ability to concentrate specific metallic elements are shown. Next step to proceed this study would be to create an adequate database on separative and extractive function of microbes in water solution and to search unknown microbes in field works.

Survey on mechanism of concentration of metallic element in plasma

Mechanisms of metallic elements transfer and accumulation process in the plasma were surveyed in literatures from the point of view of chemical metallurgy.

Contents of metallic elements inside plasma membrane are controlled by active and passive transport of metallic ions with selective action of transport proteins in plasma membrane. Especially, active transport, which is up-hill directional against electrochemical potential between inside and outside membrane, is interesting in chemical metallurgical application. The following mechanism is becoming clear by recent development in molecular biology. Conformation changes in membrane proteins brings transport of specific ions through membrane and these processes utilizes energies in hydrosis of ATP on membrane and/or electrochemical gradient of other ions across membrane.

The techniques of removing proteins in membrane of plasma and rebuilding it in riposome or artificial lipid bylayer are studied in the area of biochemistry and these methods are confirmed to be applicable in some fields such as drag delivery.

Application of these transplantation methods to experiment would be effective for development of new separation and extraction process.

Gaseous process

⑫③ Development of Shape Memory Thin Films Formed by PVD Method

April 1993 to March 1998
A. Takei, 3rd Research Group
Keywords: micromachine, shape memory, Ti-Ni, sputtering

Micromachines such as micromanipulators and fluid microvalves are expected to be used in the near future in various fields such as biotechnology, medicine and the semiconductor industry. In order to produce such a micromachine, the development of an effective microactuator is essential.

We have already demonstrated that perfect shape memory effect can be achieved even in thin films of Ti-Ni formed by sputtering under a certain condition (See our report in "Research topics" of this journal). However there must be many factors affecting the shape memory effect of thin films. Sputtering conditions should affect structure of thin films, resulting in a change in their mechanical properties. Heat treatment after sputtering is also an important factor. We have the probability to control the shape memory behavior of thin films by heat treatment.

In this research programme we will investigate the relationship between the shape memory behavior of thin films and process factors.

Related Papers

Formation of Ti-Ni Shape Memory Films by Sputtering, A. Ishida, A. Takei and S. Miyazaki, Proc. of Int. Conf. on Martensitic Transformations, ICOMAT-92, California (1992): to be published.

Shape Memory Thin Film of Ti-Ni Formed by Sputtering, A. Ishida, A. Takei and S. Miyazaki, Thin Solid Films 228 (1993): 210.

Development and Characterization of Ti-Ni Shape Memory Thin Films, S. Miyazaki, A. Ishida and A. Takei, Proc. of Int. Sympo. on Measurement and Control in Robotics, Tsukuba, Japan (1992).

124 Precise Composition Control of Ordered Alloys by Chemical Transportation Techniques

April 1992 to March 1995
H. Sasano, Physical Properties Division
Keywords: ordered alloys, shape memory alloys, reversible color change alloys, chemical transportation technique

Ordered Alloys are expected to have attractive properties. However, the properties are very sensitive to the composition of the alloys. It is hard to control the composition precisely by conventional methods. We succeeded in controlling zinc or cadmium concentration in shape memory alloys and reversible color change alloys with accuracy of 0.1 percent by solid-vapor diffusion couple method. In this method, components to be applied are restricted to elements which have high vapor pressure. In this study we try to control the concentration of elements which have low vapor pressure.

We attempted to control aluminum concentration in copper alloys by controlling heating temperatures of pure copper and mixture of aluminum powder and ammonium chloride placed in a closed quartz tube independently. It was expected that aluminum chloride gas formed by the reaction of aluminum with ammonium chloride would decompose on the copper surface and then aluminum would diffuse into copper. However, silicon in addition to small amount of aluminum diffused into copper. The silicon is attributed to the reduction of the quartz tube by aluminum chloride. In this method, any silicon concentration below 8 mass% can be obtained. For large amount of aluminum to diffuse into copper, it was necessary to raise the heating temperatures to above 973 K. In this condition, aluminum content on the surface was higher than 80 mass%. We are trying to get copper alloys of optional concentration of aluminum by developing the CVD method.

Related Papers

Control of Zinc Concentration and Growth Rate of Beta Phase in Copper-Zinc Alloy by Heating in Zinc Vapor, H. Sasano, H. Arai and T. Suzuki, J. Jap. Inst. Metals 57 (1993): 440–44 (in Japanese).

Preparation and Characterization of Cu-Zn-Al Shape Memory Alloy by Heating in Zinc Vapor, H. Sasano, H. Arai and T. Suzuki, J. Jap. Inst. Metals 57 (1993): 445–48 (in Japanese).

125 Synthesis and Characterization of Oxide Superconductors

April 1988 to March 1994
K. Nakamura, 1st Research Group
Keywords: high-Tc oxide superconductors, thin film, MBE, oxygen deficiency, intergrowth, super-lattice

Among the various technique in synthesizing films having multicomponent layered structure, alternate sequential deposition using multi evaporation source and accurate shutter interval is a most promising method in controlling the structure of such systems. In fabrication of oxide superconductor films, we have been applied this method to control the number of CuO_2 layers in a unit cell of Bi system and have succeeded to control the number n up to 7. Furthermore, we have inves-

tigated in detail structure of the films and have found that intergrowth structure is inevitably realized when the amount of evaporating flux from the source is somewhat different from the stoichiometric ratio. We found that such intergrowth occurs periodically and can be characterized as having a statistical mixture of neighboring two phases having different number of CuO_2 planes, i.e., n and n + 1. On the other hand, we have succeeded to synthesize superlattices such as $(3)_2(4)_2$ repeated 10 times, where 3 and 4 in the parentheses means unit cells having 3 and 4 CuO_2 planes, respectively. From the measured T_c vs. average number CuO_2 planes of these intergrowth and superlattice films, we concluded that the diffusion of holes takes place in a range more than a unit layer.

To control oxygen deficiency and to characterize accurate oxygen content and structure change accompanied by oxygen deficiency which have not been established in thin YBCO films are another target in this study. We have found that not only the c-axial length but also the diffraction line intensity caused by the change in the z-coordinate of heavier cations changes appreciably with oxygen deficiency and proposed new method to determine accurate oxygen deficiency from the intensity change. We also investigate in detail structural change in thin YBCO films accompanied by the ordering of cations due to annealing of thin films.

126 Study on Fabrication Process of High-T_c Oxide Superconductors

April 1988 to March 1994
Y. Tanaka, 1st Research Group
Keywords: YBaCuO film, deposition, BiSrCaCuO, AgCu sheath, powder-in-tube method

The feasibility of preparing YBaCuO films on metallic substrates has been studied in an attempt to fabricate a superconducting tape. Deposition methods are rf magnetron sputtering, excimer laser ablation, and low pressure thermal plasma flash evaporation. In order to achieve high critical current density, J_c, problems must be solved with respect to intergranular weak-links at high angle grain boundaries. Particular attention, therefore, is given to the deposition of YSZ buffer layers with in-plain texturing. A new bias-sputtering technique installed with a hollow-cathode type electrode has been developed. Using this technique, triaxially aligned YSZ buffer layers are successfully obtained on polycrystalline substrates. The critical temperature, T_c of the YBaCuO thin films laser-deposited on Hastelloy C with an in-plain textured YSZ buffer layer is 90 K, and J_c increases to as high as 2×10^5 A/cm^2 at 77 K.

Powder-in-tube method using Ag-sheath is also a candidate method for fabricating BiSrCaCuO superconducting wires. However, in order to fabricate practical wires, high homogeneity in J_c along a long length as well as sufficient mechanical strength has to be realized for magnet or transmission applications. Factors for the inhomogeneity in J_c are as follows; Ag sheath swelling during sintering, cracks in oxide core by mishandling and, in addition, compositional deviation, carbon existence at grain boundary and second phase segregations which are attributed to inadequate raw powder material and/or deformation processes. The sheath swelling is one of the important factors. A Bi2212 Ag sheathed tape is prepared by partial melting followed by controlled slow-cooling to form highly oriented crytalline structure. Oxygen gas isolated rapidly upon partial melting expands within softened Ag sheath at high temperature and causes the swelling. Then, segregations occur and quite low J_c values appear. To avoid the swelling it is useful to prepare a raw calcined powder in a reduced oxygen atmosphere. AgCu alloy sheathed tapes with high-density oxide core and flat sheath/core interface have been fabricated by an improved deformation process.

127 Processing and Development of Isotopically Controlled Materials (ICM)

April 1992 to March 1996
T. Noda, 2nd Research Group
Keywords: isotopically controlled materials, ICM processing facility, laser CVD, chemical vapor infiltration

Materials composed of isotopically selected elements realize the essential solution of subjects such as induced activity, He embrittlement, and compositional change caused by reactions with energetic particles.

The objectives of the program are (1) R & D of *in-situ* ICM processing facility (ICMPF) utilizing infrared multi-photon decomposition reaction, (2) search of working materials for isotope separation, (3) development of *in-situ* synthesis of isotopically controlled SiC, Si_3N_4, BN etc. and (4) development of ceramics and their composites with advanced properties.

The following results were obtained.

1. The setup of pulse infrared laser with a maximum energy of 3.5 J/pulse was completed. 60 laser lines between 9.2 ~ 10.8 μm could be evolved.
2. Si_2F_6, working gas for Si isotope separation, was successfully synthesized from Si_2Cl_6 and ZnF_2.
3. The simulation code, IRAC, calculating transmutation and induced activity, and decay heat under various neutron irradiation conditions covering thermal to 14 MeV neutrons predicted superiority of ICM to conventional materials.

4. Low temperature synthesis of SiC film using laser CVD was studied. Polycrystalline SiC film could be formed on graphite substrates from Si_2H_6 and C_2H_2 even at 518 K under a proper laser beam condition.
5. Chemical vapor infiltration process to obtain SiC composite with a high purity and improved mechanical properties is being developed. Carbon fiber/SiC composite with a toughness three times higher than that of monolithic SiC was obtained.

Related Papers

Preparation of Carbon Fiber/SiC Composite by Chemical Vapor Infiltration, T. Noda, H. Araki, F. Abe, H. Suzuki and M. Okada, ISIJ Int'l 32 (1992): 926–31.

Interfacial Structure of CVI Carbon Fiber/SiC Composite, H. Araki, T. Noda, F. Abe, H. Suzuki, J. Mat. Sci. Letters 11 (1992): 1582–84.

Microstructure and Mechanical Properties of CVI Carbon Fiber/SiC Composites, T. Noda, H. Araki, F. Abe and M. Okada, J. Nucl. Mat. 191–94 (1992): 539–43.

Liquid state process

(128) Metastable Phase Solidification from Undercooled Liquid by Introducing External Nucleation Seed

April 1993 to March 1996

S. Tsukamoto, Advanced Materials Processing Division

Keywords: solidification, metastable phase, levitation melting, undercooling

Metastable metallic materials produced from deeply undercooled melts can provide some interesting materials properties. In the previous work, we indicated that the metastable phase solidification could be induced with relative ease if the barrier to the nucleation could be eliminated due to an epitaxial growth from pre-existing matrix of different solidification mode in rapid solidification of electron beam skin melting. The aim of this investigation is to elucidate the role of nucleation and dendrite growth velocities on competitive phase selection of equilibrium and metastable phases during the solidification of undercooled melts. A levitation melting technique is used to obtain large undercoolings. An external seeding is also tried to clarify the role of nucleation and to develop a new technique for producing metastable bulk materials.

Collaboration Research

Fundamental Study on Atom Arrangement, Design And Control of Metallic Materials: NRIM and Research Development Corporation of Japan

129 Purification of Metals by Non-Contacting Melting Method

April 1991 to March 1994

A. Fukuzawa, Chemical Processing Division

Keywords: cold crucible, levitation melting

The purpose of this study is to develop the electromagnetic levitation melting process of reactive metals and refractory metals using the cold crucible type non-contacting induction furnace. Up to now, the reaction between metal and crucible has made it difficult to purify the reactive metals and there has been no crucible materials for homogeneous melting of refractory metals. The cold crucible type melting method will solve these problems.

In these several years, we have made various kinds of trials on the cold crucible type non-contacting induction furnace and many fundamental results concerning with the cold crucible have been obtained. However, we have been developing the levitation control techniques; supplying different two frequencies in order to obtain optimum levitating conditions corresponding to any molten metals and alloys that have various physical properties such as density, electrical resistance and melting point.

In this term we are carrying out further study by setting the cold crucible in an atmosphere controlled vessel for optimum levitating and purification of molten metals such as titanium and its alloys. The shape of the cold crucible and the high frequency coil, and the electric output power have been examined in order to obtain the optimum levitating conditions in the vessel.

Now, we are developing the levitation technique concerning high-purification melting of reactive metals and refractory metals.

130 Extraction from Metal to Gas Phase

April 1992 to March 1994

A. Fukuzawa, Chemical Processing Division

Keywords: thermal plasma, low pressure plasma jet, vaporization

Thermal plasma produced by transfer or non transfer type torch is widely used for melting metals and surface lining. However, its operating pressure is usually at atmospheric pressure because of the existence of plasma jet. In some case low pressure plasma jet is used, but its pressure is not less than 100 torr.

This research work is to investigate the behavior of plasma jet in lower pressure of 10 torr order and apply to the gaseous extraction of tramp elements like Cu, Sn, Ga or Cr from liquid iron or steel by the help of ultra high temperature of plasma jet. To get the aimed pressure rotary pump of 6000 l/min was attached with plasma furnace, and in blank test the pressure in the furnace reached as low as

around 1 torr under the addition of Ar of 60 l/min as plasma source. However, in the hot run, glow discharge was observed around 10 torr.

Extraction rate of the above elements is investigated now by varying the pressure, gas composition or power supplied.

This technology can be applied for the extraction of various kinds of elements from molten metals and alloys, and especially from recycled scrap.

131 Basic Technology Development of Materials Processing in a Short-Duration Microgravity Environment

April 1992 to March 1995

A. Sato, Advanced Materials Processing Division

Keywords: microgravity, solidification, combustion synthesis, superconductor

This project is designed in order to use the drop tower facility at Kami-sunagawa in Hokkaido (10 s) and Toki in Gifu (4.5 s). This project consisted of 19 sub-themes, and three of them are being carried out in NRIM.

A study on double combustion synthesis apparatus

Combustion synthesis is a production process to produce chemical compounds from elemental powders in a short time using the heat of formation of component elements. The main purpose of this study is synthesizing the high performance intermetallic compounds using the short time microgravity environment in 10 s. We developed a "Short time double combustion synthesis apparatus" in order to conduct the experiment of combustion synthesis in 10 s duration of microgravity.

Observation of harbingering phenomena of solidification crystallization

Patterns of liquid flow during phase transformations, such as solidification, under microgravity differ from those under 1G on the ground. Nucleation behavior as well as crystal growth is influenced by gravity. We are trying to observe an embryo/embryos of organic transparent materials. The embryos are clusters of atoms/molecules whose radii are smaller than those of the critical ones that grows into nuclei. We intend to observe the effect of the gravitational force on the number and the movement of the nuclei.

Study on the synthesis of high temperature superconductors

The objective of this study is to investigate various materials aspects of oxide high temperature superconductors (HTSC), such as, phase relationships, solidification phenomena, reactions and wettability with other materials, etc., since these aspects should have influences on the synthesis of HTSC under microgravity environment. The phase change of Bi-Sr-Ca-Cu-O (BSCCO) and BSCCO/Ag composite were studied by microstructure observations and X-ray diffractions. The results indicate that the Ag dissolves into BSCCO lowering the partial melting point and that the partial molten state is the mixture of the liquid phase and (Sr, Ca)-Cu-O and Bi-Sr-Ca-O solid phases. Possibility of segregation of these solid phases during partial molten state under microgravity is discussed comparing with results of aircraft experiments.

132 Solidification Processing for Fine-grain Structure Materials

April 1991 to March 1994

A. Sato, Advanced Materials Processing Division

Keywords: solidification processing, fine grain structure, rapid solidification, vigorous agitation

Many kinds of materials composed of various grain structures can be produced by solidification processings. Grain structures can be divided roughly into three: (1) A coarse-grain structure, or a single-crystal structure in the extreme case. (2) A fine grain structure, or an amorphous structure in the extreme case. (3) A usual poly-crystal structure found in conventional castings. The coarse-grain structure or the single-crystal structure can be obtained by a slow unidirectional solidification, while the fine-grain structure or the amorphous structure can be realized by a rapid solidification. The usual poly-crystal structure is acquired at a common solidification rate.

Rods, composed of several grains solidified completely unidirectionally from its one end to its other end, can be produced by a moldless upward continuous casting process we have developed. Materials composed of the fine-grain structures or the amorphous structure are now being used for diversified objects. Therefore, it is concluded that researches on production of materials composed of the fine-grain structure as well as those composed of the coarse-grain one should be performed.

The research on the production of ingots composed of the fine-grain structure is carried on by a rapid solidification process along with vigorous agitation. An apparatus for this process has been constructed, and experiments using Al-Si alloys are carried out. The results obtained are under examination.

133 Measurements, Analyses and Evaluations of Specimens Made by FMPT

April 1992 to March 1994

A. Sato, Advanced Materials Processing Division

Keywords: microgravity, solidification, fluid flow

FMPT (First Material Processing Test of Japan) was performed in September, 1992 in Space Shuttle (SL-J mission). Researchers of our institute are responsible for following five themes out of 22 materials processings in the total of 34 themes.

Production of compound semiconductor crystals by floating zone melting

A large single crystal of indium antimonide compound semiconductor was made in an infrared image furnace. The crystal is being examined by an X-ray diffraction topography, and the electric property is also being measured. The report on the results will be published within 6 months.

Production of new superconducting materials

Monotectic Al-Pb-Bi alloys and eutectic Ag-Ln (Lanthanide)-Ba-Cu alloys were melted and solidified using continuous heating furnace during the mission. Optical micrographs of Al-Pb-Bi alloys indicate that sphere particles of Pb-Bi alloys having an average diameter of 20 μm uniformly are distributed in the Al matrix. The result suggests that the solidification occurred uniformly in spite of the Marangoni force. The microstructure analysis of Ag eutectic alloys and the formation of superconductors from the flight processed Al and Ag alloys are now in progress.

Formation mechanism of deoxidation products in iron ingot deoxidized with two or three elements

Experiments in space were manipulated successfully. All of 12 samples were melted and some of them boiled, but the most can be examined for later microscopic observation.

Preparation of particle dispersion alloys

TiC particle dispersion/nickel base alloys were melted and solidified. The temperature profile of furnace and the microstructure of the alloys were examined. The results made clear that the melting and solidification was done correctly and as scheduled. Samples made in space is more homogeneous than those on the ground.

Diffusion in liquid state of a binary alloy system

Flight specimens (diffusion couple of Au and Ag) were observed by eyes, and prepared for the further examinations by means of optical microscope, SEM, EPMA, and so on. The diffusion in some of the flight specimens proceeded faster than that of those on ground, and it is considered due to the Marangoni convection.

Solid state process

(134) Metallurgical Analysis of Micro-Machining Region

April 1993 to March 1996

S. Yamamoto, Advanced Materials Processing Division

Keywords: micro-machining, metallurgical factor, TiNi alloy, Ti alloy

The object of this investigation is to analyze metallurgical factors which affect micro-machining and to accumulate basic data with a view of microfying mechanical systems.

The range of cutting thickness is from a few μm to a few hundred μm. It is anticipated that the cutting force on the tool and the tool life change with the direction of crystals within a cutting region.

The effect of grain boundaries and microstructures is larger in micro-machining than that in the usual machining.

It is necessary to store data on various machining methods for microfying mechanical systems. In this study, data on turning, end milling and drilling of various materials will be accumulated. Work materials are a NiTi shape memory alloy as a functional material, stainless steels and Ti alloys as structural materials.

This year, the existing micro-machining device, which has functions of shaping and turning, is to be systemized with an installation of high speed air turbine spindle for micro-end milling and micro-drilling. The performance of the device is to be tested by machining materials having various microstructures and hardnesses.

135 Cooperative Phenomena of the Transformation Variants

April 1992 to March 1995

H. Miyaji, Advanced Materials Processing Division

Keywords: variant selection, martensitic transformation, Fe-30Ni alloy

To increase the ion diffusivity in thin film, the variant selection processes are studied on the martensite of ferrous alloys which have 3, 12 or 24 crystallographically equivalent orientation relation with matrix crystal. It is expected that the ion diffusivity changes dynamically corresponding to the martensitic transformation.

In the present study we investigate the effect of internal stress on the variant selection, which is induced during the processing of thin films.

The textures of Fe-30Ni alloy sheets rolled at a temperature above M_d (γ) and subjected to a sub-zero treatment (α) were determined by an x-ray pole figure method.

It was found that the rolled texture of γ phase was of typical Cu-type. The transformation texture of α phase had the pole distribution of the shape of the numeral "8" by the effect of strong interaction with internal stress.

The texture measurements of α phase, which is formed from γ phase subjected to a stress relieving annealing, are in progress.

Related Papers

Effect of Specimen Size on the Variant Selection in Martensitic Transformation, H. Miyaji and E.

Furubayashi, Textures Microstruct. 12 (1990): 189–97.

Transformation Texture Analysis of BCC and BCT Ferrous Martensite, H. Miyaji and E. Furubayashi, submitted to Textures Microstruct.

136 Materials Properties Induced by Transformation Superplasticity

April 1990 to March 1993

H. Nakajima, Advanced Materials Processing Division

Keywords: transformation superplasticity, microstructures, mechanical properties

There are two types of superplastic behavior, known as fine-grained and transformation superplasticity. In the latter, large elongations are generated by a thermal cycle through the phase transformation in a material. The main purpose of this investigation is to elucidate the change in the microstructures and the mechanical properties of steels which have been elongated by transformation superplasticity. Test material was a 0.1C-2Mn-1Cr-0.3Mo-Nb, B, Ti steel and the superplastical deformation was generated in the bainitic transformation. A specimen was heated to a temperature of 900 °C for 5 min, and then it was cooled in air. When the temperature of the specimen reached to about 650 ~ 600 °C, a tensile load up to 190 MPa was applied. The bainite transformation range is shifted to higher temperatures with increasing of applied stress and the superplastical strain increases more than in direct proportion to the applied stress. Microstructures consist of lath-like bainitic ferrite and granular bainitic ferrite in the cooling under no load. An increase of the applied stress decreases the ratio of the former and the microstructure becomes almost granular at higher applied stresses. The effect of superplastical deformation on the tensile properties was neither observed in testing at room temperature nor at –196 °C.

137 Metallurgical Analysis of Cutting Region

April 1989 to March 1993

S. Yamamoto, Advanced Materials Processing Division

Keywords: cutting force, built-up edge, chip shear region, multiple regression analysis

In machining of steels, a cutting force on a tool is very important from the point of view of a tool life and a formation mechanism of chips.

An estimating method of the cutting force is studied in a cutting speed range in which a built-up edge forms. For this purpose, it is necessary to get a shape and a deformation force of a tip region of the built-up edge, and a width and a deformation force in a chip shear region.

At first, the width of the chip shear region (Ws) and the tip radius of the built-up edge (Br) were measured with a micro-machining device.

The interrelation between both values and the hardness of work material (H) and the cutting speed (V) was obtained.

In the second place, the deformation force of the chip shear region (Kfs) and that of the built-up edge (Kfb), which were obtained by the analysis of the previous experimental results, were also correlated with the hardness of work material (H) and the cutting speed (V).

Multiple regression analysis was applied on four factors (Br, Ws, Kfs, Kfb), the hardness (H) and the cutting speed (V). It gave computation equations to estimate the cutting forces (principal force (Fc), side force (Fs) and thrust force (Ft)) from H and V values. It was found a good correlation between the calculated and the measured values. Above equations can be put into practical use.

138 Comprehensive Research and Development of Special Structural Ceramics Using Colloid Processing

April 1990 to March 1993

Y. Kaieda, Chemical Processing Division

Keywords: combustion synthesis, WC, chemical furnace

The purpose of this theme is forming of the elemental powders, instant synthesizing of the special structural compound composite using the heat of formation and its propagation, and revealing its mechanical properties. The study of the synthesis of the special compound with high melting temperature as a matrix of the composite using the chemical furnace, which is conducted by combustion synthesis, has been continued in this fiscal year. The very hard WC with high melting point is selected as an objective chemical compound in this fiscal year.

The chemical furnace consists of titanium and carbon which are both solid state below 1993 K. Three matters are in condensed state below the adiabatic temperature. Namely, carbon and titanium carbide are solid state and titanium is liquid state. While the combustion synthesis is occurred, a part of the starting powder is heated up by the propagation of heat from the adjacent part in which the combustion synthesis has already started. Since titanium and carbon keep in contact with each other in solid state below the melting point of titanium, it is difficult for both powder to make a solid solution by mutual diffusion of titanium and carbon in a short time. However, above the melting point of the titanium, the solid particles of carbon are surrounded by molten titanium. Accordingly, above this temperature up to the

adiabatic temperature, the synthesis becomes possible because of the classical reaction process in which the spherical particle is surrounded by liquid.

On the other hand, when the oxide starting powders are used in the chemical furnace and the following formula is applied,

$$3TiO_2 + 3C + 4Al = 3TiC + 2Al_2O_3,$$

solid state TiC and liquid Al_2O_3 are synthesized because the mutual diffusion becomes possible by the reaction, and the diffusion occurs in solid carbon particle surrounded by liquid aluminum and liquid TiO_2. This case is not favorable for synthesis of WC because the adiabatic temperature is too low.

Powder processing

(139) Study on Solid State Chemical Reaction, its Propagation and Materials Synthesis

April 1993 to March 1996
Y. Kaieda, Chemical Processing Division
Keywords: combustion synthesis

The fundamental study to reveal the reactions between solids (powder), solid and liquid, and solid and gas is carried out. The propagation of the reaction and the synthesis process of the materials (synthesized through the reaction) are also studied. The field of the study covers not only the grasp of the phenomena but the comprehensive understanding of the chemical reaction, the heat transfer, the mass transfer and the other aspects of the synthesis of materials in the solid phase system.

The selection of the combinations of elements, which is focussed in the present study, will be investigated. The system of the combination that might exhibit the effect of convection and pressure during the reaction and synthesis process is selected considering the system that performs the effect of liquid and gaseous phase. The system of elements, in which the safety during the experiment is assured, is selected.

Investigation by the thermal analysis with raising temperature in constant speed and/or in alternating speed is carried out to reveal the conditions for the initiation of the reaction, the propagation and the synthesis. The influence of pressure and convection on the phenomena in the reaction process of the system containing gaseous phase or liquid phase is studied using a high gaseous pressure apparatus. These experiments will reveal the phenomena of the chemical reaction between solids, the thermal conductivity, the propagation of the reaction and the mass transfer. The products synthesized by this study is examined by the x-ray diffraction analysis, SEM observation, EDX analysis and other microscopic analysis to disclose the microscopic aspects of the phenomena of the reaction, the thermal conduction, the propagation of the reaction and the synthesis. This study enables us to understand the basic phenomena of the chemical reaction between solids and its propagation and the synthesis of materials.

(140) Fundamental Study on Creation of Micro Stereome Fabrics by Powder Technology

April 1993 to March 1996
K. Halada, Failure Physics Division
Keywords: powder, porosity, sintering, structure control, ecomaterial

Minerals of biological origin have the microstructure to perform functions efficiently. It is well-known that spicules or echinoderms have three dimensional framework or porous structures, e.g. microperforate, labyrinthic, retiform fascicular etc., to perform efficient mechanical properties. We have started this study as a first step with an ambition to acquire or mimic the design and construction of materials of natural origin in the field of the inorganic materials technology.

Powder technology is noteworthy technology to create the mimetic microstructure of natural materials, because the powder can be divided to small elemental particles and can be synthesized under optional control. Prediction of microstructures and stereome morphologies of sintered materials is important to design such microstructures. One part of this study is on arrangement; to develop the way of prediction for the microstructure and the stereome morphology of sintered materials.

The feature of powder particle is also important as the element of synthesis. Embellishment of particles with finely controlled qualities is expected to enlarge the possibility of the design of stereome fabrics. The second part of the study is on assembling; to inquire the way of combination of various type of particles and to inquire the production method of appropriate powder or embellished particles for assembling.

(141) Characterization of Composite Ultrafine Particles

April 1993 to March 1995
S. Ohno, Physical Properties Division
Keywords: ultrafine particle, composite UFP, catalytic property, Fischer-Tropsch's reaction, photocatalytic decomposition

It is well known that the ultrafine particles (UFP) have many excellent physical and chemical properties. Further, the composite UFP formed by combining between foreign particles in the region of a UFP's size would be expected to improve the properties of UFP and to create a new function.

In this study, the composite UFP of metal and ceramics (e.g. metal-nitride, metal-carbide, metal-oxide, etc.) are synthesized by plasma CVD process using a DC arc plasma and an RF-plasma. Morphological, structural and thermal properties of the composite UFP are determined by means of transmission electron microscopy, energy dispersion analysis for x-ray, x-ray diffractometry and differential thermal analysis. Furthermore, measurements of Fischer-Tropsch's reaction (hydrogenation of carbon monoxide) and the photocatalytic decomposition of water and/or organic compounds are performed to characterize the catalytic properties of the composite UFP.

In collaboration with POWDER TECH Co., LTD., special research on preparation of ultrafine iron nitride particles by "reactive plasma-metal" reaction is conducted (May 1992 to March 1994).

Related Paper

Synthesis of the Composite Ultrafine Particles of Ni-TiC by "Reactive Plasma-Metal" Reaction, S. Ohno, C. Jiang, H. Okuyama and K. Honma, J. Jpn. Soc. Powder & Powder Metall. 39 (1992): 221–26 (in Japanese).

⑭② Synthesis and Characterization of Advanced Materials Utilizing Colloidal Dispersed Systems

April 1993 to March 1995

Y. Sakka, Chemical Processing Division

Keywords: colloid, fine powder, consolidation, gas desorption, nanocomposite

Key developments in processing of fine powders are (1) synthesis of fine powders with controlled sizes, shapes and chemistries, (2) consolidation techniques to control pore volume and pore size distribution, and (3) the role of powders and compacts on the evolution of microstructures during sintering. Although many kinds of techniques in preparing fine powders have been reported, little efforts have been paid on the consolidation of fine powders. In the present study, the emphasis will be on the second and third development.

Colloidal processing of nano-sized powders (Al_2O_3, ZrO_2, ZnO, Ni, etc.) is conducted to obtain porous materials with controlled pore sizes. The most important factor is how to disperse the powders. The porous materials will be used further as starting materials for fabricating nanocomposites, heterogeneous phases, biomimetic materials, etc. Electro-discharge sintering is applied to obtain the advance materials. In this procedure, the powders are heated by instantaneous high electric pulsed power application under a uniaxial pressure. Characterization of the synthesized materials is another subject. The gas (especially H_2, H_2O, CO and CO_2) sorption-desorption experiments of metal-ceramics nanocomposite particles are conducted for characterizing the catalytic properties.

Related Papers

Processing of SiC-Mullite-Al_2O_3 Nanocomposite, Y. Sakka, D.D. Bidinger, J. Liu, M. Sarikaya and I.A. Aksay, Proc. 16th Annual Conferences on Composites, Materials and Structures, Restricted Sessions (1992): 1–12.

Surface Chemistry and Sintering Characteristics of Ni Ultrafine Powders, Y. Sakka and T. Uchikoshi, Powder Metall. 36(3) (1993): in press.

Adsorption of Hydrogen on Ni and Ni-TiO_2 Composite Ultrafine Particles, T. Uchikoshi, Y. Sakka, S. Ohno, H. Okuyama and K. Yoshihara, Surface Sci. 287-88 (1993): 1082-86.

143 Coating of Fine Powders by CVD Technique in Fluidized Bed

April 1991 to March 1994

T. Itagaki, Materials Design Division

Keywords: fluidized bed, CVD, HfC, tungsten powder

This research is aimed at preparing various types of very fine powders coated with very thin layer of a second substance. The fine coated powders have various advantages when they are used for sintering. For example, if the powder is coated with a sintering agent, the sintering will finish in much shorter time or will be performed at a lower temperature as compared with the case when the agent is added as powder, because the agent is much more finely dispersed. When an alloying element is coated on powder of a refractory metal, the alloying will be more homogeneous by the same reason.

A chemical vapour deposition technique in a fluidized bed is planned to be applied to make the coating layer comprising ceramic materials. The particle size of the powder will be 1–10 microns, and thickness of the coated layer will be several nanometers. Based on the research work performed previously, we have been convinced that coating by CVD technique in a fluidized bed is technically feasible.

The first experiment was concerned with coating of HfC on tungsten powder. Until present, we attained coated layer of about 7 nanometer thickness on the surface of tungsten powder in diameter of 4 microns. The obtained powder will be sintered at a high temperature to obtain tungsten alloy dispersed with HfC.

Next experiment will be concerned with coating of sintering agent on ceramics such as silicon nitride or silicon carbide. This coating will be more difficult because the density of the powder is much smaller than that in the first experiment.

144 Development of Particles Assembly Technology for Integration of Functions

April 1992 to March 1996
N. Shinya, Failure Physics Division
Keywords: intelligent materials, multiple functions, particle assembly technology

For creation of intelligent materials, technologies for systematization and integration of multiple functions should be developed in advance. Systematically coordinated multiple functions will lead to manifestation of intelligent functions, such as self-repair, self-diagnosis, feedback and so on, which can respond to environmental conditions.

In order to provide materials with the systematically coordinated multiple functions, a new approach is made through a development of particles assembly technology in this work. Each particle has a primitive function such as sensor, processor and actuator. Therefore coordinations and systematizations of these primitive functions may be realized through three dimensional particles arrangement. For the arrangement it is necessary to develop the technology which make it possible to assemble several kinds of particles according to structural designs for the manifestation of the coordination and systematization. As elemental technologies for the three dimensional particles arrangements, particle designs, particle preparation, controls of particle movement and treatments of assembled particles are being studied at the first stage.

Pure metal particles were coated with thin conductive polymer. The interface between the metal and the polymer showed non-linear voltage/ampere relation due to the shotteky barrier. The coated particles were collected, and the assembled particles showed good varister properties. This is a primitive example developed by this concept.

145 Properties of Raw Powder of Superconductor for High Pressure Forming

April 1988 to March 1994
Y. Kaieda, Chemical Processing Division
Keywords: Y-system, combustion synthesis

There are many well-known methods for making Y-Ba-Cu-O system superconductor which are roughly classified into solid phase method, liquid phase method and gaseous phase method. In the most popular powder process of solid phase method Y_2O_3, $BaCO_3$ and CuO are usually used as starting powders because these substances are stable in the room temperature and relatively cheap. In this process the mixture of the powder of the starting materials is calcined in the furnace with flowing oxygen gas for several hours, then it is pulverized and mixed again and sintered in the furnace for long hours.

Many ceramics and intermetallic compounds are made by combustion synthesis using the heat of formation of the combination of the elemental powders in the system. If the combustion synthesis is applied for making Y-Ba-Cu-O system superconductor, the elemental powders should be used for getting the heat of formation in the reaction between the starting metallic powders and an oxygen gas in order to start and to propagate the combustion synthesis. However, the pure metallic yttrium powder is unstable and easily oxidized in the air at room temperature and reactive to water. Pure metallic barium is also unstable and oxidized in the air at room temperature and reactive to water and toxic to human body. To the contrary, pure copper is relatively stable in the air and not reactive to water. It may be instinctive to use pure copper powder as a key material for performing combustion synthesis of Y-Ba-Cu-O system superconductor. The values of the heat of formation of copper oxides, $-\Delta H_{298}$, are 167.4 kJ/mol for Cu_2O and 155.3 kJ/mol for CuO.

In the present experiment, the combustion synthesis of Y-Ba-Cu-O system superconductor was performed, using the heat of formation of copper oxide, under the absolute pressure range of pure oxygen gas at 1.3 kPa to 12.6 MPa to examine if those values of heat of formation of copper oxides are enough for sustaining the propagation of the combustion synthesis and synthesizing the Y-Ba-Cu-O system superconductor. The process of combustion synthesis of Y-Ba-Cu-O system superconductor using pure copper powder and pure oxygen gas was revealed and the samples made by combustion synthesis were characterized.

146 Study on Rapidly Solidified Powders for Superconductive Materials

October 1988 to March 1994
K. Halada, Failure Physics Division
Keywords: superconductive materials, rapid solidification, powder, sintering

Rapidly solidified Bi-Sr-Ca-Cu-O glassy ceramics was produced by gas atomization and centrifugal atomization from molten oxide. By the centrifugal atomization ligaments and spheroidized glassy powder 0.1 to 1 mm in diameter were obtained. Gas atomized powder was composed of fine spherical powder less than 20 μm in diameter and thin fiber with round heads at the end. All of them were amorphous, which had the crystallization temperatures around 500 °C.

While the mixed powder showed a simple shrinkage behavior above 700 °C, the atomized powder once shrank above 500 °C, followed by the second shrinkage around 700 °C, and characteristi-

cally expanded from 820 °C before rapid shrinkage above 860 °C. From the atomized powder $Bi_2Sr_2CuO_6$ crystallized above 500 °C. $Bi_2Sr_2CaCu_2O_8$ (superconductive phase) appeared above 800 °C, and the partial melting took place around 860 °C. Below the temperature of the remarkable partial melting extraordinary growth of Ca_2CuO_3 phase was observed. The phase separation generated Bi-rich part as the counter result of the growing of Ca_2CuO_3 phase. These phase separation was confirmed by newly developed EPMA composition analysis method. The Bi-rich part prevented from producing the stable high-T_c phase, because the liquid phase broke out from the Bi-rich part below the temperature to make the high-T_c phase stable.

Related Papers

Sintering of Bi-Sr-Ca-Cu-O Superconductive Material Atomized from Molten Oxide, K. Halada, K. Minagawa, H. Suga, H. Okuyama, S. Ohno and Y. Muramatsu, Advances in Powder Metallurgy & Particulate Materials 8 (1992): 281–92.

EPMA Composition-coordinate Mapping Analysis of the Phase Change of Atomized Bi-Sr-Ca-Cu Oxide, K. Halada, K. Honma, K. Minagawa and H. Okuyama, J. Jpn. Soc. Powder Metall. 39 5 390–96 (in Japanese).

147 Preparation and Characterization of Ultrafine Powders Used for Making Oxide Superconductors

April 1988 to March 1994
S. Ohno, Physical Properties Division
Keywords: superconducting oxides, ultrafine powder, gas desorption, degradation

Improvement of homogeneity, sinterability, and preferable orientation is expected using finer powders as raw materials for superconducting oxide. One objective of this study is to synthesize the ultrafine powders suitable for making superconducting oxide. Various preparation methods are conducted such as reactive plasma-metal reaction, CVD in RF-plasma, oxalate coprecipitation and citrate sol-gel methods. Then the factor affecting the superconductivity properties is examined, especially on the appropriate composition, nonstoichiometry, particle size, and effect of Ag addition.

For technological applications of superconductors, informations about the degradation under open environmental condition and its prevention is indispensable. We have examined the reaction of superconductors with water vapour and carbon dioxide. The degradation by water vapour is more obvious for Y-oxide system ($YBa_2Cu_3O_{7-\delta}$) than for Bi-oxide system. In the Y-oxide system, the relation between the amount of the sorption of water vapour and the oxygen deficiency δ is determined quantitatively. Moreover, the effect of the surface treatment in carbon dioxide on the sorption-desorption characteristics and the effect of Ag addition are investigated in detail to prevent the degradation.

148 Combustion Synthesis for Production of Ceramic and Intermetallic Materials

April 1992 to March 1993
Y. Kaieda, Chemical Processing Division
Keywords: combustion synthesis

National Research Institute for Metals cooperates with New York State College of Ceramics at Alfred, N.Y. in U.S.A. under the auspices of the Japanese and the U.S. Government in conducting a basic research to develop the production process of ceramic and intermetallic materials and the characterization of the synthesized materials. The international cooperative research will enhance the level of the field of the combustion synthesis and will develop the production system of the advanced materials.

The institute makes an effort to develop this materials production process, which exploits hot, exothermic, usually rapid, chemical reactions to form useful materials. In the process, heat is supplied from the reaction itself, not an external or expensive source. As its primary research goal, the institute intends to develop a basic, fundamental understanding of the combustion synthesis process and foster prototype manufacturing technologies that can be transferred or licensed for manufacturing.

Research has been focused on the areas of functionally gradient materials; joining ceramic to metal, ceramic to intermetallic compounds, and ceramic to ceramic materials; coatings of ceramic on metal, intermetallic or ceramic materials; cemented carbides; dense refractory monoliths; high-temperature, corrosion-resistant filters; and fundamental studies.

To determine the major areas in which the combustion synthesis processing is most cost effective and practical, the institute has been investigating specific areas in which the process can be most fruitful. Current research projects involve the study of functionally gradient materials; creep-resistant intermetallic-matrix composites. Researchers are also exploring the outer limits of the combustion synthesis processing with high-temperature superconductors and the basic aspects of multi-component oxide powder synthesis and fundamentals of the process.

149 Production and Characterization of Advanced Powders

April 1988 to March 1993
K. Yoshihara, 4th Research Group

Keywords: mechano-chemical synthesis, ultrafine particle, sintering, composite, rapid diffusion

This research topic comprises the six, subthemes described in the following sections.

1. Production of fine grain carbide powder by mechano-chemical synthesis; Mechano-chemical reactions in the planetary ball mill, and the annealing conditions of mixed powders (Ti-C and W-C etc.) are investigated to produce fine grain carbide powders of transition metals.
2. Synthesis and consolidation of composite ultrafine particles; Composite ultrafine particles of metal and ceramic such as metal-nitride, metal-oxide and metal-carbide etc. are synthesized by a reactive plasma-metal reaction or an RF-plasma CVD method. Sintering characteristics and photocatalytic properties are investigated. Various ultrafine powders are also prepared by a sol-gel method and their characterization are conducted.
3. Characterization of ultrafine particles and their bonded bodies; Gas adsorption and desorption characteristics of ultrafine particles (Fe, Ni, and their composite with ceramics) are investigated by specially developed thermal desorption method. Electro-discharge sintering under a presure are conducted to make porous or dense nano-structure materials.
4. Production of advanced powders by centrifugal atomization; Fundamentals of the centrifugal atomization are investigated. Atomization mechanisms and atomizing parameters has been elucidated. Microstructure of solidified powders were also studied from the view point of the solidification mechanisms. The effect of super-cooling was found to be significant in the solidification of atomized powder.
5. Sintering of metal-ceramic mixed powders; Sintering of Cu-Al_2O_3, Cu-Y_2O_3 and Cu-W mixed powders were investigated to develop high strength and high conductivity copper base composites. Correlations between wettability and sintering characteristics were discussed, and mechanical properties of these sintered composites were examined from the view point of high density and wettability.
6. Reaction in metal thin film; Titanium-segregated layer on Nb film, which is formed by heating Nb film on Ti substrate in a vacuum, is found to be thermodynamically stable in the form of multi-layer segregation and is analyzed by introducing aeolotropic interaction between atoms.

Related Papers

Effect of Milling Methods on the Reaction of TiC Formation, S. Wanikawa and T. Takeda, J. Jpn. Soc. Powder Metall. 39 (1992): 1145–50 (in Japanese).

Sintering Characteristics of Fe and FeCo Alloy Ultrafine Powders, Y. Sakka, T. Uchikoshi and E. Ozawa, J. Mater. Sci. 28 (1993): 203–17.

Joining

⑮⓪ Fundamental Study on Brazing under a Micro Gravity

April 1993 to March 1995

K. Sasabe, Advanced Materials Processing Division

Keywords: brazing, micro gravitation, temperature distribution, capillary penetration

The purpose of this study is to establish the method to find process parameters for brazing in space. Brazing is one of the most important and practical joining technique in the space environment because thin walled cylindrical rods will be used widely for the constructions in space. Moreover, a vacuum and a micro-gravity, the typical characteristic of the space environment, can be used as positive conditions for brazing actively.

Under the microgravity, the capillary flow of liquid is not limited or stabilized by the gravity but dominated by the surface tension only. Temperature distribution of joint during brazing under the micro gravity is, therefore, important to get perfect penetration of filler metal in a joint gap, because capillary gap penetration of filler metal must be controlled by the temperature distribution.

We will investigate the relationships between flow phenomena of molten liquid and temperature field change during brazing and try to propose process parameters for the brazing in space.

151 Corrosion of Dissimilar Metals Joints in Reactor Fuel Reprocessing Plants

April 1991 to March 1996

H. Nakamura, Advanced Materials Processing Division

Keywords: diffusion welding, titanium, zirconium, stainless steel, laser speckle method

Dissimilar metals joints are to be used in a new reactor fuel reprocessing plant in Japan. The joints composed of stainless steels and valve metals are made by solid state joining. It is necessary for the safety of plant to assure sufficient mechanical strength and also corrosion resistance.

Diffusion welding of zirconium to 304L type stainless steel was necessary to insert a tantalum foil for the protection against intermetallic compounds formation. An annealed soft foil was preferred and a sufficient tensile strength of 480 MPa was obtained at welding temperature of 1123 K. Solid solution of tantalum in zirconium at Zr/Ta interface and mutual diffusion at 304L/Ta interface were observed but no intermetallic compound.

Corrosion test in boiling 3N nitric acid with addition of Cr^{+6} ion of 1 g/l was performed. Surface observations of immersed specimens of three kinds of weld specimens, that is, diffusion welds, friction welds and explosive welds, showed almost uniform intergranular corrosion at the 304L stainless steel portion of each specimen after 144 hours immersion. It is therefore presumed that all these solid state joining might be acceptable to the reprocessing plant.

Elastic analysis of thermal stress of dissimilar metal joints due to heating up was done with various mesh sizes. Diameter of laser spot reasonably correspondent to small mesh size analysis was checked and the valve of 0.1 mm was enough for the evaluation.

152 Joining of Intermetallic Compounds Utilizing Resistance Heating by Direct Current

April 1991 to March 1993

S. Fukushima, Advanced Materials Processing Division

Keywords: joining technique, titanium aluminide, microscopic observation, bending strength

The aim of this study is to clarify the possibility of the joining of intermetallic compounds, an advanced structural material. An applied joining technique consists of a reaction sintering process and a liquid-phase diffusion bonding process. The two processes proceed simultaneously under a certain welding condition.

Aluminum power in intermediate metal melts selectively through heating. The aluminum melt reacts on base metal surface and on titanium particles in the intermediate metal, and makes thin alloy layers at their interface. From this, it is confirmed that the applied joining process is very effective.

When an excessive high welding force was applied, the aluminum melt was pushed out towards a periphery of intermediate metal due to collapse of a skeleton which consisted of titanium particles. This led to microstructural dissimilarity in the intermediate metal. On the other hand, when an excessive low welding force was applied, the aluminum melt did not reach the base metal surface and voids in the intermediate metal did not disappear. From these facts, it was concluded that a suitable welding force (pressure) existed and this welding pressure was in the range of 10 MPa to 14 MPa for the original area of intermediate metal.

A welding time of 10 min or more at 1473 K and 40 min or more at 1373 K were required to obtain a good weld at the aforementioned welding pressure. Four-point bending test at a room temperature revealed that welds produced at the above welding conditions had a bending strength of 200 MPa or more at the tension side of the bending specimen.

Further experiments are necessary for the analysis of wetting phenomenon between aluminum melt and base metal surface and for the confirmation of tensile strength of the joint at an elevated temperature.

153 Low Energy Joining with Controlled Surface Composition and Misorientation Angle

April 1990 to March 1993

O. Ohashi, Advanced Materials Processing Division

Keywords: joining, surface composition, hydrogen permeability

As a part of a National Project in Japan which focuses on "Materials Interconnection" there is an interest in fundamental research designed to create new functional materials by controlling the surface composition, structure and shape of joining surfaces. Research work undertaken at NRIM aims to develop low energy joining techniques based on the control of surface composition and misorientation angle between two contacting surfaces. Furthermore, work is being carried out to develop materials for a special function, i.e., hydrogen purification and silicon devices for semi-conductor applications. The characteristics of the prepared surfaces are examined using an ultra high vacuum equipment developed for diffusion welding with facilities that enable surface control and analysis. In addition, surface modification techniques by vapor deposition have been examined to improve the hydrogen permeability of some developed membranes.

We have obtained the following results:

1. when bonding single silicon crystal, with a misorientation angle of less than 2 degrees high joint strengths were achieved with adsorbed OH^- on the joint surfaces and when bonds were made in air in contrast to those made in vacuum;
2. argon ion bombardment had the effect of cleaning bonding surfaces, but also increased the surface roughness as the accelerating voltage was increased. For example, copper bonds could be made at 300 °C after ion bombardment using an accelerating voltage of 2 ~ 3 kV. However, with an accelerating voltage of 4 kV or greater copper failed to bond;
3. yttrium-deposition was demonstrated to be effective in modifying the interface between palladium-overlayer and vanadium-based alloys (V-15Ni-0.05Ti). The hydrogen permeability of this membrane was found to increase markedly with yttrium-deposition. Auger analysis revealed that yttrium reduced the vanadium oxide on the alloy surface by forming yttrium oxide.

Related Papers

Model Calculation of Electronic Property near Transition Metal Interfaces, S. Suga and O. Ohashi, Physica Scripta 45 (1992): 458–62.

Effects of Metallic Atoms on Insulator Surfaces, S. Suga and O. Ohashi, Physica Status Solidi 169 (1992): k13–15.

Effect of Twist Angle on Tensile Strength of Diffusion-Welded Joints in Molybdenum Single Crystal, O. Ohashi and S. Suga, Q. J. Jpn. Weld. Soc. 10 (1992): 53–58 (in Japanese).

Effect of Surface Composition on Diffusion Welding in Stainless Steel, O. Ohashi and S. Suga, J. Jpn. Inst. Metals 56 (1992): 579–85 (in Japanese).

Effects of Deoxidizer Addition on the Hydrogen Permeation Characteristics of V-Ni Alloy Membranes, M. Komaki, C. Nishimura and M. Amano, J. Jpn. Inst. Metals 56 (1992): 729–33 (in Japanese).

154 Effects of Temperature Distribution on Capillary Gap Penetration

April 1991 to March 1993

K. Sasabe, Advanced Materials Processing Division

Keywords: brazing, micro gravitation, temperature distribution, capillary flow, simulation

Brazing is one of the most suitable joining method for metals in space because of a vacuum and a micro gravity of the space environment. The driving force of capillary flow is the capillary pressure ΔP which is written as a function of the radius of meniscus d and the surface tension of liquid γ as $\Delta P = 2\gamma/d$. ΔP changes depending on temperature because surface tension depends on temperature.

We studied on temperature distribution dependencies of capillary flow in order to understand fundamental behavior of brazing under the micro gravity.

The method to presume the temperature distributions of joint during brazing was investigated by the finite-difference calculus for the two dimensional cross section of the joint. Moreover, the precise observations of capillary flow under various temperature distributions were carried out by a model experiment using acrylic plates and paraffin. We found that the initial condition of penetration of liquid into the capillary gap dominated the subsequent penetration behavior totally and was very sensitive to the temperature distribution.

Composite process

155 Study on the Melting Effects of Spray Particles on Properties of Deposited Coatings

April 1993 to March 1996

S. Kitahara, Advanced Materials Processing Division

Keywords: plasma spraying, spray particle, melting effect, coating property

In the process of deposition of coatings formed by applying the thermal spraying, the melting degree of spray particles is one of the most important factors to get a high quality coating with a good property in heat, wear or corrosion resistance. The coating is necessary to be produced by deposition of spray particles which are in the proper melting state corresponding to the physical, chemical and metallurgical properties of spray powders.

In this experiment, we are making clear the relationship between melting degree of spray particles and properties of deposited coatings. Ni, Ni-base alloy and ceramics (Al_2O_3, TiC etc.) powders are spray materials. The plasma spraying is used to form a coating.

The degree of melting of spray particles is controlled by changing the particle size and the spray parameters, i.e., plasma operating current, gas flow rate and spray distance. The coatings are produced by deposition of the controlled melting particles, and the formed coatings are examined the properties of coating structure, adhesiveness, denseness and so on.

Through the results of the experiments, we investigate the effects of melting degree of spray particles on properties of deposited coatings, and accumulate the basic informations to form high quality coatings in plasma spraying.

Related Paper

Formation of Gradient Coatings by a Plasma Spraying Process, S. Kitahara, T. Fukushima and S. Kuroda, Report of the 123rd Committee on Heat-Resisting Metals and Alloys, Jpn. Soc. for the Promotion of Sci. 32 (1991): 89–96.

156 Forced Infiltration Process for Making Composite Structures

April 1992 to March 1995

T. Dendo, Advanced Materials Processing Division

Keywords: infiltration, semi-molten state, intermetallic compound

Forced infiltration technique is applied to two different processing purposes in this theme.

The first is to make a composite layer structure in surface portion of a porous ceramic compact by infiltration under semi-molten state. The infiltrating metals employed are Pb-Sn alloys which have wide range of semi-molten state in which liquid and solid co-exist. The porous compacts used are made of alumina powder having mean particle size of 1 μm, and their porosities are controlled in the range of 75 to 95% in relative density by choosing sintering condition. Feature and feasibility of this new process are explored by

examining the effects of process parameters such as volume fraction of liquid, porosity of ceramic compact, infiltration pressure and so on.

The other is to synthesize intermetallic compounds by infiltration into a porous metallic preform. At present, some attempts are being made for synthesizing Ti-Al compounds through solid-liquid reaction during infiltrating process. From some preliminary experiments, it is confirmed that three kinds of compounds i.e. Ti_3Al, TiAl and $TiAl_3$, are synthesized in this process and each fraction of them strongly depends on the thermal conditions such as pre-heating temperature and pouring temperature.

Related Paper

Synthesis of Ti-Al Intermetallic Compounds by Reaction during Pressure Infiltration, T. Shirota, T. Hashimoto, M. Nakamura, H. Doi, T. Kimura and T. Dendo, Proc. 43rd Join. Conf. Tech. Plast. (1992): 483–86 (in Japanese).

157 Coating Formation by Molten and Electrified Powders

April 1991 to March 1995

S. Kuroda, Advanced Materials Processing Division

Keywords: plasma spray, surface coating, deposition phenomena, interface, semi-transferred arc

This research aims to clarify the deposition phenomena of molten particles onto solid surface with a special interest in spray deposition of coatings in mind. The collision of a high velocity molten particle onto a solid surface and the subsequent solidification are very fast and complicated phenomena, on which various coating processes such as plasma spraying are based. With the aid of a technique developed to measure the velocity and temperature of flying particles, morphology of quenched splats as well as the pore structure of the deposited coatings have been related to those parameters.

The mechanical property as well as the microstructure of thus formed coating/substrate interface are examined by using various mechanical testing methods and microscopic techniques. Low pressure plasma spraying of NiCrAlY and 8%Y_2O_3-ZrO_2 have been investigated for the purpose of densification and improvement of adhesion of sprayed coatings. Application of a semi-transferred arc during spraying under low pressure shows a promise to these ends. In addition, feasibility of employing electrostatic force to control the motion of fine powders are examined.

Related Papers

The Quenching Stress in Thermally Sprayed Coatings, S. Kuroda and T. W. Clyne, Thin Solid Films 200 (1991): 49–66.

Gradient Coatings Formed by Plasma Twin Torches and Those Properties, T. Fukushima, S. Kuroda and S. Kitahara, Proc. 1st Int. Symp. FGM (1990): 145–50.

Measurement of Temperature and Velocity of Thermally Sprayed Particles Using Thermal Radiation, S. Kuroda, H. Fujimori, T. Fukushima and S. Kitahara, Trans. Jpn. Welding. Soc. 22 (1991): 82–89.

Significance of the Quenching Stress in the Cohesion and Adhesion of Thermally Sprayed Coatings, S. Kuroda, T. Fukushima and S. Kitahara, J. Thermal Spray Technol. 1 (1993): 325–32.

Process with aid of beam technology

158 Diagnostics of Laser Photoionization Induced Plasma

April 1992 to March 1995

Y. Ogawa, Chemical Processing Division

Keywords: laser photoionization, laser induced plasma, drift velocity, ion and electron temperatures, plasma density

Resonance stepwise photoionization method has acquired a wide variety of applications. Novel applications of laser photoionization include its emergence as a feasible method for the processing of high-purity materials and the separation of commercially valuable isotopes, when using as the detection of trace elements, and ion sources for ion implantation, etc. Furthermore, the extraordinary sensitivity and versatility of resonance photoionization spectroscopy have already applied to the identification of high-lying atomic levels, the measurement of transition cross sections, and the studies of chemical reaction, etc.

These applications are mainly based on laser stepwise excitation of atoms and on extraction of ions from weakly ionized plasma produced by the photoionization. The method of laser stepwise resonant photoionization of atoms was suggested more than ten years ago and the basic features and characteristics of this method have been fundamentally realized. However, little is known about the microscopic and macroscopic properties of the laser induced plasma (such as drift velocity, ion and electron temperatures, plasma density and so on) or about the extraction behavior of ions under the applied electric field. We have planned this research work to establish the diagnostic techniques for the weakly ionized plasma, which will fully contribute to the understanding of ion extraction behavior.

Related Paper

Laser Material Purification of Neodymium, Y. Ogawa et. al., J. Jpn. Inst. Met. 55 (1991): 545–52.

159 Study on Evaporation Process by High Energy Density Beams

April 1992 to March 1995

H. Irie, Advanced Materials Processing Division

Keywords: electron beam, laser, evaporation, plasma temperature

The electron beam evaporation process has been widely used in coating industry, but it has been used at very low evaporation rate because of large production rate of sputter. These coating process has been done on the base of experiences because of shortage of knowledge of evaporation mechanism. On the other hand, laser has been considered as a good heat source to produce material vapors in controlled environment. But laser itself is the same kind of heat source as the electron beam and it will face the same problem as the electron beam does.

The laser, especially CO_2 laser of infrared wave length, has a unique property of heating a plasma by the inverse Bremstrahlung effect with free electron.

The objective of this research is to make clear what happens in evaporation and diffusion of evaporated materials processes by the electron beam and the laser heating. In order to obtain information on these procedures, the light spectroscopic observation and other plasma observation methods are very useful. In this year, the light spectroscopic method was tried to apply to the laser melting process. In a laser melting process of pure iron with a high power CO_2 laser and Ar shielding gas, the plasma state very rapidly changed with time and it was very difficult to scan with respect to wave length. The observation of time average of a specific line showed that the plasma temperature increased with the laser power and the evaporated material mainly distributed at the circumference of plasma. Then for direct superheating of the plasma of evaporated material by the laser, the gas flow has to be arranged. In order to investigate laser evaporation process and also laser heating process of evaporated plasma, a chamber of controllable atmosphere was experimentally produced.

160 Study on Synthesis of Special Compounds by a Combined Use of Ion Implantation and Deposition

April 1991 to March 1994

K. Saito, Surface and Interface Division

Keywords: ion implantation, deposition, BiSrCaCuO, $Fe_{16}N_2$, TiAl

A combined use of ion implantation and sputter deposition is a promising technique for synthesizing novel materials with specific atomic and electronic structures in highly controlled manner. We synthesized high-quality superconducting BiSrCaCuO thin films of thicknesses below several tens nanometers. Since the maximum T_c of 108 K was obtained at a thickness of 300 Å, T_c of 78 K and 76 K were achieved at thicknesses of 150 Å and 75 Å, respectively. Furthermore, we are synthesizing a specific magnetic films of $Fe_{16}N_2$ with giant magnetization. Nitrogen implantation at a temperature as low as 10 K followed by annealing at a relatively low temperature of 423 K was found to be efficient in view of the thermodynamic driving force for its metastable phase formation.

On the other hand, the atomic structure of intermetallic compound TiAl implanted with nitrogen ions has been studied by high-resolution electron microscopy to investigate the atomic mechanism for modifying the brittle nature of the matrix and/or the grain boundaries.

Related Papers

Fabrication of 300 Å thick BiSrCaCuO thin films with T_c of 108 K by Use of Ion Implantation, K. Saito and M. Kaise, Jpn. J. Appl. Phys. 31 (1992): L1047.

Fabrication of 30 nm Thick Superconducting BiSrCaCuO Thin Films by Single-Target Magnetron Sputtering Method, M. Kaise and K. Saito, J. Japan. Inst. Metals, 57 (1993): 103 (in Japanese).

Surface of Modification of Intermetallic Compound TiAl by Nitrogen Ion Implantation, T. Matsushima and K. Saito, J. Japan Inst. Metals 57 (1993): 325 (in Japanese).

161 Study on Molten Metal Behavior in Surface Modification Process with High Temperature Heat Sources

April 1992 to March 1993

H. Irie, Advanced Materials Processing Division

Keywords: electron beam, laser, arc, surface modification, sulfur content

In surface modification using high temperature heat sources such as laser, electron beam and arc plasma, where materials are heated above 3000 K, the surface roughness of fused zone is an important factor in practice. Among various factors, the influence of sulfur content and power distribution of heat sources on the surface roughness has been investigated. Grey and nodular cast irons of several grades of sulfur content for practical use in Australia were melted by laser in Japan and arc plasma in Australia last year. The results showed that in specimen of 0.012 mass% sulfur the fusion zone was flat and smooth, but in one of 0.022 mass% it heaped up at low melting speed and humped at high speed. In these practical specimens, many other elements are contained. In order to investigate the influence of sulfur content much more clearly, 7 kinds of cast iron, in which only

sulfur content varies from less than 0.001 to 0.1 mass% were examined in this year.

When the sulfur content is less than 0.002 mass%, all of the specimens showed very smooth and flat fusion surface at any melting speed. On the contrary, in the case of more than 0.007 mass% sulfur content, the fusion zone heaped up, but did not humped even at higher melting speed. The shape of fusion zone in cross section in the former specimens, showed wine cup shape and changed to well type at more than 0.05 mass% through a triangular type in the intermediate sulfur region. At a high melting speed, the shape was of a bowl type at any speed.

These results were quite different from that for arc melting, where the fusion zone of high sulfur content humped at higher melting speed.

The considerable differences in fusion zone, between laser and arc melting, between in practical and experimental specimens, and among sulfur content could not be clear. Not only the dependence of surface tension on sulfur content, but also other factors such as heat distribution and other alloying elements may contribute to the change of molten metal behavior.

This research was carried out to back up a collaboration program of bilateral science and technology agreement between Australia and Japan involving mutual exchange of scientists of each country.

Processing in special environment

⑯② Development of New Material Phases in the Extremely High Vacuum

April 1993 to March 1995

K. Yoshihara, 4th Research Group

Keywords: extremely high vacuum, boron nitride, SET, thin film

The objective of this research is to establish the basic concepts for controlling the surface energy of metals, and to find new phases on solid surfaces. To carry out this research, we have to treat specimens in an extremely high vacuum system to avoid any contaminations on solid surfaces. This research is composed of the following three projects.

1. The development of the extremely high vacuum system; We have already found that BN precipitated on the surface of the stainless steel doped with B and N, and the precipitated BN is inert to the adsorption of gases. The main residual gas component in an extremely high vacuum is H_2. Therefore, we are now investigating the H_2 permeation rate through BN thin films. The precipitated BN is also expected to be a lubricant material in a vacuum. The atomic force on the precipitated BN is also measured.
2. The development of new surface analysis technique; The objective of the project is to establish the technology to create the very thin films on the solid materials and also to develop the new technique called "Surface Electron Spectroscopic Tomography: (SET)." SET is the technique to make the surface atomic structure visible by analyzing the whole angle of energy spectrum of the electrons exited in the films. The electron exited in the bulk will loose the characteristic energy at the surface region. Therefore it will be possible to make the surface atomic structure visible when the tomographic technique is combined with electron spectroscopy.
3. The segregation behavior of metal thin films; The substrate materials rapidly diffuses through the deposited thin films when it is heated in a vacuum. This segregation behavior of substrate materials is controlled by the surface free energy of thin metal films. The basic rule to control this rapid diffusion phenomena are investigated.

163 Development of Quantum Microstructure in Ultra Clean Vacuum

April 1990 to March 1995

K. Yoshihara, 4th Research Group

Keywords: quantum microstructure, ultra clean vacuum

It is expected that materials with quantum microstructures will possess new and useful properties. However, to create these materials, it is necessary to handle the materials in extremely clean and high vacuum environment. Otherwise, impurities from the environment will deteriorate the material properties. This project is divided into two phases. In the first phase (Apr. 1990–Mar. 1993), we will introduce the sample transfer system by a magnetic levitation system. By using this system, we will transfer specimens from one station to the other station without any exposure to contaminating environment. In the second phase (Apr. 1993–March. 1995), we will create materials with quantum microstructures by using this ultra clean vacuum system.

Since April 1990, we have constructed the extremely high vacuum system. The main chamber has achieved vacuum pressure of 10^{-10} Pa by using new vacuum pumps and special gate valves. In 1991, we developed two types of magnetic levitation transport system in the extremely high vacuum system. One is a linear motor system composed of four stators and a carrier. The carrier is transferred over stators with three samples. The other system uses couples of the magnets made of

super conductive material and permanent magnets. We manufactured a large cryostat in which super conductive magnets moved at a temperature lower than 100 K. These magnetic levitation transport system installed in the main chamber can transfer specimens in the vacuum of less than 10^{-8} Pa. These transport system have lower out gassing rate than that of the traditional transport systems using a 'feedthrough' manipulator or an all-metal magnet coupling.

Publications

❒ Papers Published in 1992

Characterization/Properties

Electronic and nuclear properties

1. *AC Susceptibility and Magnetization of Nb-Tube Processed Nb_3Al Composite Wires*, K. Itoh, M. Yuyama, T. Kuroda and H. Wada, Advances in Cryogenic Eng. Mater. 38 (1992): 805–12.
2. *Unusual Vortex States in High-T_c Superconductors—What Determines J_c-Value?*, K. Kadowaki, Advances in Superconductivity IV (1992): 395–400.
3. *Mixed Valence State of Cerium in Bis(phthalocyaninato)cerium Complex*, H. Isago and M. Shimoda, Chemistry Letters (1992): 147–50.
4. *Development of High Resolution Magnet System and Applications*, H. Aoki, S. Uji and T. Shimizu, Cryogenic Eng. 27 (1992): 21–29 (in Japanese).
5. *Voltex Dynamics and Unusual Vortex State of High T_c Superconductors*, K. Kadowaki, Electronic Properties and Mechanisms of High T_c Superconductors (1992): 209–20.
6. *A Model for the Dissipation Mechanism in the Highly Anisotropic Layered Superconductors*, K. Kadowaki, Electronic Properties and Mechanisms of High T_c Superconductors (1992): 373–77.
7. *Macroscopic Quantum Tunneling Effects of Bloch Walls in Small Ferromagnetic Particles*, *C. Paulsen, †L.C. Sampaio, †B. Barbara, D. Fruchart (Laboratoire de Cristallographie), †A. Marchand (†Laboratoire Louis Néel), *J.L. Tholence (*Laboratoire de Recherches sur les Très Basse Températures) and M. Uehara, Euro-Phys. Letters 19 (1992): 643–45.
8. *Silver Sheathed Superconducting Tapes Made from the Bi-System Oxide Powders Mixed with Metal Ag or Cu Powders*, T. Asano, Y. Tanaka, M. Fukutomi, M. Komori, K. Inoue, H. Maeda, *M. Yoshikawa and *M. Naitoh (*Hosokawa Micron Co.), IEEE Trans. Mag. 28 (1992): 884–87.
9. *Heavy Cyclotron Mass in Ferromagnetic Substance UGe_2*, *K. Satoh, *S.W. Yun, *I. Ukoh, *I. Umehara, *Y. Onuki (*Univ. of Tsukuba), H. Aoki, S. Uji, T. Shimizu, †M. Hunt, †P. Meeson, †P.A. Probst and †M. Springford (†Bristol Univ.), J. Mag. Mag. Mater. 104–07 (1992): 39–40.
10. *Pressure Effects on the Yb Valence State in $YbIn_{1-x}Ag_xCu_4$ (x = 0–0.2)*, T. Matsumoto, T. Shimizu, Y. Yamada and K. Yoshimura (Kyoto Univ.), J. Mag. Mag. Mater. 104–07 (1992): 647–48.
11. *MBE Growth of $CeSi_2$ Thin Films and Their Electrical Transport Properties*, H. Aoki, M. Yata, Y. Isoda and S. Uji, J. Mag. Mag. Mater. 104–07 (1992): 1905–06.
12. *Mesoscopic Quantum Tunneling in Small Ferromagnetic Particles*, *C. Paulsen, †L.C. Sampaio, †R.T. Tachoueres, †B. Barbara, D. Fruchart (Laboratoire de Cristallographie), †A. Marchand (†Laboratoire Louis Néel), *J.L. Tholence (*Laboratoire de Recherches sur les Très Basse Températures) and M. Uehara, J. Mag. Mag. Mater. 116 (1992): 67–69.
13. *Fermi Surfaces and Transport Properties of $YBa_2Cu_4O_8$*, T. Oguchi and T. Sasaki, J. Phys. Chem. Solids B 53 (1992): 1525–32.
14. *Indentification and Vibrational Properties of the Mixed Oxide (1–X) V_2O_5 + $XMoO_3$ ($X \leq 0.3$)*, T. Hirata and H.Y. Zhu (Zhejiang Univ.), J. Phys. Condens. Mater. 4 (1992): 7377–88.
15. *de Haas-van Alphen Effect in VGe_2*, *K. Satoh, *S.W. Yun, *I. Umehara, *Y. Onuki (*Univ. of Tsukuba), S. Uji, T. Shimizu and H. Aoki, J. Phys. Soc. Jpn. 61 (1992): 1827–28.
16. *Observation of Heavy Electrons in $CeRu_2Si_2$ via the dHvA Effect*, H. Aoki, S. Uji, *A.A. Keiko and *Y. Onuki (*Univ. of Tsukuba), J. Phys. Soc. Jpn. 61 (1992): 3457–61.
17. *Crystal Structures of the Two Dimensional Antiferromagnets RFe_2O_4 (R = Y, Er) and Their Magnetic Properties under Pressure*, T. Matsumoto, N. Mohri (Univ. of Tokyo), *J. Iida, *M. Tanaka (*Ochanomizu Univ.), K. Shiratori (Osaka Univ.), F. Izumi (NIRIM) and H. Asano (Univ. of Tsukuba), Physica B 180–81 (1992): 603–05.
18. *Observation of Anisotropic Pinning Effect in $Bi_2Sr_2CaCu_2O_{8+\delta}$ Single Crystals*, *S. Kawamata, *N. Itoh, *K. Okuda (*Univ. of Osaka Pref.), T. Mochiku and K. Kadowaki, Physica C 195 (1992): 103–08.
19. *Anomalous Magnetization Behavior of Single Crystalline $Bi_2Sr_2CaCu_2O_{8+\delta}$*, K. Kadowaki and T. Mochiku, Physica C 195 (1992): 127–34.

20. *dHvA Effect of Nb in Low Fields Down to H_{c2}*, H. Aoki, S. Uji, T. Shimizu and Y. Onuki (Univ. of Tsukuba), Physica C 198 (1992): 323–27.

21. *Effects of Ce Substitution and Reduction on Conduction in $Nd_{2-x}Ce_xCuO_4$ Single Crystals*, S. Uji and H. Aoki, Physica C 199 (1992): 231–39.

22. *Alternating Change of Allowed and Forbidden Optical Transitions in $(Si)_{2m}/(Ge)_{10-2m}$ Superlattices with (001) Stacking*, *M. Ikeda, *K. Terakura (*Univ. of Tokyo) and T. Oguchi, Phys. Rev. B 45 (1992): 1496–99.

23. *Novel Interplay of Fermi Surface Behavior and Magnetism in a Low Dimensional Conductor*, *J.S. Brooks, †C.C. Agosta, S. J. Klepper (MIT), ‡M. Tokumoto, ‡N. Kinoshita, ‡H. Anzai (‡ETL), S. Uji, H. Aoki, *A.S. Perel, *G.J. Athas (*Boston Univ.) and †P.H. Howe (†Clark Univ.), Phys. Rev. Letter 69 (1992): 156–59.

24. *Model Calculation of Electronic Properties Near Transition Metal Interfaces*, S. Suga (Osaka Univ.) and O. Ohashi, Phys. Scr. 45 (1992): 458–62.

25. *Effects of Adsorbed Metallic Atoms on Insulator Surface*, S. Suga (Osaka Univ.) and O. Ohashi, Phys. Status Solidi 169 (1992): K13–15.

26. *Observation of Quantum Tunneling of the Magnetization Vector in Small Particles without Domain Walls*, *B. Barbara, †C. Paulsen, *L.C. Sampaio, M. Uehara, D. Fruchart (Laboratoire de Cristallographie), †J.L. Tholence (†Laboratoire de Recherches sur les Très Basse Températures), *A. Marchand (*Laboratoire Louis Néel), J. Tejada (Univ. of Barcelona) and S. Linderoth (Univ. of Denmark), Proc. of Int. Workshop on Studies of Magnetic Properties of Fine Particles and Their Relevance to Materials Science (1992): 235–43.

27. *Anisotropic Superconducting Properties of Single Crystalline $Bi_2Sr_2CaCu_2O_{8+\delta}$*, K. Kadowaki, K. Togano, H. Maeda and J.J.M. Franse (Univ. of Amsterdam), Proc. of ISSP, PCOS (1992): 541–45.

28. *High Pressure Specific Heat Investigation of the Magnetic Transition in CeP*, A. Matsushita, *Y. Okayama, S. Takayanagi (Hokkaido–Kyouiku Univ.), *N. Mohri (*Univ. of Tokyo), T. Matsumoto, †Y.S. Kwon, †Y. Haga and †T. Suzuki (†Tohoku Univ.), Solid State Commun. 84 (1992): 761–63.

Atomistic arrangement

29. *High-Resolution Electron Microscopy Observation of Defects in 180 Mev Cu^{11+} Ion-Irradiated $Bi_2Sr_2CaCu_2O_8$ Crystals*, B. Chenevier (École Nationale Supérieure de Physique de Grenoble), S. Ikeda, H. Kumakura, K. Togano, *S. Okayasu and *Y. Kazumata (*JAERI), Jpn. J. Appl. Phys. 31 (1992): L777–79.

30. *Low-Temperature Annealing Effect on Superconducting and Structural Properties of Ion-Irradiated $Bi_2Sr_2CaCu_2O_x$ Crystals*, B. Chenevier (École Nationale Supérieure de Physique de Grenoble), H. Kumakura, S. Ikeda, K. Togano, *S. Okayasu and *Y. Kazumata (*JAERI), Jpn. J. Appl. Phys. 31 (1992): L1671–74.

31. *Infrared Spectra of Platinum-Impregnated V_2O_5 Powders on Hydrogen Insertion*, T. Hirata and K. Yagisawa, J. Alloys and Compounds 185 (1992): 177–82.

32. *Phase Separation in 12 mol% Cerium-Doped Zirconia Induced by Heat Treatment in H_2 and Ar*, H.Y. Zhu (Zhejiang Univ.), T. Hirata and Y. Muramatsu, J. Am. Ceram. Soc. 75 (1992): 2843–48.

33. *Temperature Rise of a Superconducting Oxide $Bi_2Sr_2CaCu_2O_8$ Sample during Argon Ion Milling*, B. Chenevier (École Nationale Supérieure de Physique de Grenoble) and S. Ikeda, J. Electron Microsc. 41 (1992): 196–98.

34. *Structure Images of Y_2O_3 Corresponding to the Shift of Y-Atoms*, S. Ikeda and K. Ogawa, J. Electron Microsc. 41 (1992): 330–36.

35. *Site Substitution of Additive Elements in TiAl Intermetallic Compound*, H. Doi, K. Hashimoto, K. Kasahara and T. Tsujimoto, J. Jpn. Inst. Met. 56 (1992): 232–37 (in Japanese).

36. *Growth Rate of Dislocation Loop in Fe-Ni-Cr Alloy under Kr^+ Ion and Electron Irradiation*, T. Kimoto, *C.W. Allen and *L.E. Rehn (*Argonne Natl. Lab.), J. Nucl. Mater. 191–94 (1992): 1194–97.

37. *Crystal Structure of $Pb_2Sr_2MCu_3O_{8+\delta}$ System (M = Nd, Sm, Eu, Gd, Dy, $Y_{1-x}Ca_x$, Ho and Er)*, T. Mochiku and K. Kadowaki, J. Phys. Soc. Jpn. 61 (1992): 881–90.

38. *Magnetic Properties of the Two Dimensional Antiferromagnets RFe_2O_4 (R = Y, Er) at High Pressure*, T. Matsumoto, N. Mohri (Univ. of Tokyo), *J. Iida, *M. Tanaka (*Ochanomizu Univ.) and K. Shiratori (Osaka Univ.), J. Phys. Soc. Jpn. 61 (1992): 2916–20.

39. *Structural Evidence for the Amorphization of Mechanically Alloyed Cu-Ta Powders Studied by Neutron Diffraction and EXAFS*, *C.T. Lee, *M. Mori, *T. Fukunaga, K. Sakurai and *U. Mizutani (*Nagoya Univ.), Materials Science Forum 88–90 (1992): 399–406.

40. *X-Ray Photoelectron Diffraction Studies of $Bi_2Sr_2CaCu_2O_{8+x}$*, M. Shimoda, *T. Greber, *J.

Osterwalder and *L. Schlapbach (*Université de Fribourg), Physica C 196 (1992): 236–40.

41. *Extended X-Ray-Absorption Fine-Structure Studies on Ball-Milled Powders of the Immiscible System Cu-V,* K. Sakurai, *M. Mori and *U. Mizutani (*Nagoya Univ.), Phys. Rev. B 46 (1992): 5711–14.

42. *A Fast and Accurate Infrared Pyrometer Combining Two-Wavelength Comparison with Single Waveband Detection,* N. Kishimoto and H. Amekura, Sensor Technology 12 (1992): 18–25 (in Japanese).

Phase transformation and microstructures

43. *Effect of Water Vapor on the Tetragonal to Monoclinic Transformation of Tetragonal Zirconia Powders Examined by Gas Desorption Measurement,* Y. Sakka, J. Mater. Sci. Letters 11 (1992): 18–21.

44. *Origin of Abnormally Large Tetragonality of Martensite in High Carbon Iron Alloys Containing Aluminum,* S. Uehara, S. Kajiwara and T. Kikuchi, Mater. Trans., JIM 33 (1992): 220–28.

45. *Autogenous Electron Beam Welds across Dissimilar Stainless Steels: Solidification Sequences,* S. Tsukamoto, H.K.D.H. Bhadeshia (Univ. of Cambridge) and H. Harada, Proc. of 3rd Int. Conf. on Trends in Welding Research (1992): 181–86.

46. *Microstructure of Dispersion Alloys Solidified in μG,* Y. Muramatsu, K. Harada, T. Dan, S. Yoda (NASDA) and S. Anzawa (IHI) Proc. of 18th Int. Sympo. on Space Technology and Science 18 (1992): 2255–58.

47. *Tempering of Martensite under the Influence of an Externally Applied Stress,* A. Matsuzaki (JRDC), H.K.D.H. Bhadeshia (Univ. of Cambridge) and H. Harada, Proc. of G.R. Speich Sympo. (1992): 47–52.

48. *On Experimental Aspects of the Orientation Relationship in the Primary Recrystallization of Metals,* E. Furubayashi, Scr. Metall. Mater. 27 (1992): 1493–96.

Surface and interface properties

49. *Growth of GaAs Epitaxial Microcrystals on a S-Terminated GaAs Substrate,* K. Ishige and N. Koguchi, 11th Record of Alloy Semiconductor Physics and Electronics Sympo. (1992): 245–50.

50. *A Structure Observation of GaAs Microcrystals Grown on a Se-Terminated GaAlAs Surface by Droplet Epitaxy,* T. Chikyow and N. Koguchi, 11th Record of Alloy Semiconductor Physics and Electronics Sympo. (1992): 251–58.

51. *A Microcrystal Growth on a Se-Terminated GaAlAs Surface for the Quantum Well Box Structure by Sequential Supply of Ga and As Molecular Beams,* T. Chikyow and N. Koguchi, Appl. Phys. Letters 61 (1992): 2431–33.

52. *A Selective Growth of GaAs Microcrystals on a Se-Terminated GaAlAs Surface from Ga Droplets for the Quantum Well Box Structure,* T. Chikyow and N. Koguchi, Extended Abstracts of Int. Conf. on Solid State Device and Materials (1992): 582–84.

53. *Oxidation and Degradation of Titanium Nitride Ultrafine Powders Exposed to Air,* Y. Sakka, S. Ohno and M. Uda (Nisshin Steel Co., Ltd.), J. Am. Ceram. Soc. 75 (1992): 244–48.

54. *Effect of the Film Structures on the Rapid Diffusion Behavior in Nb Film/Ti Substrate and Ti Film/Nb Substrate,* M. Yoshitake and K. Yoshihara, J. Jpn, Inst. Met. 56 (1992): 89–95 (in Japanese).

55. *Effect of Molybdenum Content on the Corrosion of 9Cr Ferritic Steels in a Flowing Sodium Environment,* I. Mutoh and T. Suzuki, J. Jpn. Inst. Met. 56 (1992): 794–801 (in Japanese).

56. *Characterization of Bi-Pb-Sr-Ca-Cu-O Oxide Powders Synthesized by the Oxalate Coprecipitation Route,* Y. Sakka and M. Ohtaguchi, J. Mater. Sci. Letters 11 (1992): 749–53.

57. *In-Situ Observation of Metal Surfaces in Aqueous Solutions with an Electrochemical STM,* N. Nagashima, H. Masuda and S. Matsuoka, JSME Int. J. 35 (1992): 442–48.

58. *STM Images of Surface Films Produced at Elevated Temperatures,* S. Matsuoka, H. Masuda, Y. Ikeda, *K. Akaie and *Y. Ochi (*Univ. of Electro-Communications), JSME Int. J. 35 (1992): 456–61.

59. *Rapid Diffusion in Thin Films,* K. Yoshihara and M. Yoshitake, Netsushori 32 (1992): 267–71 (in Japanese).

60. *A Common Data Processing System for Surface Analysis,* K. Yoshihara, Oyo Butsuri 61 (1992): 1246–50 (in Japanese).

61. *Linearity in Electron Counting and Detection Systems,* M.P. Seah (Natl. Phys. Lab.) and M. Tosa, Surface and Interface Analysis 18 (1992): 240–46.

62. *Surface Segregation of Substrate Element on Metal Films in Film/Substrate Combinations with Nb, Ti and Cu,* M. Yoshitake and K. Yoshihara, Surface and Interface Analysis 18 (1992): 509–13.

63. *A Common Data Processing System for Surface Analysis,* K. Yoshihara, M. Yoshitake and the VAMAS-SCA Community, Surface and Interface Analysis 18 (1992): 724–28.

64. *Surface Structure Dependence of GaAs Microcrystal Size Grown by As-Incorporation to Ga Droplets*, T. Chikyow, S. Takahashi and N. Koguchi, Surf. Sci. 267 (1992): 241–44.

65. *Effect of Non-Metallic Inclusions on Rotating Bending Fatigue Properties of Spring Steels*, K. Kanazawa and T. Abe, Trans. J. Soc. Spring Research 37 (1992): 15–23 (in Japanese).

66. *Prediction of Burn-off of a C/C-Composite in Air and in O_2/N_2 Gas Mixtures*, A. Miyazaki, I. Tomizuka, S. Nakazawa and Y. Koizumi, Zairyo-to-Kankyo 41 (1992): 83–88 (in Japanese).

67. *Effects of Variations of Temperature and Stress on Stress Corrosion Cracking of STPT42 Carbon Steel in High Temperature Water*, S. Ohashi and T. Ishihara, Zairyo-to-Kankyo 41 (1992): 224–30 (in Japanese).

68. *High Temperature Oxidation of a Series of Nickel-Base Superalloys on a Single Tye-Line and its Extension*, S. Nakazawa, I. Tomizuka, Y. Koizumi and A. Miyazaki, Zairyo-to-Kankyo 41 (1992): 379–84 (in Japanese).

69. *Specific Surface Area and Pore Size Distribution of Rusted Steel after Chemical Conversion in a $0.1_M Na_2MoO_4$-H_3PO_4 Aqueous Solution*, K. Kurosawa and T. Fukushima (Univ. of Ryukyus), Zairyo-to-Kankyo 41 (1992): 393–98 (in Japanese).

70. *Evaluation of Biomedical Stainless Steels by Fretting Corrosion Test*, A. Hoshino, Zairyo-to-Kankyo 41 (1992): 399–405 (in Japanese).

71. *High Temperature Oxidation of C/C-Composites and Their Components from Viewpoint of Material Design*, A. Miyazaki, I. Tomizuka, S. Nakazawa and Y. Koizumi, Zairyo-to-Kankyo 41 (1992): 597–604 (in Japanese).

Mechanical properties

72. *Environmental Embrittlement in $L1_2$-Ordered (Co, Fe)$_3$V Alloys*, C. Nishimura and C.T. Liu (Oak Ridge Natl. Lab.), Acta Metall. Mater. 40 (1992): 723–31.

73. *The Effect of Grain Boundary Deformation on the Creep Micro-Deformation of Copper*, N. Shinya, R.A. Carolan (Birmingham Univ.), M. Egashira and S. Kishimoto, Acta Metall. Mater. 40 (1992): 1629–36.

74. *VAMAS Second Round-Robin Test of Structural Materials at Liquid Helium Temperature*, T. Ogata, K. Nagai, K. Ishikawa, K. Shibata (Univ. of Tokyo) and S. Murase (Toshiba Co.), Advances in Cryogenic Eng. Mater. 38 (1992): 69–76.

75. *Deformation Structures in High-Cycle Fatigue of 0.1N-32Mn-7Cr Steel at Cryogenic Temperatures*, O. Umezawa and K. Ishikawa, Advances in Cryogenic Eng. Mater. 38 (1992): 141–48.

76. *High-Cycle Fatigue Properties of Titanium Alloys at Cryogenic Temperatures*, O. Umezawa, K. Nagai, T. Yuri, T. Ogata and K. Ishikawa, Advances in Cryogenic Eng. Mater. 38 (1992): 175–82.

77. *Effect of Contact Pressure on Fretting Fatigue of High Strength Steel and Titanium Alloy*, K. Nakazawa, M. Sumita and N. Maruyama, ASTM, STP (1992): 115–25.

78. *Effect of Strain Rate on Tensile Behavior of Some Alloys at Liquid Helium Temperature*, K. Ishikawa, T. Ogata, T. Yuri, K. Nagai and O. Umezawa, Cryogenics 32 (1992); 67–70.

79. *Fatigue Properties of Cold-Rolled and Sensitized SUS347 Austenitic Stainless Steels at Cryogenic Temperatures*, T. Yuri, K. Ishikawa, K. Nagai, T. Ogata and O. Umezawa, Cryogenics 32 (1992): 89–92.

80. *Effect of Young's Modulus on Basic Crack Propagation Properties near the Fatigue Threshold*, A. Ohta, N. Suzuki and T. Mawari, Int. J. Fatigue 14 (1992): 224–26.

81. *Minor Role of Fractographic Features in Basic Fatigue Crack Propagation Properties*, N. Suzuki, T. Mawari and A. Ohta, Int. J. Fract. 54 (1992): 131–38.

82. *Creep Rupture Properties of a Ni-Base Heat-Resistant Alloy Hastelloy XR under Varying Stress Condition*, *H. Tsuji, T. Tanabe, Y. Nakasone and *H. Nakajima (*JAERI), JAERI-M 92-074 (1992): 1–19 (in Japanese).

83. *Low-Cycle Fatigue Properties of TiAl Intermetallic Compounds*, K. Yamaguchi, M. Shimodaira and S. Nishijima, J. Iron and Steel Inst. Jpn. 78 (1992): 134–40 (in Japanese).

84. *Effect of Stress Amplitude Transient on Fatigue Crack Initiation and Propagation of High Strength Steel in Synthetic Sea Water under Cathodic Protection*, N. Maruyama and M. Sumita, J. Iron and Steel Inst. Jpn. 78 (1992): 640–46 (in Japanese).

85. *Evaluation of Creep Deformation and Rupture Life of 1.3Mn-0.5Mo-0.5Ni Steel by Modified θ Projection Concept*, H. Kushima, T. Watanabe, K. Yagi and K. Maruyama (Tohoku Univ.), J. Iron and Steel Inst. Jpn. 78 (1992): 918–25 (in Japanese).

86. *Effect of Graphite Nodule Spacing and Temperature on Fracture Toughness in a Thick Walled Ferritic Spheroidal Graphite Cast Iron*, K. Nakano and T. Yasunaka, J. Iron and Steel Inst. Jpn. 78 (1992): 926–33 (in Japanese).

87. *Creep Fracture Modes at High Temperature in SUS321H*, H. Tanaka, M. Murata and N. Shinya, J. Iron and Steel Inst. Jpn. 78 (1992): 934–40 (in Japanese).

88. *Fatigue Damage in Ceramic Materials Caused by Repeated Indentation*, E. Takakura and S. Horibe, J. Mater. Sci. 27 (1992): 6151–58.

89. *High-Temperature Strength of Simple and Solute-Modified 10Cr-30Mn Austenitic Steels*, F. Abe, T. Noda, H. Araki and S. Nakazawa, J. Nucl. Mater. 191–94 (1992): 668–71.

90. *Tensile Properties of Neutron Irradiated 9Cr-WVTa Steels*, F. Abe, T. Noda, H. Araki, *M. Narui and *H. Kayano (*Tohoku Univ.) J. Nucl. Mater. 191–94 (1992): 845–49.

91. *System Design of Pilot Data-Free-Way (Distributed Database for Advanced Nuclear Materials)*, *H. Nakajima, *N. Yokoyama (*JAERI), †S. Nomura, †F. Ueno (†PNC), M. Fujita, Y. Kurihara and S. Iwata (Univ. of Tokyo), J. Nucl. Mater. 191–94 (1992): 1046–50.

92. *Applicability of Creep Damage Rules to a Nickel-Base Heat-Resistant Alloy Hastelloy XR*, *H. Tsuji, T. Tanabe, Y. Nakasone and *H. Nakajima (*JAERI), J. Nucl. Mater. 199 (1992): 43–49.

93. *Creep Crack Growth Behavior in Ni-Base Superalloys in 1,273 K Helium Gas Environment*, Y. Nakasone, K. Hiraga and T. Tanabe, J. Nucl. Sci. & Technol. 29 (1992): 422–26.

94. *Long-Term Creep Crack Growth Behavior of 316 Stainless Steel*, M. Tabuchi, K. Kubo and K. Yagi, J. Soc. Mater. Sci. Jpn. 41 (1992): 1255–60 (in Japanese).

95. *Effect of Flow Rate on Fatigue Crack Growth Behavior of A533B Steels in High Temperature Pressurized Water*, J. Soc. Mater. Sci. Jpn. 41 (1992): 1648–54 (in Japanese).

96. *Stress Rupture Factor for Butt Welded Joints of 304 Stainless Steel*, M. Yamazaki, T. Watanabe, H. Hongo, Y. Monma and C. Tanaka, J. Soc. Mater. Sci. Jpn. 41 (1992): 1779–85 (in Japanese).

97. *Inhibition of Surface Cracking during Creep by Shot Peening*, H. Tanaka, H. Kushima, M. Murata and N. Shinya, J. Soc. Shot Peening Technol. Jpn. 4 (1992): 50–55 (in Japanese).

98. *Results of an Intercomparison of Creep Crack Growth Tests Made in Japan*, T. Yokobori (Teikyo Univ.), C. Tanaka, K. Yagi, *M. Kitagawa, *A. Fuji (*IHI), T. Yokobori, Jr. (Tohoku Univ.) and M. Tabuchi, Materials at High Temperatures 10 (1992): 97–107.

99. *Effects of Test Environment and Grain Size on the Tensile Properties of $L1_2$-Ordered (Co, Fe)$_3$V Alloys*, C. Nishimura and C.T. Liu (Oak Ridge Natl. Lab.), Mater. Sci. Eng. A 152 (1992): 146–52.

100. *The Effect of Microstructural Evolution in Bainite, Martensite and δ-Ferrite on the Toughness of Cr-2W Steels*, F. Abe, H. Araki and T. Noda, Mater. Sci. Technol. 8 (1992): 767–73.

101. *The Microstructural Evolution and Creep Behavior of Bainitic, Martensitic and Martensite/Ferrite Dual Phase Cr-2W Steels*, F. Abe and S. Nakazawa, Mater. Sci. Technol. 8 (1992): 1063–69.

102. *Dislocation Pinning and Channeling in a Neutron-Irradiated 10 mass%Cr-30 mass%Mn Austenitic Steel*, F. Abe, *M. Narui and *H. Kayano (*Tohoku Univ.), Mater. Trans., JIM 33 (1992): 1123–29.

103. *The Role of Microstructural Instability on Creep Behavior of a Martensitic 9Cr-2W Steel*, F. Abe, S. Nakazawa, H. Araki and T. Noda, Metall. Trans. A 23 (1992): 469–77.

104. *The Effect of Tungsten on Creep Behavior of Tempered Martensitic 9Cr Steels*, F. Abe and S. Nakazawa, Metall. Trans. A 23 (1992): 3025–34.

105. *Function and Utilization of Data-Free-Way System (Distributed Database for Advanced Nuclear Materials)*, M. Fujita, Y. Kurihara, *H. Nakajima, *N. Yokoyama (*JAERI), †F. Ueno, †S. Kano (†PNC) and S. Iwata (Univ. of Tokyo), Proc. of 2nd Int. Conf. on Computer Applications to Materials and Molecular Science and Engineering (1992): 81–84.

106. *Evaluation of Creep-Fatigue Interaction Based on Creep Damage Mode*, K. Yagi and K. Kubo, Proc. of 3rd Int. Conf. on Low Cycle Fatigue and Elasto-Plastic Behavior of Material (1992): 242–47.

107. *Development of a Distributed Database for Advanced Nuclear Materials*, M. Fujita, Y. Kurihara, *H. Nakajima, *N. Yokoyama (*JAERI), †F. Ueno, †S. Nomura (†PNC) and S. Iwata (Univ. of Tokyo), Proc. of 4th Int. Sympo. on Advanced Nuclear Energy Research (1992): 402–09.

108. *The Use of Miniature Specimen for Assessment of Residual Life by Temperature-Accelerated Test*, *K. Sonoya, *M. Kitagawa (*IHI), M. Murata, H. Tanaka and K. Yagi, Proc. of 5th Int. Conf. on Creep of Materials (1992); 75–79.

109. *Creep Crack Growth Behavior of Ni-26Cr-17W-0.5Mo Alloy in Air and Helium Gas Environment at 1,273 K*, M. Tabuchi, K. Yagi, Y. Nakasone and T. Tanabe, Proc. of 5th Int. Conf. on Creep of Materials (1992): 297–304.

110. *Size and Shape Effects of Welded Joint Specimen on Creep Behavior*, Y. Muramatsu, M. Yamazaki, H. Hongo and Y. Monma, Proc. of 7th ICPVT (1992); 1–17.

111. *Present Status and Future Direction of Data-Free-Way (Distributed Database for Advanced Nuclear Materials)*, M. Fujita, Y. Kurihara, *H. Nakajima, *N. Yokoyama (*JAERI), †F. Ueno, †S. Kano (†PNC) and S. Iwata (Univ. of Tokyo), Proc. of Int. Sympo. on Material Chemistry (1992): 601–11.

112. *Effects of Oxidation on High-Temperature, High-Cycle Fatigue Properties of Engineering Steels*, K. Kanazawa, M. Sato and M. Kimura, Proc. of 1992 SINO–JAPAN Bilateral Sympo. on High Temperature Strength of Materials (1992): 228–38.

113. *Governing Factors of the Inherent Creep Strength of Ferritic Steels*, K. Kimura, H. Kushima, K. Yagi and C. Tanaka, Report of 123rd Committee on Heat-Resisting Metals and Alloys Jpn. Soc. for the Promotion of Sci. 33 (1992): 131–41 (in Japanese).

114. *Evaluation of Creep Deformation Behaviors and Rupture Life of Cr-Mo Type Steels by a Modified θ Projection Concept*, H. Kushima, T. Watanabe, K. Yagi, C. Tanaka and K. Maruyama (Tohoku Univ.), Report of 123rd Committee on Heat-Resisting Metals and Alloys Jpn. Soc. for the Promotion of Sci. 33 (1992): 143–57 (in Japanese).

115. *Effect of Microstructures on Creep Rupture Properties for SUS347H*, H. Tanaka, M. Murata, K. Yagi and C. Tanaka, Report of 123rd Committee on Heat-Resisting Metals and Alloys Jpn. Soc. for the Promotion of Sci. 33 (1992): 313–21 (in Japanese).

116. *Creep Crack Growth Properties of IN100 Superalloy*, M. Tabuchi, K. Kubo and K. Yagi, Report of 123rd Committee on Heat-Resisting Metals and Alloys Jpn. Soc. for the Promotion of Sci. 33 (1992): 343–49 (in Japanese).

117. *Ferritic/Martensitic Steels: Promises and Problems*, R.L. Klueh (Oak Ridge Natl. Lab.), K. Ehrlich (Kernforschungszentrum Karlsruhe) and F. Abe, Report of DOE/ER-0313/12 (1992): 131–41.

118. *Cold Rolling of Boron-Free Polycrystalline Ni_3Al Grown by Unidirectional Solidification*, T. Hirano and T. Mawari, Scr. Metall. Mater. 26 (1992): 597–600.

119. *Effects of Alloy Stoichiometry on Environmental Embrittlement in $L1_2$-Ordered (Co, Fe)$_3$V Alloys*, C. Nishimura and C.T. Liu (Oak Ridge Natl. Lab.), Scr. Metall. Mater. 27 (1992): 1307–11.

120. *Fatigue Properties of Butt-Welded Joints for 5083-O Aluminum Alloy*, H. Hirukawa, S. Matsuoka, E. Takeuchi and S. Nishijima, Trans. Jpn. Soc. Mech. Eng. 58 (1992): 676–82 (in Japanese).

121. *Fracture Characteristics and Mechanisms of GFRTP*, H. Hirukawa, *A. Todoroki, *H. Kobayashi and *H. Nakamura (*Tokyo Inst. Technol.), Trans. Jpn. Soc. Mech. Eng. 58 (1992): 845–51 (in Japanese).

Measurement and evaluation

122. *Results on the First VAMAS Intercomparison of AC Loss Measurements*, K. Itoh, H. Wada and K. Tachikawa (Tokai Univ.), Advances in Cryogenic Eng. Mater. 38 (1992): 459–68.

123. *Layer Thickness Determination of Thin Films by Grazing Incidence X-Ray Experiments Using Interference Effect*, K. Sakurai and A. Iida (Natl. Lab. for High Energy Physics), Adv. in X-Ray Anal. 35 (1992): 813–18.

124. *Electrical and Thermal Conductivities and Magnetization of Some Austenitic Steels Titanium and Titanium Alloys at Cryogenic Temperatures*, O. Umezawa and K. Ishikawa, Cryogenics 32 (1992): 873–80.

125. *Development of 40 Tesla Class Hybrid Magnet System*, K. Inoue, T. Takeuchi, T. Kiyoshi, K. Itoh, H. Wada, H. Maeda, *T. Fujioka, *S. Murase, *Y. Wachi, *S. Hanai and *T. Sasaki (*Toshiba Co.), IEEE Trans. Mag. 28 (1992): 493–96.

126. *Fourier Analysis of Interference Structure in X-Ray Specular Reflection from Thin Films*, K. Sakurai and A. Iida (Natl. Lab. for High Energy Physics), Jpn. J. Appl. Phys. 31 (1992): L113–15.

127. *On-line Enrichment and Determination of Trace Sulfur in High-purity Iron Samples by Flow Injection and Inductively Coupled Plasma Atomic Emission Spectrometry*, K. Yamada, C.W. McLeod (Sheffield City Polytechnic), O. Kujirai and H. Okochi, J. Anal. Atomic Spectr. 7 (1992): 661–65.

128. *VAMAS Low Cycle Fatigue Round-Robin Tests*, M. Kitagawa (IHI) and K. Yamaguchi, J. Iron and Steel Inst. Jpn. 78 (1992): 1431–40 (in Japanese).

129. *Determination of Low Contents of Oxygen in High Purity Iron by Inert Gas Fusion Infrared Absorption Method Using Impulse Heating Technique*, T. Yoshioka and H. Okochi, J. Jpn. Inst. Met. 56 (1992): 81–88 (in Japanese).

130. *Study on Segregation of Small Amount of Ga in Iron Ores by Means of Computer Processing of EPMA X-Ray Image*, T. Kimura, M. Fukamachi and A. Ohba, J. Jpn. Inst. Met. 56 (1992): 1179–84 (in Japanese).

131. *The Quantitative Evaluation System of Surface Flaw on the Magnetic Flux Leakage Testing Method*, I. Uetake, H. Itoh and T. Saito, J. JSNDI 41 (1992): 657–64 (in Japanese).

132. *The Relation between Measured Value of Magnetic Flux Leakage and Sensor Size*, I. Uetake, H. Itoh and T. Saito, Nondestructive Testing & Evaluation 7 (1992): 347–59.

133. *In Situ Deformation and Unfaulting of Interstitial Loops in Proton-Irradiated Steels*, *M. Suzuki, *A. Sato, *T. Mori (*Tokyo Inst. Technol.), J. Nagakawa, N. Yamamoto and H. Shiraishi, Phil. Mag. A 65 (1992): 1309–26.

134. *High-Field Facilities under Development and Construction at the National Research Institute for Metals, Japan*, K. Inoue, T. Asano, T. Kiyoshi, Y. Sakai, T. Takeuchi, K. Itoh and H. Maeda, Physica B 177 (1992): 7–15.

135. *Local Strain Sensing Using Piezoelectric Polymer*, M. Egashira and N. Shinya, Proc. of lst Int. Conf. on Intelligent Materials (1992): 143–46.

136. *Determination of Trace Elements in High Concentration of Matrix Solutions of Iron Zirconium and Molybdenum by Graphite Furnace Atomic Absorption Spectrometry*, T. Kobayashi, K. Ide, S. Hasegawa and H. Okochi, Proc. of 3rd Int. Conf. on Progress of Analytical Chemistry in the Iron and Steel Industry (1992): 234–40.

137. *3-D High Resolution X-Ray Tomography for Small Objects*, Y. Yamauchi, N. Kishimoto and T. Ikuta (Osaka Electro-Communication Univ.), Proc. of 4th Int. Sympo. on Advanced Nuclear Energy Research (1992): 285–88.

138. *Effects of Product Form and Boron Addition on the Creep Damage in the Modified Hastelloy X Alloys in a Simulated HTGR Helium Gas Environment*, Y. Nakasone, *H. Tsuji, *H. Nakajima (*JAERI) and T. Tanabe, Proc. of 4th Int. Sympo. on Advanced Nuclear Energy Research (1992): 561–66.

139. *Creep Damage of Hastelloy XR at Very High Temperatures in Simulated HTGR Helium Gas*, Y. Nakasone, T. Tanabe, *H. Tsuji, *H. Nakajima (*JAERI), T. Ohba and K. Yagi, Proc. of 5th Int. Conf. on Creep of Materials (1992): 551–55.

140. *Single Crystal Growth and Characterization of* $Bi_2Sr_2CaCu_2O_{8+\delta}$, K. Kadowaki and T. Mochiku, Proc. of Int. Workshop on Superconductivity (1992): 112–14.

141. *Determination of Alloying Elements and Trace Titanium in 2.25Cr-1Mo Steel by Glow Discharge Mass Spectrometry*, S. Itoh, F. Hirose and R. Hasegawa, Spectrochem. Acta B 47 (1992): 1241–45.

142. *Application of the Laser Speckle Method to Strain Measurement in the Welding Process*, Y. Muramatsu and S. Kuroda, Q. J. Jpn. Weld. Soc. 10 (1992): 125–31 (in Japanese).

Simulation and theory

143. *Scatter in Creep-Rupture Data and Long-Time Extrapolation for Ferritic Heat-Resisting Steels*, M. Sakamoto, H. Yoshizu and Y. Monma, J. Soc. Mater. Sci. Jpn. 41 (1992): 1655–61 (in Japanese).

144. *Computer Simulation of Laser-Generated Elastic Waves in Solid*, H. Yamawaki and T. Saito, Nondestructive Testing & Evaluation 7 (1992): 165–77.

145. *Numerical Calculation of Surface Waves Using New Nodal Equations*, H. Yamawaki and T. Saito, Nondestructive Testing & Evaluation 7 (1992): 379–89.

146. *Calculational Evaluation of Radiation Induced Deformation*, J. Nagakawa, Proc. of 4th Int. Sympo. on Advanced Nuclear Energy Research (1992): 387–91.

147. *Development and Perspective on Materials Database*, S. Nishijima, Proc. of ASCA Seminar on Materials Database Technol. (1992): 101–11.

148. *VAMAS TWA10 Round-Robin on Creep and Fatigue Data Evaluation*, Y. Monma, Proc. of ASCA Seminar on Materials Database Technol. (1992): 136–45.

149. *Attempt to Predict Creep Rupture Strength Form Short-Time Tensile Strength of Heat-Resisting Steels and Alloys*, H. Yoshizu, M. Sakamoto and Y. Monma, Report of 123rd Committee on Heat-Resisting Metals and Alloys Jpn. Soc. for the Promotion of Sci. 33 (1992): 169–80 (in Japanese).

150. *Fatigue Life Prediction Considering Constraint of Notches*, M. Nihei and T. Konno, Trans. Jpn. Soc. Mech. Eng. 58 (1992): 160–65 (in Japanese).

151. *Prediction of Fatigue Strength Properties Using Material Strength Database (1st Report, Prediction of High-Cycle Fatigue Strength)*, M. Nihei and T. Konno, Trans. Jpn. Soc. Mech. Eng. 58 (1992): 1287–92 (in Japanese).

152. *Database System on the Information for Phase Transformation in Binary Alloy System*, T. Yokokawa and M. Fujita, Zairyoukagaku 29 (1992): 38–46 (in Japanese).

Materials

Non-ferrous materials

153. *Development of a High Strength, High Conductivity Copper-Silver Alloy for Pulsed Magnets*, Y. Sakai, K. Inoue, T. Asano and H. Maeda, IEEE Trans. Mag. 28 (1992): 888–91.
154. *In Situ Observations of the Growth Process of C-Axis-Oriented $Bi_2Sr_2Ca_1Cu_2O_x$ Superconducting Phase*, *T. Hasebe, Y. Tanaka, *T. Yanagiya (*Sumitomo Heavy Industries, Ltd.), T. Asano, M. Fukutomi and H. Maeda, Jpn. J. Appl. Phys. 31 (1992): L21–24.
155. *Fabrication and Superconducting Properties of AgCu Alloy-Sheathed BiSrCaCuO Oxide Tapes*, Y. Tanaka, T. Asano, T. Yanagiya (Sumitomo Heavy Industries, Ltd.), M. Fukutomi, K. Komori and H. Maeda, Jpn. J. Appl. Phys. 31 (1992): L235–38.

Intermetallic compounds

156. *TiAl Melting in CaO Crucible and Its Mechanical Properties*, N. Sakuma, T. Mitsui, H. Kurabe and T. Tsujimoto, J. Iron and Steel Inst. Jpn. 78 (1992): 680–87 (in Japanese).
157. *Electrical Conductivity of Solid Beryllium Sulfide*, H. Nakamura, Y. Ogawa, A. Kasahara and S. Iwasaki, J. Jpn. Inst. Met. 56 (1992): 1408–13 (in Japanese).
158. *Microstructural Evolution and Tensile Properties of Ti-rich TiAl Alloys*, M. Takeyama, Mater. Sci. Eng. A 152 (1992): 269–76.
159. *Alloy Design for Improvement of Ductility and Workability of Alloys Based on Intermetallic Compound TiAl*, T. Tsujimoto, K. Hashimoto and M. Nobuki, Mater. Trans., JIM 33 (1992): 989–1003.

Materials for mechanical application

160. *Mechanical Properties of Particulate Reinforced Titanium-Based Metal Matrix Composites Produced by the Blended Elemental P/M Route*, M. Hagiwara, N. Arimoto (Osaka Titanium Manufacturing Co.), S. Emura, Y. Kawabe and H. Suzuki (Nippon Steel Co.), ISIJ Int. 32 (1992): 909–16.
161. *Strengthening Capability in Titanium Alloys*, Y. Kawabe, J. Jpn. Soc. for Heat Treatment 32 (1992): 249–55 (in Japanese).
162. *Particulates Dispersion-Strengthened Titanium-Based Alloys*, M. Hagiwara, Kinzoku 62 (1992): 41–47 (in Japanese).

Materials for electronics application

163. *Effects of Strain on Critical Currents in Ag-Sheathed BiSrCaCuO Tapes*, T. Kuroda, M. Yuyama, K. Itoh and H. Wada, Advances in Cryogenic Eng. Mater. 38 (1992): 1045–51.
164. *Fabrication of $Bi_2Sr_2CaCu_2O_8$ Tapes and Coils*, H. Kumakura, Advances in Superconductivity IV (1992): 547–52.
165. *High-Temperature X-Ray Diffraction Analysis for $Bi_2Sr_2CaCu_2O_y$*, *T. Hasegawa, *T. Kitamura, *H. Kobayashi (*Showa Electric Wire & Cable Co., Ltd.), H. Kumakura, H. Kitaguchi and K. Togano, Appl. Phys. Letters 60 (1992): 2692–94.
166. *Fabrication and Properties of $Bi_2Sr_2CaCu_2O_8$/Ag Composite Tapes and Coils*, H. Kumakura, H. Kitaguchi, K. Togano, H. Maeda, *J. Shimoyama, *T. Morimoto (*Asahi Glass Co., Ltd.), †K. Nomura and †M. Seido (†Hitachi Cable Ltd.), Cryogenics 32 (1992): 489–95.
167. *Anisotropy in D.C. Magnetization in Textured $Y_{0.9}Ca_{0.1}Ba_2Cu_4O_8$ Superconductors*, H. Kumakura, H. Kitaguchi, K. Togano, *T. Hasegawa and *F. Takeshita (*Showa Electric Wire & Cable Co., Ltd.), Jpn. J. Appl. Phys. 31 (1992): L1031–33.
168. *Effect of Cooling Rate on Critical Current Density for $Bi_2Sr_2CaCu_2O_{8+\delta}$/Ag Composite Tapes*, *J. Shimoyama, *J. Kase, *T. Morimoto (*Asahi Glass Co., Ltd.), H. Kitaguchi, H. Kumakura, K. Togano and H. Maeda, Jpn. J. Appl. Phys. 31 (1992): L1167–69.
169. *Flux Pinning Characteristics in 180 MeV Cu^{11+}-Irradiated $Bi_2Sr_2CaCu_2O_x$*, H. Kumakura, H. Kitaguchi, K. Togano, H. Maeda, J. Shimoyama (Asahi Glass Co., Ltd.), *S. Okayasu and *Y. Kazumata (*JAERI), Jpn. J. Appl. Phys. 31 (1992): L1408–10.
170. *Improvement of Reproducibility of High Transport J_c for $Bi_2Sr_2CaCu_2O_y$/Ag Tapes by Controlling Bi Content*, *J. Shimoyama, *N. Tomita, *T. Morimoto (*Asahi Glass Co., Ltd.), H. Kitaguchi, H. Kumakura, K. Togano, H. Maeda, †K. Nomura and †M. Seido (†Hitachi Cable Ltd.), Jpn. J. Appl. Phys. 31 (1992): L1328–31.
171. *Enhancement of Flux Pinning in $Bi_2Sr_2CaCu_2O_8$ by 180 MeV Cu^{11+} Irradiation*, H. Kumakura, S. Ikeda, H. Kitaguchi, K. Togano, H. Maeda, *J. Kase, *T. Morimoto (*Asahi Glass Co., Ltd.), †S. Okayasu and †Y. Kazumata (†JAERI), J. Appl. Phys. 72 (1992): 800–02.
172. *Development of Nb Tube Processed Nb_3Al Multifilamentary Superconductor*, T. Takeuchi, T. Kuroda, K. Itoh, M. Kosuge, Y. Iijima, T. Kiyoshi, F. Matsumoto and K. Inoue, J. Fusion Energy 11 (1992): 7–18.

173. *Bi-Oxide High T_c Superconductors*, H. Maeda, J. Surf. Finishing Soc. Jpn. 43 (1992): 806–12 (in Japanese).

Materials for energy application

174. *Study on Deuterium Absorption of Pd at High Pressure D_2 Gas and Low Temperature*, M. Kitajima, G. Maizza (Politechnico di Torino), K. Nakamura and M. Fujitsuka, IL Nuovo Cimento 14 (1992): 27–32.

175. *Prospect of Material Processes for Low Activation*, T. Noda, F. Abe, H. Araki, H. Suzuki and M. Okada, JAERI-M 92–207 (1992): 567–72.

176. *Real-Time Raman Measurement of Si (111) under Low Energy Ar^+ Ion Irradiation*, K. Nakamura and M. Kitajima, J. Appl. Phys. 71 (1992): 3645–47.

177. *Plasma Density Dependence of Oxidation Rate of Si by In Situ during Rapid Ellipsometry*, *H. Kuroki, H. Shinno, K. Nakamura, M. Kitajima and *T. Kawabe (*Univ. of Tsukuba), J. Appl. Phys. 71 (1992): 5278–80.

178. *Effects of Deoxidizer Addition on the Hydrogen Permeation Characteristics of V-Ni Alloy Membranes*, M. Komaki, C. Nishimura and M. Amano, J. Jpn. Inst. Met. 56 (1992): 729–33 (in Japanese).

179. *Real-Time Raman Measurements of Graphite Surface under Ion Irradiation*, K. Nakamura, E. Asari (Univ. of Tsukuba) and M. Kitajima, J. Jpn. Soc. Surf. Sci. 13 (1992): 261–65 (in Japanese).

180. *Raman Spectra of K_xMoO_3 ($X < 0.33$) and Its Laser Annealing*, K. Nakamura, M. Kitajima and T. Hirata, J. Mater. Sci. Letters 11 (1992): 805–06.

181. *The Energy Dependence on Lattice Damage of Graphite by Low Energy He-Ion Irradiation*, K. Nakamura, *E. Asari, M. Kitajima and *T. Kawabe (*Univ. of Tsukuba), J. Nucl. Mater. 187 (1992): 294–97.

182. *Ferritic/Martensitic Steels for Fusion Applications: Promises and Problems*, R. L. Klueh (Oak Ridge Natl. Lab.), K. Ehrlich (Kernforschungszentrum Karlsruhe) and F. Abe, J. Nucl. Mater. 191–94 (1992): 116–24.

183. *Initial Damage in Graphite under Ion Irradiation Studies by Real-Time Raman Measurements*, M. Kitajima and K. Nakamura, J. Nucl. Mater. 191–94 (1992): 356–59.

184. *Thermal Properties of Carbon-Boron-Titanium Compounds as Plasma Facing Materials*, T. Tanabe, *T. Baba, *A. Ono (*NRLM), M. Fujitsuka, T. Shikama (Tohoku Univ.) and H. Shinno, J. Nucl. Mater. 191–94 (1992): 382–85.

185. *Irradiation Behavior of Carbon-Boron Compounds and Silicon Carbide Composites Developed as Fusion Reactor Materials*, T. Shikama (Tohoku Univ.), M. Fujitsuka, H. Araki, T. Noda, T. Tanabe and H. Shinno, J. Nucl. Mater. 191–94 (1992): 611–15.

186. *Optimum Alloy Compositions in Reduced-Activation Martensitic 9Cr Steels for Fusion Reactor*, F. Abe, T. Noda and M. Okada, J. Nucl. Mater. 195 (1992): 51–67.

187. *Ion-Irradiation Effects on Phonon Correlation Length of Graphite Studied by Raman Spectroscopy*, K. Nakamura and M. Kitajima, Phys. Rev. B 45 (1992): 78–82.

188. *Raman Studies of Graphite Lattice Disordering Kinetics under Low Energy He Ion Irradiation*, K. Nakamura and M. Kitajima, Phys. Rev. B 45 (1992): 5672–74.

189. *Study of Surface under Ion Irradiation by Real-Time In Situ Measurements*, M. Kitajima, Proc. of Int. Sympo. on Material Chemistry (1992): 157–66.

190. *Plasma Oxidation Process of Silicon and Plasma Characteristics*, *H. Kuroki, H. Shinno, K. Nakamura, M. Kitajima and *T. Kawabe (*Univ. of Tsukuba), Proc. of Int. Sympo. on Material Chemistry (1992): 407–14.

191. *Low Energy He^+ Irradiation Effect on Graphite Surface*, *E. Asari, K. Nakamura, M. Kitajima and *T. Kawabe (*Univ. of Tsukuba), Proc. of Int. Sympo. on Material Chemistry (1992): 581–90.

192. *Experimental Study of Plasma Effect on Oxidation of Solid Surface*, M. Kitajima, *H. Kuroki, H. Shinno and *T. Kawabe (*Univ. of Tsukuba), Proc. of Int. Conf. on Plasma Physics (1992): 13–22.

193. *Real-Time Raman Measurement on Irradiation Effect*, M. Kitajima, Proc. of Int. Workshop on Ceramic Breeder Blanket Interactions (1992): 38–42.

194. *Raman Scattering from Graphite Irradiated by Deuterium Ions*, K. Nakamura and M. Kitajima, Solid State Commun. 82 (1992): 475–77.

195. *Thermal Relaxation of Lattice Disorder in Graphite Induced by Ion Irradiation*, K. Nakamura, E. Asari (Univ. of Tsukuba) and M. Kitajima, Solid State Commun. 82 (1992); 569–71.

196. *Growth of Silicon Oxide on Silicon in the Thin Film Region in an Oxygen Plasma*, M. Kitajima, H. Kuroki (Univ. of Tsukuba), H. Shinno and K. Nakamura, Solid State Commun. 83 (1992): 385–88.

197. *Research and Development of Residual Life Prediction for Materials Used in Plants*, N. Shinya, Zairyoukagaku 29 (1992): 1–7 (in Japanese).

Materials for environmental performance

198. *Ecomaterial—New Step of Material towards the 21st Century,* K. Halada, Bull. Jpn. Inst. Met. 31 (1992): 505–11 (in Japanese).

199. *Functional Ecomaterial—An Approach to Nature-Created Material,* K. Halada, Nihon no Kagaku 33 (1992): 63–68 (in Japanese).

Processing

Gaseous process

200. *Preparation of Carbon Fiber/SiC Composite by Chemical Vapor Infiltration,* T. Noda, H. Araki, F. Abe, H. Suzuki and M. Okada, ISIJ Int. 32 (1992): 926–31.

201. *Synthesis and Characterization of $Bi_2Sr_2Ca_{n-1}Cu_nO_y$ (n = 1 – 7) Thin Films Grown by Off-Axis, Three Target Magnetron Sputtering,* H. Narita (Yasukawa Electric Mfg. Co., Ltd.), T. Hatano and K. Nakamura, J. Appl. Phys. 72 (1992): 5778–85.

202. *Formation of Polycrystalline SiC Film by Excimer Laser CVD,* T. Noda, Y. Suzuki, H. Araki, F. Abe and M. Okada, J. Mater. Sci. Letters 11 (1992): 477–78.

203. *Interfacial Structural of Chemical Vapor Infiltration Carbon Fiber/SiC Composite,* H. Araki, T. Noda, F. Abe and M. Okada, J. Mater. Sci. Letters 11 (1992): 1582–84.

204. *Microstructure and Mechanical Properties of CVI Carbon Fiber/SiC Composites,* T. Noda, H. Araki, F. Abe and M. Okada, J. Nucl. Mater. 191–92 (1992): 539–43.

205. *Oxidation Resistance of Ni-TiC Composite Film Formed by Reactive Ion Plating,* A. Ishida, A. Takei, *Y. Tsuji and *H. Imai (*Shibaura Inst. Technol.), J. Surf. Finishing Soc. Jpn 43 (1992): 126–30 (in Japanese).

206. *Composition Change of Ni-TiC Composites Films Formed by Ion Plating with Single Source,* T. Masui (Mie Ind. Res. Inst.), Y. Tsuji (Shibaura Inst. Technol.), A. Ishida and A. Takei, J. Surf. Finishing Soc. Jpn. 43 (1992): 227–28 (in Japanese).

Liquid state process

207. *Attack on Magnesia Crucible by Molten Iron,* T. Dan, N. Aritomi , K. Ogawa, K. Honma and T. Kimura, J. Jpn. Inst. Met. 56 (1992): 53–59 (in Japanese).

208. *Production of Aluminum Profile Rods by a moldless Upward Continuous Casting Process Using Formers,* A. Sato, Y. Ohsawa and G. Aragane, Mater. Trans., JIM 33 (1992): 66–72.

Solid state process

209. *Grain Size-Gradient Structure by Heat Treatment Using Internal Nitridation Method and It's Effect on High Temperature Fatigue Life,* J. Kyono and N. Shinya, J. Iron and Steel Inst. Jpn. 78 (1992): 1838–45 (in Japanese).

Powder processing

210. *Sintering of Bi-Sr-Ca-Cu-O Superconductive Material Atomized from Molten State,* K. Halada, K. Minagawa, H. Suga, H. Okuyama, S. Ohno and Y. Muramatsu, Advances in Powder Metall. & Particulate Mater. 8 (1992): 281–91.

211. *Combustion Synthesis of an Oxide-Superconductor,* Y. Kaieda, M. Ohtaguchi and N. Oguro, Int. J. Self-Propagating High-Temperature Synthesis 1 (1992): 246–56.

212. *Effects of Cold Isostatic Pressure on the Sintering Behavior of Nickel Ultrafine Powders,* Y. Sakka, J. Alloys and Compounds 190 (1992): 31–33.

213. *EPMA Composition-Coordinate Mapping Analysis of the Phase Change of Atomized Bi-Sr-Ca-Cu Oxide,* K. Halada, K. Honma, K. Minagawa and H. Okuyama, J. Jpn. Soc. Powder Powder Metall. 39 (1992): 390–96 (in Japanese).

214. *Effect of Milling Methods on the Reaction of TiC Formation,* S. Wanikawa and T. Takeda, J. Jpn. Soc. Powder Powder Metall. 39 (1992): 1145–50 (in Japanese).

215. *Combustion Synthesis of Intermetallic Compounds,* Y. Kaieda, Metals (1992): 76–81 (in Japanese).

216. *Development of New Production Process of Intermetallic Compounds,* Y. Kaieda and T. Oie (Kyouritsu Ceramic Materials Co., Ltd.), New Ceramics (1992): 87–91 (in Japanese).

217. *Processing of SiC-Mullite-Al_2O_3 Nanocomposite,* Y. Sakka, *D.D. Bidinger, *J. Liu, *M. Sarikaya, *I.A. Aksay (*Univ. of Washington), Proc. of 16th Annual Conf. on Composites, Materials and Structures (1992): 1–12.

218. *Sintering Characteristics of Iron Ultrafine Powders,* Y. Sakka, T. Uchikoshi and S. Ohno, Solid State Phenomena 25–26 (1992): 179–86.

219. *Reaction Sintering of Nb_3Al to Near Full Density,* C. Nishimura and C.T. Liu (Oak Ridge Natl. Lab.), Scr. Metall. Mater. 26 (1992): 381–85.

Joining

220. *Effect of Surface Composition on Diffusion Welding in Stainless Steel*, O. Ohashi and S. Suga (Osaka Univ.), J. Jpn Inst. Met. 56 (1992): 579–85 (in Japanese).
221. *Effect of Twist Angle on Tensile Strength of Diffusion-Welded Joints in Molybdenum Single Crystal*, O. Ohashi and S. Suga (Osaka Univ.), J. Jpn. Weld. Soc. 10 (1992): 53–58 (in Japanese).

Composite process

222. *Anodic Oxidation Behavior of Aluminium Die Casting Alloy ADC12 in 13M and 1.5M Sulfuric Acid Solution*, Y. Fukuda and T. Fukushima (Univ. of Ryukyus), J. Surf. Finishing Soc. Jpn. 43 (1992): 48–54.
223. *Significance of Quenching Stress in the Cohesion and Adhesion of Thermally Sprayed Coatings*, S. Kuroda, T. Fukushima and S. Kitahara, J. Thermal Spray Technol. 1 (1992): 325–32.
224. *Aluminized Coatings on Titanium Alloys and TiAl Intermetallic Compound*, A. Takei and A. Ishida, Proc. of Int. Sympo. on Solid State Chemistry of Advanced Materials (1992): 317–24.
225. *Significance of the Quenching Stress in the Cohesion and Adhesion of Thermally Sprayed Coatings*, S. Kuroda, T. Fukushima and S. Kitahara, Proc. of Int. Thermal Spray Conf. (1992): 903–09.

Process with aid of beam technology

226. *Fabrication of 300Å* Thick BiSrCaCuO Thin Films with T_c of 108 K by Use of Ion Implantation, K. Saito and M. Kaise, Jpn. J. Appl. Phys. 31 (1992): L1047–50.
227. *Displacement Damage Effects and Related Phase Changes of Ar-Ion-Irradiated BiSrCaCuO System Superconducting Thin Films*, K. Saito and M. Kaise, Jpn. J. Appl. Phys. 31 (1992): 3533–38.
228. *Thermal Spike and Displacement Damage Effects in BiSrCaCuO Thin Films by Ar Ion Beams*, K. Saito and M. Kaise, Jpn. J. Appl. Phys. 31 (1992): 3539–45.
229. *Local Plasma Compositions at Anode Surface in Mixed Gas Shielding GAT*, K. Hiraoka, Q. J. Jpn. Weld. Soc. 10 (1992): 58–64 (in Japanese).

Processing in special environment

230. *Development of 20 T Class Superconducting Magnet with Large Bore*, T. Kiyoshi, K. Inoue, K. Itoh, T. Takeuchi, H. Wada, H. Maeda, *K. Kuroishi, *F. Suzuki, *T. Takizawa and *N. Tada (*Hitachi, Ltd.), IEEE Trans. Mag. 28 (1992): 497–500.
231. *Mechanism of Surface Precipitation of Highly Oriented Hexagonal Boron Nitride in Austenitic Stainless Steel*, D. Fujita, K. Yoshihara and T. Homma (Univ. of Tokyo), J. Jpn. Int. Met. 56 (1992): 406–14 (in Japanese).
232. *Application of Factor Analysis and AES to the Chemical State Depth Profiling of TiN/Ti/Si*, D. Fujita and K. Yoshihara, J. Surf. Sci. Soc. Jpn 13 (1992): 286–93 (in Japanese).
233. *The Effect of BN Coating on the Hydrogen Permeation through Stainless Steel Membranes*, A. Itakura, M. Tosa and K. Yoshihara, J. Vac. Soc. Jpn. 35 (1992): 313–16 (in Japanese).
234. *Extremely-High Vacuum System for the Long-Distance Transport System*, M. Tosa, A. Itakura and K. Yoshihara, J. Vac. Soc. Jpn. 35 (1992): 325–27 (in Japanese).
235. *Extremely-High Vacuum Station for Material Art*, M. Tosa and K. Yoshihara, J. Vac. Soc. Jpn. 35 (1992): 588–93 (in Japanese).

❐ NRIM Publications (Apr. 1992 to Mar. 1993)

1. Bulletin of National Research Institute for Metals, in Japanese.
   No. 14 (Jan. 1993)
2. Annual Report of National Research Institute for Metals, in Japanese.
   For fiscal year of 1991 (Nov. 1992)
3. Kinzaigiken News, in Japanese.
   Nos. 4 to 12 (1992) and Nos. 1 to 3 (1993)
4. NRIM Research Activities, in English.
   (Oct. 1992)
5. NRIM Special Report, in English.
   Nos. SR-93-1 and 2 (Mar. 1993)
6. Material Strength Data Sheet, in English.
   NRIM Creep Data Sheet,
   Nos. 37A and 39A (Sep. 1992)
   Nos. 22B and 34B (Mar. 1993)

   NRIM Fatigue Data Sheet,
   Nos. 69 to 72 (Dec. 1992)

International Exchange Apr. 1992 to Mar. 1993

❒ International Collaboration Research

Australia

1. Study on Surface Modification of Metals with Ultra-High Temperature Heat Sources. (CSIRO)

Brazil

1. Study on Ni-Base Superalloys. (Fundacao de Technologia Industrial)

Canada

1. Damage Evaluation and Remaining Life Prediction of Structural Materials. (Canadian Center for Mineral and Energy Technology)

China

1. Investigation of High Temperature Titanium Alloy for Application over 600 °C. (Northwest Institute for Non-Ferrous Metal Research)
2. Studies on Structural Control and Superconducting Properties of High Temperature Superconductors. (Institute of Metal Research Academia Sinica)
3. Study on the Combustion Synthesis of Intermetallic Compounds. (Northwest Institute for Non-Ferrous Metal Research)
4. Fundamental Study on the Improvement of Superconductivity for High-T_c Oxide. (Northwest Institute for Non-Ferrous Metal Research)
5. Study of Localized Corrosion Damage of Corrosion Resistance Alloys in High Temperature Aqueous Solution. (Shanhai Jiao Tong University)

Finland

1. Development of Superconductive Thin Oxide Coatings. (Tampere University of Technology)

France

1. Superconducting and Cryogenic Magnetic Materials. (Service National des Champs Intenses, Centre National de la Recherche Scientifique Grenoble and Others)

Germany

1. Development of Superconducting Materials. (Kernforschungszentrum Kerlsruhe)
2. Exchange of Creep and Fatigue Data Sheet. (5 Institutes)

Italy

1. Superconducting Properties of Advanced Superconductors in Time-Varying Magnetic Fields. (CISE Spa, Technologia Innovative Thermophysics & Cryogenics Sec.)
2. Intercomparison of Methods and Materials for Strain Measurements at Cryogenic Temperatures. (Instituto di Metrogia "G. Colonettie"-C.N.R.)
3. Study on the Mechanism of Deformation, Fracture and Corrosion in Ni-Based Superalloys. (Instituto per la Tecnologia dei Materiali Metallicinon Tradizionali)

Korea

1. Exchange in Materials Strength Property Data. (Korea Standards Research Institute)
2. Development of the Aluminaid-Base Intermetallic Compounds for Structural. (Korea Institute of Machinery and Metals)
3. Studies on Fabrication Process of High Temperature Superconductor. (Korea Institute of Machinery and Metals)
4. Characterization of the Composite Film with Dispersion of Carbide Phase by PVD and CVD Process and the Establishment of the Process Parameters Leading to Fabrication Techniques. (Korea Institute of Machinery and Metals)
5. Performance Characterization of Materials at High-Temperature. (Korea Standards Research Institute)

Sweden

1. Application of Advanced Electromagnetic Technology to the Metallurgical Processing. (Royal Institute of Technology)

U.K.

1. Evaluation of Life and Remaining Life Prediction of Huge Structures under Service Operation. (Welding Institute)

U.S.A.

1. Combustion Synthesis for Production of Ce-

ramic, Intermetallic and Composite Materials. (Alfred University)
2. Research and Development on Systems and Materials for Magnetic Refrigerators. (Francis Bitter National Magnet Laboratory)
3. Database of Properties for High-Temperature Superconducting Materials. (National Institute of Standards and Technology)
4. Studies of High-Strength/High Conductive Materials and Their Application to High-Field Magnets. (Francis Bitter National Magnet Laboratory)
5. Fundamental Studies on the Conductor Fabrication of High Temperature Oxide Superconducting Materials. (University of Illinois)
6. Evaluation Methods for Superconductors. (National Institute of Standards and Technology)

❒ List of Guest Researchers

*STA Fellowship

Nationality and Name	Affiliation	Term	Research Subject
Australia			
Dr. I.E. French	Institute of Industrial Technology, CSIRO	1993.3.15. to 1993.3.26.	Study on Molten Metal Behavior in Laser and Electron Beam Processing
Dr. B.I. Selling	Institute of Industrial Technology, CSIRO	1993.3.17. to 1993.3.31.	Study on Molten Metal Behavior in Laser and Electron Beam Processing of Non-Ferrous Metal
Belgium			
Dr. D. Vanderschueren*	Catholic University Leuven	1992.3.1. to 1993.2.17.	Superplasticity in a Vanadium Alloyed Gamma Plus Beta Phased Ti-Al Intermetallic
Dr. L.V. Bockstal	Catholic University Leuven	1993.3.2. to 1993.3.15.	Coil-Winding Procedure for High Strength/High-Conductivity Wire
Canada			
Dr. W.R. Datars	McMaster University	1992.12.1. to 1992.12.15.	Physical Properties of Graphite Intercalated Compounds and C_{60}
China			
Dr. H.Y. Zhu*	Zhejiang University	1991.5.15. to 1992.5.14.	Structure and Electronic Properties of Metal Oxides
Dr. Lian Zhou	Northwest Institute for Non-Ferrous Metal Research	1992.11.8. to 1992.11.28.	Developments of High Performance High-T_c Superconductors
Mr. Zhao Wenjin	Nuclear Power Institute of China	1993.2.25. to 1993.3.31.	Technique of Transmission Electron Microscope and *In-Situ* Observation of Radiation Damage in Materials
Miss Wen Zhang	Nuclear Power Institute of China	1993.2.25. to 1993.3.31.	Effect of Post-Heat Treatment on Crystallization of Laser CVD SiC Film
Czecho			
Dr. B. Strnadel*	Technical University, Institute of Metal Science	1993.2.1. to 1994.1.31.	Cyclic $\gamma \longleftrightarrow \varepsilon$ Transformation Behavior and Its Effect on the Shape Memory Characteristics in Fe-Mn-Si-Cr-Ni Alloy
France			
Dr. B. Chenevier*	École Nationale Supérieure de Physique de Grenoble	1991.1.11. to 1992.10.10.	High Resolution Electron Microscopy Analysis of High-T_c Superconducting Materials
Dr. J.J.B. Pape*	University of Bordeaux	1992.1.9. to 1993.7.8.	Deformation Mechanisms of Metal Matrix Composites
Germany			
Dr. U. Welp	Argonne National Laboratory	1992.9.3. to 1992.9.24.	Direct Observation of Vortex State in Superconductor by Means of Magnetic Force Microscope
Dr. H. Noerenberg*	Rostock University	1993.3.3. to 1993.4.21.	Investigation of Arsenic Adsorption on GaAs(001) Using RHEED and HRSEM

Nationality and Name	Affiliation	Term	Research Subject
Dr. H.G. Gross*	Association of Quality Assurance in Material Welding Techniques	1993.3.22. to 1993.9.21.	Investigation for Correlation between Laser Speckle Method and Mechanical Properties during Welding Cycle
India			
Dr. R. Chatterjee	Indian Institute of Technology	1993.2.16. to 1994.2.15.	Development of High-T_c Superconducting Tape by Vapor Deposition Technique
Korea			
Dr. Yong-Hak Huh	Korea Standards Research Institute	1992.4.3. to 1992.7.3.	Evaluation of Creep Crack Groeth Properties of Metals
Dr. Joung Soo Kim	Korea Atomic Energy Research Institute	1992.11.15. to 1993.3.31.	Study on the Straining Electrode Behavior of Austenitic Alloys in High Temperature Solutions
Dr. Jung-Ho Ahn	Korea Institute of Machinery and Metals	1993.2.8. to 1993.3.29.	Fabrication of Low-T_c Multifilamentary Superconductors
Netherlands			
Dr. J.P. Zijp*	Delft Technical University	1990.11.11. to 1992.11.11.	Vaporization Phenomena in Arc Plasmas
Dr. J.E. Bie	Delft Technical University	1992.3.1. to 1992.5.31.	Production of Advanced Powder
Philippines			
Ms. L.A. Guzman	Industrial Technology Development Institute	1993.7.15. to 1992.6.10.	Japan–ASEAN Cooperation Program on Materials Science and Technology, Philippine Project on Atmospheric Corrosion (Metallic Coating)
Ms. S. Murdiati	Research and Development Center for Metallurgy-LIPI	1992.4.10. to 1992.6.10.	Same as above
Ms. R.G. Principe	Industrial Technology Development Institute	1992.8.4. to 1992.12.3.	Same as above
Ms. E.L. Enriquez	Industrial Technology Development Institute	1992.8.4. to 1992.12.3.	Same as above
Russia			
Dr. A.K. Kuprin*	Moscow State University	1992.3.31. to 1993.9.30.	Hydrogen and Its Effects on the Electric Properties of Metals and Semiconductors by Using the *In-Situ* Analysis in the Electron Microscope
Slovakia			
Dr. R. Sandrik	Institute of Physics, Slovak Academy of Science	1993.3.4. to 1993.3.18.	Characterization of Thin Films of Oxide Superconductors Using PIXE-RBS Method
Switzerland			
Prof. Dr. R. Flükiger	University of Geneva	1993.3.11. to 1993.3.17.	Discussions on J_c Properties of High Temperature Superconductors
Thailand			
Ms. N. Thanuddhanusilp	Thailand Institute of Science and Technological Research	1992.3.9. to 1992.7.3.	Japan–ASEAN Cooperation Program on Materials Science and Technology, Thai Project on Atmospheric Corrosion (Organic Coating)
Mr. P. Suanpoot	Chiang Mai University	1992.4.20. to 1992.7.3.	Same as above
Mr. Tasrif	Research and Development Center for Applied Chemistry-LIPI	1992.4.20. to 1992.9.4.	Same as above
Ms. N. Chulasai	Thailand Institute of Science and Technological Research	1992.11.16. to 1993.1.29.	Same as above
Ms. Waraporn Rungruangkanokkul	Chulalorykorn University	1992.11.16. to 1993.1.29.	Same as above
U.K.			
Dr. R.C. Reed*	Imperial College of Science, Technology and Medicine	1992.4.1. to 1992.9.30.	Computer Modeling of Phase Transformation in Steels

Nationality and Name	Affiliation	Term	Research Subject
Dr. T.I. Khan*	University of Cambridge	1993.2.7. to 1994.2.7.	Study Changes in Diffusion Bonding Surface Structure Using RHEED after Ion Bombardment and Atom-Radical Surface Modification Techniques
U.S.A.			
Dr. A.L. William	Stanford University	1992.6.26. to 1992.8.22.	Real-Time Measurements and Kinetic Modeling on Changes in the Surface Structure and Chemical Bondings during Ion or Molecular Beam Irradiation
Dr. N.H. MacMillan	Alfred University	1992.12.14. to 1993.1.7.	Mechanical and Thermomechanical Characterization of Functionally Gradient (Ceramic/Intermetallic) Composite Joints Formed by Self-Propagating High Temperature Synthesis
Dr. Jian-Min Zuo	Arizona State University	1993.3.5. to 1993.3.31.	Study on Cooled CCD Camera Imaging System Attached to Transmission Electron Microscope
Dr. Y. Iwasa	Francis Bitter National Magnet Laboratory	1993.3.10. to 1993.3.29.	Evaluation and Application of Cu-Ag Alloy as Conductor Material in High Field

❒ List of Visitors

M: Meguro Main Site T: Tsukuba Laboratories

Nationality and Name	Affiliation	Site	Date
Argentine			
Mrs. Rosa Maria	Center of Mineral Resources and Ceramic Technology	T	Jul. 1992
Dr. E.J. Lenta	INTI Cordoba Laboratory	M, T	Sep. 1992
Belgium			
Mr. E. Ponthieu and his party	Univ. des Sci. et des Tech. de Lille	M	Aug. 1992
Brazil			
Mr. Jose Garibaldi	University of Santa Catarina	T	Jul. 1992
Canada			
Mr. Gavin M. Hood	Atomic Energy of Canada Ltd.	T	Sep. 1992
China			
Mr. Cai Jian Guo and his party	Guangxi Research Institute of Metallurgy	T	Jul. 1992
Mr. Cui Jiao Lin	Ningbo College	T	Jul. 1992
Ms. Chen Shu Hua	China Steel Corporation	M	Sep. 1992
Prof. Luo Weili	Shanghai Research Institute of Materials	M	Oct. 1992
Mr. Ding Ya Ping	Shanghai Nuclear Engineering Research & Design Institute	M	Nov. 1992
Prof. Peng Shiji and his party	China University of Mining and Technology	M	Dec. 1992
Mr. Yang Zhifei and his party	China Electronic Product Reliability & Environmental Testing Research Institute	M	Mar. 1993
Dr. Jian Min Zuo	Arizona State University	T	Mar. 1993
Prof. Ma Jusheng and her party	Tsinghua University	M	Mar. 1993
Egypt			
Prof. M.R. Moharam and his party	Al-Azhar University	T	Jun. 1992
Formosa			
Mr. T.T. Chen and his party	National Tsing Hua University	T	Oct. 1992
France			
Prof. C. Bathias and his party	Conservatoire National des Arts et Métiers	M	Apr. 1992

Nationality and Name	Affiliation	Site	Date
Prof. Jean Le Coze	Ecole des Mine de Sainte-Etinne	T	Jun. 1992
Dr. B. Barbara	Laboratoire de Magnetsme Louis Neel Grenoble	T	Aug. 1992
Dr. P.E.A. Turchi	Lawrence Livermore National Laboratory	M	Oct. 1992
Prof. G. Aubert and his party	Cantre National de La Recherche Scientifique	T	Feb. 1993
Germany			
Dr. H. Assman	Giemens AG	T	Nov. 1992
Dr. B. Schönfeld	Institut für Angewandte Physik	T	Jan. 1993
Hungary			
Dr. Laszlo Kover	Institute of Nuclear Research of the Hungarian Academy of Sciences	T	Nov. 1992
Israel			
Dr. L.A. Bendersky	National Institute of Standards and Technology	M	Apr. 1992
Italy			
Dr. P. Schiller	Institute for Advanced Materials, Joint Research Center	M, T	Feb. 1993
Mr. M. Mirabile and his party	ILVA	M	Mar. 1993
Korea			
Mr. Choi Jung Sik and his party	Hyundai Motor Company	M	Apr. 1992
Mr. Cho Seong Jai and his party	New Material Evaluation Center	M	May 1992
Dr. Hhn Yoo Dong and his party	Korea Institute of Machinery and Metals	M	May 1992
Mr. Zheong G. Kim	Seoul National University	T	May 1992
Dr. Hai Doo Kim	Korea Institute of Machinery and Metals	T	May 1992
Dr. Yoom Jeong Mo and his party	Chon-Buk National University	M	Jul. 1992
Mr. T.H. Lee and his party	Hyundai Motor Company	M	Nov. 1992
Mr. Kim Jae Shik and his party	Ministry of Science & Technology	M	Dec. 1992
Mexico			
Mr. Sergio Modesto	Technical Education Center	T	Jul. 1992
Netherlands			
Dr. M. Bon	Elsevier North-Holand	T	Apr. 1992
Pakistan			
Dr. Mian Suhail Aslam	Embassy of the Islamic Republic of Pakistan	T	Jun. 1992
Spain			
Mr. S. Breso and his party	Asociacion de Investigacion de la Industria Metal Mecanica Afines Y Conexas	M	Jun. 1992
Sweden			
Prof. A. Melander	Swedish Institute for Metals Research	M	Jul. 1992
Thailand			
Dr. B. Udomsakdhi and his party	The Siam Cement Co., Ltd.	T	Oct. 1992
U.K.			
Dr. K.C. Mills	National Physical Laboratory	M	Jun. 1992
Prof. C. Humphreys	University of Cambridge	M, T	Jul. 1992
Prof. B. Wilshire	University of Wales	M	Feb. 1993
U.S.A.			
Dr. J.M. Vitek	Oak Ridge National Laboratory	M	Apr. 1992
Dr. R.M. Fantazier and his party	Armstrong R & D	M	Jun. 1992
Dr. J.A. Horton, Jr.	Oak Ridge National Laboratory	M	Jun. 1992
Prof. B.L. Bozeman and his party	Syracuse University	M	Jun. 1992
Dr. A.L. Dragoo	US Department of Energy	M, T	Jun. 1992
Mr. D.E. Debord and his party	Inco Alloys International Company	T	Jun. 1992

Nationality and Name	Affiliation	Site	Date
Mr. B. Sokolowski and his party	National Aeronautics and Space Administration	T	Aug. 1992
Mr. David Chu	Lawrence Berkeley Laboratory	T	Aug. 1992
Prof. R.K. Bitting and his party	Alfred University	M	Sep. 1992
Dr. J.E. Crow and his party	National High Magnetic Field Laboratory	T	Sep. 1992
Dr. M. Chase and his party	National Institute of Standards and Technology	M	Oct. 1992
Prof. G. Krauss	Colorado School of Mines	T	Nov. 1992
Dr. S. Freiman and his party	National Institute of Standards and Technology	T	Nov. 1992
Dr. D.O. Welch and his party	Brookhaven National Laboratory	T	Nov. 1992
Prof. A.J. McEvily, Jr.	University of Connecticut	M	Dec. 1992

❒ Brief Introduction of STA Fellowship

The Science and Technology Agency (STA), an administrative organ of the Government of Japan, offers opportunities for promising young foreign researchers in the fields of science and technology to conduct research at Japan's national laboratories and public research corporations (excluding universities and university-affiliated institutes). The program is managed by the Research Development Corporation of Japan (JRDC), a statutory organization under the supervision of STA in cooperation with the Japan International Science and Technology Exchange Center (JISTEC).

Fellowship qualifications are as follows:

1. Possession of doctor's degree.
2. Less than 35 years of age, in principle.
3. Sufficient good health for research work and life in Japan.
4. Sufficient language ability in Japanese or English.

The tenure will be 6 months to 2 years. JRDC provides expenses for round-trip, monthly living with family, initial setting-in and travel in Japan. Research expenses will be paid for the host institute. Further information can be obtained at:

Japan International Science and Technology Exchange Center (JISTEC)
2-20-5, Takezono,
Tsukuba City, Ibaraki Pref. 305, Japan
Phone +81-298-53-8250
Fax +81-298-53-8260

Organization of NRIM

❒ Organization

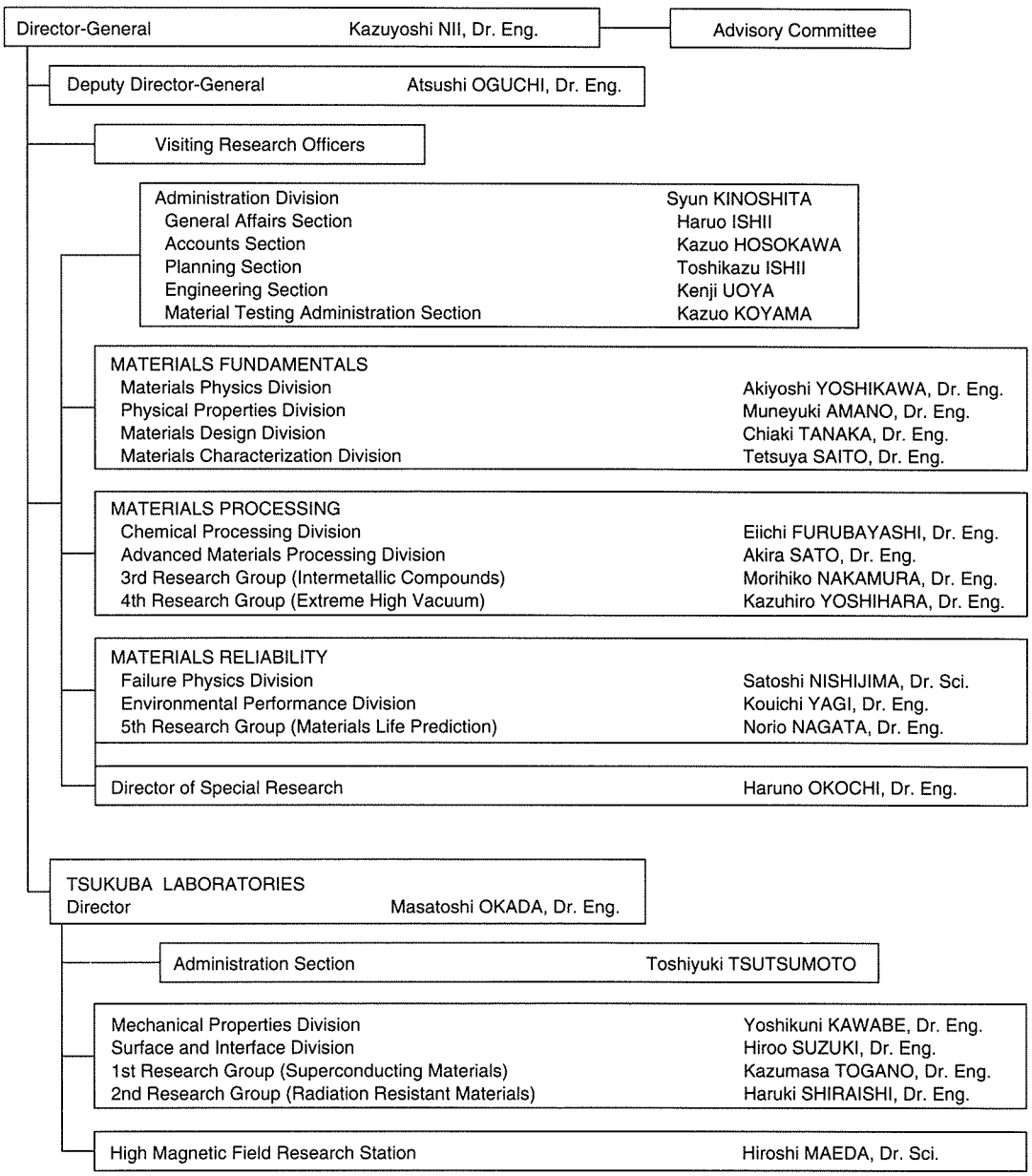

❒ Budget and Personnel in Fiscal Year of 1993

Budget	
Research and facilities	4,366
Personnel expenses	3,598
Total	7,964

unit: million yen

Personnel	
Administrative staffs	94 (10)
Researchers	331 (102)
Total	425 (112)

Number in parenthesis: Tsukuba laboratories

How to get to NRIM

To NRIM Meguro Main Site
2-3-12, Nakameguro, Meguro-ku, Tokyo 153
Phone +81–3–3719–2271 Fax +81–3–3792–3337

Narita Airport
↓ by train, JR Narita Express <60 min.>
Tokyo Station
↓ by train, JR Yamanote Line <25 min.>
Ebisu Station
↓ by taxi <5 min.> or on foot <15 min.>
NRIM

To NRIM Tsukuba Laboratories
1–2–1, Sengen, Tsukuba-shi, Ibaraki 305
Phone +81–298–53–1000 Fax +81–298–53–1005

Narita Airport
↓ by train, JR Narita Express <60 min.>
Tokyo Station
Tokyo Station Yaesu-Minami-Guchi
↓ by bus, Joban Highway Bus for Tsukuba Center <70 min.>
Tsukuba Center Bus Terminal
↓ by taxi <5 min.> or on foot <15 min.>
NRIM

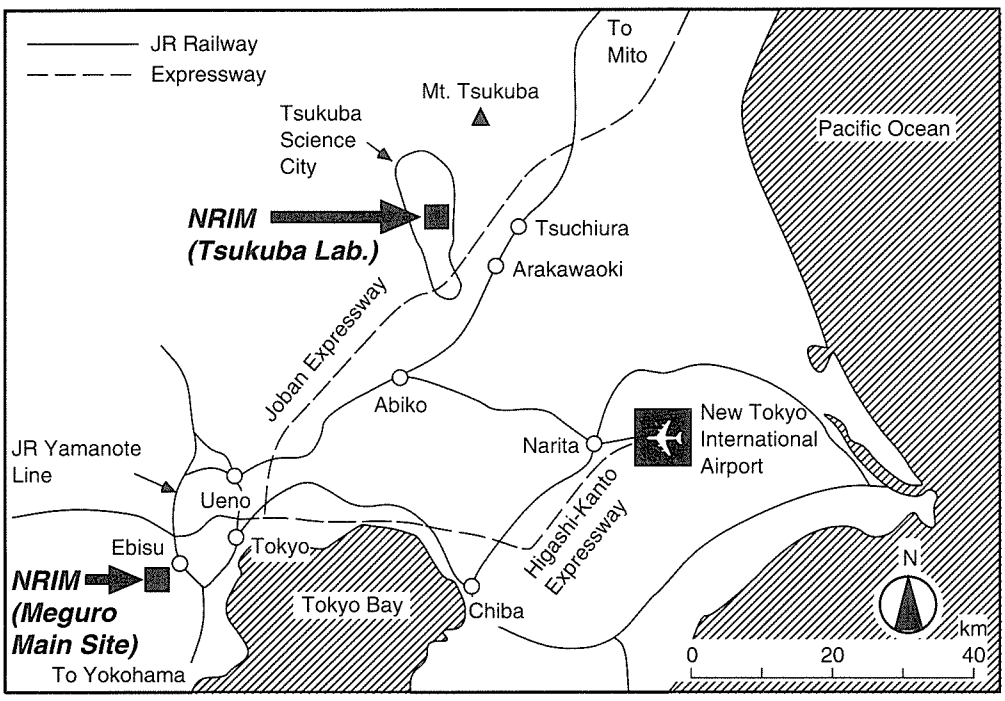

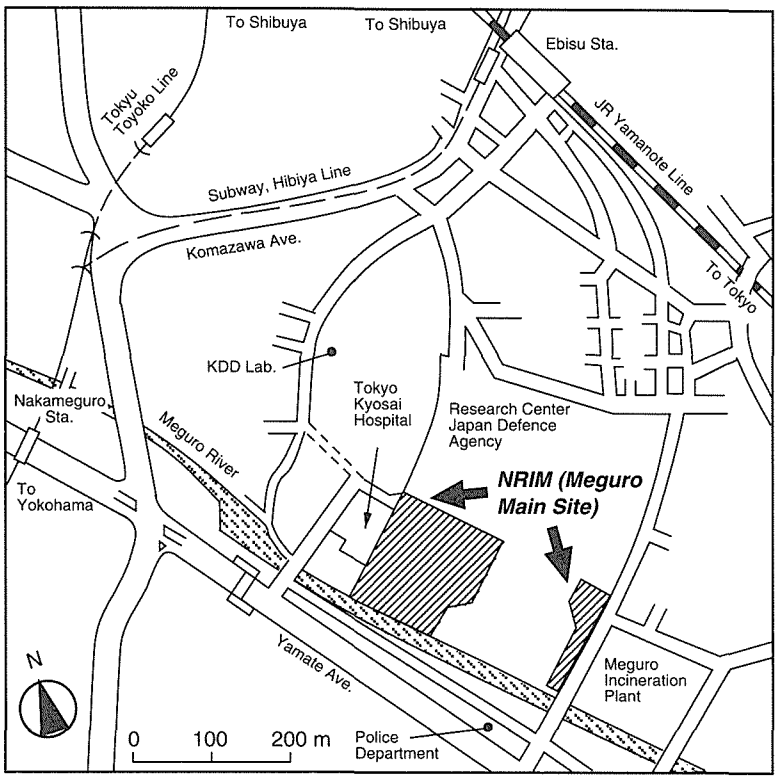

Meguro Main Site

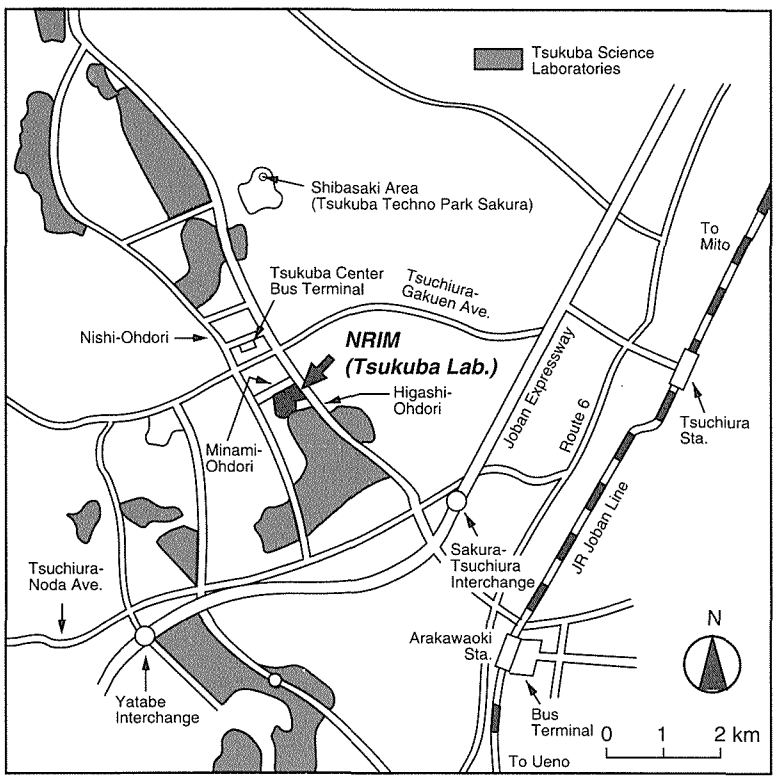

Tsukuba Laboratories

List of Keywords

NRIM Research Activities
1993
Date of Issue: 29 October, 1993

Publisher:
Toshikazu ISHII
Planning Section of Administration Division
National Research Institute for Metals
2-3-12, Nakameguro, Meguro-ku, Tokyo 153 Japan
Phone: +81-3-3719-2271, Fax: +81-3-3792-3337

Typeset using SGML by Uniscope Inc., Tokyo

NRIM Research Activities

1993